

Determination of Trace Elements in the Aquatic Environment Using Diffusive Gradients in Thin Films Technique

Smolíková, Vendula

Publication date:
2022

Document Version:
Final published version

[Link to publication](#)

Citation for published version (APA):
Smolíková, V. (2022). *Determination of Trace Elements in the Aquatic Environment Using Diffusive Gradients in Thin Films Technique*.

General rights

Copyright and moral rights for the publications made accessible in the public portal are retained by the authors and/or other copyright owners and it is a condition of accessing publications that users recognise and abide by the legal requirements associated with these rights.

- Users may download and print one copy of any publication from the public portal for the purpose of private study or research.
- You may not further distribute the material or use it for any profit-making activity or commercial gain
- You may freely distribute the URL identifying the publication in the public portal

Take down policy

If you believe that this document breaches copyright please contact us providing details, and we will remove access to the work immediately and investigate your claim.

Mendel University in Brno
Faculty of AgriSciences
Department of Chemistry and Biochemistry
&
Vrije Universiteit Brussel
Faculty of Sciences and Bio-engineering Sciences
Analytical, Environmental & Geo- Chemistry department



**Determination of Trace Elements in the Aquatic Environment Using
Diffusive Gradients in Thin Films Technique**
Dissertation thesis

Supervisors:

Assoc. Prof. Mgr. Pavlína Pelcová, Ph.D.
Prof. Dr. Martine Leermakers

Co-supervisor:

Ing. Andrea Ridošková, Ph.D.

Author:

Ing. Vendula Smolíková

EXAMINATION COMMITTEE

Supervisors:

Assoc. Prof. Mgr. Pavlína Pelcová, Ph.D.
Prof. Dr. Martine Leermakers

DCB, Mendel University in Brno
AMGC, Vrije Universiteit Brussel

Co-supervisor:

Ing. Andrea Ridošková, Ph.D.

DCB, Mendel University in Brno

Jury members:

Assoc. Prof. Mgr. Markéta Vaculovičová, Ph.D.
Chair

DCB, Mendel University in Brno

Prof. Dr. Yue Gao
Secretary

AMGC, Vrije Universiteit Brussel

prof. RNDr. Vojtěch Adam, Ph.D.

DCB, Mendel University in Brno

Prof. Dr. Frederik Tielens

ALGC, Vrije Universiteit Brussel

Prof. Dr. ir. Eveline Peeters

MICR, Vrije Universiteit Brussel

External members:

Prof. Dr. Gabriel Billon

LASIRE, University of Lille

Prof. RnDr. Viktor Kanický, DrSc.

Department of Chemistry,
Masaryk University

Assoc.Prof. Ing. Miroslav Fišera, CSc.

Department of Food Analysis and
Chemistry, Tomas Bata University in Zlín

Joint PhD between Mendel University in Brno and Vrije Universiteit in Brussel.

The dissertation thesis is submitted to Mendel University in Brno and Vrije Universiteit in Brussel in partial fulfilment of the requirements for the double degree of Doctor (Ph.D.) from Mendel University in Brno and Doctor of Sciences (Dr.) from Vrije Universiteit Brussel.

Declaration

I hereby declare that this thesis entitled *Determination of Trace Elements in the Aquatic Environment Using Diffusive Gradients in Thin Films Technique* was written and completed by me. I also declare that all the sources and information used to complete the thesis are included in the list of references. I agree that the thesis could be made public in accordance with Article 47b of Act No. 111/1998 Coll., Higher Education Institutions and on Amendments and Supplements to Some Other Acts (the Higher Education Act), and in accordance with the current Directive on publishing of the final thesis. I declare that the printed version of the thesis and electronic version of the thesis published in the application of the Final Thesis in the University Information System is identical.

I am aware that my thesis is written in accordance to Act. 121/2000 Coll., on Copyright and therefore Mendel University in Brno has the right to conclude licence agreements on the utilization of the thesis as a school work in accordance with Article 60(1) of the Copyright Act.

Before concluding a licence agreement on utilization of the work by another person, I will request a written statement from the university that the licence agreement is not in contradiction to legitimate interests of the university, and I will also pay a prospective fee to cover the cost incurred in creating the work to the full amount of such costs.

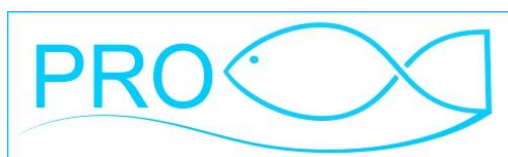
The research results of the thesis are the property of Mendel University in Brno and Vrije Universiteit Brussel.

Where the thesis would contain any commercially exploitable research results, the researcher is bound by the Valorisation Regulation of Vrije Universiteit Brussel and these results must be reported to VUB Tech Transfer before publication with a view to possible protection, e.g. through patent applications.

Date:.....

.....

signature



This work was created within CEITEC – Central European Institute of Technology, with research infrastructure supported by the project CEITEC 2020 LQ1601 financed from European Regional Development Fund. It was also financially supported by the Internal Grant Agency of Faculty of AgriSciences, Mendel University in Brno under the project IGA AF no. AF-IGA2019-IP055, by the project PROFISH CZ.02.1.01/0.0/0.0/16_019/0000869, which is financed by European Regional Development Fund in the Operational Programme Research, Development and Education and The Czech Ministry of Education, Youth and Sports, and by the Orano Mining France.

ACKNOWLEDGEMENTS

I would like to thank both of my supervisors, Assoc. Prof. Mgr. Pavlína Pelcová, Ph.D. and Prof. Dr. Martine Leermakers, as well as my co-supervisor Ing. Andrea Ridošková, Ph.D for their support. I was introduced to the world of scientific research at MENDELU where thanks to the dedicated guidance, expert advice, and determination from Pavlína and Andrea, I gained the knowledge and skills necessary for work in the field of analytical chemistry and the development of new methods. I also deeply appreciate their support to complete an internship abroad which unexpectedly changed my life. What started as an internship at VUB turned into an amazing journey filled with adventurous expeditions thanks to the support and encouragement from Martine. Her scientific insights, ideas, dedication, and enthusiasm greatly inspired me, and I deeply appreciate her attitude which always made me feel like everything is possible.

Since my research was performed in the framework of a Joint PhD I would like to express my thanks to the people involved in this process. I am especially grateful to Prof. RNDr. Vojtěch Adam, Ph.D. without whose support, encouragement, and unfading enthusiasm I would not be able to go through this. I would also like to acknowledge people from Orano Mining France and particularly Dr. Michael Descostes for allowing me to undertake my research at VUB and giving me the opportunity to join amazing missions in France. I also greatly appreciate the help from the study departments of both universities that were involved in managing my Joint PhD.

I would also like to thank all members of the DCB and AMGC departments who I had the honour to work with, for creating an inspiring, supportive, and especially friendly environment. A special thanks belong to my dear friend Ing. Eliška Sedláčková, Ph.D. with whom we shared the entire period of our studies, to RNDr. Josef Hedbávný who guided me in the lab and shared his knowledge with me, and to Ing. Marek Reichstädter, Ph.D. who encouraged me to my PhD journey in Belgium.

I am eternally grateful to all my friends and family who supported me in the difficult times and shared joy in the good ones. Tereza, Kateřina, Šárka, Silvia, Viktor, Oriana, Carla, Matthias, and Gwen – you might be in my life for a long or short time, but you have shared this important path with me, and I am very grateful for your friendship. I sincerely thank my mom, dad, and brother who always encouraged me, and I am proud of what I have been able to achieve thanks to them. Finally, the sincerest thanks belong to my partner Martin. Wherever I have been and whatever I have done, you believed in me and stood by me, and I would never be where I am now without you.

ABSTRACT

Water is an essential premise of life on Earth and thus the pollution of the aquatic environment nowadays receives increasing attention from researchers as well as the decision-makers and public. Besides other pollutants, monitoring of toxic metals and metalloids remains at the centre of research interests due to their persistent and bioaccumulative nature in the environment as well as because of the need to understand their biogeochemical behaviour. The Diffusive Gradients in Thin Films (DGT) technique is a tool that can improve the knowledge about the processes that influence the bioavailability of trace elements. Thus, the main objective of this PhD study was the development and application of the DGT technique for the evaluation of selected trace elements (arsenic and uranium) in the aquatic environment. A novel DGT resin gel utilizing the commercially available resin Lewatit FO 36 for an effective evaluation of arsenic contamination in aquatic ecosystems was developed. The technique was validated by *in-situ* application in the aquatic environments (*e.g.*, water reservoir Zákalská and mineral springs Hronovka and Regnerka (Czech Republic), and Zenne River (Belgium)). The geochemistry and distribution of As species in water and sediments of the Zenne River were further investigated based on the research findings from the years 2010–2021. The combination of active and passive sampling of the water together with analysis of sediments brought new findings regarding the As pollution of the Zenne River. The DGT technique utilizing Lewatit FO 36 resin was also tested for the simultaneous determination of both elements - arsenic and uranium - that are studied in this work. For these purposes, a new elution protocol was optimized, and the technique was evaluated by *in-situ* application in the Scheldt estuary (Belgium). Here, an extensive comparative study investigating the influence of the salinity gradient on the performance of selected DGT techniques (utilizing Chelex-100, Dow-PIWBA, Diphonix, and Lewatit FO 36) for the determination of uranium was performed. The results demonstrated that the thorough testing of the DGT performance in a real environment and especially in complex matrices such as seawater is essential for the selection of the best DGT design for environmental applications. The results of this thesis provided a new DGT design for arsenic and uranium monitoring and at the same time brought valuable information about their geochemistry in the aquatic environment.

KEYWORDS: Diffusive gradients in thin films, arsenic, uranium, aquatic ecosystems.

ABSTRAKT

Voda je základním předpokladem života na Zemi, a proto je v současné době problematice jejího znečištění věnována stále větší pozornost z hlediska výzkumu, ale rovněž rozhodujících orgánů a veřejnosti. Mimo jiných kontaminantů zůstává monitoring toxických kovů a polokovů středem zájmu výzkumu vzhledem k jejich perzistentní a bioakumulativní povaze v životním prostředí a rovněž kvůli potřebě porozumět jejich biogeochemickému cyklu. Technika difúzního gradientu v tenkých filmech (DGT) je nástroj, který může rozšířit znalosti o procesech ovlivňujících biologickou dostupnost stopových prvků. Hlavním cílem této disertační práce tak byl vývoj a aplikace techniky DGT pro hodnocení vybraných stopových prvků (arsen a uran) ve vodních ekosystémech. V rámci práce byl vyvinut nový DGT sorpční gel využívající komerčně dostupný sorbent Lewatit FO 36 pro efektivní hodnocení kontaminace vodního prostředí arsenem. Nová metoda byla validována řadou *in-situ* aplikací ve vodním prostředí (např. vodní nádrž Zászkalská, minerální prameny Hronovka a Regnerka (Česká republika), řeka Zenne (Belgie)). Geochemie a distribuce specií arsenu ve vodě a sedimentech řeky Zenne byly blíže zkoumány na základě výsledků z období 2010–2021. Kombinace aktivního a pasivního vzorkování vody společně s analýzou sedimentů přineslo nová zjištění ohledně kontaminace řeky Zenne arsenem. Technika DGT využívající pryskyřici Lewatit FO 36 byla také testována pro simultánní stanovení obou prvků, kterými se tato práce zabývá – arsenu i uranu. Pro tyto účely byl optimalizován nový eluční protokol a technika DGT byla aplikována *in-situ* v ústí řeky Šeldy (Belgie). Zde byla rovněž provedena rozsáhlá komparativní studie zkoumající vliv gradientu salinity na účinnost vybraných DGT technik (využívajících sorbenty Chelex-100, Diphonix, Dow-PIWBA a Lewatit FO 36) při hodnocení uranu. Výsledky studie ukázaly, že důkladné testování účinnosti techniky DGT v reálném prostředí a zejména v komplexních matricích, jako je mořská voda, je nezbytné pro výběr nejlepšího designu techniky pro environmentální aplikace. Tato práce poskytla nový design techniky DGT pro monitorování arsenu a uranu, a zároveň přinesla cenné informace o jejich geochemii ve vodním prostředí.

KLÍČOVÁ SLOVA: Difúzní gradient v tenkých filmech; arsen; uran; vodní ekosystémy.

ABSTRACT

Water is essentieel voor het leven op Aarde waardoor de vervuiling van het aquatisch milieu tegenwoordig in toenemende mate aandacht krijgt van onderzoekers, beleidsmakers en het brede publiek. Zowel door hun persistentie en bioaccumulatieve aard in het milieu als de nood om beter inzicht in hun biogeochemisch gedrag te krijgen, blijft het monitoren van giftige metalen en metaloïden, naast andere pollutanten, centraal staan in het onderzoek. De “Diffusive Gradients in Thin Films” (DGT) techniek is een methode die de kennis over processen, die de biologische beschikbaarheid van sporenelementen beïnvloeden, kan verbeteren. Aldus, hethoofddoel van dit doctoraat was het ontwikkelen en toepassen van de DGT techniek bij de evaluatie van geselecteerde sporenelementen (arseen en uranium) in het aquatisch milieu. Een nieuw DGT methode werd ontwikkeld, gebruik makend van het commercieel beschikbaar hars Lewatit FO 36, voor effectieve evaluatie van arseen contaminatie in aquatische ecosystemen. De techniek werd gevalideerd door in-situ toepassing in aquatische systemen (bijvoorbeeld het Zákalská waterreservoir en de minerale bronnen Hronovka en Regnerka (Tsjechië), en de Zenne rivier (België)). De geochemie en distributie van arseen species in het water en sediment van de Zenne werden verder onderzocht op basis van de onderzoeksresultaten uit de periodes 2010–2021. De combinatie van actieve en passieve bemonstering van het water, samen met de analyse van sedimenten bracht nieuwe bevindingen met betrekking tot de As vervuiling van de Zenne. De DGT techniek werd ook getest, gebruik makend van het Lewatit FO 36 hars, voor het gelijktijdig bepalen van beide elementen uit deze studie – arseen en uranium. Hiervoor werd een nieuw elutie protocol geoptimaliseerd, en werd de techniek geëvalueerd door *in-situ* toepassing in het Schelde estuarium (België). Hier werd een uitgebreide vergelijkende studie uitgevoerd die invloed van de zoutgradiënt op de prestatie van de geselecteerde DGT technieken (gebruik makend van Chelex-100, Dow-PIWBA, Diphonix en Lewatit FO 36) voor de bepaling van uranium onderzocht. De resultaten toonden aan dat het grondig testen, van de prestatie van DGT in een echt milieu en vooral in complexe matrices zoals zeewater, essentieel is voor de selectie van het beste DGT ontwerp. De resultaten van deze thesis boden een nieuw DGT ontwerp voor het monitoren van arseen en uranium, en brachten belangrijke informatie over hun geochemie in het aquatisch milieu.

SLEUTELWOORDEN: Diffusive gradients in thin films; arseen; uranium; aquatische ecosystemen.

CONTENTS

1	General introduction	17
2	Aims	19
3	Literature overview	21
3.1	Trace elements	21
3.1.1	Arsenic in the environment	22
3.1.2	Uranium in the environment	24
3.2	Bioavailability and toxicity of trace elements	26
3.2.1	Arsenic toxicity	30
3.2.2	Uranium toxicity	31
3.3	Analysis of trace elements in relation to their bioavailability	32
3.3.1	Sample pre-treatment for speciation analysis	33
3.3.2	Speciation analysis of trace elements	34
3.3.2.1	Direct techniques	35
3.3.2.2	Separation and detection techniques	36
3.3.3	Modelling methods	37
3.3.4	Techniques evaluating bioavailability of trace elements	39
3.3.4.1	Diffusive equilibrium in thin films	40
3.3.4.2	Donnan membrane technique	40
3.3.4.3	Gellyfish sampler	41
3.3.4.4	Permeation liquid membrane	41
3.3.4.5	Chemcatcher sampler	42
3.4	Diffusive Gradients in Thin films technique	43
3.4.1	Principle of the DGT technique	43
3.4.1.1	Diffusive layer	46
3.4.1.2	Binding layer	48

3.4.2	Application of the DGT technique	50
4	Materials and methods.....	53
4.1	Reagents and chemicals	53
4.2	Protocol for preparation and processing of DGT	53
4.2.1	Preparation of diffusive and resin gels.....	53
4.2.2	DGT assembly and deployment.....	56
4.2.3	Elution of the resin gel.....	57
4.3	Laboratory experiments for DGT characterization	58
4.3.1	Uptake and elution efficiency	59
4.3.2	Sorption capacity of the resin gel.....	59
4.3.3	Determination of the diffusion coefficient.....	60
4.3.4	Estimation of the diffusive boundary layer.....	60
4.4	Analytical methods.....	61
4.4.1	Modified ET-AAS method for the determination of arsenic in solution with a high concentration of chlorides	62
5	Results and discussion.....	69
5.1	Development and evaluation of the DGT technique utilizing commercially available resin Lewatit FO 36 for determination of arsenic species in the aquatic environment.....	71
5.2	Evaluation of arsenic bioavailability in mineral springs (Czech Republic) using Lewatit FO 36-DGT technique	83
5.3	Arsenic distribution and geochemistry in the Zenne River (Belgium)	91
5.4	Optimization of elution protocol for simultaneous determination of arsenic and uranium by Lewatit FO 36-DGT.....	130
5.5	Comparative study evaluating the salinity influence on the performance of different DGT binding phases for uranium determination – the Scheldt Estuary (Belgium)	138
6	Conclusions	151
7	Future perspectives.....	156
8	References	159

9	Abbreviations.....	188
10	List of figures	192
11	List of tables	193
12	List of annexes.....	194
12.1	Supplementary Information to Chapter 5.3.....	194
12.2	Supplementary Information to Chapter 5.4.....	203
12.3	Supplementary Information to Chapter 5.5.....	206
12.4	Curriculum Vitae.....	211

1 GENERAL INTRODUCTION

With 274 journals in the database of the Web of Science, the Environmental Sciences is the 8th largest category out of 254 in total [1]. Besides other research interests within this category such as climate change, environmental health, geology or monitoring, environmental pollution, and toxicology are among the most important ones. Since the majority of the planet's surface is covered in water, which is an essential premise of life on Earth, the issue of its pollution receives nowadays increasing attention from researchers as well as the decision-makers and public [2]. Although the trends in water pollution monitoring have turned over the years towards microplastic or organic pollutants such as antibiotics, hormones, pesticides, or drugs, the monitoring of trace elements remains at the centre of research attention. This is not only because of the increasing pollution by toxic trace elements and their persistent and bioaccumulative nature in the environment but also due to the need to understand the biogeochemical behaviour of elements that are essential nutrients in the aquatic environment.

Regarding the trace elements studied in this work, their essentiality for living organisms is either none (uranium) or not demonstrated yet (arsenic) according to the World Health Organization (WHO) [3, 4]. Both elements are in fact highly toxic for humans and monitoring of their appearance in the natural environment is due to their potential adverse effect on human health. Although arsenic and uranium, occur naturally in the environment, they are significant environmental contaminants, which are released into the ecosystems mainly from anthropogenic sources (*i.e.*, as a result of industrial, agricultural, and mining activities). The authorities of the European Union recognize water quality threshold limits only for total dissolved As ($10 \mu\text{g L}^{-1}$) and U ($30 \mu\text{g L}^{-1}$) set by the Directive (EU) 2020/2184 in water intended for human consumption. However, both elements are not included on the priority list of substances in the EU Water Framework Directive and their threshold levels in surface water and groundwater are thus set by the individual Member States – based on their own risk identification and assessment. Nevertheless, the authorities generally recognize that determining only the total dissolved concentration of an element in the environment does not necessarily

indicate its bioavailability to the biota. The bioavailability of trace elements is closely related to their chemical speciation which is influenced by various physico-chemical properties and the co-existence of other elements and compounds in the environment. It is, therefore, crucial to determine the bioavailable fraction of these trace elements in addition to the determination of their total concentration in the environment as it may better reflect their potential toxicity to biota.

The Diffusive Gradients in Thin films (DGT) is a technique that can fill the gap in knowledge of the processes of trace elements bioavailability in the environment. It was developed by Zhang and Davison in 1994 [5] and has been used by many researchers within the last three decades [6, 7]. The various approaches of the DGT technique application involve the evaluation of elemental speciation and lability [8-11], the bioavailability of elements to biota [12-16], long-term monitoring of time-weighted average concentrations [17-19], investigation of elements' geochemistry and cycling in sediments and soils [20-23], or 2D imaging of fluxes of elements in sediments and soils [24-27]. However, in all cases, it is necessary to choose the most suitable DGT design and perform its thorough validation.

Therefore, this work is dealing mostly with the development and evaluation of new DGT techniques or validation of existing DGT designs in real aquatic environments. The research is targeting the determination of arsenic and uranium in the water ecosystems, as they often occur simultaneously in the environment and can be especially found in the vicinity of mining sites [28-30].

2 AIMS

- Literature overview on studied trace elements (arsenic and uranium) and the approaches of their monitoring in the environment with a focus on the Diffusive Gradients in Thin films (DGT) technique.
- Development and optimization of new DGT technique for the determination of arsenic and/or uranium utilizing commercially available resin Lewatit FO 36.
- Optimization of extraction procedures and analytical methods related to the application of the DGT technique.
- Validation of new DGT techniques by *in-situ* applications in the aquatic environment.
- Investigation whether the DGT technique can be used as a monitoring tool of studied trace elements in various environmental conditions.

3 LITERATURE OVERVIEW

3.1 Trace elements

In analytical chemistry, the term “trace elements” refers to chemical elements occurring in nature in an average concentration lower than $100\ \mu\text{g g}^{-1}$ [31] and includes metals and metalloids. Therefore, this term is used for the purpose of this study which focuses on arsenic (metalloid) and uranium (metal).

Regarding the role of trace elements in living organisms and their participation in biological processes, they can be referred to as essential or toxic trace elements. While non-essential trace elements like Cd, Pb, Hg, or U have no physiological function and are considered toxic, the essential trace elements like Co, Cu, Fe, Mn, Se, and Zn have an important biochemical role (*i.e.*, as active centres or structural factors of enzymes) [32]. The essentiality of trace elements refers to the adverse consequences of their deficiency in the organism. However, the essential trace elements may also become toxic at sufficiently high intakes. The line between essentiality and toxicity varies widely – different organisms require different essential trace elements and so the threshold limit regarding their deficiency or excess is organism-specific as well [33]. There is also a group of metal(loid)s that are on the border between essential and non-essential trace elements and despite their toxic effect on the living organisms it is believed they may have some physiological function which is not known yet. An example is As which was demonstrated to be an essential nutrient for goats and chickens. Arsenic deficiency in goat’s organisms can cause a significant reduction of serum triglyceride levels which can lead to death. In the organism of poultry, it is essential for the synthesis of methionine metabolites, including cysteine. Nevertheless, the mechanism of its physiological role has not been demonstrated yet and there is no evidence of its essential role for humans [34-37].

3.1.1 Arsenic in the environment

Arsenic is a naturally occurring metalloid which despite being a trace element is commonly associated with crustal rocks. Its average concentration in the Earth's crust is 1–1.8 mg kg⁻¹ which makes it the 20th most abundant element. The typical concentration found in open oceans is about 1.5 µg L⁻¹, however, the concentration in freshwater or groundwater may be higher (but generally < 10 µg L⁻¹) [38-40]. Over 200 minerals contain As but the most abundant arsenic-containing minerals are arsenopyrite (FeAsS), realgar (AsS), and orpiment (As₂S₃). Elevated concentrations of arsenic in the environment are associated with mining activities because among the gold-bearing ores which accompany native gold deposits, arsenopyrite is the most important one. After exposure of mine tailings to air, arsenopyrite oxidises during weathering and releases Fe oxides, As and large amounts of SO₄²⁻, causing acid mine drainage [41-43].

Arsenic may occur in four oxidation states in the environment (–III, 0, III, V) but it is mostly present in inorganic form as trivalent or pentavalent oxyanions (arsenite AsO₃³⁻ and arsenate AsO₄³⁻) in aquatic ecosystems [44, 45]. Arsenic speciation in solution is therefore dependent on the pH and redox potential (Eh) of the environment (for Eh-pH diagram see **Fig. 3-1**). Under anoxic conditions, the reduced As^{III} is present as uncharged H₃AsO₃ which predominates up to pH = 9 while above this pH, the AsO(OH)₂⁻, AsO₂(OH)²⁻, or AsO₃³⁻ occur. Under oxic conditions, the oxidized As^V can hydrolyse to four species which occur with increasing pH in this order – H₃AsO₄, H₂AsO₄⁻, HAsO₄²⁻, and AsO₄³⁻ (**Fig. 3-2**) [46]. Nevertheless, As^{III} and As^V can also co-exist in both, oxic and anoxic waters, as a result of biotic or abiotic (*e.g.*, oxidation by manganese oxides) processes [47]. Besides inorganic species, organic methylated compounds or even larger As complex compounds such as arsenobetaine can be found in the aquatic environment. The methylated arsenic compounds (monomethylarsonic acid (MMA), dimethylarsinic acid (DMA), and trimethylarsine oxide (TMAO) are formed by a biotic pathway mediated by microorganisms (*e.g.*, bacteria, phytoplankton) as a result of their detoxifying mechanism [48].

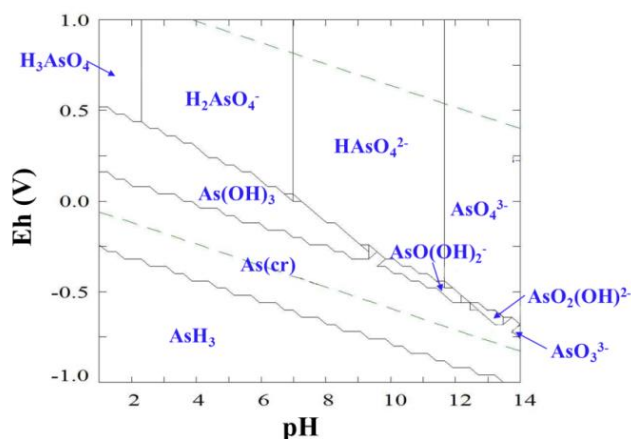


Fig. 3-1 Illustrative Pourbaix Eh-pH diagram of As-H-O system ($\text{As} = 10^{-5} \text{ M}$, $T = 25^\circ \text{C}$, created with Medusa Software (Royal Institute of Technology, Sweden)).

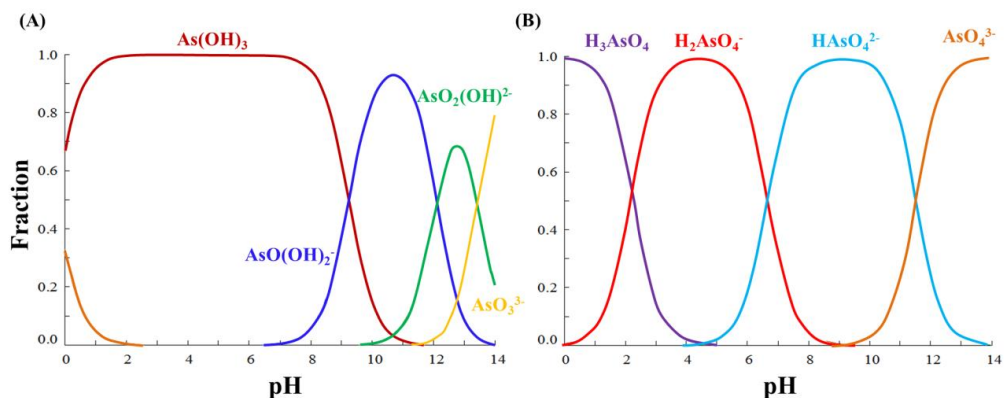


Fig. 3-2 Illustrative distribution diagram of arsenite (A) and arsenate (B) fractions in aqueous solution under different pH conditions ($\text{As} = 10^{-5} \text{ M}$, created with Medusa Software (Royal Institute of Technology, Sweden)).

Compared to the other oxyanions, arsenic is relatively mobile over a wide range of redox conditions. Its mobility in water is controlled by adsorption/desorption onto solid phases or precipitation/dissolution of arsenic-containing minerals taking place on the mineral/sediment-water interface. The most important factors limiting arsenic mobility are Fe, Mn, or Al (hydr)oxides, dissolved organic matter (DOM), and clay minerals. Iron and manganese (oxyhydr)oxides are generally accepted as the most important ones that remove arsenic from solution by sedimentation. But with the increase of reducing conditions in sediments, arsenic can be released back to solution by the reductive

desorption/dissolution of the hosting (oxyhydr)oxide [44, 49, 50]. By interfering with the adsorption of arsenic onto metal oxide surfaces, DOM may immobilize arsenic from rocks and sediments to surface water. The humic acid (HA) or fulvic acid (FA) can increase the mobility of arsenic by competing for binding sites on minerals, or by direct formation of As-DOM or As-Fe-DOM complexes [51, 52]. It has been demonstrated that As weakly bound to DOM is bioavailable for bacteria [53].

3.1.2 Uranium in the environment

Uranium belongs among actinides and occurs in nature as the mixture of three isotopes ^{238}U , ^{235}U , and ^{234}U with the relative abundances of approximately 99.275%, 0.720%, and 0.005%, respectively. The average concentration of U in the igneous rocks of the Earth's crust is 1–10 mg kg⁻¹. Uranium can be found in all rock types but the primary minerals like uraninite, pitchblende, and coffinite, as well as secondary minerals like carnotite and uranophane, belong among the most important [54, 55]. In natural freshwater, the average uranium concentration is about 0.3 µg L⁻¹, but since the conservative behaviour of uranium is generally observed within estuaries, the U concentrations are increasing with the salinity to the average concentration of 3.3 µg L⁻¹ in seawater [56, 57]. As with other toxic elements, the risk of increased uranium concentrations may arise as a result of anthropogenic activities – in particular from the mining (tailings) or other stages of the nuclear fuel cycle (spent fuel or fission product wastes) [58].

Uranium may occur in four oxidation states (III, IV, V, VI) but in the natural environment under oxic and suboxic conditions, it is mostly present as the hexavalent U^{VI}, while under reducing and anoxic conditions it is present as tetravalent U^{IV}. The trivalent U^{III} and pentavalent U^V forms of uranium are generally not relevant for environmental studies because they are considered unstable [54]. The speciation of uranium in solution is controlled by pH-Eh conditions (**Fig. 3-3**) and by the concentration and availability of complexing ions. One of the most important uranium complexes generally found in the natural aquatic environment is represented by uranyl carbonates with the $\text{UO}_2(\text{CO}_3)_x$ species dominating between pH 4–12 [57]. Nevertheless,

the chemistry of uranium in solutions is a very complex matter and the resulting models may differ from author to author due to the variability between databases used as an input. An illustrative distribution diagram of uranium in the non-complexing environment under oxic conditions, and in the presence of carbonates is shown in (Fig. 3-4) but it must be borne in mind that the software used for modelling in this work does not have a uranium-specialized database.

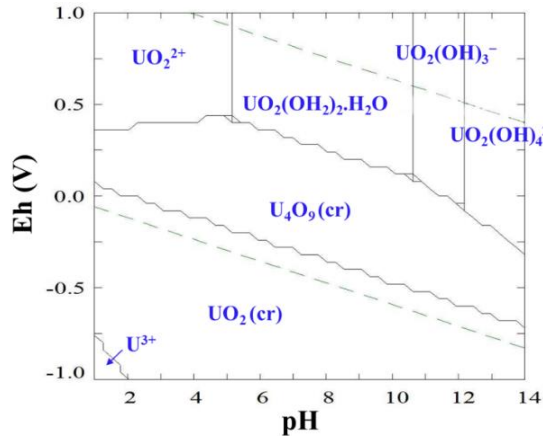


Fig. 3-3 Illustrative Pourbaix Eh-pH diagram of U-H-O system ($U = 10^{-5}$ M, $T = 25$ °C, created with Medusa Software (Royal Institute of Technology, Sweden)).

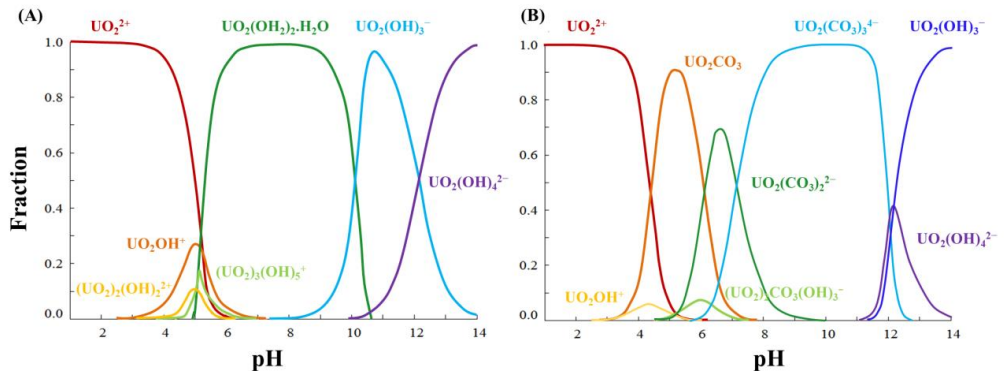


Fig. 3-4 Illustrative distribution diagram of uranium fractions under different pH conditions in non-complexing environment (A) and in the presence of carbonates (B) ($U = 10^{-5}$ M, $CO_3^{2-} = 10^{-2}$ M created with Medusa Software (Royal Institute of Technology, Sweden)).

The mobility of uranium is influenced by its speciation and sorption on the solid phases. In groundwater, the U^{VI} is reduced to insoluble U^{IV} compounds. Hexavalent

compounds are, on the other hand, highly soluble and mobile and are present either as free uranyl ion (UO_2^{2+}) or as soluble complexes with inorganic ligands such as OH^- , CO_3^{2-} , PO_4^{3-} , SO_4^{2-} , F^- , Cl^- [59]. The formation of ternary complexes of uranyl carbonates with alkaline earth metals (especially Ca^{2+} and Mg^{2+}) facilitates the mobility of uranium [60-62]. Natural DOM can also effectively form complexes with uranium and depending on the solubility of HS (humic substances) influence U mobility. The HS may act as a uranium sink when the insoluble uranyl-HA complexes are formed or increase its mobility by the formation of soluble uranyl-FA complexes. Humic substances may also compete with uranium for sorption sites on Fe, Al, or Si (hydr)oxides, and clay minerals (*e.g.*, smectite or montmorillonite) which would otherwise reduce the uranium mobility [57, 63, 64].

3.2 Bioavailability and toxicity of trace elements

Bioavailability is in chemistry generally defined as the fraction of chemical compounds in the environment that can be taken up by an organism and can interact with its metabolism [65]. Bioavailability of trace elements is generally influenced by a number of physico-chemical parameters of the environment such as pH, redox conditions, ionic strength, temperature, salinity, presence of competing elements, and available complexing agents – altogether influencing the chemical form or speciation of the element. But it is also linked to biotic factors of the organism that interacts with the trace elements such as the type and species of organism, its uptake mechanism and metabolism, age, etc. [66-69]. The total concentration of trace elements present in the environment does not necessarily reflect its potential bioavailability. Therefore, the determination of the bioavailable fractions of trace elements is gaining in importance since it provides information about the likelihood of their interaction with living organisms and thus allows an estimation of the potential toxicity of trace elements to biota in the aquatic environment.

Trace elements entering the environment naturally (*e.g.*, rock weathering or erosion, volcanic activity) or as a result of anthropogenic activities (*e.g.*, agriculture, industry, mining) are in the aquatic environment generally distributed between particulate and

dissolved fractions (**Fig. 3-5**). Particulate fraction represented by elements associated with particulate matter of organic (*e.g.*, bacteria, algae, protozoans) or inorganic origin (amorphous organic matter, detritus, as well as suspended inorganic sediment) is not a bioavailable fraction but play an important role in trace elements' transport and regulation of their concentration in the water column due to the processes of adsorption or precipitation, and subsequent sedimentation. The distribution between the particulate and dissolved fraction depends on the presence and availability of potential sorbents in the aquatic environment. A higher ratio of the particulate fraction of some trace elements can therefore be found in turbid environments (*e.g.*, estuaries) or wastewaters [70-72]. Nevertheless, from the point of view of the potential bioavailability of trace elements to biota, it is necessary to go beyond the distinction between particulate and dissolved fractions. The dissolved fraction which is generally separated by filtration of the water sample (pore size 0.20–0.45 μm) can be further divided into colloidal and truly dissolved (labile) fractions. A colloid-size fraction of dissolved elements is mainly formed with humic acids, non-humic macromolecules (*e.g.*, polysaccharides, proteins, or amino sugars), or inorganic colloids like Fe and Mn (oxyhydr)oxides, Al oxides, and silicates. But only truly dissolved fraction, which is composed of constituents with a molecular weight less than 1–10 kDa, is considered labile and therefore readily available for living organisms. Free or hydrated ions and weak metal complexes with either inorganic (*e.g.*, OH^-) or organic (*e.g.*, FA) ligands which can easily dissociate belong among the labile fraction of trace elements [73-76].

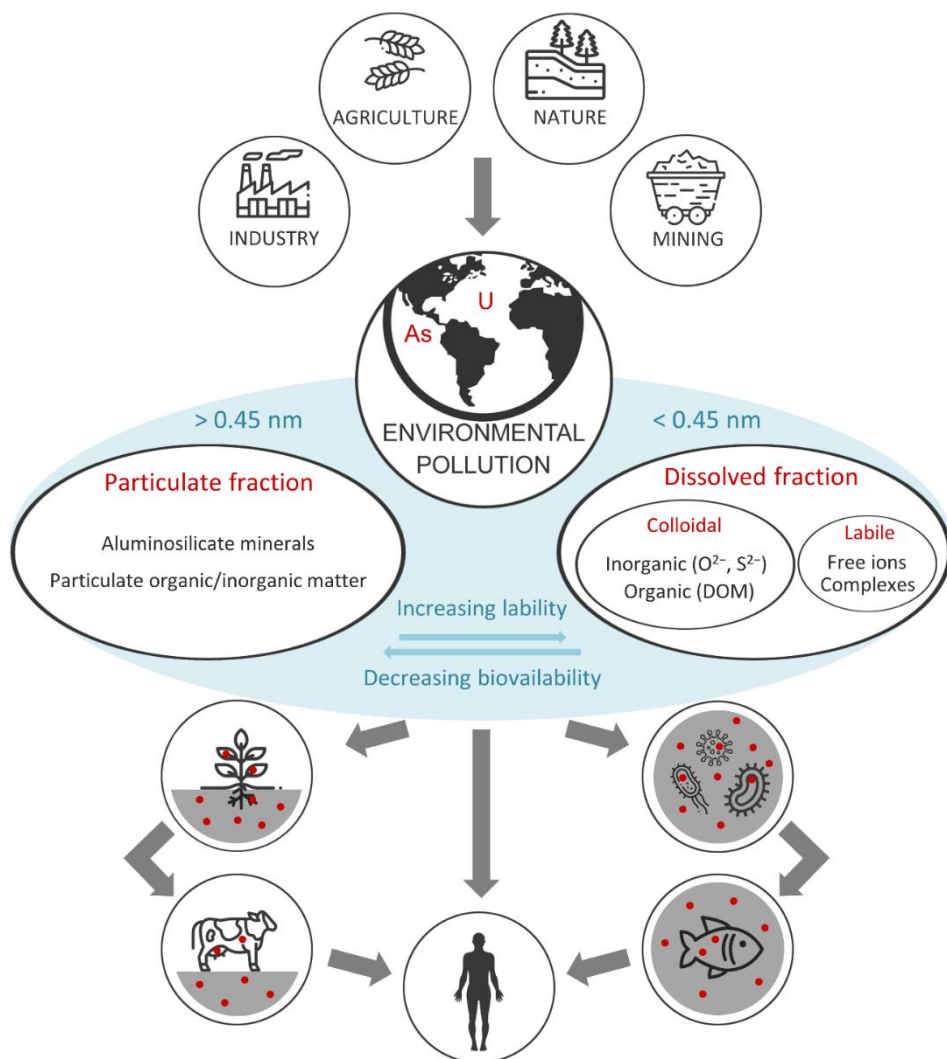


Fig. 3-5 Illustrative scheme of trace elements pathways to aquatic ecosystems, their fractionation in water, and potential exposure pathways for living organisms.

The bioavailable fraction of trace elements in water may enter the organisms and subsequently interact with them. For simplicity, the uptake of trace elements (metals or metalloids) from the aquatic environment is usually described for simple unicellular organisms. In complex organisms, several aspects of the uptake must be taken into account. For example, in the human body, the primary uptake is through the gastrointestinal tract, and therefore, the transport from the duodenum through mucosal cells to the bloodstream and subsequent transport to cells and potential targeted cell's

organelle must be considered [69, 77]. Generally, trace elements interaction with organisms includes:

- 1) diffusion of the metal in the bulk solution to the surface of the cell membrane,
- 2) sorption or surface complexation of the metal to the binding sites of the cell membrane surface,
- 3) transport of the metal through the cell membrane [78].

The examples of possible paths of trace elements uptake by a cell from the solution are illustrated in **Fig. 3-6**. The surface of the organism may be represented by the gill, gut, root-tip, epithelium, or simply a surface of a unicellular organism for the above-mentioned reason. Weak metal complexes dissociate within their transport until reaching the biological surface. Subsequent association of metal with the biological membrane is known as biosorption and includes reactions such as ion-exchange, chemisorption, complexation, chelation, microprecipitation, or surface adsorption. Afterwards, this step may be followed by the biological transport of trace elements into the cell and interaction with the cell [67, 79, 80]. The transport across the plasma membrane of the cell may take place as a direct penetration through the phospholipid layer (especially non-polar lipophilic compounds such as alkyl-metals), which is essentially mediated by passive diffusion. However, active transport mediated by a specific carrier or through an ion pump/channel, or by endocytosis occurs as well [81, 82]. After entering the cell, metal ions may interact with various intracellular sites and organelles (*e.g.*, mitochondria, ribosomes, lysosomes, nucleus, metallothioneins), some of which may result in metabolic consequences [65, 81].

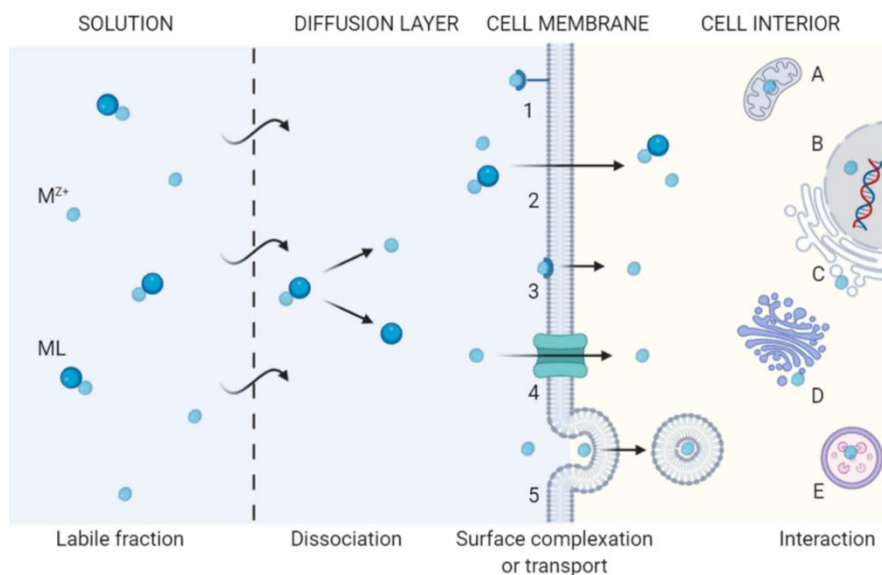


Fig. 3-6 Trace element (metal(loid)) uptake by cell (M^{Z+} – free metal ion; ML – weak complex of metal and ligand; 1 – surface complexation; 2 – penetration of M or ML through the phospholipid layer; 3 – mediated transport; 4 – transport through ion pump/channel; 5 – endocytosis, A – mitochondria, B – nucleus, C – endoplasmic reticulum with ribosomes, D – Golgi apparatus, E - lysosome) (inspired by [65, 81, 83] and created with BioRender.com).

Once entering the living organism, trace elements may interact with its metabolism. In general, exceeding the threshold concentration of essential and/or non-essential trace elements in organisms may lead to the disruption of homeostasis, accumulation, and eventually toxic effects. The toxicity of trace elements is influenced by various factors – the dose, the ability to penetrate through protective barriers of the organism and to react with the organism, the ability to transform in the organism and increase/decrease its toxic effect, and the ability of the organism to eliminate them [33, 79].

3.2.1 Arsenic toxicity

The toxicity of arsenic is given primarily by its speciation. Generally, inorganic arsenic species of As^{III} and As^V are more toxic and mobile than organic arsenic species like MMA or DMA [84, 85]. In oxygenated water, As^V predominates in the form of $H_2AsO_4^-$ and $HAsO_4^{2-}$ which have nearly identical chemical properties as phosphate that occur as $H_2PO_4^-$ and HPO_4^{2-} under the same conditions. Arsenate can therefore compete with

phosphate which is an important nutrient for many aquatic organisms. However, some organisms (*e.g.*, phytoplankton) developed a detoxification mechanism for the reduction of As^{V} to As^{III} . But while resulting As^{III} is not toxic for phytoplankton, it is highly toxic for higher organisms such as zooplankton and fish. This biotransformation thus leads to the increased concentration of As^{III} species even under oxidizing conditions. Other organisms degrade the arsenate by its methylation resulting in the formation of MMAs and DMAs which can be excreted. But unlike As^{III} these organic compounds display low toxicity for higher organisms which is in contrast to other metals that generally show higher toxicity in a methylated form (*e.g.*, methyl mercury) because these compounds are lipophilic and are thus able to easily penetrate the cell membrane [48, 86, 87].

After entering the cell, arsenate can replace phosphate in metabolic pathways due to its similar structure. The disruption of the phosphodiester bond in adenosine triphosphate (ATP) or substitution of PO_4^{3-} by AsO_4^{3-} in adenosine diphosphate (ADP) may result in depletion of ATP stores that produce cellular energy. Arsenate may also be reduced in the cell by glutathione (GSH). The formed arsenite has a higher rate of accumulation in the cellular system compared to arsenate. This together with the high affinity of As^{III} for sulfhydryl groups (-SH) causes its interaction with proteins, enzymes, and low molecular weight compounds such as GSH or cysteine thereby making them inactive. Since GSH is involved in the antioxidant defence of organisms, its homeostasis disruption increases reactive oxygen species (ROS) in cells and thus causing cell damage. The absorbed arsenic is generally detoxified by S-adenosylmethionine (SAM) initiated methylation with resulting MMA or DMA that are excreted by the urine [88-90].

3.2.2 Uranium toxicity

Uranium is unique for its dual toxicity – chemical and radiological. But it has been determined that the adverse health effect of naturally occurring uranium and depleted uranium is primarily a result of its chemical rather than radiological character. Enriched uranium produced during the nuclear fuel cycle may pose ~50 times higher radiotoxicity than natural uranium and up to ~100 times higher radiotoxicity than depleted U [91-93].

The radiological toxicity of U is given by its concentration in the environment and by the isotopic composition. Chemical toxicity is closely related to uranium chemical speciation and the associated properties of U such as solubility, mobility and thus overall bioavailability for living organisms [94, 95].

The radiological toxicity of uranium is related to the emission of α (mostly) or β particles, or possibly γ rays during the decay of U isotopes. There are different decay series based on the initial U isotope, but the process generally continues through a series of radionuclides until reaching a stable, non-radioactive isotope of Pb [96]. From the point of view of the radiological impact of uranium on the organism, the emitted α particles as the most common ones, are hardly able to penetrate the outer layer of skin and do not constitute a hazard when emitted outside the body. But they may pose a risk after inhalation or ingestion of U resulting in DNA damage caused by direct ionization by the alpha particles or the indirect production of ROS [92, 97].

The chemical toxicity of uranium is given by its oxidation state. After entering the organism, uranium generally exists as a hexavalent uranyl ion which can enter the organism directly or is formed by oxidation of tetravalent uranium. Uranyl ion forms complexes with citrate or bicarbonate in blood or with proteins in plasma [91]. The most sensitive target organ of the chemical toxicity of uranium has been reported to be the kidney where uranium is released from bicarbonate, forms complexes with phosphate, and causes damage to the tubular wall [96, 98].

3.3 Analysis of trace elements in relation to their bioavailability

There are different approaches to the analysis of trace elements in the environment. From the fundamental determination of the total concentration of elements, over determining their speciation or fractionation, to the evaluation of their bioavailability. Knowing the concentration of trace elements in the environment represents only a part of the whole in terms of understanding their biological and geochemical interactions. The total concentration of trace elements is often a poor predictor of their bioavailability, toxicity, or reactivity [86]. Not only trace elements are distributed between particulate and dissolved phases in the aquatic environment but within the dissolved phase, trace

elements may exist as different chemical species that differ by their oxidation or electronic state, isotopic composition, and/or complex or molecular structure [66]. It is, therefore, crucial to gain comprehensive knowledge of the trace elements' speciation and their bioavailability for living organisms in order to assess the potential risk they may pose. For this reason, different approaches for analysis and evaluation of trace elements' speciation and bioavailability relevant for this work are presented in this chapter.

3.3.1 Sample pre-treatment for speciation analysis

Fractionation of analyte or group of analytes from a certain sample based on their physical (*e.g.*, size, solubility) or chemical (*e.g.*, bonding, reactivity) properties may be performed before speciation analysis. Filtration, ultrafiltration, and dialysis of water samples may be carried out to evaluate the distribution of trace elements between dissolved or particulate fractions occurring in the water column. This is usually done by a series of filtering through filters with different pore sizes and possibly from different materials. The fraction that does not pass through the filter with a pore size of 0.45 μm is generally considered a particulate phase. The colloidal fraction is separated by filters with pore sizes between 0.45 μm and 10 nm. The truly dissolved (labile) and potentially bioavailable fraction is usually separated by ultrafiltration, with the pore size corresponding to 10 kDa or less [66, 99, 100].

For fractionation of trace elements associated with the solid phase (sediments or soils), sequential extractions may be performed. Obtaining information about the leachability of elements from the solid phase may give a rough estimation of their potential mobility. Sequential extractions provide specific soil/sediment fractions of trace elements within the successive extraction steps which dissolve different sediment phases and extract elements associated with them. Total digestion of samples by strong acids (*e.g.*, HF, *aqua regia*) is generally used in the last step for the residual fraction as well as for the determination of total concentration. Generally, trace elements are distributed between water-soluble, acid extractable, reducible, and oxidizable fractions.

These can be also presented as (1) water-soluble, (2) exchangeable, (3) sorbed, (4) carbonate, (5) Fe and Mn oxides, (6) organic, (7) sulphide, and (8) residual fractions:

- (1) free or hydrated ions and weak complexes,
- (2) sorption by electrostatic attraction to negatively charged sites on colloid particles,
- (3) adsorption on specific sites of colloid particles (not exchangeable),
- (4) precipitation in soils with a high content of CaCO_3 , bicarbonate, and alkalinity,
- (5) adsorption on colloidal Fe/Mn oxides,
- (6) complexation with an organic fraction (chelated and/or organic bound),
- (7) highly insoluble and stable metal-sulphides compounds,
- (8) fixation within crystalline lattices of mineral (aluminosilicate) particles.

Nevertheless, various metals exhibit different distribution among these fractions and therefore the order of these groups may vary in the literature [65, 101-103]. Different protocols of sequential extractions have been used by researchers, but they are mostly modifications of the original protocols proposed by Tessier et al. [104] and by the Community Bureau of Reference (BCR) [105].

3.3.2 Speciation analysis of trace elements

Over the last few decades, the use of analytical methods has been enhanced to speciation analysis. The procedure of speciation analysis generally consists of direct detection of chemical species or their separation and subsequent detection by analytical instruments (**Fig. 3-7**). The choice of the analytical procedure depends on the nature of the analysed sample (*e.g.*, aqueous or solid samples), the species to be determined, required accuracy, sample volume, and cost [106].

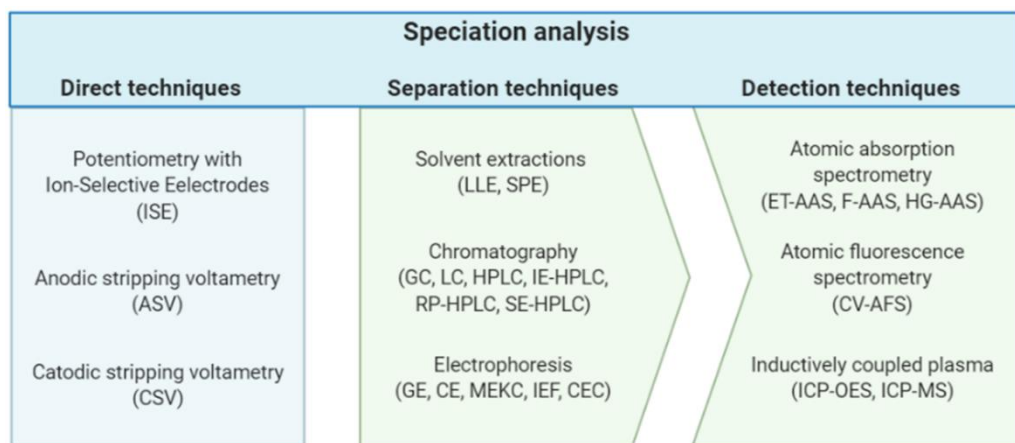


Fig. 3-7 Overview of selected analytical techniques used for elemental speciation analysis.

3.3.2.1 Direct techniques

Since the speciation of analytes may change during sampling, storage of the samples, or their pre-treatment, the ideal solution would be to perform a direct speciation analysis. Speciation analysis in natural waters may be carried out by direct techniques that do not require any additional separation method and can directly quantify the species. These are generally electrochemical techniques such as potentiometry with ion-selective electrodes (ISE) and voltammetry – anodic stripping voltammetry (ASV) or cathodic stripping voltammetry (CSV) [66, 83]. Electrochemical techniques are generally cheap, fast, and enable analysis *in-situ*. Potentiometry with ion-selective electrodes enables direct analysis of free metal ions in natural waters but its disadvantage lies in relatively high detection limits which are not suitable for analysis of trace concentrations in complex natural matrices. Voltammetry methods have on the other hand low detection limits and are therefore suitable for environmental analysis. Anodic stripping voltammetry enables the determination of not only free metal ions but also labile fractions of metals, *i.e.*, weak complexes that dissociate within their transport to the electrode surface. Analyses of these labile complexes which also contribute to the metal flux to the organism may thus provide valuable information regarding the bioavailability of trace elements [83, 107, 108]. However, electrochemical techniques do not achieve the same sensitivity and selectivity in comparison to the use of separation and detection

techniques as described in the following chapter. Nevertheless, voltammetry methods are particularly interesting due to their similarities with the DGT technique used in this work. Both techniques are measuring the diffusion flux of labile analyte species toward a device and thus the results of both approaches when applied simultaneously are generally well correlated [9, 109]. The differences between DGT and voltammetry results are related to the thickness of the diffusive layer. Since the contribution of complexes that can dissociate within their transport through the diffusive layer increase in direct proportion to the thickness of this layer, the DGT determined fraction is generally bigger [110-112].

3.3.2.2 Separation and detection techniques

Other techniques require the separation of species as the first step before analysis. The separation methods include solvent extractions (*e.g.*, liquid-liquid (LLE), solid-phase extraction (SPE)) [113] or analytical separation techniques such as liquid chromatography (LC), gas chromatography (GC), capillary electrophoresis (CE), and gel electrophoresis (GE) [114, 115]. Liquid chromatography is generally preferred before gas chromatography because GC requires a derivatization step inducing sufficiently volatile and stable compounds for analysis and may therefore influence the analyte speciation. High-performance liquid chromatography (HPLC) is nowadays frequently used with different separation modes such as ion-exchange (IE), reversed-phase (RP), or size-exclusion (SE) [114, 116]. Electrophoresis is then frequently used for the separation of species based on their charge (CE) or charge and size (GE). Capillary electrophoresis can use different modes – capillary zone electrophoresis (CZE), micellar electrokinetic capillary electrochromatography (MEKC), isoelectric focusing (IEF), or capillary electrochromatography (CEC) [66, 114, 117]. The choice of the technique is given by the physico-chemical properties (*e.g.*, size, shape, charge, oxidation state) of targeted analyte species. Moreover, the combination of two or more separation methods is sometimes necessary for the separation of chemical species [118].

After the separation procedure, the detection methods are used either combined (off-line) or hyphenated (on-line). Detection methods include spectral techniques such as

atomic absorption spectrometry with electrothermal (ET-AAS) or flame (F-AAS) atomization [66]. The main advantage of AAS lies in its lower operation costs and simplicity of its setup and run. However, it has generally higher detection limits, lower sensitivity, it only allows analysis of a single element per run and has a smaller operational range. Nevertheless, the atomic spectrometry techniques may also be coupled with the derivatization step of cold vapour generation (CV-AFS) or hydride generation (HG-AAS) which allow the speciation analysis of volatile metals (Hg) or metalloids (As, Se, Te, and others) with better detection limits [119-122]. However, nowadays the lowest detection limits or the widest range of use may be achieved using inductively coupled plasma with optical emission spectrometry (ICP-OES) or mass spectrometry (ICP-MS) (**Fig. 3-8**). Both techniques allow fast, robust, sensitive, and flexible analysis with the possibility of multi-elemental analysis. Moreover, the ICP-MS may be used for the isotopic analysis which is gaining importance for environmental monitoring of uranium and other elements [66, 114, 123, 124].

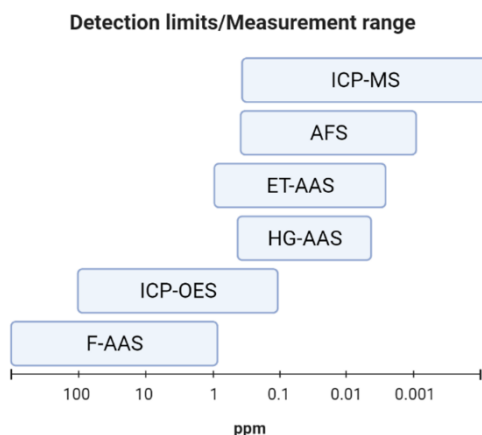


Fig. 3-8 Schematic comparison of detection limits/measurement range of selected analytical techniques used for elemental analysis (adapted from [125, 126]).

3.3.3 Modelling methods

The natural environment, either aquatic or terrestrial, is generally a very complex system and it may be therefore difficult to interpret the results obtained by instrumental analysis of environmental samples. The geochemical modelling by computer programs that

calculate solution equilibria allows to solve this problem and can provide valuable information to complement speciation analysis. There are several computer software such as MINEQL [127], MINTEQA2 [128], PhreeQC [129], CHESS [130], Geochemist WorkBench [131], MEDUSA [132], or WHAM [133]. The latter is unique for incorporating the humic-ion binding model and is, therefore, most commonly used as an input because it takes into account the complexation effects. The computer programmes work with specific databases containing thermodynamic and kinetic parameters. These are used together with concentrations of analytes or other parameters determined by analytical instruments as input. Based on the modelling code (set of mathematical equations describing chemical equilibria) the programmes produce results describing a geochemical model for a particular chemical system [134]. The codes used within the above-mentioned software generally perform the same type of calculation but the use of different thermodynamical databases may generate different results. The computer software tools commonly have their own databases, but they can be combined with others such as the database created under the Thermochemical DataBase (TDB) project from the Nuclear Energy Agency (NEA) within the Organization for the Economic Co-operation and Development (OECD) [135], the Lawrence Livermore National Laboratory (LLNL) thermodynamic database [136], ThermoChimie database [137], or PRODATA database [138], which is specifically dedicated to the modelling of uranium in mining-impacted environments. It is, therefore, crucial to compare the results of different databases to achieve objective information because the geochemical modelling is always dependent on the knowledge and experiences of each user.

Another modelling approach lies in utilizing equilibrium principles for the evaluation of potential bioavailability and toxicity of chemical species. Free Ion Activity Model (FIAM) [139] assumes that the free metal ion activity reflects its chemical reactivity and toxicity. But this principle assumption is its main disadvantage at the same time precisely because in this model the biological response of the organism to elements is related only to the free metal ions in the solution [140]. But some of the metal species are not able to react directly with the cell membrane surface and they are thus considered non-bioavailable in this model [78]. Therefore, another modelling approach called the Biotic Ligand Model (BLM) [141] was developed in order to overcome these limitations.

A biotic ligand refers to a biochemical receptor that binds metals on the surface of the cell membrane (*e.g.*, first described for fish gills) [142, 143]. The BLM then takes into account not only free metal ions but also weak metal complexes and competing ions that interact with the sensitive sites on the biological surface. The BLM model is therefore a complex combination of geochemical equilibrium principles, metal-organic binding models, and toxicological models.

3.3.4 Techniques evaluating bioavailability of trace elements

The aquatic environment is a dynamic system and the assessment of trace elements' bioavailability thus may be a challenging task. Modelling methods presented in the previous chapter only apply if full equilibrium exists in the environmental surroundings of the organism. The equilibrium is achieved only if the uptake of trace elements by the cell is relatively slow in comparison with the rate of metal diffusion outside the cell. In such a case, the metal bioavailability is controlled by its thermodynamics. But the rate of metal internalization by organisms may be faster in comparison with the metal diffusion in the solution. This would generate a concentration gradient around the cell surface and enable the weak metal complexes to dissociate within their diffusion and the bioavailability would be in this case controlled by kinetic factors [83, 112].

The techniques allowing the determination of bioavailability of trace elements in the aquatic environments have been developed and enhanced within the last few decades. The origin of these techniques is related to the research of sediment geochemistry and the development of the so-called peepers – passive samplers for the determination of solutes (originally phosphates and methane) in sediment porewater [144]. The compartments of the peeper sampler were filled with deionized water, covered by a dialysis membrane, and the peeper was inserted in sediment. After deployment to sediment, the equilibrium between solutes in porewater and water in the peeper was reached and so the dissolved chemical fraction in the porewater could be determined by analysis of the solution from the sampler [144-146]. The original design utilized quite big volumes of “sampling solution” in the peeper and therefore required a long time to reach equilibrium (*i.e.*, within weeks). However, the development of other techniques

inspired by this design followed, and the range of their use was broadened not only for the sediment analysis but also for application in natural waters [147].

The general principle of techniques evaluating the bioavailability of solutes (especially elements) is usually based either on the equilibrium processes or dynamic processes. Equilibrium-based samplers include for example diffusive equilibrium in thin films (DET), Donnan membrane technique (DMT), or the Gellyfish sampler. Samplers based on dynamic processes include the diffusive gradients in thin films (DGT), permeation liquid membrane (PLM), or the Chemcatcher sampler [16, 112, 148]. The principle of these selected techniques is briefly described in the following chapters with a focus on the DGT technique.

3.3.4.1 *Diffusive equilibrium in thin films*

The DET is a passive sampling technique and its principle is the same as of original peepers but utilizes hydrogels instead of compartments filled with water [149]. A thin layer of a hydrogel is covered by a membrane filter and solutes from porewater equilibrate with the non-bound water of the hydrogel layer. The hydrogel layer is very thin (~1 mm) and the equilibrium is thus reached faster. On the other hand, since the technique is based on equilibrium and the solutes are not pre-concentrated, it may be difficult to use DETs for the analysis of trace elements. It is therefore mostly used for the analysis of major elements such as Fe or Mn. The design of the plastic housing is similar to DGT probes used for sediment deployments but DET probes are constrained within small compartments in order to prevent vertical diffusion of the trapped metals. Their principles differ as well – while DET relies on establishing equilibrium between solutes in the solution and in the device, the DGT technique utilizes a binding layer where the solutes are progressively accumulated and thus measures their dynamic flux [145, 147, 148, 150, 151].

3.3.4.2 *Donnan membrane technique*

The DMT [152] originates from the Donnan dialysis method which is based on the equilibrium theory of electrolytes described already in 1924 by F.G. Donnan [153].

Its principle lies in selective dialysis of solutes between donor and acceptor solutions separated by a semi-permeable ion-exchange membrane. Regarding the nature of the used membrane, it allows the selective diffusion of anions or cations from one solution to the other. For metal analysis, the membrane carries a negative charge in order to allow the diffusion of positively charged free metal ions through the membrane until the equilibrium is reached [83, 154, 155]. Original designs by Helmke and co-workers [156] were limited by the small volume of acceptor solution that could have been insufficient for analysis, but the following designs solved this problem [152]. Nevertheless, similarly to DET, its application for speciation of trace elements is limited by the absence of analytes' pre-concentration [83]. Although it is mostly used for experiments under laboratory conditions, there is also a possibility to use DMT with specially designated cells for *in-situ* measurements [157-160].

3.3.4.3 Gellyfish sampler

The Gellyfish [161] is a passive sampler utilizing metal-binding resin with functional groups of iminodiacetic acid (IDA) embedded in polyacrylamide hydrogel. But even though the functional groups are identical to the most widely DGT utilizing resin (*i.e.*, Chelex-100®), the Gellyfish sampler is an equilibrium-based technique and does not determine the metal fluxes. The amount of the used resin is also relatively small compared to the DGT technique. The sampler is deployed in the water column until the equilibrium is reached and the concentration of metal accumulated in the resin is therefore corresponding to the concentration of free metal ions in the surrounding solution. The main disadvantage, a very long time required for the equilibration (~7 days), of the original sampler design was reduced to ~2 days by reducing the thickness of the hydrogel [148, 161-163].

3.3.4.4 Permeation liquid membrane

The PLM (also called supported liquid membranes (SLM)) was initiated for mimicking the process of metal transport through biological membranes [164]. The principle is based on the use of a carrier which mediates metal transport through a hydrophobic

membrane. This porous membrane consisting of a water-insoluble organic solvent with an organic carrier molecule selective for targeted metal is sandwiched between sample solution and a receiving (stripping) solution which contains a strong chelating agent allowing the pre-concentration of the analyte [83, 112, 165]. The PLM measurement may represent either concentration of free metals or all dynamic species based on the permeability of the membrane [166]. The technique is overall similar to DMT but surpasses it by shorter analysis time (1–2 h versus 2–3 days) and by the pre-concentration of metals which enables the analysis of trace concentrations of analytes [167]. As DMT, it is not a technique that would be commonly applied *in-situ* and is mostly used for analysis or simulative experiments under laboratory conditions. However, there are some designs such as hollow fibre permeable liquid membranes (HFPLM) which are suitable for *in-situ* analysis as well [168].

3.3.4.5 Chemcatcher sampler

The Chemcatcher [169] has a similar design to Gellyfish sampler or DGT technique but it is a dynamic-based passive sampler, therefore more alike to the latter one. The Teflon housing consists of two watertight parts which enclose a receiving phase (for analysis of metals it is mostly a 47 mm C18 Empore™ chelating disk) and a diffusion-limiting membrane (cellulose acetate). Solutes diffuse across the membrane and are accumulated on the receiving phase and their mass is subsequently analysed. Although the principle of the technique is the same as of DGTs, the approach to their calibration and therefore data interpretation is different. While the DGT-determined concentration of analytes is calculated from the mass accumulated on the binding phase using laboratory determined diffusion coefficients, the Chemcatcher uses metal-specific uptake rates for calculations. Nevertheless, both techniques are able to provide the time-weighted average (TWA) concentrations of labile fractions of analytes [163, 170-173].

3.4 Diffusive Gradients in Thin films technique

The Diffusive Gradients in Thin films (DGT) technique was developed by Zhang and Davison in 1994 and used for the first time as a passive sampler for evaluation of Zn labile fraction in seawater [5]. Ever since the DGT technique has been most frequently used by many researchers for the determination of divalent metal ions (*i.e.*, Cd, Co, Cu, Ni, Pb, Zn) [110, 174] but its application has also been broadened to the evaluation of nutrients [175-178], radioactive elements [179-184], platinum group elements [185-187], oxyanions [188-191], or rare-earth elements [192, 193]. It has also been frequently used for the determination of various organic compounds such as antibiotics, bisphenols, endocrine disruptors, household and personal care products, illicit drugs, nitrochlorobenzenes, organophosphate flame retardants, pesticides and herbicides, perfluorinated compounds, and pharmaceuticals [194]. The nature of its application has also expanded from various aquatic environments (*i.e.*, freshwater, seawater, brackish water of estuaries, wastewaters) to sediments or soils where the labile fluxes of analytes from porewater have been determined, but also to other unusual matrices such as fish or soy sauces [195, 196]. Among the other techniques used for the evaluation of trace elements bioavailability mentioned in the previous chapters, the DGT is one of the most widely used [145]. By the time this thesis was being prepared, more than 1,444 papers could be found in the Web of Science Core Collection under the keyword “diffusive gradients in thin films”.

3.4.1 Principle of the DGT technique

The standard DGT design consists of two layers – a binding layer and a diffusive layer. The binding layer is most commonly a hydrogel incorporating a binding phase (sorbent) in its structure, which selectively binds an analyte or a group of analytes. This layer is by many researchers referred to as a resin gel because the original, and up to date the most frequently used DGT design, utilized Chelex-100 resin. But nowadays, the binding layer may utilize another type of sorbents besides resins as well (*e.g.*, nanoparticles). The binding layer is covered by a diffusive gel and a membrane filter which together form

concentration gradient of the analyte is generated within the diffusive layer. This steady-state flux of the analyte toward the binding layer is created only if the analyte is bound rapidly, strongly, and irreversibly by the binding phase and therefore the analyte concentration approaches zero on the interface of the diffusive and binding layer. But this situation applies only if the analyte is fully labile and thus generally describes the course of accumulation of free metal ions (M^{Z+}). In the case of metal complexes with ligands (ML), the dissociation of these complexes may take place during their diffusion through a diffusive layer. Based on the dissociation rate it is possible to recognise fully labile, partially labile, and inert metal complexes (**Fig. 3-9B**) [5, 147, 197, 199]. After deployment, the total accumulated mass of the analyte is determined by its elution (usually by strong acid) from the binding layer and subsequent analysis of the analyte concentration in the eluate by analytical technique (*i.e.*, AAS, CV-AFS, ICP-OES, ICP-MS). Elution protocols differ according to the nature of the binding layer and so the choice of the analytical technique varies based on the targeted analyte.

Since the accumulated mass of analyte (M , ng), the time of the deployment (t , s), and the area of the DGT device that has been exposed to the solution (A , cm²) are known, the flux of the analyte (J , ng cm⁻² s⁻¹), can be calculated using **Eq. 1**.

$$J = \frac{M}{A * t} \quad (1)$$

The metal transport through the diffusive layer is also controlled by Fick's law, where the flux of the analyte is proportional to the analyte concentration in the solution (c_{SOL} , µg L⁻¹), the diffusion coefficient of the analyte (D , cm² s⁻¹), and inversely related to the thickness of the diffusive layer (Δg , cm) **Eq. 2**.

$$J = \frac{c_{SOL} * D}{\Delta g} \quad (2)$$

Both relations combined together result in **Eq. 3**, which is used for the calculation of the so-called DGT-measured concentration (c_{DGT} , µg L⁻¹) of the analyte, which depending on the conditions, may not equate to c_{SOL} , because in a complexing environment, some of the occurring metal complexes may be partially labile or even

inert as described previously. In such a case, the c_{DGT} would appear to be lower in comparison to c_{SOL} .

$$c_{DGT} = \frac{M * \Delta g}{D * A * t} \quad (3)$$

The Δg in this equation is related to the thickness of the material diffusive layer (MDL), also referred to as δ^{MDL} in the literature, consisting of the diffusive gel and membrane filter. Nevertheless, when deploying DGTs under field conditions it is important to also consider the diffusive boundary layer (DBL) which is a layer adjacent to the surface of the DGT device where there is effectively no flow. The higher the solution flow is, the thinner the created DBL. Therefore, the thickness of the DBL layer (δ^{DBL}) should be estimated and added to the Δg to achieve sufficient accuracy of the measurement, especially when the DGTs are deployed in stagnant waters (*e.g.*, lake, groundwater) [5, 147, 194, 198, 200]. The procedure of estimation of the DBL is described in **Chapter 4.3.4**.

Another very important variable in the calculations is the diffusion coefficient which describes the diffusion rate of the solute through the diffusive layer and is generally lower than the diffusion coefficient in water. It is usually experimentally determined in a simple solution under laboratory conditions when a new technique is developed or when the DGTs are deployed in a specific and complex matrix. The diffusion coefficients are temperature-dependent and therefore, the measurement of the temperature during the DGT deployment is a crucial factor in order to obtain accurate results [198, 201]. The procedure of evaluation of the diffusion coefficient and its adjustment to temperature is described in **Chapter 4.3.3**.

3.4.1.1 Diffusive layer

Diffusion-limited separation of labile metal species is achieved within their transport through the diffusive layer. Even though the contribution of the DBL in the solution also contributes to the total thickness of the diffusive layer, for the purpose of this chapter, only the material part of the diffusive layer is considered. The material diffusive layer

consisting of the diffusive hydrogel and membrane filter is a key element for the DGT performance [83, 201].

The membrane filter covering the diffusive gel is usually commercially available cellulose nitrate, cellulose acetate, polyvinyl fluoride (PVFD), or polyethersulphone (PES) membrane. These have defined pore size, commonly 0.45 μm , and therefore prevent the interaction of the particulate fraction with the diffusive gel. The thickness of the membrane filter (usually ~ 0.013 cm) contributes to the total Δg . The main purpose of the filter membrane is to protect the diffusive gel. During long-term deployment in natural water, the biofilm may be formed on the filter surface and thus affect the DGT performance. Therefore, some researchers applied protective impregnation (antibiotics, Cu, and Ag) or additional membrane (polycarbonate) to prevent biofouling [83, 194, 202, 203].

The diffusive gel is characterized as a hydrogel having properties between solid and liquid. It contains over 95% of free water (just a minimum fraction of water is bound in the three-dimensional polymer chains structure) that represents an available medium for the diffusion of the solutes. The DGT diffusive gel is generally prepared as agarose (AG), agarose cross-linked polyacrylamide (APA), or bis-acrylamide cross-linked polyacrylamide gel (also called restricted gel (RG)) [201]. Different diffusive gels are being used for different purposes. The main assumption of diffusive gel is its inertness toward the targeted analyte. For this reason, agarose diffusive gel is preferred over APA gel for analysis of mercury since it can be significantly bound by the APA gel [204–206]. The RG gel has generally smaller pore size (< 1 nm) compared to the APA gel (5–20 nm) and therefore enables the determination of free metal ions and small inorganic complexes only. Simultaneous deployment of DGTs with RG and APA diffusive gels is thus used for the *in-situ* distinction between inorganic metal species and metal complexes with larger organic ligands (*i.e.*, humic acid). For comparison, the agarose gel has an approximate pore size of 35–47 nm. However, the pore size may vary depending on the ratio of reagents used during gel preparation. The mentioned pore sizes are relevant for 1.5% agarose gel and APA gel prepared with 15% acrylamide and 0.3% agarose-derived cross-linker [201, 207, 208]. In this work, APA diffusive gel (for preparation protocol see **Chapter 4.2.1**) combined with PES or PVFD membrane filters

were mostly used. The agarose gels were used for the preparation of gels for arsenic speciation.

Besides the hydrogel diffusive layer, other phases have been used by some researchers such as cellulose acetate dialysis membrane (in the combination with liquid binding layer) [209], Nafion-coated cellulose acetate membranes [210, 211], Nafion membrane [212], or chromatographic paper [213-215].

3.4.1.2 Binding layer

The key assumption for a good binding phase is that it binds the analyte rapidly, strongly, and irreversibly and that its sorption capacity is sufficient for analyte uptake and does not become saturated within the deployment of DGTs. In general, the most common binding phases are polyacrylamide/agarose-based hydrogels incorporating a sorbent (*i.e.*, resin or synthesized micro- or nanomaterials). There have also been reported other binding phases such as liquid binding phase with nanoparticulate Fe_3O_4 (for As measurement) [216], polymer-bound Schiff base (for Cu, Cd, and Pb) [217], sodium polyacrylate (for Cd and Cu) [218], poly(4-styrenesulphonate) (for Cd and Cu) [219], or poly(ethyleneimine) (for Cu, Cd, and Pb) [220]. However, the first and most frequently used binding layer consists of a polyacrylamide hydrogel utilizing Chelex-100 chelating resin as a binding phase. This resin is selective for transition metals over alkali and alkaline earth metals and is therefore broadly used for the determination of divalent metals such as Cd, Co, Cr, Cu, Fe, Mn, Ni, Pd, or Zn [174, 221, 222]. Nevertheless, this resin is generally not suitable for the determination of arsenic since it is present in an anionic or neutral form in aquatic environments under oxic conditions. Similarly, uranium predominantly occurs in a neutral or anionic form of free uranyl ion or the most common carbonate complexes in the solutions with the $\text{pH} > 4$ (see **Fig. 3-2** and **Fig. 3-4**). Therefore, other binding phases are usually used for the determination of these two elements. The overview of the binding phases used for the determination of As and U, and therefore relevant for this work, can be found in **Table 3-1**.

Table 3-1 Overview of binding phases used for analysis of arsenic or uranium by the DGT technique.

Targeted analyte	Binding phase	Ref
Arsenic	Activated carbon	[223]
	Amberlite IRA 910	[224]
	Cerium dioxide	[225]
	Ferrihydrite (Fh)	[226, 227]
	Iron hydroxide	[228]
	Metsorb	[176, 229]
	Nanoparticulate Fe ₃ O ₄ (Fe ₃ O ₄ NPs)*	[216]
	Nanoparticulate lanthanum oxide (nano-La ₂ O ₃)	[191]
	Mixture of sulphonated and phosphonated cross-linked polyethylenimine (SCPEI-PCPEI)	[230]
	Titatium dioxide	[231]
	Zinc ferrite (Zn-ferrite)	[232]
	Zirconium dioxide	[233, 234]
	3-mercaptopropyl-functionalized silica (3-MFS)	[235]
Uranium	Chelex-100	[236, 237]
	Diphonix	[238]
	Dowex 2×8-400	[239]
	Manganese dioxide	[240]
	Metsorb	[241]
	Dow-PIWBA	[242]
	Spheron-Oxin	[243]
	Whatman DE 81	[236]

*Liquid binding phase.

A number of resins have been used as the DGT binding phase for the determination of arsenic. In a recent work of Gorny, et al. [244], a comparison of five binding phases for As (Fh, Metsorb, Zn-ferrite, and ZrO₂, 3-MFS) was performed, showing that all of them are possibly providing similar results in oxic freshwater and seawater over a wide

range of pH (5–9) for deployment period over 96 h for. While most of the resins are used for the measurement of total As concentration, the DGTs utilizing the 3-MFS or Amberlite IRA 910 sorbents determine As^{III} and As^V, respectively. Therefore, the deployment of DGTs utilizing the 3-MFS or Amberlite IRA 910 binding layers alongside some other sorbent determining total As concentration (*e.g.*, Metsorb), provide a speciation analysis of inorganic As species [224, 235]. Some researchers have also used a mixed binding layer (MBL) in order to improve the DGT performance or to simultaneously analyse labile forms of arsenic together with other analytes (*e.g.*, metals, oxyanions, sulphide, phosphate) by combining Fh–Chelex-100 [245], Metsorb–Chelex-100 [246], ZrO₂–Chelex-100 [247], AgI–Fh [248], AgI–ZrO₂ [249], ZrO₂–SPR-IDA (suspended particulate reagent-iminodiacetate) [250].

Regarding U determination, many studies revealed that the performance of Chelex-100 may be hampered in a complex environment with a high concentration of competing ions such as Ca or Mg, (*i.e.*, mining-impacted environment or seawater) [180, 240, 241]. Therefore, other binding phases are usually used for U analysis (see **Table 3-1**). The same MBL of AgI–Fh that has originally been used for the analysis of P, V, As, and S [248] was subsequently used even for the determination of Mo, Sb, W, and U [25]. An extensive evaluation by *in-situ* applications of selected binding phases for the determination of uranium has been carried out by Husson et al. [22], Pedrobon et al. [251], or Drozdak et al. [252]. Nevertheless, up to date, there is no DGT binding phase for simultaneous determination of As and U.

3.4.2 Application of the DGT technique

The main advantages of the DGT technique are the ability to pre-concentrate the analytes *in-situ*, the elimination of the potential adverse effect of the solution matrix on the analytical procedure, the provision of the time-weighted average concentration of the analyte over long time periods (in the scale of days to weeks), and the evaluation of the analyte bioavailability to biota [253]. The DGT is therefore broadly used for the analysis of trace elements, it is applied in an environment where the direct sampling is

complicated due to the matrix nature (*e.g.*, seawater), or for long-term monitoring purposes.

The DGT technique is also frequently used for elemental speciation analysis in natural waters and its performance is often combined with the filtration and ultrafiltration techniques. Discrete grab water samples are usually processed by filtration (0.45 μm or 0.22 μm pore size) to distinguish between the particulate and dissolved fractions. The additional ultrafiltration through various filters of different pore sizes (*e.g.*, 500 kDa, 100 kDa, 10 kDa, 1 kDa) may be performed and the analysed fractions of the element are compared with the DGT-labile concentration. In general, the fraction passing through the 100 kDa or 10 kDa is recognized as a truly dissolved fraction (labile) and is sometimes used to reflect the bioavailability of metals and thus should correlate with the DGT results. However, the ultrafiltration methods have some disadvantages compared to the DGT technique due to:

- 1) providing a concentration of single grab sample vs. time-weighted average concentration,
- 2) sample transport and storage vs. *in-situ* conservation of analytes,
- 3) complicated procedure vs. relatively simple handling.

Moreover, the fractions obtained by ultrafiltration are only discriminated by their size while the DGT-determined fraction also includes the metal complexes which are able to dissociate within their diffusion. Nevertheless, the combination of both techniques provides valuable knowledge about the lability and potential bioavailability of trace elements in the aquatic environment [10, 252, 254-257].

Since the principle of the analyte uptake by DGT is very similar to the uptake of elements by biological cells of a living organism (see similarities between **Fig. 3-6** and **Fig. 3-9B**), there are several studies dedicated to the investigation of the potential of the DGT technique to mimic and possibly predict the accumulation of trace elements to biota. Most of these studies are dealing with the bioavailability of trace elements in soil-plant systems by a comparison of the concentrations accumulated in plant parts with the DGT-determined concentration [258, 259]. Other researchers used the DGT technique to mimic the bioavailability of metals from soils to invertebrates [260, 261]. Nevertheless, only a few studies are dealing with such an investigation in the aquatic

environment. Uptake by aquatic organisms is probably more often under the control of the analyte internalization through the cell membrane. In cases where the uptake is under diffusion control (*i.e.*, microorganisms), the actual thickness of the diffusive layer is much thinner compared to the diffusive layer in the DGT technique, and therefore the metal uptake by biota in water is probably more correlated with the performance of voltammetry electrodes [110]. However, some studies indicate that DGT-labile concentration of some elements (Hg, Al, Cu, Cr, Ni, Zn, Cd, and Pb) correlates with the concentration determined in input organs (gills, skin, scales, or eyes) of fish, in clams, or freshwater snails [13, 262-266]. Moreover, the DGT technique was also used in *in vitro* unified barge method (UBM) solution to predict the metals (Pb, Zn, and Cu) bioaccessibility through the intestine in the human body [267-269].

4 MATERIALS AND METHODS

4.1 Reagents and chemicals

Since the experimental part of this thesis was carried out within two research facilities of both universities, the amount of used material was enormous. For this reason, the usual list of all reagents and chemicals is not presented as each chapter devoted to research results is supplemented by a precisely specified list of used material. Overall, the used reagents and chemicals were of analytical reagent grade or higher.

4.2 Protocol for preparation and processing of DGT

The basic premise for working with the DGT technique is to work in a clean environment so that the results are not distorted by cross-contamination. This includes the use of personal protective laboratory equipment and the work in a clean laboratory. All the used plastic equipment and glassware necessary for the manufacturing of DGT gels and containers for experimental deployment solutions were always pre-cleaned in 10% (v/v) HNO₃ for at least 24 h and thoroughly rinsed with Milli-Q water ($> 18.2 \text{ M}\Omega \text{ cm}^{-1}$ Millipore, USA).

4.2.1 Preparation of diffusive and resin gels

For the preparation of agarose cross-linked polyacrylamide (APA) diffusive gels that were used within this work, it is necessary to prepare the gel solution first. This consists of 15% of acrylamide, 0.3% (v/v) of DGT agarose-derived cross-linker, and Milli-Q water. The gels were prepared by polymerizing the gel solution by the initiator and catalyser of the polymerization reaction, which are typically ammonium persulphate (APS) and N,N,N',N'-tetramethylethylenediamine (TEMED). When preparing the APA diffusive gels, 10 mL of gel solution was mixed with 70 μL of freshly prepared 10% (w/v) APS and 25 μL of TEMED according to the protocol described in the literature [270]. The agarose-based (AG) diffusive gels were only used for DGTs utilizing 3-MFS

and were prepared by dissolution of agarose in Milli-Q water (1.5% solution) at 80 °C [271].

For the preparation of resin gels, the appropriate amount of sorbent was added to the gel mixture as well. Different types of resin gels require different pre-treatment and different ratios of polymerizing agents in order to obtain the best gel structure, which should be strong, flexible, and elastic with the uniform distribution of sorbent particles. The Diphonix, Dow-PIWBA, Lewatit FO 36, and Metsorb resins were ground (in a mortar grinder or by Pulverisette Type 02.102, Fritsch, Germany) and sieved on Teflon sieve (50 µm). Only the 3-MFS resin gels were prepared in AG according to protocol by Pommier et al. [272]. The ratios of used sorbents and polymerizing agents used for resin gels prepared within this work are presented in **Table 4-1**.

Table 4-1 Preparation protocol of resin gels (reagents used per 10 mL of gel solution).

	Resin (g)	10% APS (µl)	TEMED (µl)
3-MFS* [207]	1	-	-
Chelex-100 [270]	4	50	15
Diphonix [180]	2	360	90
Dow-PIWBA [242]	2	300	120
Lewatit FO 36 [273]	1.25	240	120
Metsorb [229]	1	60	15

*The 3-MFS resin gel was prepared in agarose and thus no APS and TEMED were added.

After thorough stirring, the gel solution was slowly cast between two glass plates separated by the plastic spacer of the thickness of 0.050 cm or 0.025 cm for the diffusive and resin gel, respectively, and enclosed by clips. If bubbles occurred, they were removed by gentle pressure on the glass while held in a vertical position. Glass plates were then placed in the preheated oven at approximately 40–45°C for 1 h or longer until the gel was formed. Polymerized gel sheets were then removed from the glass plates and let hydrated in Milli-Q water for at least 24 h with several changes of the water (at least three times in the case of diffusive gels, minimum once in the case of resin gels). The use of well-defined spacers resulted in a thickness of 0.08 cm and 0.04 cm of the

diffusive and resin gels, respectively, after hydration. The thickness of diffusive gel can be modified by combining the spacers (*e.g.*, for the purpose of determination of the DBL as described in **Chapter 4.3.4**). Hydrated gel sheets were cut using a plastic circle cutter (diameter 2.5 cm) or Teflon coated razor blade (for the appropriate size of gel strip for sediment probes). Diffusive gels were stored in 0.01 M NaNO₃ and resin gels in Milli-Q water at 4 °C prior to use. Since the APA gel-type was majorly used in this work, an illustrative scheme of the APA resin gel production is shown in **Fig. 4-1**.

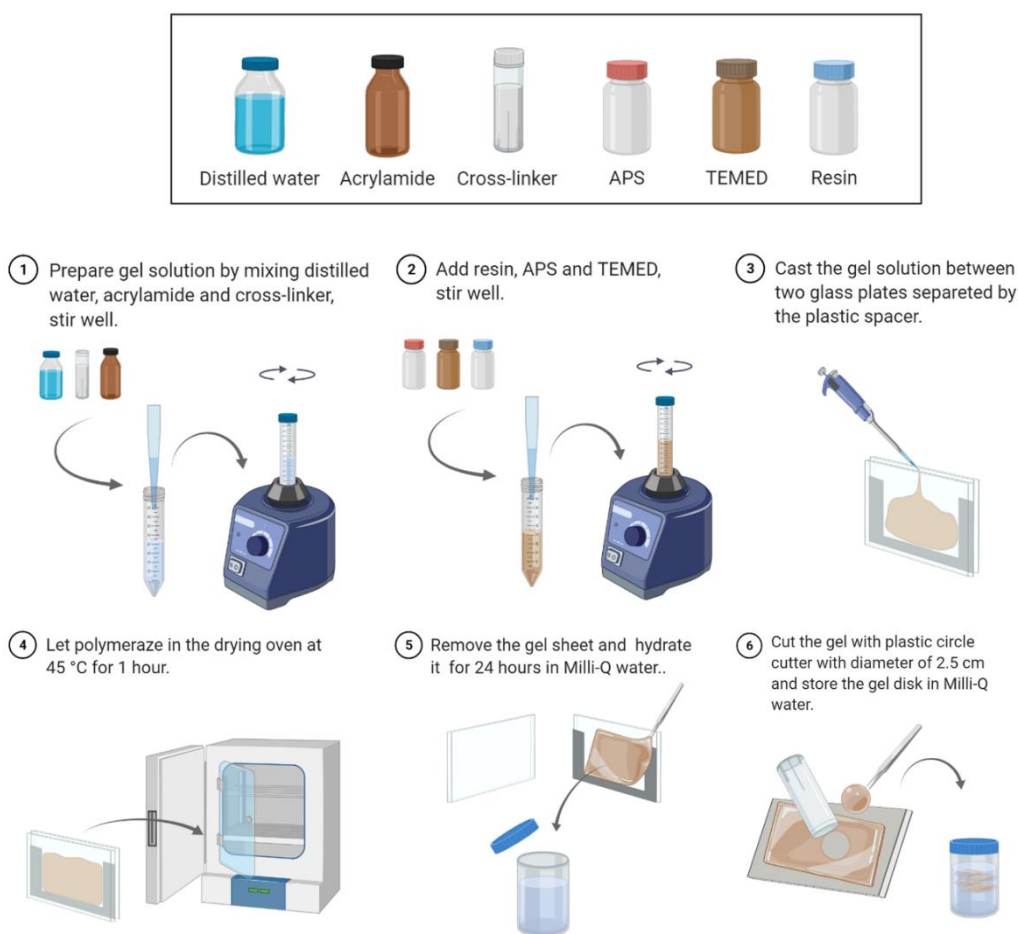


Fig. 4-1 Illustrative protocol for preparation of the DGT APA resin gel (created with BioRender.com).

4.2.2 DGT assembly and deployment

DGT pistons and probes (DGT Research Ltd., UK) with an exposure window of 3.14 cm² and 27 cm², respectively, designed for water and sediment deployment were used in this work. Polyethersulphone (PES) Supor® 450 (Pall Corporation, USA) or polyvinyl fluoride (PVDF) Durapore® (Merck, Germany) membrane filters of 0.45 µm pore size were pre-cleaned in 5% (v/v) HNO₃ for 24 h and thoroughly rinsed with Milli-Q water prior to use. The DGT plastic housings were loaded with resin gel disc, covered by diffusive gel and membrane filter, and enclosed by a cap with an exposure window. Assembled DGT units were stored at 4 °C in zip-lock bags and kept moisturized with a few drops of 0.01 M NaNO₃ prior to deployment. The sediment probes were deoxygenated by purging in a 0.01–0.1 M NaCl (depending on the salinity of the environment) for at least 4 h prior to deployment.

For laboratory experiments (*e.g.*, determination of diffusion coefficients or investigation of the influence of the external factors on the DGT performance), the DGT units were loaded into Perspex holder and deployed in plastic or glass containers with the deployment solution under constant stirring (**Fig. 4-2A**). When deploying DGTs *in-situ*, the units were either tied together with the fishing line or loaded into Perspex open plates and eventually enclosed into filter tubes or plastic cages to avoid their damage during deployment. To ensure the placement of DGTs in the well-defined depth of the water column, the device was attached by ropes either to the two sticks that were pushed in the sediment (**Fig. 4-2B**) or to the buoy (**Fig. 4-2C**) on top and to the weight or anchor on the bottom. For sediment deployment, the probes were either deployed in the sediment core that was taken in the plexiglass tube (in deep seawater) or directly pushed in sediments (in rivers) (**Fig. 4-2D**).

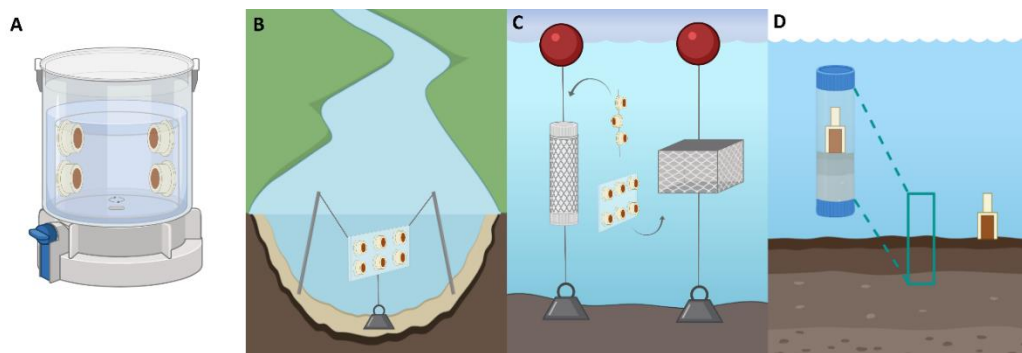


Fig. 4-2 Schematic illustration of DGT deployment method when performing laboratory experiment (A) or when applied *in-situ* in streams (B) or deeper water of lake or sea (C) and deployment of DGT probes in sediments (D) (created with BioRender.com).

Whether deploying DGTs under laboratory conditions or *in-situ* the exact time of deployment was always recorded. At the same time, the crucial physico-chemical parameters of water (*i.e.*, temperature, pH, Eh, dissolved O₂, conductivity, and salinity) were measured. Point samples of deployment solution or natural water for the analysis of total or dissolved trace metals were collected at the beginning and end of each deployment. When analysing the dissolved fraction of trace metal concentration, the samples were filtered through 0.45 µm membrane syringe filters first and acidified to 1% HNO₃. After retrieving, the DGTs were rinsed with Milli-Q water and stored in zip-lock bags at 4 °C until disassembling in the laboratory.

4.2.3 Elution of the resin gel

The DGT pistons were dismantled by cracking the cap by twisting the screwdriver in the groove of the outer sleeve or removing the cap with a knife. The resin gel disc was rinsed with Milli-Q water and placed in the clean tube. In the case of sediment probes, the gel strips were sliced by Teflon coated razor at 0.5–1 cm interval and placed in the clean tube. The reagents used for the elution of each type of resin gel together with the optimized elution procedures are described in **Table 4-2**. After elution, the samples were diluted ten times by Milli-Q water or 2% HNO₃ (in the case where elution reagent was not an acid), centrifuged if necessary, and stored at 4 °C until analysis by AAS or ICP-MS (see **Chapter 4.4**).

Table 4-2 Elution protocols for resin gels used within this work.

Resin gel	Reagent	Volume ^a	Elution procedure
3-MFS [235]	1 M HNO ₃ + 0.01 M KIO ₃	1 mL	LT*, 24 h
Chelex-100 [270]	1 M HNO ₃	1 mL	LT, 24 h
Diphonix [180]	1 M HEDPA**	1 mL	LT, 24 h
Dow-PIWBA [242]	conc. HNO ₃	1 mL	70 °C, 24 h
Lewatit FO 36 [273, 274]	0.17 M NaCl + 0.25 M NaOH ^b / 1 M NaOH ^c	10 mL ^b / 5 mL ^c	MW extraction ^{b***} / 70 °C, 24 h ^c
Metsorb [229]	1 M HNO ₃	1 mL	LT, 24 h

* LT – Laboratory temperature (20 °C)

** HEDPA – 1-hydroxyethane-1,1-diphosphonic acid

*** Microwave extraction – 130 °C, 16 min

^a The eluent volume per gel disc. Half the volume of eluent was used for the extraction of gel slices from sediment probes.

^b Original extraction protocol followed by analysis by modified ET-AAS method [273].

^c Optimized extraction protocol suitable for ICP-MS analysis [274].

4.3 Laboratory experiments for DGT characterization

When developing a new DGT technique, it is always necessary to perform thorough laboratory testing for its characterization. Therefore, the experimental designs for uptake and elution efficiency, determination of the sorption capacity, diffusion coefficients, and estimation of the diffusive boundary layer are described in this chapter.

All DGT tests were performed at laboratory temperature (18–22 °C) using plastic or glass containers of 2 or 3 L volume. The deployment solution generally consisted of 0.01 M NaNO₃ spiked with the investigated analyte, As and/or U, and eventually enriched with other compounds whose influence on sorption was evaluated. The deployment solutions were prepared 24 h prior to DGT deployment so that the solution was equilibrated. The solutions were stirred well (500–800 rpm) during the whole experiment. All experiments were performed with at least two replicates of resin gel discs or DGT units.

4.3.1 Uptake and elution efficiency

A single resin gel disc was immersed into a small volume (10–20 mL) of deployment solution spiked with As and/or U for 24 h. The samples of the solution were taken at the beginning and end of the experiment and the concentration of the investigated analyte was determined by analytical method (AAS/ICP-MS). The uptake efficiency was expressed as the uptake factor (f_u), which was calculated using the **Eq. 4** from the difference between initial mass (M_i) and remaining mass (M_r) of the analyte in the solution.

$$f_u = (M_i - M_r)/M_i * 100\% \quad (4)$$

The resin gel disc that was retrieved from the deployment solution was rinsed with Milli-Q water and immersed in a tested elution reagent. Different reagents and their mixtures were tested in the combination of different volume and extraction temperatures. The mass of analyte eluted from the gel (M_e) and the mass accumulated on the gel disc (M_a , which equals to the $M_i - M_r$ difference) were used for calculation of the elution factor (f_e) using the **Eq. 5**.

$$f_e = (M_e/M_a) * 100\% \quad (5)$$

4.3.2 Sorption capacity of the resin gel

A single resin gel disc was immersed into the series of deployment solutions spiked with increasing concentration of a single-element standard solution. After 24 h, the gel discs were removed from the solution, rinsed with Milli-Q water, and eluted. The mass of the analyte eluted from the gel and analysed by analytical technique was plotted versus the concentration in the deployment solution. The resulting adsorption isotherm describes the course of analyte accumulation, and the total sorption capacity of resin gel is determined at the point where the adsorption equilibrium is reached. The linear part of the adsorption isotherms is then recognised as the effective sorption capacity of the resin gel.

4.3.3 Determination of the diffusion coefficient

Diffusion coefficients of As towards tested resin gel were determined by time-dependence experiment. The DGT units were deployed in the spiked deployment solution and at least 2 replicates were removed after certain time intervals and the resin gels were eluted. The diffusion coefficients (D , $\text{cm}^2 \text{s}^{-1}$) were calculated from the slope (s) of the linear regression of the analyte mass accumulated on resin gel (M , ng) as a function of time using **Eq. 6**, where Δg is the thickness of diffusive layer consisting of diffusive gel (0.0080 cm) and membrane filter (0.013 cm), A is the exposed area (3.14 cm^2), and c is the concentration of analyte in the solution measured in a grab sample ($\mu\text{g L}^{-1}$). Obtained diffusion coefficients (D_T) determined in the solution of the temperature T ($^{\circ}\text{C}$) were corrected to reference temperature T_{ref} (25°C) and expressed as $D_{T_{ref}}$ using the Stokes-Einstein relation (**Eq. 7**) [275].

$$D = \frac{s * \Delta g}{A * c} \quad (6)$$

$$\log D_T = \frac{1.37023(T - T_{ref}) + 8.36 * 10^{-4}(T - T_{ref})^2}{109 + T} + \log \frac{D_{T_{ref}}(273 + T)}{(273 + T_{ref})} \quad (7)$$

4.3.4 Estimation of the diffusive boundary layer

Where applicable, the thickness of the diffusive boundary layer was estimated by deploying the triplicate of DGTs with three different thicknesses of diffusive gels (0.04, 0.08, and 0.12 cm) into the solution for 24 h. The DBL (δ^{dbl} , cm) was calculated by dividing the intercept (y) by the slope (s) of a linear regression of the reciprocal analyte mass accumulated on resin gel ($1/M$) as a function of the diffusive layer thickness (Δg , cm). The **Eq. 8**, where D_w and D_{gel} are diffusion coefficients of the analyte in water and in the diffusive gel, respectively, was used for calculation [7]. Since the DBL represents an extension of the diffusive layer thickness, the analyte concentration determined by DGT (c_{DGT} , $\mu\text{g L}^{-1}$) is then calculated using **Eq. 9**, where the total diffusive layer is represented by the combination of the material diffusive layer (diffusive gel and

membrane filter, Δg also referred to as δ^{dbl} in the literature) and diffusive boundary layer (δ^{dbl}).

$$\delta = \frac{y}{s} * \frac{D_w}{D_{gel}} \quad (8)$$

$$c_{DGT} = \frac{M * (\Delta g + \delta^{dbl})}{D * A * t} \quad (9)$$

4.4 Analytical methods

Because this work was created at laboratories of two partner universities, different analytical instruments were used for the analysis of studied trace elements. The atomic absorption spectrometer 280Z AA with electrothermal atomization (ET-AAS, Agilent Technologies, USA) and Zeeman background correction was mainly used within the first part of this work dealing with the development of new resin gel for the determination of arsenic. The development of a novel ET-AAS method for arsenic determination in these gels is described in the next **Chapter 4.4.1**. For the uranium analysis or simultaneous analysis of uranium and arsenic, high-resolution sector field inductively coupled plasma mass spectrometry (SF-ICP-MS, Element II, Thermo Fisher Scientific Bremen GmbH, Germany) was used. For instrumental parameters of As and U analysis by SF-ICP-MS used in this work see **Chapter 12.2**. The analyses were overall performed by optimized methodologies with instrument setups that were validated by both laboratories in the long term. The accuracy of sample analysis was regularly verified by the analysis of reference samples (river water – SLRS-6, National Research Council Canada; surface water level 2 – SW2, Spectrapure Standards AS, Norway; trace elements and methylmercury in estuarine sediment – IAEA-405, International Atomic Energy Agency, Austria). The concentrations of analysed elements in these reference materials were generally within the range of 10% of the certified values.

4.4.1 Modified ET-AAS method for the determination of arsenic in solution with a high concentration of chlorides

Smolíková, V., Pelcová, P., Hedbávný, J., Zlámalová, L., Ridošková, A. Modification of electrothermal atomic absorption spectrometry for determination of arsenic in high salinity samples. In: MendelNet 2018: Proceedings of International PhD Students Conference, Brno, 2018, Vol. 25, pp. 527-531.

A novel ET-AAS method for arsenic determination in samples containing high chloride concentration was proposed because the DGT resin gel for evaluation of arsenic that was developed within this work (**Chapter 5.1**) required a highly concentrated mixture of NaOH and NaCl (0.25 M and 0.17 M, respectively) for elution.

Analysis of trace elements in samples with the chloride-rich matrix is generally challenging because of the interference effects. When ICP-MS is used, high chloride concentration can cause polyatomic ion interferences by generating $^{40}\text{Ar}^{35}\text{Cl}^+$ that has the same m/z ratio as ^{75}As [276, 277]. Analysis of arsenic by ET-AAS is then particularly complicated due to the volatility of this element. The loss of arsenic content may occur during the pyrolysis step very easily especially when the sample matrix contains chlorides that may increase the volatility of this analyte [278, 279].

Generally, an ideal temperature program of graphite furnace cannot be given without the knowledge of the sample composition. But since the composition of the sample matrix, which is here represented by the eluent, is in this case known and unchanging, it was possible to adjust the temperature program so there is no loss of arsenic content during the pyrolysis step. This in combination with the use of the palladium modifier (1% (v/v) Pd) led to obtaining excellent results in the meaning of their accuracy and precision (98–100% recovery of arsenic concentration with 1% relative standard deviation). The knowledge of the matrix composition also allowed the use of the standard addition calibration method that can compensate for matrix interference arising from the chloride content.

Last but not least, the surface modification of the graphite furnace by tungsten carbides was performed because the chloride-rich matrix of samples caused rapid wear

to the graphite tubes. The modification was performed by simple impregnation of graphite tubes' surface by immersion in the aqueous solution of sodium tungstate of 50 g L^{-1} and their subsequent annealing in the ET-AAS. The changes on the surface of the graphite tube before and after surface modification were observed by scanning electron microscopy (**Fig. 4-3**). This procedure extended the lifetime of the graphite tubes five times up to 250 firing cycles.

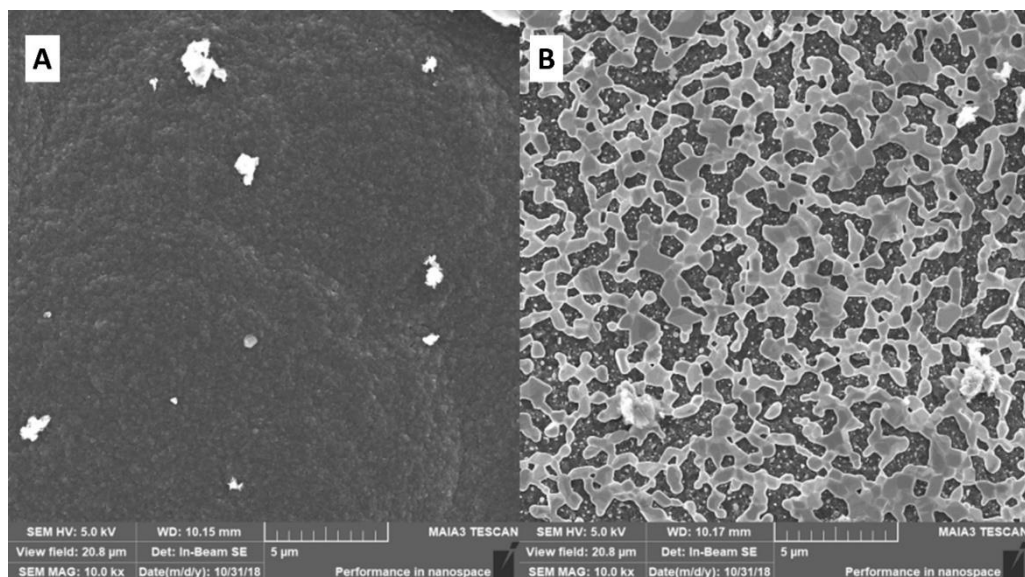


Fig. 4-3 Inner surface of the graphite tube before (A) and after (B) modification by tungsten carbides.

The optimization process of the ET-AAS method for arsenic determination in samples containing high chloride concentration as the new methodology was presented at the MendelNet2018 conference. The proceedings of this conference are regularly included in the Conference Proceedings Citation Index (Clarivate Analytics) and therefore, this peer-reviewed contribution was included as a part of this work as well. Moreover, this contribution was awarded as the best contribution in the section Applied Chemistry and Biochemistry.

Modification of electrothermal atomic absorption spectrometry for determination of arsenic in high salinity samples

Vendula Smolikova^{1,2}, Pavlina Pelcova¹, Josef Hedbavny¹, Lucie Zlamalova¹, Andrea Ridoskova^{1,2}

¹Department of Chemistry and Biochemistry
Mendel University in Brno
Zemедelska 1, 613 00 Brno

²Central European Institute of Technology
Brno University of Technology
Purkynova 123, 612 00 Brno
CZECH REPUBLIC

xsmoliko@mendelu.cz

Abstract: The electrothermal atomic absorption spectrometry (ET-AAS) method was optimized for determination of the arsenic content in high salinity samples. The combination of palladium (1 g/l) modifier, graphite furnace temperature program and graphite tube modified with tungsten carbide significantly reduced the matrix interference in the sample with NaCl concentration of 10 g/l. Optimized temperature program ensured the reduction of the background absorbance about 95–100%. The modification of graphite furnace surface by tungsten carbides ensured the shift of background absorbance prior to the absorbance of the analyte and considerable extension lifetime of graphite tubes.

Key Words: arsenic, palladium modifier, tungsten carbide, ET-AAS, background correction

INTRODUCTION

Arsenic with mutagenic and carcinogenic effects on humans belongs among the highly toxic substances in the environment. Inorganic arsenic forms, such as arsenate (As^{V}) and arsenite (As^{III}), have higher toxicities than organic arsenic species. Human populations worldwide are primarily exposed to inorganic arsenic through the consumption of contaminated water (Cubadda et al. 2017). Determination of total arsenic content in aqueous samples is usually performed by electrothermal atomic absorption spectrometry. Arsenic determination by ET-AAS may be complicated by losses of the analyte during the pyrolysis stage and interferences caused by matrix (e.g., sea water, mineralized water) (Bermejo-Barrera et al. 1996, Bozsai et al. 1990, Welz et al. 1988).

The most, palladium nitrate or palladium-magnesium nitrate modifiers are used for determination of arsenic content in high salinity samples (Bermejo-Barrera et al. 1996, Welz et al. 1988). These modifiers cause stabilization of volatile analytes, including arsenic, to higher pyrolysis temperatures, and ensure the separation of the arsenic from the matrix during the pyrolysis phase without the loss of analyte. Reducing the background absorption can also be achieved by inserting a pre-atomization cool-down step into the graphite furnace temperature program (Bozsai et al. 1990, Cabon 2000, Pszonicki and Dudek 1999) or surface-modified graphite tubes (Kulik et al. 2009, Volynsky 1998).

The aim of this study was to optimize the ET-AAS method for arsenic determination in high salinity samples. The combination of palladium modifier, graphite furnace temperature program and graphite tube modified with tungsten carbide was tested and optimized for sensitive and precise arsenic determination.

MATERIAL AND METHODS

Instrumentation

Measurements were performed using graphite furnace atomic absorption spectrometer 280Z AA (Agilent Technologies, Santa Clara, CA, USA) with Zeeman background correction. Determination of arsenic was carried out under the conditions recommended by the manufacturer for As (193.7 nm) with

a spectral bandwidth of 0.5 nm. Ultrasensitive hollow cathode lamp (Agilent Technologies, Santa Clara, CA, USA) was used as the radiation source of As (lamp current 10 mA). The ultrasonic bath Elmasonic P (Elma, Singen, Germany) was used for graphite furnace surface-modification.

Reagents

All solutions were prepared from analytical grade chemicals. Arsenic (III) standard solution with the concentration of 1000 ± 4 mg/l (Fluka, Czech Republic) was used for the preparation of calibration solutions (calibration range 0–100 $\mu\text{g/l}$). Palladium 10 g/l (Fluka, Czech Republic) was used for the preparation of 1% (v/v) Pd modifier and $\text{Na}_2\text{WO}_4 \cdot 2\text{H}_2\text{O}$ (Lachema, Czech Republic) was used for graphite furnace surface-modification. The 65% HNO_3 (Penta, Czech Republic) purified by sub-boiling distillation apparatus (Type BSB-939IR, Berghof, Eningen, Germany) and demineralized water produced by Millipore Milli Q system (Millipore, Bedford, MA, USA) were used for sample dilution.

Graphite furnace surface-modification

Pyrolytic graphite tubes were impregnated with aqueous solution Na_2WO_4 (50 g/l). Tubes were placed in the solution and soaked for 3 minutes in the ultrasonic bath under atmospheric pressure. Tubes were then carefully wiped and heated twice in the atomizer according to the graphite furnace temperature program (Table 2). The operation was repeated three times (Figure 1). Every day before the measurement starts, 10 μl of sodium tungsten solution (50 g/l) were dispensed onto the inner surface of the furnace and heated according to the graphite furnace temperature program (Table 2).

Figure 1 Scheme of graphite furnace surface-modification



Procedure

The standard arsenic solution (50 $\mu\text{g/l}$) in solution NaCl (10 g/l) was used for method optimization. The samples were acidified with 3% (v/v) HNO_3 before analysis. The palladium modifier (injection volume 10 μl) was pre-injected into graphite furnace before the sample injection (sampling volume 20 μl).

RESULTS AND DISCUSSION

Graphite furnace program optimization

Firstly, arsenic content in the sample with high concentration of NaCl (10 g/l) was measured under the graphite furnace temperature program recommended by the manufacturer of ET-AAS (Table 1). The palladium (1% v/v) was used as the modifier.

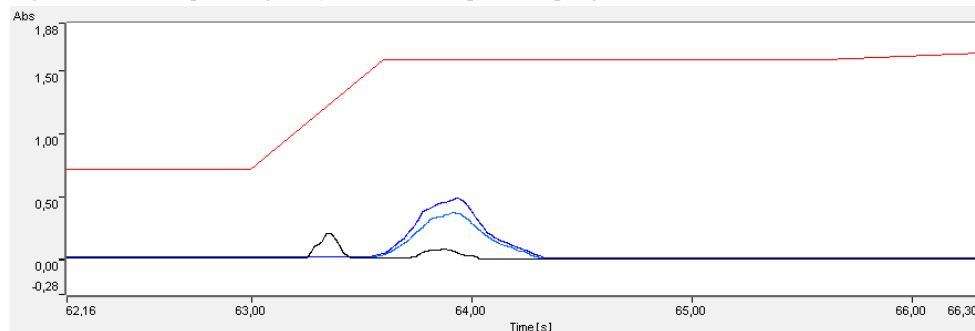
Table 1 Graphite furnace temperature program recommended by the manufacturer of ET-AAS

Step	1	2	3	4	5	6	7
Temperature, $^{\circ}\text{C}$	85	95	120	1400	1400	2600	2800
Ramp time, sec	5	40	10	5		0.6	2
Hold time, sec				1	2	2	
Read						ON	
Argon flow, l/min	0.3	0.3	0.3	0.3	0	0	0.3

Legend: 1,2,3 – drying steps; 4,5 – pyrolysis steps; 6 – atomization step; 7 – cleaning step

High concentration of sodium chloride in the sample matrix generated high background absorbance which deformed the absorbance of analyte (Figure 2). When the temperature program recommended by the manufacturer was used for arsenic determination, the method recovery of arsenic in the sample with high salinity was only 50–70% with RSD = 17.8%. The limit of detection for As in solution NaCl (10 g/l) was 12.2 µg/l (sample volume 20 µl, 10 replicates).

Figure 2 The absorption signal of arsenic at temperature program stated in Table 1



Legend: Red line – temperature program; blue line – analyte absorbance; black line – background absorbance

To reduce the background absorption a cool-down step before atomization was incorporated into the graphite furnace temperature program (Table 2). Longer duration of drying step prevented boiling of the sample in the graphite tube.

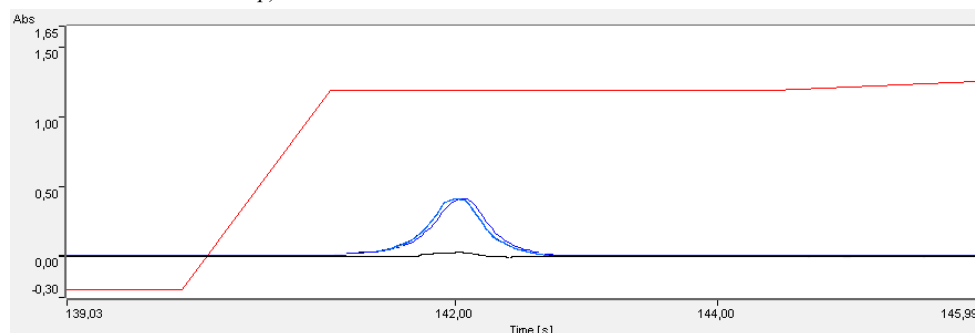
Table 2 Graphite furnace temperature program with pre-atomization cool-down step

Step	1	2	3	4	5	6	7
Temperature, °C	90	150	300	1300	130	2300	2650
Ramp time, sec	9	30	25	10	15	1	5
Hold time, sec		20		30	1	3	
Read						ON	
Argon flow, l/min	0.3	0.3	0.3	0.3	0.3	0	0.3

Legend: 1,2,3 – drying steps; 4 – pyrolysis step; 5 – cool-down step; 6 – atomization step; 7 – cleaning step

A cool-down step between the steps of pyrolysis and atomization ensured that the sample matrix effect was reduced, and the background absorption was lower about 95–100% (Figure 3). The RSD was decreased to less than 1%. The method recovery of arsenic with temperature program using cool-down step was 98–100%. Limit of detection for As in solution NaCl (10 g/l) was decreased to 1.1 µg/l (sample volume 20 µl, 10 replicates).

Figure 3 The absorption signal of arsenic at temperature program stated in Table 2 (with pre-atomization cool-down step)



Legend: Red line – temperature program; blue line – analyte absorbance; black line – background absorbance

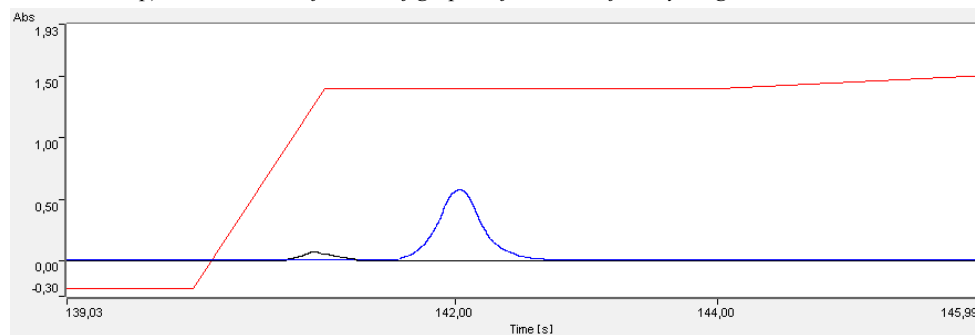
Bozsai et al. (1990) achieved similar results using palladium-magnesium nitrate modifier, pyrolysis temperature 1300 °C and the temperature drop after the pyrolysis step. It is assumed that high background absorbance is caused by Rayleigh scattering by larger salt particles in the cooler regions at the tube ends. When the pre-atomization cool-down step is incorporated into the graphite furnace temperature program, the tube is heated more uniformly and the effect of the cool tube ends is avoided almost completely (Bozsai et al. 1990).

Moreover, standard addition calibration method instead of matrix-free calibration was used to reduction matrix interferences. This step improved the performance of the methodology and made it independent of the knowledge of the NaCl concentration in the sample.

Graphite furnace surface-modification

Although we have achieved very good results of arsenic recovery through temperature program improvement, the lifetime of the graphite tube was reduced due to the aggressive composition of the sample matrix. The surface of the graphite tube was significantly damaged after about 50 firing cycles. For this reason, we have combined the cool-down step temperature program with the modification of graphite furnace surface by tungsten carbides.

Figure 4 The absorption signal of arsenic at temperature program stated in Table 2 (pre-atomization cool-down step) and at the modification of graphite furnace surface by tungsten carbides



Legend: Red line – temperature program; blue line – analyte absorbance; black line – background absorbance

The modification of graphite furnace surface by tungsten carbides led to the shift of the total background absorbance prior to the actual absorbance of the analyte. This prevents the distortion of the analyte absorbance (Figure 4). The lifetime of the graphite tube was significantly increased to 250 firing cycles.

CONCLUSION

The sensitive and precise method has been proposed and optimized for arsenic determination in samples containing high concentrations of chlorides. The interference effect of the sample matrix was reduced by the combination of palladium (1 g/l) modifier, graphite furnace temperature program with the cool-down pre-atomization step and graphite tube modified with tungsten carbides. The background absorbance was reduced about 95–100%. The new methodology allowed the determination of arsenic in solution NaCl (10 g/l) with the recovery of 98–100%. Limit of detection was decreased 11.3 times. Moreover, the lifetime of the graphite tube was increased five times.

ACKNOWLEDGEMENTS

This research was carried out with the support of the Ministry of Education, Youth and Sports of the Czech Republic under the project CEITEC 2020 (LQ1601). The research has been supported by grant no. AF-IGA-2018-tym005.

REFERENCES

- Bermejo-Barrera, P. et al. 1996. Comparison of different chemical modifiers for the direct determination of arsenic in sea water by electrothermal atomic absorption spectrometry. *Fresenius Journal of Analytical Chemistry*, 355: 174–179.
- Bozsai, G. et al. 1990. Determination of arsenic, cadmium, lead and selenium in highly mineralized waters by graphite-furnace atomic-absorption spectrometry. *Talanta*, 37(6): 554–553.
- Cabon, J.Y. 2000. Effects of various salts on the determination of arsenic by graphite furnace atomic absorption spectrometry. Direct determination in seawater. *Fresenius Journal of Analytical Chemistry*, 367: 714–721.
- Cubadda, F. et al. 2017. Human exposure to dietary inorganic arsenic and other arsenic species: State of knowledge, gaps and uncertainties. *Science of the Total Environment*, 579: 1228–1239.
- Kulik, A.N. et al. 2009. Tungsten-assisted modification of graphite furnaces for an atomic absorption spectrometer. *Journal of Applied Spectroscopy*, 76(4): 564–569.
- Pszonicki, L., Dudek, J. 1999. Modifier effects in the determination of arsenic, antimony and bismuth by electrothermal atomic absorption spectrometry. *Journal of Analytical Atomic Spectrometry*, 14: 1755–1760.
- Volynsky, A.B. 1998. Graphite atomizers modified with high-melting carbides for electrothermal atomic absorption spectrometry. II. Practical aspects. *Spectrochimica Acta Part B: Atomic Spectroscopy*, 53(12): 1607–1644.
- Welz, B. et al. 1988. Palladium nitrate – magnesium nitrate modifier for graphite furnace atomic absorption spectrometry. Part 2. Determination of arsenic, cadmium, copper, manganese, lead, antimony, selenium and thallium in water. *Journal of Analytical Atomic Spectrometry*, 3: 695–701.

5 RESULTS AND DISCUSSION

The results of this dissertation thesis are provided within this chapter as individual scientific publications that have already been published/are in preparation for submission to peer-reviewed journals. These publications are supplemented by brief author's comments.



(Picture taken in the former mining open pit during sampling campaign in the Pays de Loire, France in 2020).

5.1 Development and evaluation of the DGT technique utilizing commercially available resin Lewatit FO 36 for determination of arsenic species in the aquatic environment

Smolíková, V., Pelcová, P., Ridošková, A., Hedbávný, J., Grmela, J. Development and evaluation of the iron oxide-hydroxide based resin gel for the diffusive gradient in thin films technique. *Analytica Chimica Acta*. 2020, 1102, 36-45, IF 6.228.

The DGT technique for the determination of arsenic generally utilizes binding phases containing iron hydroxide, ferrihydrite, titanium dioxide, zirconium oxide, or cerium oxide [225, 226, 228, 231, 233]. Nevertheless, the use of commercially available resins is generally preferred due to the stable quality of the product and their undemanding use (usually require no or minor pre-treatment in the meaning of grinding). But only two commercially available resins appeared in the literature so far – Metsorb and Amberlite IRA 910 [224, 229]. Metsorb is a titanium dioxide-based granular adsorbent while Amberlite IRA 910 is a strongly basic anion exchange resin with dimethyl ethanol ammonium functional groups. But both of them have unsatisfactory total sorption capacity of As ($8.5 \mu\text{g As}^{\text{III}} \text{ gel disc}^{-1}$ and $82.0 \mu\text{g As}^{\text{V}} \text{ gel disc}^{-1}$ for Metsorb [17], $0.3 \mu\text{g As}^{\text{V}} \text{ gel disc}^{-1}$ for Amberlite IRA 910 [16]).

For this reason, a commercially available resin Lewatit FO 36 was used as a DGT binding phase for the first time in this work. Lewatit FO 36 is polystyrene-based resin with tertiary amine groups ($-\text{CH}_2-\text{N}(\text{CH}_3)_2$) doped with nano-scaled film of $\text{FeO}(\text{OH})$ (**Fig. 5-1**). Oxyanions are bond by a specific, reversible reaction involving hydroxy-groups on the iron oxide-hydroxide surface. The formed complexes of As with iron are inner-sphere complexes. The resin is highly selective for oxyanions such as arsenite and arsenate, and its performance is not influenced by the presence of other anions, such as chloride, sulphate, or nitrate [280]. This was in agreement with the results of this study where a new DGT technique with excellent total sorption capacity ($\sim 535 \mu\text{g gel disc}^{-1}$ of each tested species – As^{III} , As^{V} , monomethylarsonic acid (MMA), and dimethylarsinic acid (DMA)) was developed. No significant influence on the DGT performance was

observed in the pH range 4–8 or in the presence of chlorides ($0\text{--}0.5\text{ mol L}^{-1}$) and humic acid ($0\text{--}100\text{ mg L}^{-1}$). Due to the chemical analogy of arsenate and phosphate, the competition for binding sites can be observed, but only at a very high concentration of phosphates (10 mg L^{-1}). However, with regard to the average concentration of phosphates found in European rivers which is generally very low (total phosphorus $\sim 0.05\text{ mg L}^{-1}$ [281]), this effect may be neglected. Similarly, a high concentration of iron in solution ($\text{Fe } 1\text{ mg L}^{-1}$) resulted in its complexation with arsenic which thus became less labile and therefore the DGT-determined fraction of As was lower compared to the total concentration in the solution. But regarding the common concentrations of iron (less than 0.3 mg L^{-1}), the negative effect may be considered negligible in most natural waters. The performance of the novel Lewatit FO 36-DGT was evaluated by laboratory experiment with natural water sample (river Svatka, Brno, Czech Republic) and by *in-situ* application in the Zászkalská water reservoir (Neřežín, Czech Republic). Good agreement between the concentrations determined by DGT (c_{DGT}) and concentrations in grab samples of the solution (c_{SOL}) was observed with the resulting ratio of $c_{\text{DGT}}/c_{\text{SOL}}$ varying between 0.99–1.04 in the spiked river water. The $c_{\text{DGT}}/c_{\text{SOL}}$ ratio in the Zászkalská reservoir was 0.91–0.93 even after 49 days of deployment.

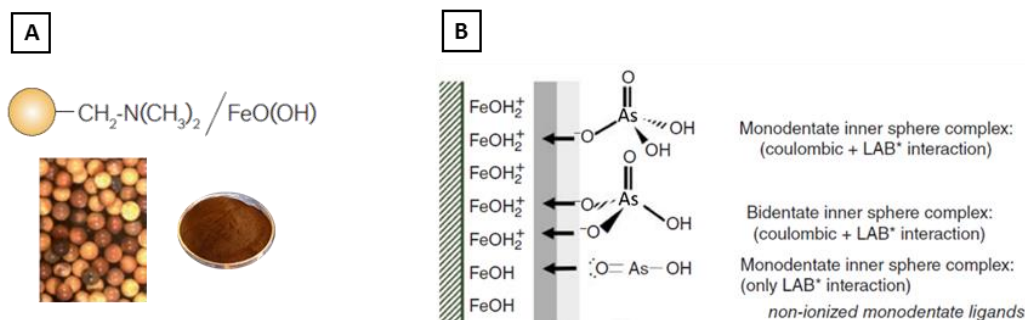


Fig. 5-1 (A) Chemical structure and appearance of Lewatit FO 36 [280]; (B) illustration of interactions between arsenic inorganic species with iron oxide-hydroxide functional groups (adapted from [282]).



Development and evaluation of the iron oxide-hydroxide based resin gel for the diffusive gradient in thin films technique

Vendula Smolíková^{a,b}, Pavlína Pelcová^{a,*}, Andrea Ridošková^a, Josef Hedbávný^a, Jan Grmela^c

^a Department of Chemistry and Biochemistry, Mendel University in Brno, Zemedelska 1, CZ-613 00, Brno, Czech Republic

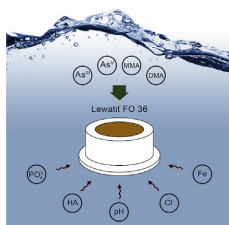
^b Central European Institute of Technology, Brno University of Technology, Purkynova 123, CZ-612 00, Brno, Czech Republic

^c Department of Zoology, Fisheries, Hydrobiology and Apiculture, Mendel University in Brno, Zemedelska 1, CZ-613 00, Brno, Czech Republic

HIGHLIGHTS

- New DGT resin gel utilizing Lewatit® FO 36 resin was developed.
- High total sorption capacity of four arsenic species (As^{III} , As^{V} , MMA, DMA).
- Influence of various external factors (pH, iron, chlorides, humic acid, phosphates) was tested.
- Evaluation of DGT method on real samples (in laboratory and *in-situ*).

GRAPHICAL ABSTRACT



ARTICLE INFO

Article history:

Received 13 August 2019

Received in revised form

13 December 2019

Accepted 14 December 2019

Available online 17 December 2019

Keywords:

Diffusive gradient in thin films technique

Arsenic species

Atomic absorption spectrometry

Aquatic environment

ABSTRACT

An ion-exchange resin Lewatit FO 36 was used for the preparation of a new resin gel for the diffusive gradient in thin films technique (DGT). The DGT method was optimized for the accumulation of four bioavailable arsenic species (As^{III} , As^{V} , monomethylarsonic acid, dimethylarsinic acid) in the aquatic environment. The total sorption capacity of Lewatit FO 36 resin gel was $535 \mu\text{g As disc}^{-1}$. The microwave-assisted extraction in the presence of NaCl (10 g L^{-1}) and NaOH (10 g L^{-1}) was used for the isolation of arsenic species from the Lewatit FO 36 resin gel. The elution efficiency of arsenic was $98.4 \pm 2.0\%$. Arsenic was determined by the optimized electrothermal atomic absorption spectrometry (ET-AAS) method using palladium modifier, pre-atomization cool-down step and tungsten carbides coating of graphite tube. The Lewatit FO 36 resin gel provides accurate results ($c_{\text{DGT}}/c_{\text{SOL}}$ ratio 0.86–1.00) in the pH range 4–8. No significant influence of experimental conditions was observed in the presence of chlorides (0 – 0.5 mol L^{-1}) and humic acid (0 – 100 mg L^{-1}). Only a very high concentration of phosphates (10 mg L^{-1}) caused a slight decrease in the diffusion coefficients of MMA and As^{V} species (8.4% and 12.4%, respectively). The presence of iron (0 – 1 mg L^{-1}) caused a decrease in the diffusion coefficients, but with regard to the common concentrations of iron (less than 0.3 mg L^{-1}), the negative effect was considered not significant for As^{III} and DMA in natural water. The DGT-ET-AAS method was applied for the determination of bioavailable arsenic species in the spiked river water samples and also *in-situ* in the water reservoir. The new resin gel was characterized by a homogeneous gel structure with excellent

Abbreviations: DGT, diffusive gradient in thin films technique; ET-AAS, electrothermal atomic absorption spectrometry; MMA, monomethylarsonic acid; DMA, dimethylarsinic acid; PAM, polyacrylamide; HA, humic acid; D, diffusive coefficient; DOM, dissolved organic matter.

* Corresponding author. Department of Chemistry and Biochemistry, Mendel University, Zemedelská 1, Brno, 61300, Czech Republic.

E-mail address: pavlina.pelcova@mendelu.cz (P. Pelcová).

<https://doi.org/10.1016/j.aca.2019.12.042>

0003-2670/© 2019 Elsevier B.V. All rights reserved.

reproducibility (< 5% variation of results between batches) and high sorption capacity which suggests its possible long-term application (up to 286 days in the environment with the arsenic concentration of 100 $\mu\text{g L}^{-1}$).

© 2019 Elsevier B.V. All rights reserved.

1. Introduction

Since heavy metals belong to persistent contaminants of the environment, they present a worldwide problem. Arsenic with its mutagenic and carcinogenic effects is one of the most toxic metalloids that can occur in the aquatic, as well as sediment and soil ecosystems [1,2]. Toxicity and bioavailability of arsenic are closely related to its chemical forms. The most frequent inorganic species are arsenite (As^{III}) and arsenate (As^{V}). Reduced arsenite species are 10 times more toxic and mobile than oxidized inorganic ones and both have generally higher toxicities (70–100 times more) than organic arsenic species, such as monomethylarsonic acid (MMA) or dimethylarsinic acid (DMA) [3–6]. Methylation of inorganic arsenic compounds in the environment does not generally occur under abiotic conditions even in the presence of carbon sources, and therefore organic compounds are almost entirely produced by bacterial methylation. The transformation process is reversible, and the balance of methylation/demethylation processes is influenced by various external factors, i.e. pH, redox potential (Eh), temperature, availability of carbon sources to As-methylating microorganisms [7,8]. Depending on the transformation of arsenic species there are significant changes in their toxicity and mobility and therefore, it is important to determine not only the inorganic but also the organic species of arsenic.

In a number of ecotoxicological studies, toxic effects of metals on living organisms have been related to measuring the total concentration of metals in the environment. But total metal content provides a limited forecast of its availability to biota. Therefore, the determination of labile metal flows from the environment using the diffusive gradient in thin films technique (DGT) appears to be a suitable alternative to conventional methods which can also cause unpredictable changes of analyte chemical forms during sampling, sample transfer and processing [9]. The DGT technique can provide information about bioavailability of metals from the environment, it stands out for its simplicity, low cost, and time intensity. Moreover, the possibility of *in-situ* application of DGT over a long time period provides obtaining more detailed results of time-weighted average (TWA) concentrations than the single grab sampling. The DGT technique can simulate the process of metal uptake by biota using the diffusive gel membrane (an equivalent of the biological membranes, e.g. gills, roots) and the binding gel layer (an equivalent of the biota tissues). Therefore, the DGT has a great potential not only to measure the available portion of analyte in the environment but also to predict the metal concentration in biota before any sacrifice of living organisms [10].

In most of published works dealing with arsenic and DGT, binding gels contain synthesized binding micro- or nano-components such as iron-hydroxide [3], ferrihydrite [11], titanium dioxide [12], zirconium oxide [13] or cerium oxide [14], as well as resins such as Metsorb [15], Amberlite IRA 910 [16], 3-mercaptopropyl-functionalized silica [17] or even activated carbon [18]. Some researchers also combined the binding components to achieve better results or to perform a multi-elemental analysis [19–24]. However, the laboratory synthesis of binding microparticles and nanoparticles is time-consuming, and it may be difficult to ensure the reproducibility of the micro- and nanoparticles'

properties of each batch. This fact requires a thorough characterization of each batch of microparticles to ensure the constant quality. Also, sufficient homogeneity of gel structure may not be achieved using the laboratory synthesized wet micro- or nanoparticles (when drying the particles by pressure between the filter papers or weighing them after centrifugation and decantation of excess water). On the other hand, the preparation of resin-containing gels is generally less time-consuming because resins are commercially available, sorbent quality is stable and the sorption properties of the formed gels are repeatable batch-to-batch. The main disadvantage and limitation of resin-containing gels is their unsatisfactory sorption capacity – 8.5 $\mu\text{g As}^{\text{III}}$ gel disc⁻¹ and 82.0 $\mu\text{g As}^{\text{V}}$ gel disc⁻¹ for Metsorb [17], 0.3 $\mu\text{g As}^{\text{V}}$ gel disc⁻¹ for Amberlite IRA 910 [16], 77.5 $\mu\text{g As}^{\text{III}}$ gel disc⁻¹ for 3-mercaptopropyl-functionalized silica [17].

In this work, the commercial anion-exchange resin Lewatit FO 36 containing iron oxide-hydroxide functional groups is tested for the manufacture of resin DGT gels. Lewatit FO 36 is commercially available in stable quality and combines simplicity and undemanding use of resin and high sorption capacity which is usually typical for micro or nanoparticles. Because of the strong ability of iron compounds to bind arsenic, they are commonly used in many arsenic removal technologies for the treatment of drinking water. Lewatit FO 36 resin is originally designed to reduce arsenic contamination in potable water supplies. It adsorbs arsenite as well as arsenate compounds and according to the manufacturer, the sorption capacity of this resin is not influenced by the presence of other anions such as chlorides, sulfates or nitrates. Nevertheless, the use of this resin for the preparation of DGT resin gels has not yet been discussed in the literature. Here we present a detailed description of the gel preparation, characterization of prepared resin gels and optimization of the elution process and the analysis procedure for arsenic determination. Sorption capabilities of the newly formed Lewatit FO 36 resin gel were compared to those of iron-hydroxide gel [3] because both binding components have similar functional groups. The influence of relevant factors (pH, iron, chlorides, humic acid and phosphates) that may affect the sorption of arsenic was evaluated. Suitability of the new Lewatit FO 36 gel-DGT-AAS method for determining arsenic in the aquatic environment was verified by the analysis of spiked river water sample and by the field trial.

2. Materials and methods

2.1. Reagents and chemicals

All chemicals were of analytical grade. Standard solutions of As^{III} ($c = 999 \pm 4 \text{ mg L}^{-1}$ in 2% (v/v) HNO_3) and As^{V} ($c = 995 \pm 3 \text{ mg L}^{-1}$ in H_2O) (Sigma-Aldrich, Germany) were used for the preparation of arsenite and arsenate stock and calibration solutions. Disodium methylarsenate hexahydrate $\text{CH}_3\text{AsNa}_2\text{O}_3 \times 6\text{H}_2\text{O}$ (Chem Service, USA) and dimethylarsinic acid $(\text{CH}_3)_2\text{AsO}_2\text{H}$ (Fisher Scientific, Czech Republic) were used for the preparation of MMA and DMA stock and calibration solutions without any further purification. All solutions were prepared using Milli-Q water produced by Millipore Milli Q system (Millipore, Bedford, MA, USA).

The 65% HNO_3 (VWR, Czech Republic) purified by the distillation apparatus (Type BSB-939 IR, Germany) and NaOH (Penta, Czech Republic) were used for pH adjustment. Sodium chloride and sodium nitrate (Penta, Czech Republic) were of analytical grade. Humic acid, Fe^{3+} standard solution ($c = 10 \pm 0.05 \text{ g L}^{-1}$ in 3% (v/v) HNO_3) (Sigma-Aldrich, Germany) and potassium phosphate (Penta, Czech Republic) were used for testing the influence of experimental conditions on accumulation arsenic.

Palladium 10 g L^{-1} (Analytika, Czech Republic) was used for the preparation of Pd modifier (1% (v/v)) and $\text{Na}_2\text{WO}_4 \times 2\text{H}_2\text{O}$ (Sigma-Aldrich, Germany) was used for the coating of graphite furnace.

DGT resin gels were prepared using acrylamide 40% (w/v) (Merck, Germany), ammonium persulfate (Honeywell Fluka, Germany), N,N,N',N'-tetramethylethylenediamine (TEMED) (Sigma-Aldrich, Germany), agarose-derived DGT cross-linker (2%) (DGT Research Ltd., UK) and Lewatit® FO 36 resin (Lanxess, Germany). For the preparation of iron-hydroxide, ferric nitrate nonahydrate $\text{Fe}(\text{NO}_3)_3 \times 9\text{H}_2\text{O}$ (Sigma-Aldrich, Germany) was used.

2.2. Instrumentation and DGT devices

Determination of arsenic content in samples was performed using the atomic absorption spectrometer 280Z AA (Agilent Technologies, USA) with electrothermal atomization and using Zeeman background correction. Arsenic concentration was analyzed at a wavelength of 193.7 nm with a spectral bandwidth of 0.5 nm. As a light source, an ultrasensitive hollow cathode lamp (Agilent Technologies, USA) with lamp current 10 mA was used.

DGT pistons with an exposure area of 3.14 cm^2 (DGT Research Ltd., UK) and membrane filters of $0.45 \mu\text{m}$ pore size and 0.013 cm thickness (Pall Corporation, USA) were used for the experiments. All glass, plastic spacers, and components were cleaned by soaking in 10% HNO_3 for at least 48 h and rinsed with Milli-Q water prior to use.

2.3. Preparation of Lewatit FO 36

The Lewatit FO 36 resin was used for the manufacture of new DGT resin gels. Prior to use, the resin was purified using a solution of sodium hydroxide (10 g L^{-1}) and sodium chloride (10 g L^{-1}) according to the manufacturer's instructions. After 24 h of regeneration, the resin was filtrated, washed with Milli-Q water and dried at 35°C . The purified resin was ground and sieved through a Teflon sieve ($150 \mu\text{m}$).

2.4. Preparation of iron-hydroxide

Iron-hydroxide was prepared according to a protocol given in the literature [25]. The precipitate of iron-hydroxide was formed by the titration of 4% (w/v) $\text{Fe}(\text{NO}_3)_3 \times 9\text{H}_2\text{O}$ solution with 1 M NaOH to pH 7.0. The resulting brown-red precipitate was decanted and then washed several times with Milli-Q water. Iron-hydroxide was stored at 4°C under Milli-Q water.

2.5. Production of diffusive and resin gels

Polyacrylamide type of diffusive gels (PAM) consists of 10 mL of gel solution (15% of acrylamide, 0.3% of cross-linker and Milli-Q water), $70 \mu\text{L}$ of 10% (w/v) ammonium persulfate and $25 \mu\text{L}$ of TEMED. Diffusive gels were produced according to the protocol stated in the literature [26] using a 0.050 cm plastic spacer.

Resin gels were prepared by mixing 0.375 g of processed Lewatit FO 36 powder and 3 mL of gel solution. Under constant stirring $36 \mu\text{L}$ of TEMED and $72 \mu\text{L}$ of 10% (w/v) ammonium persulfate were added to the mixture. The resulting solution was pipetted between

two glass plates separated by a plastic spacer (0.025 cm) to create a gel of defined thickness. The resin gel was then allowed to polymerize in the drying oven at 40°C for 1 h.

Iron-hydroxide based gels were prepared using 0.750 g of iron-hydroxide precipitate (after its filtration and removal of excess water by compressing between two filter papers) in 3 mL of gel solution. After thorough mixing, $4.5 \mu\text{L}$ of TEMED and $18 \mu\text{L}$ of 10% (w/v) ammonium persulfate were added to the solution. The iron-hydroxide based gel was then processed in the same manner as the previous gel type, but it was polymerized at 45°C for 1 h.

After the polymerization of gel sheets in the drying oven, the diffusive gel and both types of binding gels were conditioned in Milli-Q water for 24 h with several changes of water (at least three times). The gel sheets were then cut into discs (diameter 2.5 cm) and stored at 4°C under Milli-Q water. The thickness of diffusive gels after conditioning in demineralized water was $0.080 \pm 0.002 \text{ cm}$ ($n = 10$).

2.6. Optimization of the arsenic elution from the Lewatit FO 36 resin gel

One Lewatit FO 36 resin gel disc (5 replicates) was deployed into 20 mL of 0.01 M NaNO_3 solution (pH 5.0) with concentration 5 mg L^{-1} of As. After 24 h, gel discs were removed from the solution, rinsed with Milli-Q water and inserted into various elution agents (1 M/6 M/conc. HNO_3 ; 6 M/conc. HCl ; 1 M H_2SO_4 or their combination either at room temperature or at $70/130/150^\circ\text{C}$ in microwave extraction oven). The mixture of sodium hydroxide and sodium chloride with the mass ratio of 1:1 recommended by the manufacturer as a regeneration agent of Lewatit FO 36 resin was used as well. The remaining concentration of arsenic in the initial solution and the concentration of arsenic released from the gel disc through the elution process were measured by the atomic absorption spectrometer and used for the calculation of elution efficiency. The concentration of elution agent, elution time and temperature of microwave extraction were among the optimized parameters of the elution procedure.

2.7. Optimization of the ET-AAS determination

Since the highly concentrated mixture of NaOH and NaCl was used as an elution agent for the release of arsenic from Lewatit FO 36 resin gels, the determination of As content in eluates was complicated by the loss of arsenic content during the pyrolysis step and interferences caused by the matrix of elution agent. Therefore, the ET-AAS method was optimized for the determination of As in high salinity samples by combining the palladium modifier (1% (v/v)), cool-down step (130°C) incorporated into the temperature program and graphite tube coating by tungsten carbides [27].

2.7.1. Graphite furnace temperature program

Because the interference effect of chlorides presence cannot be reduced by increasing pyrolysis temperature due to the volatile character of the arsenic, the incorporation of a cool-down step before atomization was used to minimize the matrix effect (Table 1). The extension of drying steps to 84 s (original manufacturer's recommended duration was 55 s) prevented boiling of the sample in the graphite tube.

2.7.2. Graphite furnace surface-modification

To prevent the damage of the graphite tube inner surface caused by the aggressive composition of elution agent, pyrolytic graphite tubes were impregnated with an aqueous solution of sodium tungsten. The tubes were soaked in the Na_2WO_4 solution (50 g L^{-1}) for 3 min in the ultrasonic bath. After careful wiping of the outer

Table 1

Graphite furnace temperature program with pre-atomization cool-down step.

Step ^a	1	2	3	4	5	6	7
Temperature, °C	90	150	300	1300	130	2300	2650
Ramp time, sec	9	30	25	10	15	1	5
Hold time, sec		20		30	1	3	
Read						ON	
Argon flow, Lmin ⁻¹	0.3	0.3	0.3	0.3	0.3	0	0.3

^a 1, 2, 3 – drying; 4 – pyrolysis; 5 – cool-down; 6 – atomization; 7 – cleaning.

surface by cellulose wipes, they were heated in the AAS according to the above mentioned optimized program. The process was repeated three times. Every day prior to the start of analysis, 10 µL of Na₂WO₄ solution was applied by sampler dispensing capillary into the graphite furnace and heated according to the graphite furnace temperature program.

2.7.3. Determination of arsenic

The samples were acidified with 3% (v/v) HNO₃ before analysis. The 1% (v/v) palladium modifier (volume 10 µL) was pre-injected into the graphite furnace before the sample injection (volume 20 µL). The standard addition calibration method was used to reduce possible matrix interferences.

2.8. Sorption capacity of resin gels

Resin gels containing Lewatit FO 36 were characterized by the determination of sorption capacity of gel discs in a standard solution of each arsenic species (As^{III}, As^V, MMA and DMA). Single resin gel disc (5 replicates) was deployed into 20 mL of 0.01 M NaNO₃ solution (pH 5.0) with concentration 0.1–300 mg L⁻¹ of As^{III} or As^V and 0.1–1500 mg L⁻¹ of MMA or DMA for 24 h under constant stirring. The gel discs were then removed from the solution, rinsed with Milli-Q water and eluted. The concentration of arsenic in the eluate was analyzed by ET-AAS and used for the calculation of arsenic mass accumulated per resin gel disc. The sorption capacity of iron-hydroxide based gels was determined in the same way.

2.9. Measurement of diffusion coefficients by time-dependence experiment

Time-dependence experiment was carried out using the complete DGT units. The Lewatit FO 36 resin gel was placed on the top of the plastic piston, covered with PAM diffusive gel and membrane filter, and capped by a tight-fitting outer sleeve with an exposure window. The DGT units were deployed into 3 L of the 0.01 M NaNO₃ solution (pH 5.0) with the concentration 1 mg L⁻¹ of individual As species under constant stirring (for neglecting the diffusive boundary layer). The DGT units (5 replicates) were removed from the solution after 2, 4, 6 and 8 h. The diffusion coefficients (D , cm² s⁻¹) of As^{III}, As^V, MMA, and DMA were calculated from the slope of a linear plot, using Eq. (1) [26], where Δg is the thickness of diffusive layer consisting of diffusive gel and membrane filter (0.080 ± 0.013 cm), C is the concentration of arsenic (1000 µg L⁻¹) in solution and A is the exposed area (3.14 cm²).

$$D = \frac{\text{slope } \Delta g}{CA} \quad (1)$$

Obtained diffusive coefficients were corrected to the temperature of 25 °C using Eq. (2) [28].

$$\log D_T = \frac{1.37023(T - T_{ref}) + 8.36 \cdot 10^{-4}(T - T_{ref})^2}{109 + T} + \log \frac{D_{T_{ref}}(273 + T)}{(273 + T_{ref})} \quad (2)$$

2.10. Influence of external factors on as species accumulation by DGT

The effect of pH (range 1.5–11.0), presence of iron (Fe³⁺ concentration 0–1 mg L⁻¹), chlorides (Cl⁻ concentration 0–0.5 mol L⁻¹), humic acid (HA concentration 0–100 mg L⁻¹) and phosphates (PO₄³⁻ concentration 0–10 mg L⁻¹) on the accumulation of arsenic by the DGT was monitored. The five DGT units were deployed into 3 L of the 0.01 M NaNO₃ solution (pH 5.0, except for the pH influence experiment) with the known concentration ($C = 1000 \mu\text{g L}^{-1}$) of individual As species for 4 h ($t = 14\,400 \text{ s}$) under constant stirring. The mass of arsenic (M , ng) determined by ET-AAS in the eluate was used for the calculation of diffusion coefficient using Eq. (3) [28].

$$D = \frac{M \Delta g}{A t C} \quad (3)$$

2.11. Real samples

The efficiency of Lewatit FO 36 resin gels was evaluated by deploying the DGT units into the sample of natural river water. The sampling point on the Svratka River with GPS coordinates 49°07'55.3"N 16°37'37.9"E was selected. The sampling of river water was performed in February 2019. The river water had a pH of 7.9 and contained 0.19 mg L⁻¹ Fe (determined by F-AAS Agilent Technologies, USA), 81.5 mg L⁻¹ SO₄²⁻, 0.22 mg L⁻¹ PO₄³⁻, 59.6 mg L⁻¹ Cl⁻, 65 mg L⁻¹ NO₃⁻, 0.1 mg L⁻¹ NO₂⁻. The total concentration of As in the sample was below the method detection limit (LOD = 1.1 µg L⁻¹). Therefore, the river water was spiked with individual arsenic species ($c = 1 \text{ mg L}^{-1}$). Five DGT units were deployed into 3 L of the spiked river water under constant stirring. The DGT units were removed from the solution after 4 h. The mass of arsenic species accumulated by Lewatit FO 36 resin gels was determined by ET-AAS.

For *in-situ* application, the DGTs (5 replicates for each sampling time) were deployed in the Žáskalská water reservoir located in the vicinity of a former cinnabar mine called Jedová hora (49°47'28.4"N 13°52'42.0"E). The deployment was performed in June 2019, with the maximum deployment time of 49 days. After the deployment, the DGT units were rinsed with water and transported to the laboratory in plastic bags. The water of Žáskalská reservoir contained 0.09 mg L⁻¹ Fe (determined by F-AAS Agilent Technologies, USA). The concentration of As in the water was determined by ET-AAS after pre-concentration by evaporation of liquid under nitrogen flow by Ultravap 96 (Porvair Sciences limited, USA) and subsequent dissolution of the residue in 5% HNO₃.

2.12. Statistical analysis of results

Analytical software Statistica 13 (StatSoft, Czech Republic) was used for data analysis. One-way ANOVA was used to evaluate the significance of the influence of experimental conditions on the diffusion coefficients. Statistical significance was declared when p -

value was < 0.05.

3. Results and discussion

3.1. Elution efficiency

The elution efficiency was characterized as a percentage of arsenic released from the total amount of arsenic adsorbed on the gel disc. Unfortunately, none of the commonly used elution agent such as 1 M/6 M HNO_3 , 6 M HCl or 1 M H_2SO_4 provided satisfactory results neither at room temperature nor after microwave extraction (elution efficiency $30.8 \pm 90.6\%$ – $74.1 \pm 26.5\%$). Moreover, concentrated acids caused dissolution of resin gel and even filtrated eluates generated nonspecific interference effects during the AAS analysis (elution efficiency $112.2 \pm 35.6\%$ – $551.3 \pm 22.9\%$). The best results with quantitative elution yields ($98.4 \pm 2.0\%$) of arsenic content from resin gel were obtained, when the mixture of sodium chloride (10 g L^{-1}) and sodium hydroxide (10 g L^{-1}) was used as elution agent for microwave-assisted extraction at 130°C for 16 min (Fig. 1). After this extraction process, the gel disc could be easily removed from the solution and eluate sample can be directly analyzed.

3.2. Analytical performance

The high concentrations of NaOH and NaCl in the matrix of eluate generated high background absorbance which caused deformation of the analyte absorbance signal. The incorporation of the cool-down step (130°C) before the atomization ensured that the background absorption was lower by 95–100%. Limit of detection of the method was decreased eleven times to $1.1 \mu\text{g L}^{-1}$. The accuracy of the method in terms of measuring the arsenic content in the presence NaOH (10 g L^{-1}) and NaCl (10 g L^{-1}) was 98–100% with high precision ($\text{RSD} = 1.0\%$). The inner surface of the graphite tube was also modified by tungsten carbides. This step led to a five-fold extension of the lifetime of the graphite tube (to 250 firing cycles) which was otherwise very rapidly damaged by the matrix of the elution agent. The optimized ET-AAS method enabled a sensitive, precise and fast determination of arsenic content eluted from the Lewatit FO 36 resin gel.

3.3. Sorption capacity

The total and effective sorption capacity of the Lewatit FO 36 gel towards As^{III} , As^{V} , MMA and DMA was evaluated by the determination of adsorption isotherms, which express the dependence of the arsenic mass accumulated per gel disc on the concentration of individual arsenic species in the initial solution (Fig. 2).

The total sorption capacity of Lewatit FO 36 resin gel at pH 5.0 towards each arsenic species was $\sim 535 \mu\text{g gel disc}^{-1}$. The sorption of As^{III} and As^{V} was linear until reaching the total sorption capacity of resin gel. The effective sorption capacities of MMA and DMA species were lower (up to $\sim 321 \mu\text{g gel disc}^{-1}$ and $\sim 226 \mu\text{g gel disc}^{-1}$, respectively). Contents of arsenic in PAM gels and Lewatit FO 36 gel blanks were below the limit of detection ($\text{LOD} = 1.1 \mu\text{g L}^{-1}$). The high sorption capacity of Lewatit FO 36 gel suggests its possible deployment in field experiments for a long time period with regard to common arsenic concentrations in aquatic ecosystems (less than $10 \mu\text{g L}^{-1}$ and frequently less than $1 \mu\text{g L}^{-1}$) [29]. Even if the concentration of arsenic in a contaminated area reached $100 \mu\text{g L}^{-1}$, the sorption capacity would be filled in 286 days.

In comparison to iron-hydroxide based gel which has a similar functional group as Lewatit FO 36 resin, the total sorption capacity is 4.5 times higher (compared to $\sim 118 \mu\text{g As gel disc}^{-1}$ determined in our laboratory). In comparison with microparticles containing gels used for the determination of arsenic, the Lewatit FO 36 resin gel provides better sorption capabilities toward As^{III} than ZrO_2 ($\sim 400 \mu\text{g As gel disc}^{-1}$) and TiO_2 ($\sim 275 \mu\text{g As gel disc}^{-1}$) binding gels. Moreover, the sorption capacity of Lewatit FO 36 resin gel toward As^{V} is higher than the sorption capacities of CeO_2 ($\sim 375 \mu\text{g As gel disc}^{-1}$) and TiO_2 ($\sim 275 \mu\text{g As gel disc}^{-1}$) binding gels [14].

3.4. Measurement of diffusion coefficients by time-dependence experiment

Time-dependence experiment was performed to obtain diffusive coefficients (D) of individual arsenic species which were calculated from the slope of a linear plot of arsenic mass accumulated per gel disc as a function of time using Eq. (1). Due to the almost identical character of As^{V} , MMA and DMA curves, only the one of As^{V} is shown in Fig. 3 for better clarity.

The calculated diffusion coefficients of individual arsenic species (in 0.01 M NaNO_3 solution, pH 5.0, at 25°C) were

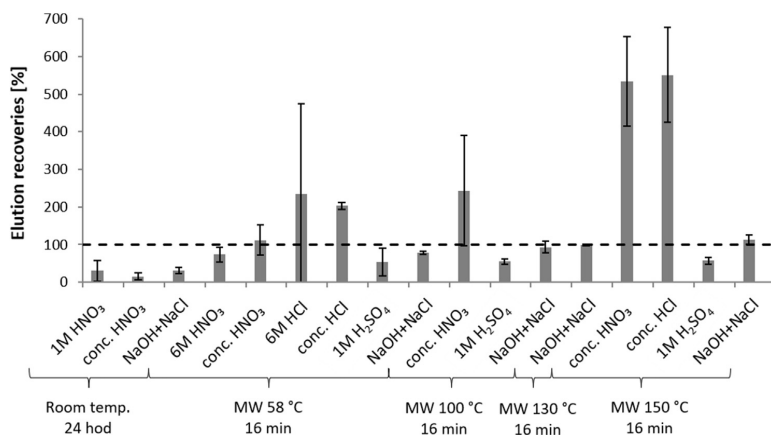


Fig. 1. Comparison of the elution efficiency of individual elution agents under different temperature conditions ($n = 5$).

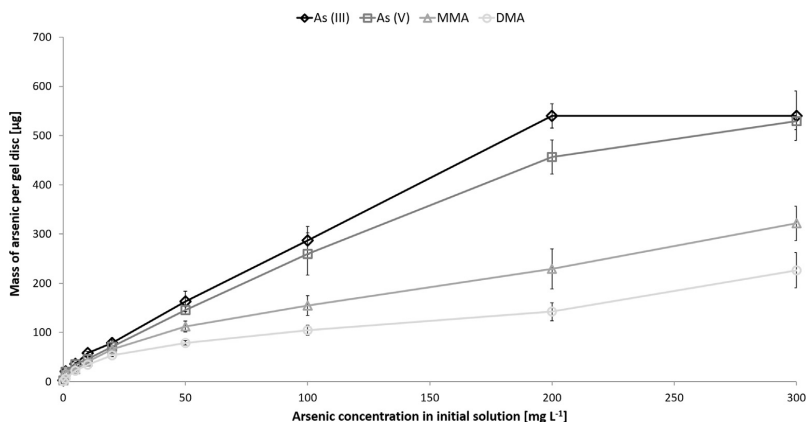


Fig. 2. Sorption capacity of Lewatit FO 36 resin gels towards As^{III}, As^V, MMA and DMA (accumulation time 24 h, n = 5).

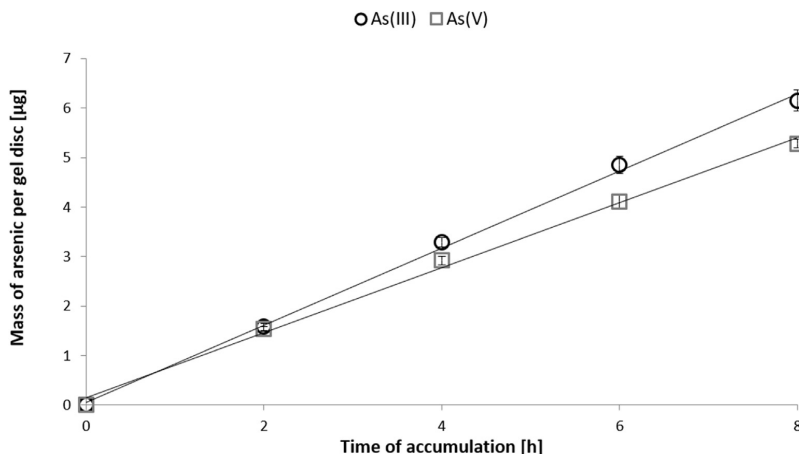


Fig. 3. Time-dependence experiment of arsenic species (arsenic species concentration 1 mg L⁻¹, n = 5).

$7.08 \pm 0.07 \times 10^{-6} \text{ cm}^2 \text{ s}^{-1}$ for As^{III}, $6.16 \pm 0.13 \times 10^{-6} \text{ cm}^2 \text{ s}^{-1}$ for As^V, $6.13 \pm 0.17 \times 10^{-6} \text{ cm}^2 \text{ s}^{-1}$ for MMA and $5.74 \pm 0.16 \times 10^{-6} \text{ cm}^2 \text{ s}^{-1}$ for DMA. Diffusion coefficients of individual species vary widely in many studies [3,4,13–15] and closest to our results were those stated by Price et al. [30] with $7.45 \times 10^{-6} \text{ cm}^2 \text{ s}^{-1}$ for As^{III} and $6.05 \times 10^{-6} \text{ cm}^2 \text{ s}^{-1}$ for As^V. Compared to Gorny et al. [4], the same downward trend in the mobility of arsenic species was obtained in this study (As^{III} > As^V = MMA > DMA). These results also agree with the molar masses of each arsenic species. Differences in the diffusion course of individual arsenic species could be also explained by their different hydration size. Arsenite species are at pH 5.0 represented by neutral form H₃AsO₃ while arsenate species are represented by H₂AsO₄⁻ (pH 2–7) as shown in the distribution diagrams (Fig. 4) created by the Medusa Software (Royal Institute of Technology, Sweden). More dissociated species are characterized by a thicker hydration layer, which causes their slower diffusion through the diffusive layer [31–33].

Since there are differences in the diffusion coefficients of

individual arsenic species, it may be difficult to choose which one should be used for the determination of total arsenic concentration without the knowledge of its speciation in real ecosystems. The use of the average diffusion coefficient ($6.41 \times 10^{-6} \text{ cm}^2 \text{ s}^{-1}$) calculated from the highest and lowest D values presented in this work only generate 11.6% error in terms of underestimation of DMA concentration. In the case of 100% representation of As^{III} in the sample, its concentration would be overestimated by 9.5%. This level of uncertainty is two times lower than the one stated by Österlund et al. [34] who determined D values of the same arsenic species for ferrihydrite-backed resin gel. Therefore, the use of average diffusion coefficient is acceptable for the determination of total arsenic contamination in real ecosystems.

3.5. External influences on as species uptake by DGT

3.5.1. Influence of pH

The influence of pH in the range of 1.5–11.0 on the diffusion coefficients of individual arsenic species was monitored (Fig. 5A).

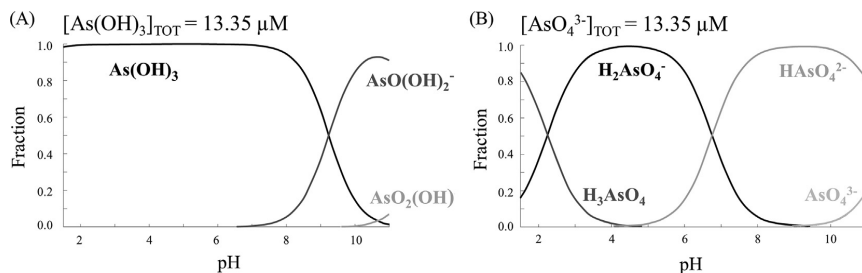


Fig. 4. Distribution diagram of arsenite (A) and arsenate (B) fractions under different pH conditions.

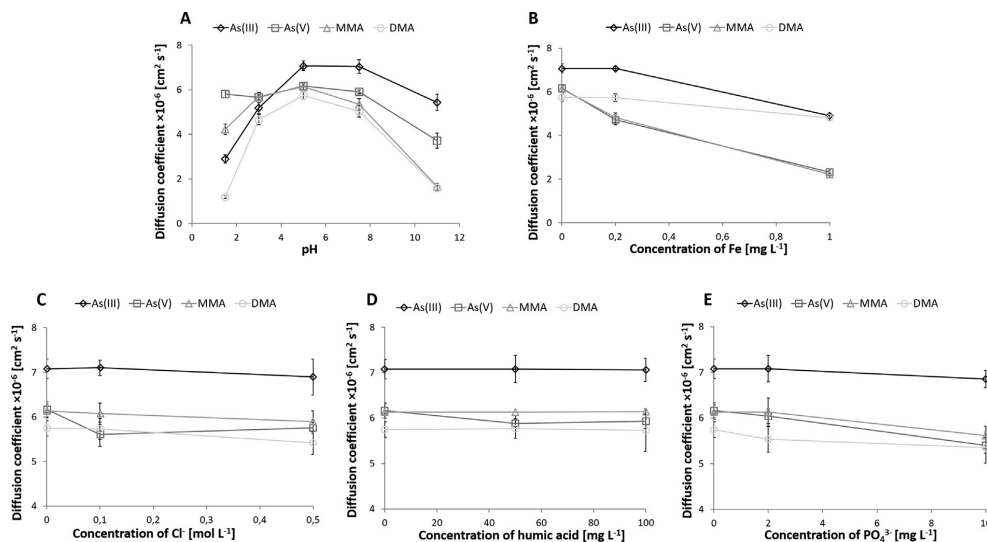


Fig. 5. Influence of pH (A), iron (B), chlorides (C), humic acid (D) and phosphates (E) on the diffusive coefficients of arsenic species (arsenic species concentration 1 mg L^{-1} , accumulation time 4 h, $n = 5$).

No statistically significant difference ($p > 0.05$) in the diffusion coefficients of individual arsenic species was observed in the pH range 4–8. In strongly acidic conditions, a decrease in diffusion coefficients was observed for As^{III} (pH < 4), MMA, and DMA (pH < 3). The diffusion coefficient of As^{IV} remained stable up to pH of 1.5. In strongly alkaline conditions, a decrease in the diffusion coefficients of all species was observed (pH = 9–11). Changes in the diffusion coefficients can be caused by the dissociation of all arsenic species as shown in Fig. 4. The observed decrease in D values in acidic conditions can be also caused by the dissolution of iron oxide-hydroxide at a pH lower than 4, which is also pointed out by the manufacturer of the Lewatit FO 36 resin. However, pH in natural water is in the range of 4–8 and therefore the Lewatit FO 36 resin gel can be considered suitable for field applications.

3.5.2. Influence of iron

The presence of ferric compounds in the aqueous environment affects the mobility of arsenic [35,36] and thus the influence of iron on the accumulation of arsenic by DGT units was investigated. Iron in the concentration range of 0–1 mg L^{-1} was used for the experiment. As shown in Fig. 5B, a statistically significant difference

($p < 0.05$) in the diffusion coefficients of all individual arsenic species was observed. The decrease in D values was caused by the binding of As species to iron, resulting in the loss of arsenic availability to DGT. However, with regard to the common concentrations of iron in natural water (less than 0.3 mg L^{-1} , rarely exceeds 1 mg L^{-1}) [37,38], the negative effect is considered not significant for As^{III} and DMA. Obtained results indicate that it is important to consider the influence of iron on the diffusion coefficient of arsenic species particularly in mineral water or wastewater, where higher concentrations of iron can occur.

3.5.3. Influence of chlorides

Lewatit FO 36 is a strongly basic anion-exchange resin and therefore the influence of commonly occurring anions was studied. Due to the high concentration of chlorides in natural water (common concentration of Cl^- in river water is less than 50 mg L^{-1} , majority of seawater contains $17\text{--}35 \text{ g L}^{-1}$ [39]), the influence of these anions was tested. No statistically significant difference ($p > 0.05$) in the diffusion coefficients of individual arsenic species was observed in the range of chlorides concentration 0–0.5 mol L^{-1} (Fig. 5C). These results indicate the possible application of Lewatit

Table 2

The comparison of the arsenic concentration obtained by DGT and by direct ET-AAS measurement.

Arsenic species	c_{DGT} (mg L ⁻¹) ^a	c_{SOL} (mg L ⁻¹) ^b	c_{DGT}/c_{SOL}
As ^{III}	1.02 ± 0.03	1.02 ± 0.02	0.99 ± 0.01
As ^V	1.03 ± 0.03	1.04 ± 0.02	0.99 ± 0.01
MMA	1.08 ± 0.05	1.04 ± 0.01	1.04 ± 0.03
DMA	1.01 ± 0.04	1.02 ± 0.02	0.99 ± 0.01

^a Measured by DGT (5 replicates) using diffusion coefficients determined at 0.20 mg L⁻¹ Fe (7.08×10^{-6} cm² s⁻¹ for As^{III}, 4.73×10^{-6} cm² s⁻¹ for As^V, 4.82×10^{-6} cm² s⁻¹ for MMA, 5.74×10^{-6} cm² s⁻¹ for DMA).

^b Measured directly by ET-AAS.

FO 36 resin gels even in high salinity natural waters.

3.5.4. Influence of humic acid

Humic acid (HA) together with fulvic acid (FA) are two main fractions of dissolved organic matter (DOM). The concentration of DOM varies widely in natural water sources, especially in backwater, lakes or ponds, where it could reach the concentration up to 60 mg L⁻¹ [40]. The effect of the presence of humic acid was investigated because it can form complexes with arsenic and thus influence its mobility (Fig. 5D) [40,41]. No statistically significant difference ($p > 0.05$) in the diffusion coefficients of individual arsenic species was observed in the range of humic acid concentration 0–100 mg L⁻¹. These results correspond to those stated by Panther et al. [3] for iron-hydroxide gel.

3.5.5. Influence of phosphates

According to the manufacturer, the sorption abilities of Lewatit FO 36 resin should not be influenced by the presence of anions such as chlorides, sulfates, and nitrates. Nevertheless, the presence of phosphates can cause competition of arsenic accumulation, because phosphorus and arsenic are chemical analogs which form similar molecules. Therefore, competitive inhibition of arsenate accumulation in the presence of phosphate can be assumed [42,43]. Diffusion coefficients of all arsenic species showed a slight downward trend with the increasing phosphate concentration (Fig. 5E). A statistically significant difference ($p < 0.05$) in D values of As^V and MMA (by 12.4% and 8.4%, respectively) was observed at phosphates

concentration of 10 mg L⁻¹. This is due to the similarity of As^V and methylated MMA chemical structures to phosphate. No statistically significant difference ($p > 0.05$) in the diffusion coefficients of As^{III} and DMA was observed. The presence of phosphates can affect the sorption of arsenic, but with regard to common phosphate concentrations in natural water which are generally very low (1–24 µg L⁻¹ in major rivers [44]), this effect can be considered neglectable. However, consideration should be given to the phosphate content in the case of wastewater analysis.

3.6. Real samples

3.6.1. Laboratory evaluation of Lewatit FO 36 gel on the river sample

To evaluate the performance of Lewatit FO 36-DGT-AAS method for the determination of arsenic contamination, the DGT devices were deployed in the natural water sample under laboratory conditions. Due to the natural content of arsenic in the Svratka river water below the limit of detection (LOD = 1.1 µg L⁻¹), samples were spiked with individual arsenic species. No other treatment of water sample was made to preserve its natural properties.

The comparison of the arsenic concentration directly measured by ET-AAS in the solution (c_{SOL}) and concentration obtained by DGT units (c_{DGT}) using Eq. (3) is shown in Table 2. Since the river water contained 0.19 mg L⁻¹ Fe, the diffusion coefficients of As^V and MMA determined in the presence of 0.20 mg L⁻¹ Fe were used for the calculation of c_{DGT} . Because the diffusive coefficients of As^{III} and DMA are not influenced by this iron concentration, those D values determined in 0.01 M NaNO₃ solution were used for calculations.

Using these D values, good agreement between c_{DGT} and c_{SOL} was observed for all arsenic species. Based on these results, it can be assumed that the method provides accurate results and can be used for applications in real ecosystems.

3.6.2. In-situ application of Lewatit FO 36 resin gel

Good linearity of arsenic mass accumulated on the Lewatit FO 36 resin gels up to 14 days was obtained. Arsenic accumulation during longer immersion of DGT units (49 days) was influenced by the formation of biofilm on the DGT units, which led to the 6.1% decrease of accumulated mass (Fig. 6). In order to avoid the influence of slow water flow in the Zákalská water reservoir on the

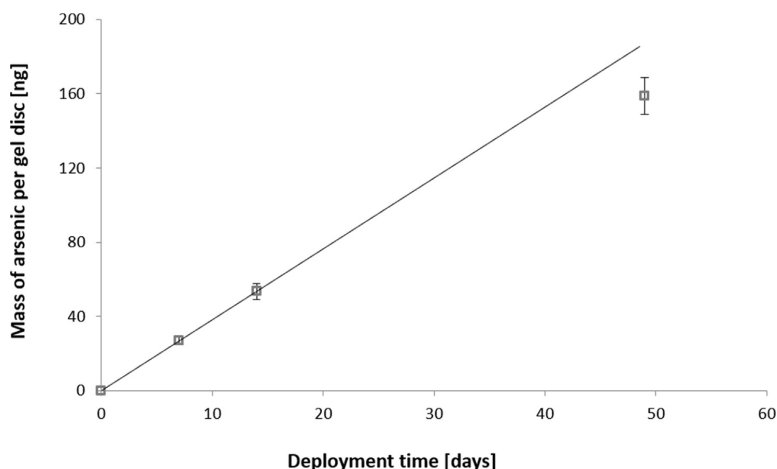


Fig. 6. Accumulation of arsenic in the Zákalská water reservoir.

sorption of arsenic, the diffusion coefficient was calculated from the dependence of accumulated arsenic mass on the time of each sampling (7, 14 and 49 days) using Eq. (1). The obtained D value $2.20 \times 10^{-6} \text{ cm}^2 \text{ s}^{-1}$ was used for the calculation of c_{DGT} . The arsenic concentration measured by Lewatit FO 36-DGT after 14 days was $0.59 \pm 0.08 \mu\text{g L}^{-1}$, while the concentration of arsenic in Zászkalská water after its pre-concentration was $0.54 \pm 0.03 \mu\text{g L}^{-1}$. There was a good agreement between c_{DGT} and c_{SOL} values with the relative deviation of 10.4%.

4. Conclusions

This study presents the use of newly created DGT resin gel utilizing the ion-exchange resin Lewatit FO 36. The Lewatit FO 36 resin gel is characterized by homogeneous gel structure with excellent reproducibility and low time-consuming production. The high sorption capacity ($\sim 535 \mu\text{g gel disc}^{-1}$) of Lewatit FO 36 gel towards four arsenic species (As^{III} , As^{V} , MMA, DMA) suggests its possible long-term application (up to 286 days in the environment with the arsenic concentration of $100 \mu\text{g L}^{-1}$) to obtain time-weighted average concentrations of arsenic in natural waters. This allows obtaining more representative results than simple grab sampling. The sorption abilities of Lewatit FO 36 gel remained stable in the pH range 4–8 relevant to natural waters. Diffusion coefficients of all tested arsenic species were influenced neither by high concentrations of chlorides nor by humic acid. Only a very high concentration of phosphates (10 mg L^{-1}) caused a slight decrease in the diffusion coefficients of As^{V} and MMA species (12.4% and 8.4%, respectively), while those of As^{III} and DMA remained stable. With respect to common iron concentrations in natural water (less than 0.3 mg L^{-1}), the influence of iron presence is negligible for the determination of As^{III} and DMA. However, it is important to consider the influence of iron on the diffusion coefficients of arsenic species particularly in areas, where higher concentrations of iron can occur and consequently to select the appropriate diffusion coefficient for calculations. However, the Lewatit FO 36-DGT-AAS method provided excellent results in the determination of arsenic content in the real river water and during a long term (up to 49 days) *in-situ* application in the Zászkalská water reservoir.

Author contribution

Vendula Smolíková: Investigation, Conceptualization, Validation, Methodology, Formal analysis, Writing – Original Draft, Visualization. Pavlína Pelcová: Conceptualization, Supervision, Methodology, Writing – Review & Editing, Resources. Andrea Ridošková: Conceptualization, Supervision, Writing – Review & Editing, Resources. Josef Hedbávný: Methodology. Jan Grmela: Investigation.

Declaration of competing interest

The authors declare that they have no known competing financial interests or personal relationships that could have appeared to influence the work reported in this paper.

Acknowledgements

This work was supported by the CEITEC 2020 (LQ1601), IGA MENDELÚ grant (no. AF-IGA2019-IP055), and by the project PRO-FISH CZ.02.1.01/0.0/0.0/16_019/0000869, which is financed by the European Regional Development Fund in the Operational Programme Research, Development and Education and The Czech Ministry of Education, Youth and Sports. We are also grateful to Lanxess CEE s.r.o. and RADKA spol. s.r.o. Pardubice for providing the

Lewatit FO 36 resin sample.

References

- [1] R. Singh, S. Singh, P. Parihar, V.P. Singh, S.M. Prasad, Arsenic contamination, consequences and remediation techniques: a review, *Ecotoxicol. Environ. Saf.* 112 (2015) 247–270.
- [2] A. Sattar, S. Xie, M.A. Hafeez, X. Wang, H.I. Hussain, Z. Iqbal, Y. Pan, M. Iqbal, M.A. Shabbir, Z. Yuan, Metabolism and toxicity of arsenicals in mammals, *Environ. Toxicol. Pharmacol.* 48 (2016) 214–224.
- [3] J.G. Panther, K.P. Stillwell, K.J. Powell, A.J. Downard, Development and application of the diffusive gradients in thin films technique for the measurement of total dissolved inorganic arsenic in waters, *Anal. Chim. Acta* 622 (1–2) (2008) 133–142.
- [4] J. Corny, L. Lesven, G. Billon, D. Dumoulin, C. Noiriél, C. Pirovano, B. Made, Determination of total arsenic using a novel Zn-ferrite binding gel for DGT techniques: application to the redox speciation of arsenic in river sediments, *Talanta* 144 (2015) 890–898.
- [5] M. Kumaresan, P. Riyazuddin, Overview of speciation chemistry of arsenic, *Curr. Sci.* (2001) 837–846.
- [6] K.F. Akter, G. Owens, D.E. Davey, R. Naidu, Arsenic Speciation and Toxicity in Biological Systems, *Reviews of Environmental Contamination and Toxicology*, Springer, 2005, pp. 97–149.
- [7] L. Ascar, I. Ahumada, P. Richter, Influence of redox potential (Eh) on the availability of arsenic species in soils and soils amended with biosolid, *Chemosphere* 72 (10) (2008) 1548–1552.
- [8] W. Zhai, M.T. Wong, F. Luo, M.Z. Hashmi, X. Liu, E.A. Edwards, X. Tang, J. Xu, Arsenic methylation and its relationship to abundance and diversity of *arsM* genes in composting manure, *Sci. Rep.* 7 (2017) 42198.
- [9] C. Li, S. Ding, L. Yang, Y. Wang, M. Ren, M. Chen, X. Fan, E. Lichtfouse, Diffusive gradients in thin films: devices, materials and applications, *Environ. Chem. Lett.* (2018) 1–31.
- [10] H. Dočekalová, P. Skarpa, B. Dočekal, Diffusive gradient in thin films technique for assessment of cadmium and copper bioaccessibility to radish (*Raphanus sativus*), *Talanta* 134 (2015) 153–157.
- [11] J. Luo, H. Zhang, J. Santner, W. Davison, Performance characteristics of diffusive gradients in thin films equipped with a binding gel layer containing precipitated ferrihydrite for measuring arsenic (V), selenium (VI), vanadium (V), and antimony (V), *Anal. Chem.* 82 (21) (2010) 8903–8909.
- [12] J.-M. Garnier, J. Garnier, D. Jézéquel, B. Angeletti, Using DET and DGT probes (ferrihydrite and titanium dioxide) to investigate arsenic concentrations in soil porewater of an arsenic-contaminated paddy field in Bangladesh, *Sci. Total Environ.* 536 (2015) 306–315.
- [13] Q. Sun, J. Chen, H. Zhang, S. Ding, Z. Li, P.N. Williams, H. Cheng, C. Han, L. Wu, C. Zhang, Improved diffusive gradients in thin films (DGT) measurement of total dissolved inorganic arsenic in waters and soils using a hydrous zirconium oxide binding layer, *Anal. Chem.* 86 (6) (2014) 3060–3067.
- [14] F. Tan, X. Jiang, X. Qiao, D. Sun, J. Gao, X. Qian, J. Chen, S. Ren, Y. Wang, Development of cerium oxide-based diffusive gradients in thin films technique for *in-situ* measurement of dissolved inorganic arsenic in waters, *Anal. Chim. Acta* 1052 (2019) 65–72.
- [15] W.W. Bennett, P.R. Teasdale, J.G. Panther, D.T. Welsh, D.F. Jolley, New diffusive gradients in a thin film technique for measuring inorganic arsenic and selenium (IV) using a titanium dioxide based adsorbent, *Anal. Chem.* 82 (17) (2010) 7401–7407.
- [16] A.M. Rolisola, C.A. Suárez, A.A. Menegário, D. Gastmans, C.H. Kiang, C.D. Colaço, D.L. Garcez, R.E. Santelli, Speciation analysis of inorganic arsenic in river water by Amberlite IRA 910 resin immobilized in a polyacrylamide gel as a selective binding agent for As^{V} in diffusive gradient thin film technique, *Analyst* 139 (17) (2014) 4373–4380.
- [17] W.W. Bennett, P.R. Teasdale, J.G. Panther, D.T. Welsh, D.F. Jolley, Speciation of dissolved inorganic arsenic by diffusive gradients in thin films: selective binding of As^{III} by 3-mercaptopropyl-functionalized silica gel, *Anal. Chem.* 83 (21) (2011) 8293–8299.
- [18] A.R. Lucas, N. Reid, S.U. Salmon, A.W. Rate, technology, Quantitative assessment of the distribution of dissolved Au, as and Sb in groundwater using the diffusive gradients in thin films technique, *Environ. Sci.* 48 (20) (2014) 12141–12149.
- [19] J.G. Panther, W.W. Bennett, D.T. Welsh, P.R. Teasdale, Simultaneous measurement of trace metal and oxyanion concentrations in water using diffusive gradients in thin films with a Chelex–Metsorb mixed binding layer, *Anal. Chem.* 86 (1) (2014) 427–434.
- [20] T. Huynh, H. Zhang, B. Noller, Evaluation and application of the diffusive gradients in thin films technique using a mixed-binding gel layer for measuring inorganic arsenic and metals in mining impacted water and soil, *Anal. Chem.* 84 (22) (2012) 9988–9995.
- [21] A. Stockdale, W. Davison, H. Zhang, High-resolution two-dimensional quantitative analysis of phosphorus, vanadium and arsenic, and qualitative analysis of sulfide, in a freshwater sediment, *Environ. Chem.* 5 (2) (2008) 143–149.
- [22] L. Xu, Q. Sun, S. Ding, M. Gong, C. Zhang, Simultaneous measurements of arsenic and sulfide using diffusive gradients in thin films technique (DGT), *Environ. Geochem. Health* 40 (5) (2018) 1919–1929.
- [23] A. Kreuzeder, J. Santner, T. Prohaska, W.W. Wenzel, Gel for simultaneous chemical imaging of anionic and cationic solutes using diffusive gradients in

- thin films, *Anal. Chem.* 85 (24) (2013) 12028–12036.
- [24] Y. Wang, S. Ding, L. Shi, M. Gong, S. Xu, C. Zhang, Simultaneous measurements of cations and anions using diffusive gradients in thin films with a ZrO-Chelex mixed binding layer, *Anal. Chim. Acta* 972 (2017) 1–11.
- [25] H. Zhang, W. Davison, R. Gadi, T. Kobayashi, In situ measurement of dissolved phosphorus in natural waters using DGT, *Anal. Chim. Acta* 370 (1) (1998) 29–38.
- [26] H. Zhang, W. Davison, Diffusional characteristics of hydrogels used in DGT and DET techniques, *Anal. Chim. Acta* 398 (2–3) (1999) 329–340.
- [27] V. Smolíková, P. Pelcová, J. Hedbávný, L. Zlámalová, A. Ridošková, Modification of electrothermal atomic absorption spectrometry for determination of arsenic in high salinity samples, in: *MendelNet 2018: Proceedings of International PhD Students Conference, Brno, 2018*, pp. 527–531.
- [28] H. Zhang, W. Davison, Performance characteristics of diffusion gradients in thin films for the in situ measurement of trace metals in aqueous solution, *Anal. Chem.* 67 (19) (1995) 3391–3400.
- [29] P.L. Smedley, D. Kinniburgh, A review of the source, behaviour and distribution of arsenic in natural waters, *Appl. Geochem.* 17 (5) (2002) 517–568.
- [30] H.L. Price, P.R. Teasdale, D.F. Jolley, An evaluation of ferrihydrite-and Met-sorb™-DGT techniques for measuring oxyanion species (As, Se, V, P): effective capacity, competition and diffusion coefficients, *Anal. Chim. Acta* 803 (2013) 56–65.
- [31] S. Liu, N. Qin, J. Song, Y. Zhang, W. Cai, H. Zhang, G. Wang, H. Zhao, A nanoparticulate liquid binding phase based DGT device for aquatic arsenic measurement, *Talanta* 160 (2016) 225–232.
- [32] Y. Takahashi, M. Sakamitsu, M. Tanaka, Diffusion coefficients of arsenate and arsenite in water at various pH, *Chem. Lett.* 40 (10) (2011) 1187–1188.
- [33] M. Tanaka, Y. Takahashi, N. Yamaguchi, K.-W. Kim, G. Zheng, M. Sakamitsu, The difference of diffusion coefficients in water for arsenic compounds at various pH and its dominant factors implied by molecular simulations, *Geochem. Cosmochim. Acta* 105 (2013) 360–371.
- [34] H. Österlund, M. Faaninen, J. Ingri, D.C. Baxter, Contribution of organic arsenic species to total arsenic measurements using ferrihydrite-backed diffusive gradients in thin films (DGT), *Environ. Chem.* 9 (1) (2012) 55–62.
- [35] J. Farrell, B.K. Chaudhary, Understanding arsenate reaction kinetics with ferric hydroxides, *Environ. Sci. Technol.* 47 (15) (2013) 8342–8347.
- [36] H. Amiri, N. Jaafarzadeh, M. Ahmadi, S.S. Martínez, Application of LECA modified with Fenton in arsenite and arsenate removal as an adsorbent, *Desalination* 272 (1–3) (2011) 212–217.
- [37] W. Xing, G. Liu, Iron biogeochemistry and its environmental impacts in freshwater lakes, *Fresenius Environ. Bull.* 20 (6) (2011) 1339–1345.
- [38] A. Rabajczyk, J. Namieśnik, Speciation of iron in the aquatic environment, *Water Environ. Res.* 86 (8) (2014) 741–758.
- [39] A.C. Twort, D.D. Ratnayaka, M.J. Brandt, *Water Supply*, 2000. <https://vannpiseth.files.wordpress.com/2015/07/water-supply-1.pdf>.
- [40] S. McDonald, A.G. Bishop, P.D. Prenzler, K. Robards, Analytical chemistry of freshwater humic substances, *Anal. Chim. Acta* 527 (2) (2004) 105–124.
- [41] H. Fakour, T.-F. Lin, Experimental determination and modeling of arsenic complexation with humic and fulvic acids, *J. Hazard Mater.* 279 (2014) 569–578.
- [42] Z. Wu, H. Ren, S.P. McGrath, P. Wu, F.-J. Zhao, Investigating the contribution of the phosphate transport pathway to arsenic accumulation in rice, *Plant Physiol.* 157 (1) (2011) 498–508.
- [43] R. Knodle, P. Agarwal, M. Brown, From phosphorous to arsenic: changing the classic paradigm for the structure of biomolecules, *Biomolecules* 2 (2) (2012) 282–287.
- [44] M. Meybeck, Carbon, nitrogen, and phosphorus transport by world rivers, *Am. J. Sci.* 282 (4) (1982) 401–450.

5.2 Evaluation of arsenic bioavailability in mineral springs (Czech Republic) using Lewatit FO 36-DGT technique

Smolíková, V., Sedláčková, E., Pelcová, P., Ridošková, A., Musilová, B. Determination of arsenic bioavailability in mineral springs in the Czech Republic. In: MendelNet 2019: Proceedings of International PhD Students Conference, Brno, 2019, Vol. 26, pp. 636-641.

The DGT technique is considered an effective tool for the determination of bioavailability of various contaminants in the environment [6, 283]. The bioavailability of metals is influenced by water quality parameters (*i.e.*, pH, ionic strength, Eh, presence of organic matter, presence of other compounds which can either compete for binding sites or form complexes with metals) that together create specific conditions for the formation of different metal species [69]. Mobility and lability of arsenic are strongly influenced by the presence of iron in the solution [284]. Increased concentration of Fe(III) in the solution, thus also the concentration of FeO(OH) colloids, increases the colloidal As fraction which may have lower lability. The formation of As colloids is also significantly influenced by the presence of organic matter (humic substances such as humic and fulvic acids). If for example, fulvic acid is present in the same system, the sorption of As on Fe colloids may be limited – either by direct complexation of As and FA or by their competition for the binding sites on Fe colloids [228, 285]. The iron content in natural water is generally less than 0.3 mg L^{-1} (rarely exceeds 1 mg L^{-1}) [286, 287] and so the influence of iron on DGT performance is usually considered negligible. However, its content in mineral water may be elevated. For this reason, the availability of arsenic in two mineral springs Hronovka and Regnerka (Hronov, Czech Republic) that are characterized by naturally higher arsenic content was investigated by Lewatit FO 36-DGTs in this chapter.

Both mineral springs are characterized by naturally higher arsenic and iron content. The water from the underground aquifer is supplied by pipes and springs out from an

open tap which is available to the public. Since it was not possible to deploy DGTs *in-situ*, the water was sampled and delivered to the laboratory where the experiment was performed. The concentrations of As and Fe were analysed in both, filtered (0.45 μm) and unfiltered samples, in order to exclude the presence of a particulate phase of these elements. Subsamples of mineral water were taken directly on-site and compared with samples taken from the deployment containers at the beginning of laboratory experiments. No difference was found between the results showing both elements were present in the dissolved phase and no changes occurred during storage of the water used for experiments; however, this information was not included in the contribution. To evaluate the arsenic bioavailability, its DGT-determined concentration (c_{DGT}) was compared with As concentration in water grab sample (c_{GRAB}). Despite expectations, the resulting $c_{\text{DGT}}/c_{\text{GRAB}}$ ratio was 1.09 and 1.06 for mineral springs Hronovka and Regnerka, respectively. Arsenic was therefore fully DGT-available even though the iron content in mineral springs was 8.61 mg L^{-1} and 14.22 mg L^{-1} with molar ratios of $\text{Fe/As} = 65.9$ and 167.8 in Hronovka and Regnerka, respectively. It is therefore assumed that the composition of the mineral water (that generally contains a high concentration of sulphates, carbon dioxide, chlorides, or sulphides) prevents the complexation of arsenic and iron in the solution, and so the arsenic is completely available to Lewatit FO 36-DGTs.

This research was presented at the MendelNet2019 conference whose proceedings are regularly included in the Conference Proceedings Citation Index (Clarivate Analytics) and therefore, this peer-reviewed contribution was included as a part of this work as well. Moreover, this contribution was awarded as the best contribution in the section Applied Chemistry and Biochemistry.

Determination of arsenic bioavailability in mineral springs in the Czech Republic

Vendula Smolikova^{1,3}, Eliska Sedlackova^{1,3}, Pavlina Pelcova¹, Andrea Ridoskova¹,
Barbora Musilova²

¹Department of Chemistry and Biochemistry

²Department of Zoology, Fisheries, Hydrobiology and Apiculture

Mendel University in Brno

Zemedelska 1, 613 00 Brno

³Central European Institute of Technology

Brno University of Technology

Purkynova 123, 612 00 Brno

CZECH REPUBLIC

vendula.smolikova@mendelu.cz

Abstract: Mineral springs Hronovka and Regnerka located in the northeast Bohemia, Czech Republic are characteristic for high content of arsenic. The diffusive gradient in thin films technique (DGT) was used for determination of arsenic bioavailable fraction in both mineral water samples. Despite the high concentration of iron in both mineral water, the arsenic content measured by DGT (c_{DGT}) corresponded to the total arsenic concentration measured directly by ET-AAS in the grab sample of mineral water (c_{GRAB}) with the final ratio c_{DGT}/c_{GRAB} 1.09 for Hronovka, and 1.06 for Regnerka. These results indicate that the composition of the mineral water prevents the complexation of arsenic and iron and so arsenic in tested spring waters is completely bioavailable.

Key Words: arsenic, bioavailability, DGT, mineral spring

INTRODUCTION

In the Czech Republic, there are many natural mineral springs, some of which are traditionally used for their healing effects in spa towns. In the area of northeast Bohemia, we can find arsenic-rich mineral springs. According to the former Czechoslovakian national standard (ÚNMZ 1966) the mineral spring can be considered as arsenic spring if the arsenic content exceeds the limit of 0.7 mg/l. The current classification of mineral waters does not take into account the arsenic content (Česká Republika 2001). Legislation of the Czech Republic sets the maximum hygienic level of arsenic in drinking water to 10 µg/l (Česká Republika 2014), which is also consistent with recommendations of World Health Organization (WHO 2011).

Generally, arsenic in natural water is present in arsenite AsO_3^{3-} and arsenate AsO_4^{3-} oxoanion forms (Smedley and Kinniburgh 2002). The composition of mineral spring is influenced by the geological and hydrogeological location of the spring (Fugedi et al. 2010). Mineral water generally contains a high concentration of sulfates, carbon dioxide, chlorides or iron, which can affect the speciation and bioavailability of arsenic. In the surface geothermal waters rich in sulfides, arsenic is rather than oxyanions present as thioanions with the predominance of thioarsenates (Guo et al. 2017). The presence of ferric compounds in the aquatic environment also has a significant influence on the mobility of arsenic (Farrell et al. 2013) and thus the bioavailable fraction of arsenic can be lower compared to the total arsenic concentration in mineral springs.

In this study, the diffusive gradient in thin films technique (DGT) was used for determination of arsenic bioavailable fraction in the samples of mineral springs. The principle of the DGT technique is based on the diffusion of metals through a diffusive gel and their subsequent accumulation on a resin gel containing functional groups for targeted analytes. In real ecosystems, primarily mobile and labile forms of the metal, such as free and hydrated ions and complexes with natural ligands smaller than the pore size of the diffusion gel are able to diffuse through the diffusion gel and subsequently are bound in the resin gel (Zhang and Davison 2000). Resin gels containing iron oxyhydroxide functional

groups were used for arsenic determination. Iron oxyhydroxide is able to adsorb arsenite as well as arsenate compounds by ion-exchange mechanism and is commonly used for arsenic removal from drinking water (Giles et al. 2011).

MATERIAL AND METHODS

Reagents

All chemicals were of analytical grade or higher. Standard solution of As^{III} ($c = 1000 \pm 4 \text{ mg/l}$ in 2% (v/v) HNO_3 (Sigma-Aldrich, Germany)) was used for calibration. Palladium 10 g/l (Analytika, Czech Republic) was used as a matrix modifier for ET-AAS determination of arsenic, sodium tungsten dihydrate (Sigma-Aldrich, Germany) was used for graphite furnace surface coating. Test kit NANOCOLOR® Sulfate LR 200 (Macherey-Nagel, Germany) was used for photometric determination of sulfate. All solutions were prepared using Milli-Q water produced by Millipore Milli Q system (Millipore, Bedford, MA, USA), the 65% nitric acid (VWR, Czech Republic) was distilled by apparatus Type BSB-939IR (Berghof, Germany).

Acrylamide 40% (w/v) (Merck, Germany), ammonium persulfate (Honeywell Fluka, Germany), N,N,N',N'-tetramethylethylenediamine (TEMED) (Sigma-Aldrich, Germany), DGT cross-linker (2%) (DGT Research Ltd., UK) and iron oxyhydroxide based resin (Lanxess, Germany) were used for DGT gel preparation. Sodium chloride and sodium hydroxide (Penta, Czech Republic) were used as elution agent for the release of arsenic from resin gels.

Instrumentation and DGT devices

Measurement of arsenic was performed using atomic absorption spectrometer 280Z AA (Agilent Technologies, USA) with a graphite furnace atomizer and Zeeman background correction. The resonance line of As was set at 193.7 nm with a spectral bandwidth of 0.5 nm and the arsenic lamp (Agilent Technologies, USA) as a light source operated with a current 10 mA.

DGT pistons with an exposure area of 3.14 cm^2 (DGT Research Ltd., UK) and polyethersulfone membrane filters of $0.45 \mu\text{m}$ pore size and 0.013 cm thickness (Pall Corporation, USA) were used for experiments.

Diffusive and resin DGT gels

Diffusive gels consist of 10 ml of gel solution (15% of acrylamide, 0.3% of cross-linker and Milli-Q water), $70 \mu\text{l}$ of 10% (w/v) ammonium persulfate and $25 \mu\text{l}$ of TEMED and were produced according to the protocol stated in (Zhang and Davison 1999). Resin-containing gels were prepared in a similar manner with the addition of iron oxyhydroxide resin.

To elute the arsenic from DGT resin gel, the mixture of sodium hydroxide (10 g/l) and sodium chloride (10 g/l) in the combination with microwave-assisted extraction at 130°C for 16 min was used.

Determination of arsenic

The determination of As content in eluates of DGT resin gels was complicated by the loss of arsenic content during the pyrolysis step and interferences caused by the matrix of elution agent (10 g/l $\text{NaOH} + \text{NaCl}$). Therefore, the optimized ET-AAS method combining the palladium modifier (1% (v/v)), cool-down step (130°C) incorporated to temperature program and graphite tube coating by tungsten carbides was used. The parameters of ET-AAS method and procedure of arsenic determination are described in detail in Smolíková et al. The concentration of arsenic in the grab sample of mineral water was determined in the same way due to the high content of chlorides.

Samples

Samples of mineral springs Hronovka and Regnerka were collected in July 2019 in the park Jiráskovy sady, Hronov, Czech Republic. For direct determination of arsenic content, the samples were acidified to 1% (v/v) HNO_3 concentration (VWR, Czech Republic). All samples were collected to acid-cleaned glass bottles and stored refrigerated until analysis.

Figure 1 Mineral springs Hronovka and Regnerka (A) and their location (B) (<https://mapy.cz>)



Determination of bioavailable arsenic in mineral spring water

The DGT units (iron oxyhydroxide resin gel placed on the top of the plastic piston, covered by diffusive gel and membrane filter, and capped by outer sleeve with an exposure window) were deployed into 3 liters of the mineral water under constant stirring for 2, 4 and 6 h (5 replicates for each sampling time). After accumulation, the DGT units were removed from mineral water, disassembled and disks of resin gel were rinsed with Milli-Q water and eluted. The concentration of arsenic in the eluate represents the arsenic mass accumulated per resin gel disk (M , ng). This value was used for calculation of the arsenic concentration in mineral spring determined by DGT (c_{DGT} , $\mu\text{g/l}$) using Equation (1), where Δg is the thickness of diffusive layer (0.093 cm), D is the diffusion coefficient of the analyte, A is the exposed area (3.14 cm^2) and t is the deployment time (e.g., 21,600 s). Since arsenic speciation analysis was not performed, the average diffusion coefficient ($D = 6.41 \times 10^{-6} \text{ cm}^2 \text{ s}^{-1}$, determined in 0.01 M NaNO_3 solution (pH 5.0)) of four arsenic species (As^{III} , As^{V} , monomethylarsonic acid, and dimethylarsinic acid) which are available for iron oxyhydroxide resin gel was used for calculations.

$$c_{DGT} = \frac{M \Delta g}{D A t} \quad (1)$$

To evaluate the bioavailable fraction of arsenic in mineral spring water, the c_{DGT} value was then compared to the arsenic concentration measured directly by ET-AAS in the grab sample of mineral water (c_{GRAB}).

RESULTS AND DISCUSSION

Characterization of mineral water samples

Samples of mineral springs Hronovka and Regnerka were characterized by determination of pH, iron (determined by F-AAS Agilent Technologies, USA), sulfates, phosphates, chlorides, nitrates and nitrites (Horáková 2007) (Table 1).

Table 1 Characterization of mineral springs Hronovka and Regnerka

	Hronovka	Regnerka
pH	6.45	6.13
Fe [mg/l]	8.61	14.22
SO_4^{2-} [mg/l]	61.0	58.0
PO_4^{3-} [mg/l]	0.07	0.05
Cl^- [mg/l]	61.35	78.22
NH_4^+ [mg/l]	0.39	0.29
NO_3^- [mg/l]	0.13	< LOD
NO_2^- [mg/l]	0.13	0.09
Conductivity [$\mu\text{S/cm}$]	1570	1714

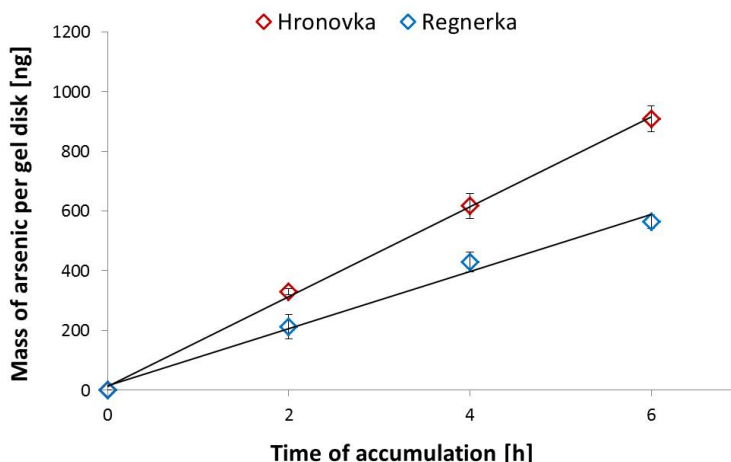
Legend: LOD – Limit of detection = 0.1 mg/l

The high concentration of iron in both samples could influence the availability of arsenic towards DGT. The previous laboratory experiments showed that the availability of arsenic towards iron oxyhydroxide resin gel is decreased by ~22% when 1 mg/l Fe^{3+} is added to the 0.01 mol/l NaNO_3 solution (pH 5.0) which is used as a standard environment for determination of diffusion coefficients of DGT resin gels.

Time-dependence experiment

Time-dependence experiment (Figure 2) was performed because the linearity of target analyte accumulation over time is the fundamental assumption of the DGT use.

Figure 2 Time-dependence experiment



The results showed that the mass of arsenic accumulated per gel disk increased linearly over the accumulation time, with a coefficient of determination $R^2 = 0.990\text{--}0.999$ for Hronovka and Regnerka, respectively. The linear course of arsenic accumulation on DGT resin gels indicates the steady-state flux of analyte under perfect sink conditions was achieved and there was no factor adversely affecting the arsenic accumulation into DGT unit (e.g., competition, saturation, kinetic effects).

Determination of bioavailable arsenic

In order to compare the concentration of arsenic measured by DGT (c_{DGT}) to the concentration measured directly by ET-AAS in the grab sample of mineral water (c_{GRAB}), the ratio of both values was calculated (Table 2).

Table 2 The comparison of the arsenic concentration obtained by DGT and by direct ET-AAS measurement

	c_{DGT} ($\mu\text{g/l}$)	c_{GRAB} ($\mu\text{g/l}$)	$c_{\text{DGT}}/c_{\text{GRAB}}$
Hronovka	192.54 ± 9.18	175.18 ± 10.51	1.09
Regnerka	120.81 ± 4.83	113.71 ± 9.32	1.06

Because speciation analysis of arsenic compounds was not performed, the average diffusion coefficient of four arsenic species was used for the calculations of c_{DGT} . The use of this D value can only generate a maximum error of 11.6% compared to the result obtained when using the diffusion coefficient of particular arsenic species. Nevertheless, the obtained ratios close to 1.00 indicates that the bioavailable fraction of arsenic concentration determined by DGT corresponds to the total arsenic concentration analyzed in grab sample of mineral water. Although previous laboratory experiments with standard solutions containing only arsenic and iron led to the reduction of arsenic availability to DGT, in real samples of mineral spring water the arsenic was fully available to the DGT despite the naturally high concentration of iron in both samples of mineral spring water. It is assumed

that this phenomenon is caused by the presence of other components (e.g., sulfates, phosphates) in the samples. The effect of sulfates and phosphates on arsenic accumulation to ferric oxide has been described in the literature (Wilkie and Hering 1996, Youngran et al. 2007).

CONCLUSION

Bioavailability of arsenic in two mineral springs Hronovka and Regnerka was evaluated using diffusive gradient in thin films technique. The linear accumulation of arsenic on iron oxyhydroxide resin gel over time indicated that the DGT measurement had a quantitative character. Although it was expected that the bioavailability of arsenic in mineral water will be reduced by the high iron content, the obtained ratios of C_{DGT}/C_{GRAB} showed that the bioavailable fraction of arsenic determined by DGT corresponds to the total arsenic concentration in grab sample in mineral water. For this reason, it is assumed that the composition of the mineral water prevents the complexation of arsenic and iron, and so arsenic is completely available to DGT as well as to the biota.

ACKNOWLEDGEMENTS

This research has been supported by grant no. AF-IGA2019-IP055 and by the Ministry of Education, Youth and Sports of the Czech Republic under the project CEITEC 2020 (LQ1601).

REFERENCES

- Česká Republika. 2001. Vyhláška Ministerstva zdravotnictví č. 423/2001 Sb., kterou se stanoví způsob a rozsah hodnocení přírodních léčivých zdrojů a zdrojů přírodních minerálních vod a další podrobnosti jejich využívání, požadavky na životní prostředí a vybavení přírodních léčebných lázní a náležitosti odborného posudku o využitelnosti přírodních léčivých zdrojů a klimatických podmínek k léčebným účelům, přírodní minerální vody k výrobě přírodních minerálních vod a o stavu životního prostředí přírodních léčebných lázní (vyhláška o zdrojích a lázních). In: Sbírka zákonů České republiky. Also available at: <https://www.zakonyprolidi.cz/cs/2001-423>. [2019-08-05].
- Česká republika. 2014. Vyhláška, kterou se mění vyhláška č. 252/2004 Sb., kterou se stanoví hygienické požadavky na pitnou a teplou vodu a četnost a rozsah kontroly pitné vody, ve znění pozdějších předpisů. In: Sbírka zákonů České republiky. Also available at: <https://www.zakonyprolidi.cz/cs/2014-8>. [2019-08-05].
- Farrel, J., Chaudhary, B.K. 2013. Understanding arsenate reaction kinetics with ferric hydroxides. *Environmental Science*, 47: 8342–8347.
- Fugedi, U. et al. 2010. Investigation of the hydrogeochemistry of some bottled mineral waters in Hungary. *Journal of Geochemical Exploration*, 107: 305–316.
- Giles, D.E. et al. 2011. Iron and aluminium based adsorption strategies for removing arsenic from water. *Journal of Environmental Management*, 92: 3011–3022.
- Guo, Q. et al. 2017. Arsenic and thioarsenic species in the hot springs of the Rehai magmatic geothermal system, Tengchong volcanic region, China. *Chemical Geology*, 453: 12–20.
- Horáková, M. 2007. *Analytika vody*. Praha: Skriptum VŠCHT.
- Smedley, P.L., Kinniburgh D. 2002. A review of the source, behaviour and distribution of arsenic in natural waters. *Applied Geochemistry*, 17(5): 517–568.
- Smolíková, V. et al. 2018. Modification of electrothermal atomic absorption spectrometry for determination of arsenic in high salinity samples. In *Proceedings of International PhD Students Conference MendelNet 2018* [Online]. Brno, Czech Republic, 7 November, Brno: Mendel University in Brno, Faculty of AgriSciences, pp. 527–531. Available at: <https://mendelnet.cz/pdfs/mnt/2018/01/112.pdf>. [2019-07-25].
- ÚNMZ. 1966. Přírodní léčivé vody a přírodní minerální vody stolní. Základní společná ustanovení. ČSN: 86 8000. Praha: Úřad pro technickou normalizaci, metrologii a státní zkušebnictví.
- Wilkie, J.A., Hering, J.G. 1996. Adsorption of arsenic onto hydrous ferric oxide: effects of adsorbate/adsorbent ratios and co-occurring solutes. *Colloids and Surfaces, A: Physicochemical and Engineering Aspects*, 107: 97–110.

WHO. 2011. Arsenic in drinking-water: Background document for development of WHO Guidelines for drinking-water quality.

Younggran, J. et al. 2007. Effect of competing solutes on arsenic (V) adsorption using iron and aluminum oxides. *Journal of Environmental Sciences*, 19: 910–919.

Zhang, H., Davison, W. 1999. Diffusional characteristics of hydrogels used in DGT and DET techniques. *Analytica Chimica Acta*, 398: 329–340.

Zhang, H., Davison, W. 2000. Direct in situ measurements of labile inorganic and organically bound metal species in synthetic solutions and natural waters using diffusive gradients in thin films. *Analytical Chemistry*, 72: 4447–4457.

5.3 Arsenic distribution and geochemistry in the Zenne River (Belgium)

Smolíková, V., Ma, T., Perrot, V., Brion, N., Gao, Y., Pelcová, P., Ridošková, A., Leermakers, M. The evolution of arsenic in the Zenne River (Belgium): distribution, geochemistry, and bioavailability. In preparation.

Water pollution by arsenic is given worldwide attention since the end of the 19th century. Historical data have relevance for the investigation of the As concentrations evolution which may signal water resource issues [288]. An example of an aquatic ecosystem whose pollution status has been monitored in a long-term is the Zenne River basin (Belgium). The Zenne represents a unique ecosystem as the river crosses a densely populated and industrial area of Brussels city and its downstream part is dominated by tidal influence. Before 2000, most of the sewage generated by the population was discharged to the river without any treatment. Fortunately, the water quality improved after the construction of wastewater treatment plants (WWTPs) in the Brussels area [289]. This is however not the case for As since no improvement was observed and peaking concentrations of As were repeatedly found in the Zenne or Scheldt rivers in the past [3, 290, 291]. For this reason, the summary of research findings is presented within this study aiming to:

- (i) assess the longitudinal profile of dissolved and particulate As distribution in the Zenne River and identify potential sources;
- (ii) evaluate the temporal changes of As in different sections of the river during dry periods, rain events and in the tidal section;
- (iii) assess the time-integrated average concentrations of labile As species using DGT;
- (iv) investigate the geochemical behaviour of As in sediment using porewater profiles, DGT profiles, and sequential extractions;
- (v) calculate fluxes of As in the Zenne River by combining data of waterflows and As concentrations as well as calculating benthic fluxes.

The results of this study revealed that downstream transport of As in the Zenne River is completely dominated by the presence of an important point source located on the tributary Tangebeek. After the confluence of Zenne with this tributary, the concentrations of As in water and sediments sharply increase. The point source results in a large temporal variability in the downstream tidal section of the Zenne River, where the water is diluted with Dijle water during rising tide. The DGT technique has been shown to be a beneficial tool for the measurement of time-weighted average concentrations in dynamic environments.

Arsenic in the sediments is mostly bound by reducible fraction and its porewater geochemistry is dominated by the reductive dissolution of Mn and Fe oxyhydroxides. The DGT-labile fraction of As accounts for 7–34% of the total dissolved As concentrations in porewater, indicating the presence of colloidal As species, which are not DGT-labile. As(III) dominates the speciation of labile As species in porewater. Although As porewater concentrations are significantly higher than the concentrations in the surface water, the calculated benthic fluxes only account for 1% of the downstream transport, highlighting the importance of the point source on the behaviour of As. For Supplementary Information see **Chapter 12.1**.



(Picture of the Zenne River taken during sampling in 2020).

Unravelling the mysteries of arsenic in the Zenne River (Belgium): sources, distribution, geochemistry, and bioavailability

Vendula Smolíková^{1,2}, Tianhui Ma¹, Vincent Perrot¹, Natacha Brion¹, Yue Gao¹, Pavlína Pelcová², Andrea Ridošková², Martine Leermakers¹

¹Analytical, Environmental and Geochemistry, Vrije Universiteit Brussel, Pleinlaan 2, Brussels, Belgium

²Department of Chemistry and Biochemistry, Mendel University in Brno, Zemedelska 1, CZ-613 00 Brno, Czech Republic

Abbreviations

CSO, combined sewer overflow; DGT, diffusive gradient in thin films technique; OM, organic matter; PW, porewater; SPM, suspended particulate matter.

Abstract

The distribution and geochemistry of arsenic (As) in water and sediments of the Zenne River, a small urban river flowing through Brussels (Belgium), were assessed on various occasions between 2010 and 2021. Although the water quality of Zenne has significantly improved in the last decades due to large investments in sewage water treatment, As concentrations remained unchanged. Concentrations of As sharply increase between Vilvoorde and Eppegem and are up to 6–8 times higher in comparison to the upstream part of the Zenne. The monitoring surveys revealed large temporal variability in As concentrations in the function of the tidal cycle. The diffusive gradients in thin films (DGT) technique using Metsorb, Lewatit FO 36, and ZrO₂ was used to assess total DGT labile species in surface waters and sediment porewater and DGT with 3-MFS was used for As(III) in porewater. Arsenic species are fully labile in surface waters as the DGT time-integrated concentrations of labile As species were in good agreement with the average concentrations calculated from the grab samplings. In sediment porewaters As is predominantly present as non-DGT labile species (66–93%) and the DGT labile As fraction is dominated by As(III). Flux calculations were performed to evaluate the relative importance of different As sources to the Zenne River and revealed the presence of a point source on a tributary of the Zenne River, the Tangebeek contributes for 87% of the As load carried by the Zenne River.

Keywords

Arsenic; Zenne River; Water; Sediment; Diffusive Gradients in Thin-films

1 Introduction

Arsenic is a ubiquitous metalloid that may enter the aquatic environment naturally (e.g., rock weathering or erosion, volcanic activity, biological activity) or as a result of anthropogenic activities (e.g., agriculture, industry, mining) [1, 2]. In natural waters and sediments, it is mostly present in inorganic form as trivalent arsenite AsO_3^{3-} (oxic conditions) or pentavalent and arsenate AsO_4^{3-} (anoxic conditions) [1, 3]. Although organic methylated compounds (monomethylarsonic acid MMA and dimethylarsinic acid DMA) or even larger As complexes such as arsenobetaine can also be found in the aquatic environment, the importance of inorganic As forms is related to their overall higher mobility and toxicity [4, 5]. To evaluate the ecotoxicological status of aquatic ecosystems and to gain further insight about As distribution and potential bioavailability to biota, the distinction between particulate and dissolved phases is usually made. Association with particles of different dimensions controls the transport of As (by diffusion, coagulation, or sedimentation) and results in diminished bioavailability [6]. On the contrary, the dissolved phase (separated by filtration on the pore size 0.20–0.45 μm) can be further divided into a colloidal fraction and truly dissolved fraction, which is closely linked to the fraction that is considered to be bioavailable [7-10]. The combination of various sampling approaches is therefore necessary to thoroughly evaluate the potential ecotoxicological impact on the environment.

The distribution of metals between particulate, colloidal, and dissolved species is influenced by the dynamics of the aquatic environment. In coastal zones and estuaries, the hydrodynamics is driven by the interaction between ocean tides and terrestrial runoffs that create areas of high turbidity, which subsequently influences the distribution of nutrients and trace elements [11, 12]. In their tidal sections, the biogeochemical cycles of trace elements significantly differ from their upstream parts due to the presence of a large amount of particulate matter and dynamic

changes in redox potential, ionic strength, salinity, and pH [13]. In macrotidal estuaries, the tidal influence also reaches much farther inland and affects the freshwater tributaries.

A great example of such a dynamic environment can be found in the Zenne River – a small urban river that originates in the Walloon part of Belgium and crosses the densely populated city of Brussels and industrial area downstream of Brussels. Although the river may seem average in terms of its length (105 km) and basin coverage (1160 km²) [14, 15], it represents a unique ecosystem which attracts attention in terms of its environmental status. Its upstream part is strongly influenced by agricultural activities (51% of the basin represented by arable land) while the downstream part is characterized by its urbanization (19% as the river crosses the densely populated capital city by about 20 km) and industrialization [15-17]. Since the Zenne is an indirect tributary of the Scheldt estuary through the Dijle and Rupel rivers, it represents a connection between terrestrial and marine ecosystems and is an important contributor regarding the pollution load [18]. Before 2000, most of the sewage generated by the population in the basin was discharged into the river without any treatment. Fortunately, the water quality improved after the application of the European Directive 91/271 on the treatment of urban wastewater [19] and construction and maintenance of wastewater treatment plants (WWTPs) in the Brussels area (WWTP Brussels South is in operation since 2000 and the WWTP Brussels North since 2007) [20]. However, the improvement of water quality observed within the last few decades does not apply to arsenic, since peaking concentrations were repeatedly reported by researchers in the past [14-17].

In this context, the distribution and geochemistry of As in the river Zenne have been investigated within the framework of several projects between the years 2010–2021. Various research approaches and techniques were applied for the analysis of As distribution and cycling in water and sediments. Filtration techniques were used for the separation of dissolved and particulate fractions of As, while the labile fraction of As was evaluated by the diffusive

gradients in thin-films (DGT) technique. Moreover, to assess the historical trends of water quality regarding As concentrations, and emission inventories, the data from Flemish Environmental Agency (Vlaamse Milieu Maatschappij – VMM) were evaluated. The aims of our study were: (i) to assess the longitudinal profile of dissolved and particulate As distribution in the Zenne River and identify potential sources; (ii) to evaluate the temporal changes of As in different sections of the river during dry periods, rain events and in the tidal section; (iii) to assess the time-integrated average concentrations of labile As species using DGT (iv) to investigate the geochemical behaviour of As in sediment using porewater profiles, DGT profiles, and sequential extractions and (v) to calculate fluxes of As in the Zenne River by combining data of waterflows and As concentrations as well as calculating benthic fluxes.

2 Materials and methods

2.1 Study site

The studied part of the Zenne River is located between Lembeek and the confluence with the Dijle River and has a length of about 60 km in total. The map of the studied area with sampling stations and their locations is shown in **Fig. 1** (the distance of each station related to the first station Z1 can be found in **Table S1**).

The area is divided into three parts – upstream of Brussels (stations Z1–Z3), the Brussels area (stations Z4–Z9), and downstream of Brussels (stations Z10–Z14). Two wastewater treatment plants are located in the Brussels area – WWTP South and WWTP North. Particularly important for this study is the area between 36 and 41 km, where the overflow from Canal Brussels-Rupel and the confluences with the Woluwe and Tangebeek rivers are located. The Tangebeek also carries the discharges of the WWTP Grimbergen. Tidal influence is visible in section between Z11 and Z14.

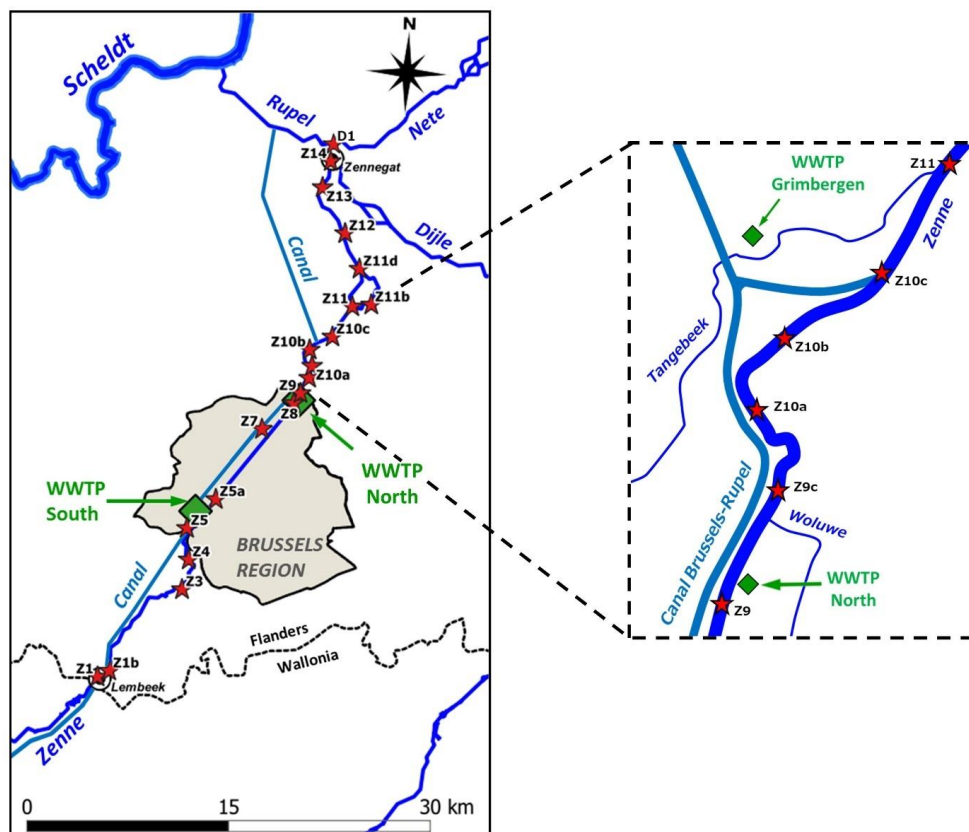


Fig. 1 Studied part of the Zenne River basin and sampling stations (Z1–Z14) between Lembeek and Zennegat with focus on the area 36 and 41 km, where the overflow from Canal Brussels-Rupel and the confluences with the Woluwe and Tangebeek rivers are located.

2.2 Sampling of water and sediments

Water samples were usually collected directly in the polyethylene (PE) 2L bottles or when necessary, from a bridge using a bucket on rope. The bottles were pre-cleaned by 1% HNO_3 for at least 24 h and thoroughly rinsed with MilliQ water and river water prior to use on-site. Water physico-chemical parameters (pH, temperature, conductivity, redox potential, dissolved O_2) were measured by multi-parameter instruments VWR MU 6100H and WTW 3430. Both working electrodes for pH and redox potential are combined with an Ag/AgCl ($[\text{KCl}] = 3 \text{ M}$)

reference electrode, with a potential equal to 220 mV versus the Standard Hydrogen Electrode (SHE). The redox potential values are expressed versus the SHE electrode (Eh vs SHE).

The sediments were sampled with the Van Veen grab sampler (for total concentrations) or using plexiglass tubes that were pushed into the sediment in order to obtain sediment core (for depth profiles). The pH and redox potential profiles were measured using plexiglass tubes with predrilled holes at 1 cm intervals. For analysis of the depth profiles, the sectioned core was used for samples collection and the sediments were sectioned at 2 cm intervals in a glove bag under a nitrogen atmosphere. Porewater samples were then taken using Rhizon samplers (Rhizosphere Research Products, Netherlands) from each section to analyze dissolved concentrations of As/Fe/Mn in porewater (As/Fe/Mn-PW).

2.3 Water samples processing

2.3.1 Determination of dissolved and particulate phase

To determine the particulate (As-SPM) and dissolved fraction (As-dis) of arsenic, 250–500 mL aliquot of water sample was filtered through the pre-weighed filter membranes with 0.45 μm pore size (Merck Millipore, Durapore®, HVLP grade) using the Nalgene filter unit with a vacuum filtration system. The 14 mL of the filtrate was then transferred to PE tube, acidified to 1% HNO_3 , and stored at 4 °C until analysis. The filters with the particulate fraction were dried in a laminar flow hood for 24 h and then weighed again. The mass difference of the filters was used for the calculation of suspended particulate matter (SPM, mg L^{-1}). To determine the concentration of particulate As fraction, the filters were digested in Teflon tubes at 70 °C using the mixture of concentrated HF (40% v/v), HCl (37% v/v), and HNO_3 (65% v/v) with the volume of 2, 3, and 1 mL, respectively. After 12 hours the samples were let to cool down, 15 mL of H_3BO_3 (4% v/v) was added to the mixture and heated again for another 3 hours. The resulting extract was transferred to PE tubes and stored at 4 °C until analysis. The resulting particulate concentration was expressed as mass of As per mass of SPM.

In order to evaluate the distribution of As between particulate and dissolved phase and its potential for migration, the distribution coefficient (K_{D-As} , L kg⁻¹) was calculated using the (1), where As-SPM is the concentration of particulate As (mg kg⁻¹) and As-dis is the concentration of dissolved As (mg L⁻¹).

$$K_{D-As} = As-SPM / As-dis \quad (1)$$

2.4 Sediment samples processing

2.4.1 Determination of total metal concentration

The total digestion was used to extract the total concentration of elements from the sediment solid phase. Sediment samples were digested in Teflon vials using a microwave oven (CEM Mars 5), working at a maximum power of 1200 W using a temperature-controlled program. To 0.1–0.2 g of sample, 4 mL concentrated HF (40% v/v), 6 mL of concentrated HNO₃ (65% v/v), and 2 mL of concentrated HCl (37% v/v) were added. The samples were gradually heated to 180 °C within 10 minutes and maintained at this temperature for another 10 minutes. After cooling down, 30 mL of H₃BO₃ (4% w/v) was added and the samples were digested again – gradually heated to 120 °C within 10 minutes and maintained at this temperature for 5 minutes. After digestion, the samples were transferred to 50 mL PE vials and stored at 4 °C until analysis.

2.4.2 Sequential extraction

To evaluate the association of As with the solid phase, the sequential extraction of the sediments was performed using the modified BCR procedure by Rauret et al. [21]. This consists of four consecutive steps (**A–D**) in which the different sediment phases are extracted by different extraction solutions: **A**) exchangeable and carbonate fraction – 0.11 mol L⁻¹ acetic acid solution; **B**) iron and manganese (oxyhydr)oxide fraction – 0.5 mol L⁻¹ hydroxylammonium chloride in 0.05 M HNO₃; **C**) organic and sulphide fraction – H₂O₂ 30% followed by dissolution in 1 mol L⁻¹ ammonium acetate solution; **D**) residual fraction – *aqua regia* (HCl 30% : HNO₃ 65% in a 3 : 1 ratio). The BCR protocol is not specific for As

fractionation but has been used because other elements were studied within the projects from which the data originates. However, the BCR protocol can still be used for the basic assessment of arsenic partitioning as the first extraction step provides sufficient estimation of the most labile forms of arsenic [22, 23].

2.4.3 Calculation of diffusive benthic fluxes

Diffusive transport of arsenic at the water-sediment interface was calculated based on the observed porewater profiles using Fick's first law of diffusion ((2):

$$F_D = -\Phi D_{sed} (dC / dx) \quad (2)$$

where the flux of an element (F_D) is given by the change in its concentration (dC) over a range in depth (dx) and its effective diffusion coefficient (D_{sed}) within the sediment of specified porosity (Φ). The effective diffusion coefficient in sediment is calculated from the diffusion coefficient in water corrected to *in-situ* temperature using the Stokes-Einstein equation (D_w) and sediment tortuosity (Θ) using ((3):

$$D_{sed} = D_w / \Theta^2 \quad (3)$$

$$\Theta^2 = 1 - \ln(\Phi^2) \quad (4)$$

The tortuosity is calculated from the sediment porosity ((4) which was calculated as the volume fraction of water in the total sediment volume [24-26].

2.5 Diffusive Gradients in Thin-films

The DGT technique was used to determine the labile fraction of As (As-DGT) in the water column and sediment porewater. Metsorb, Lewatit FO 36, ZrO_2 (for total As), 3-mercaptopropyl-functionalized silica (3-MFS; for As(III)), and Chelex-100 (for Fe and Mn) were used as binding phases of the DGT resin gels. The manufacturing protocol of the DGT gels, the elution procedure of each resin gel, and fundamental DGT calculations are described

in detail in the Supplementary Information. For deployment in water, the DGT pistons (4–6 replicates per resin gel) were loaded into Perspex open plates and enclosed in a polypropylene cage (perforation size 2 cm) to avoid their damage during the deployment. The cage was fitted with a weight on the bottom and attached to a buoy on the top to ensure the DGTs are submerged in water during tidal changes. The construction was then attached to the bridge by a nylon rope. For deployment in sediments, the DGT probes were deoxygenated by nitrogen purging in a 0.01 NaCl solution for at least 4 h prior to deployment. The probes were then vertically inserted *in-situ* in sediments (during low tide in tidal Zenne). The probes were generally arranged back-to-back, and part of the exposure window was left above the water-sediment interface to record As concentrations in the overlying water. The deployment time and water/sediment physico-chemical parameters at the beginning and end of the DGT deployment were recorded. After retrieving, the DGTs were rinsed with Milli-Q water and stored in zip-lock bags at 4 °C until disassembling in the laboratory.

2.6 Sample analysis

The analysis of trace elements was performed by Inductively Coupled Plasma-Sector Field Mass Spectrometry (ICP-SFMS) with an ELEMENT II (Thermo Instruments) using a concentric nebulizer (0.4ml/min), a cyclonic Peltier cooled spray chamber, quartz injector, and Ni cones. Indium (1ppb) was used as an internal standard. Quality control samples were run in each analysis. Standard reference materials SLRS-6 (river water, National Research Council Canada), SPS-SW2 (surface water level 2, Spectrapure Standards AS, Norway), and IAEA-405 (trace elements and methylmercury in estuarine sediment, International Atomic Energy Agency, Austria) were used. The concentrations of analysed elements (As, Fe, and Mn) in these reference materials were generally within the range of 10% of the certified values.

Analytical software STATISTICA13 (StatSoft) was used for data analysis. Pearson's correlation coefficient (r) was used to describe the relationship between parameters at the significance level of $\alpha = 0.05$.

2.7 Data collection

The data from the Flemish Environmental Agency (Vlaamse Milieu Maatschappij – VMM) obtained through the online data portals Geoview (www.geoloket.vmm.be/Geoviews/) and Waterinfo (www.waterinfo.be) were used. Water discharge data from the VMM water quality monitoring stations were selected to match the sampling periods performed within this study. The historical data of arsenic concentrations were used to evaluate the evolution of the water quality.

3 Results and discussion

3.1 Distribution of dissolved and particulate As in water along the Zenne River

The longitudinal profile of dissolved and particulate As between Lembeek (Z1, 0 km) and the mouth of the river (Z14, 58 km) was assessed in various campaigns between 2010–2013. The profiles of suspended particulate matter (SPM), pH, and conductivity are shown in **Fig. S1**. Here, the concentrations of SPM vary from 1.8 to 51.7 mg L⁻¹ and an increasing trend downstream of Brussels is observed in a majority of observations. Similarly, a slight increase in conductivity is observed at the end of the Brussels area (35 km). Contrary, the pH values decrease in this area and remain fairly constant in the tidal Zenne.

The concentrations of dissolved (As-dis) and particulate (As-SPM) arsenic are shown in **Fig. 2A+B**. General trends between the observed periods show, that As concentrations slightly decrease in the Brussels area and then sharply increase between Vilvoorde (36 km) and Eppegem, (41 km). Here, the As-dis increases from $1.6 \pm 0.4 \mu\text{g L}^{-1}$ to $9.6 \pm 5.1 \mu\text{g L}^{-1}$ while

As-SPM in this zone increases from $15.5 \pm 3.5 \mu\text{g g}^{-1}$ to $120.4 \pm 52.3 \mu\text{g g}^{-1}$. The station in Eppegem is located downstream of a section with several industries as well as the connection of the Zenne with the canal Brussels-Willebroek and a small tributary Tangebeek, which carries discharges of the industrial zone of Grimbergen and the WWTP Grimbergen. Downstream of this station, important temporal variations are observed. The distribution coefficients (K_D -As) between particulate and dissolved phases along the Zenne River did not show any specific trend (**Fig. 2C**). The dissolved fraction of As (As-dis%) represents approximately 53.7–94.5% of its total concentration with no clear trend between the observed periods (**Fig. 2D**). According to data from Foregs Geochemical Atlas of Europe [27], the median concentration of As in Europe is around $0.63 \mu\text{g L}^{-1}$ in stream water. The latest environmental quality standard for As set by VLAREM II in Belgium is $3 \mu\text{g L}^{-1}$ [28].

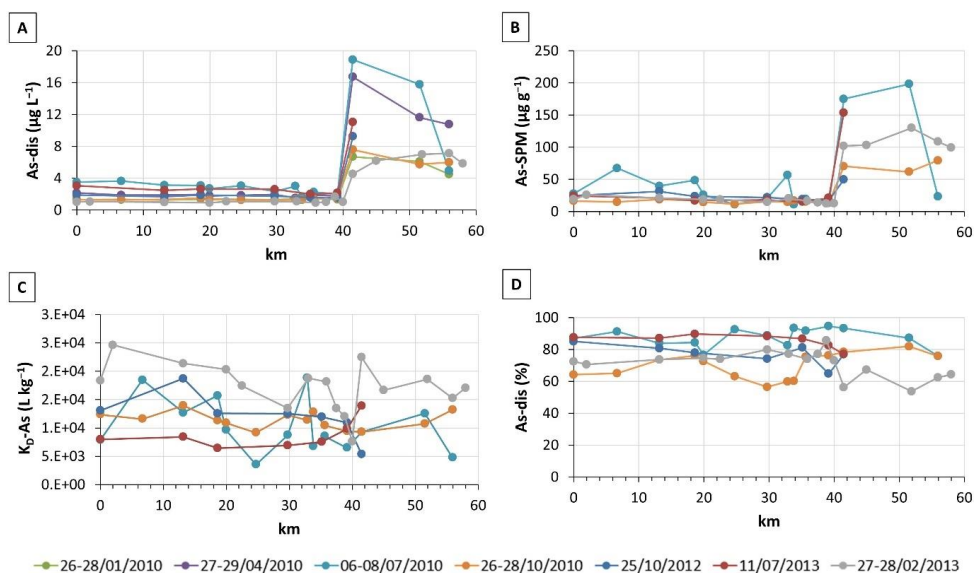


Fig. 2 Longitudinal profiles of the dissolved (A) and particulate (B) As concentrations along the Zenne River with distribution coefficients of As (C) and percentage of dissolved As (D) (0 km corresponds to station Z1 in Lembeek).

3.2 Temporal variability of As concentrations in the Zenne River

3.2.1 Influence of the weather conditions

The influence of the weather conditions on the distribution of As was evaluated during wet and dry periods. The concentrations of As-dis and As-SPM together with their inter-phase distribution indicators (K_D -As, As-dis%) were recorded within 12 or 24-hour sampling surveys. The distribution of As during dry conditions was evaluated at stations Z3, Z4, Z7, and Z9. No rain events were recorded within the sampling and the average daily water discharge according to the VMM data was maintained at 2.06, 1.74, 2.40, and 8.96 m³ s⁻¹ at stations Z3, Z4, Z7, Z9, respectively (data obtained from www.waterinfo.be for stations Lot and Vilvoorde). The results show that concentrations of dissolved and particulate arsenic, as well as its distribution between both phases, remain fairly stable during the dry periods (**Fig. 3**).

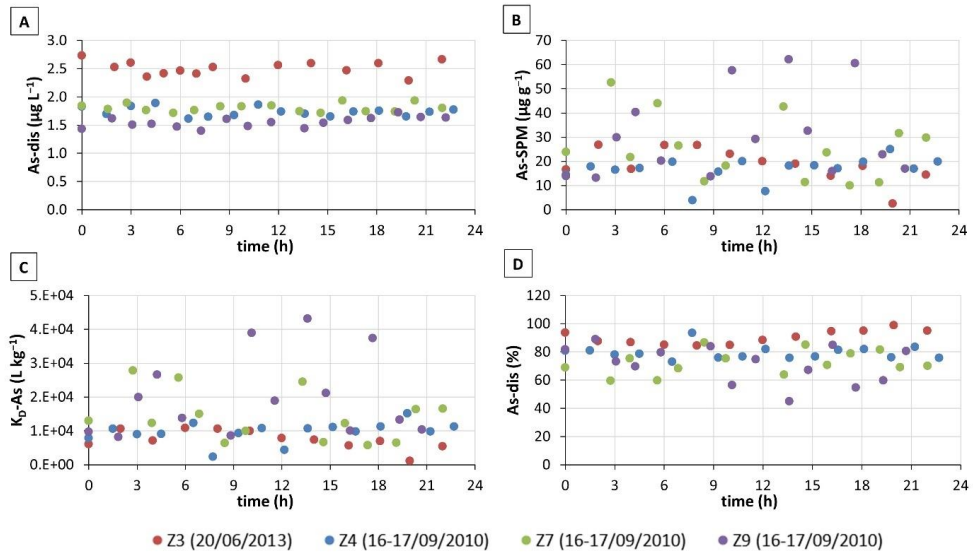


Fig. 3 Variation of the dissolved (A) and particulate (B) As concentrations during the dry periods at stations Z3, Z4, Z7, and Z9 with distribution coefficients of As (C) and percentage of dissolved As (D).

The monitoring during two rain events was performed at stations Z3 and Z9. The dynamic changes in the water discharge during the rain events together with its impact on As concentrations and distribution between particulate and dissolved fractions are shown in **Fig. 4**.

Within both rain events, the concentration of As-dis decreased with the increasing discharge due to the dilution by rainfall and surface runoffs. Since the rainwater brings particles with lower concentrations of As, the As-SPM concentrations also drop during the rain events. The affinity of As towards SPM remains fairly stable or slightly decreases. However, since the concentration of SPM in the water increased during the rain events (data not shown), the percentage of dissolved As relative to its total concentration per volume decreased from 80–90% to 50–55%.

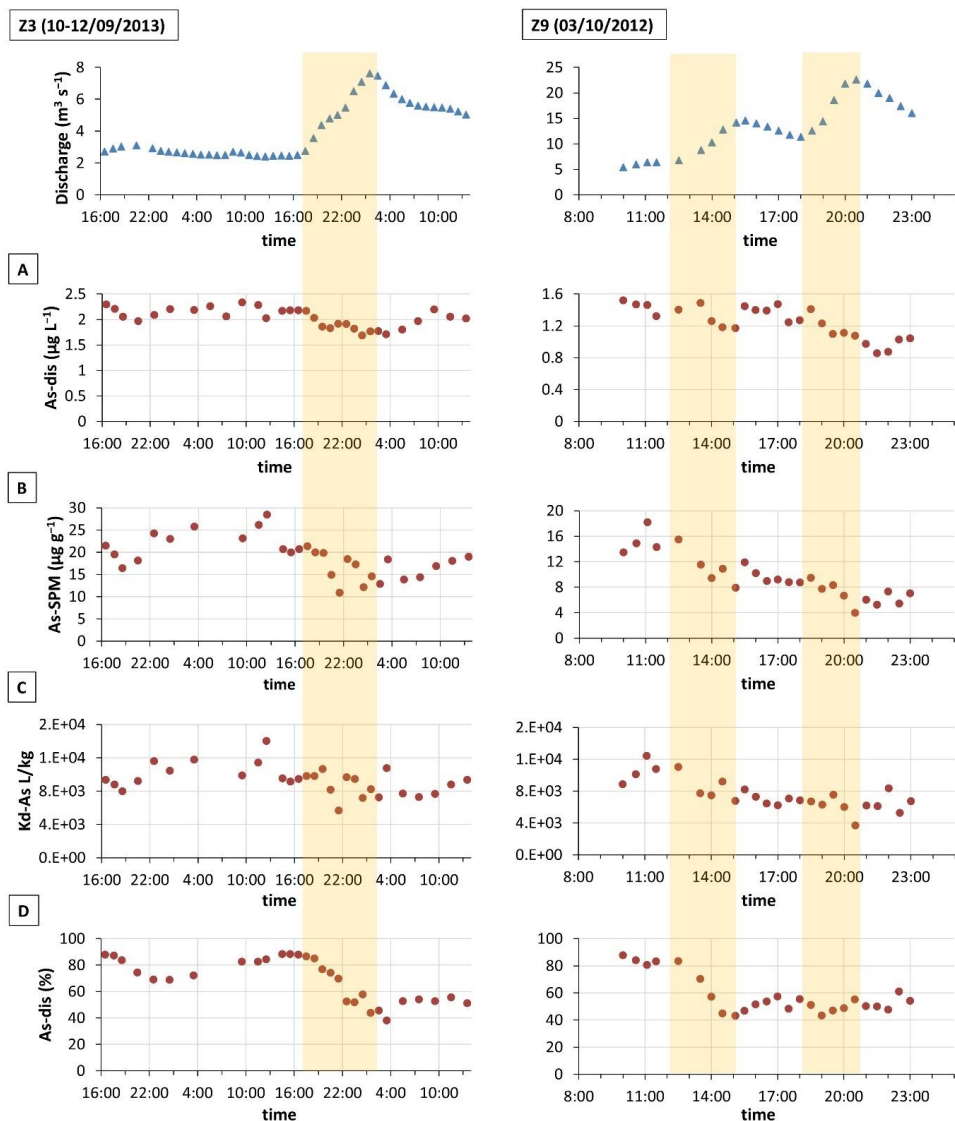


Fig. 4 Variation of the dissolved (A) and particulate (B) As concentrations during two rain events at stations Z3 and Z9 with distribution coefficients of As (C) and percentage of dissolved As (D) (yellow areas highlighting periods with increasing discharge).

3.2.2 DGT-lability of dissolved As species

Grab water sampling was combined with the application of the DGT passive sampling technique using Metsorb as binding resin in order to obtain time-integrated concentrations of labile As species. Metsorb accumulates both As(III) and As(V) as well as monomethylarsonic

acid, (MMA), and dimethylarsinic acid, (DMA). The DGTs were deployed for 2 days at two upstream stations without tidal influence (Z5, 20 km; Z9, 34 km), and one downstream station influenced by the tide (Z13, 56 km). The As-dis concentrations were analysed in grab samples that were taken only at the beginning and end of the DGT deployment and were used for the calculation of the time-weighted average As concentrations (TWA). These were then compared with the time-integrated DGT-determined concentrations (As-DGT) as shown in **Fig. 5**. A very good agreement between TWA and As-DGT is observed at all stations. However, the agreement found at station Z13 is completely coincidental since there is a large difference between As-diss concentrations at the beginning and at the end of the DGT deployment. Since the grab samples were taken at different moments of the tidal cycle (high tide on day 1 and low tide on day 2), it is obvious that As concentrations are strongly influenced by the tide. The good agreement between the DGT results and total dissolved As demonstrates that in the surface water of the Zenne River, As is present as small labile species with a negligible colloidal fraction. In previous work on As speciation in the Zenne River (Baeyens et al. 2007), no methylated As species were observed and As(V) dominated in oxygenated waters whereas As(III) dominated at O_2 concentrations $< 1\text{ mg/L}$. Thus, due to the improved O_2 conditions which are related to the operation of WWTPs [16], As(V) is currently expected to dominate the aqueous speciation.

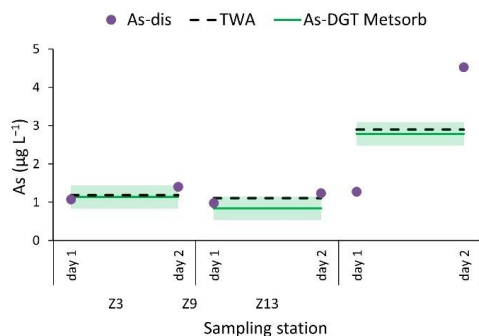


Fig. 5 Comparison of dissolved As concentrations (As-dis) and their time-weighted average values (TWA) with DGT-determined As concentrations (As-DGT Metsorb) at selected stations (the solid green line and lighter zone represent the DGT result and its standard deviation; day 1 – March 22, 2017).

3.2.3 Influence of the tidal cycle

To get a better view of the variability of As concentrations during the tidal cycle, 12 h monitoring surveys were performed at the mouth of the river (Z14, 58 km) on October 22, 2013, and on March 17, 2021. In both cases, the sampling started 1.5 h after high tide (t1) and the low tide took place between t6 and t7. The tidal range during both observed periods was about 5.3 m (data obtained from www.waterinfo.be). As-dis concentrations were determined in grab samples taken at 1-hour intervals and were used for the calculation of TWA concentration. obtain time-integrated concentrations of As, in 2013 the DGTs utilizing Metsorb resin were deployed for 2 days while in 2021 the DGTs utilizing the novel resin Lewatit FO 36 together with ZrO₂ were deployed only for the duration of the water sampling (12 h) (**Fig. 6**). Comparable to Metsorb, Lewatit FO 36 also binds As(III), As(V), MMA, and DMA [29]. During the latter survey, water samples for analysis of As-SPM were taken as well and conductivity, pH, dissolved oxygen, and SPM were measured (see profiles in **Fig. S2**). In general, pH, concentrations of dissolved oxygen, and SPM reach their maximum during high tide and vice versa. The opposite trend in the function of the tide was observed for conductivity.

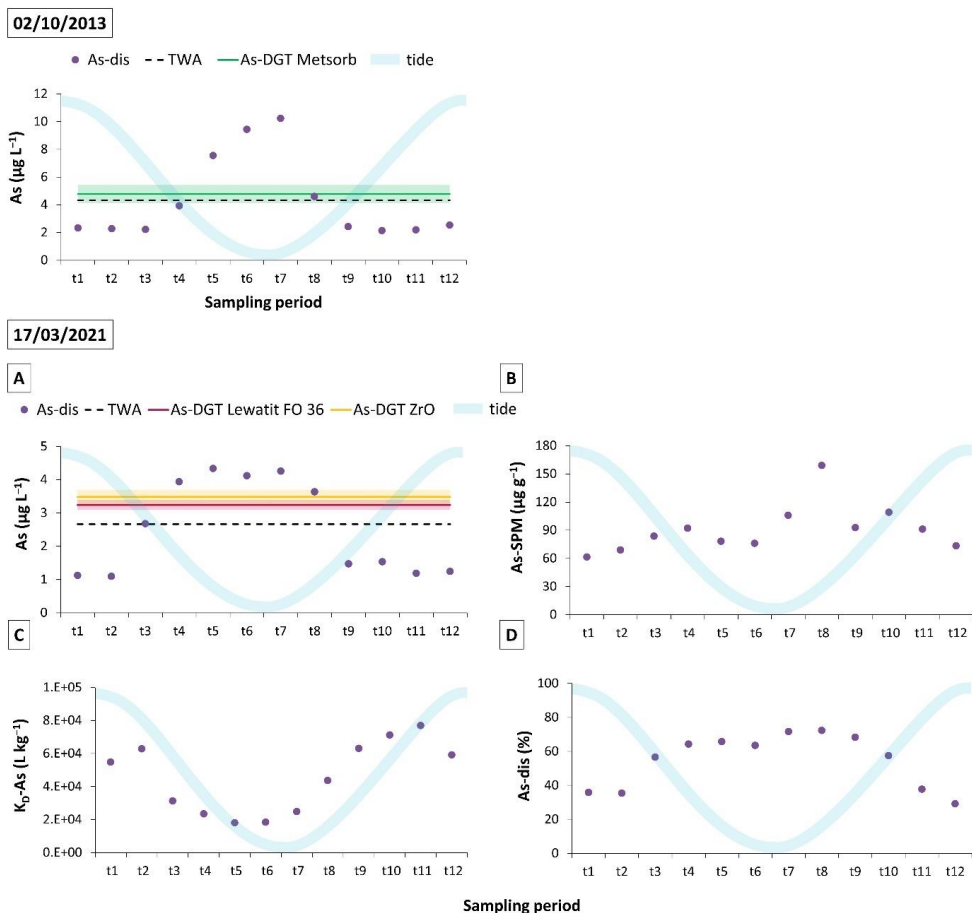


Fig. 6 Variation profiles measured at station Z14 (58 km) in October 2013 and March 2021. Variations in dissolved As concentrations (As-dis) during a tidal cycle and the comparison of their time-weighted average As concentrations (TWA) with DGT-determined As concentrations (As-DGT using Metsorb, Lewatit FO 36 or ZrO₂ resin) from both years. Variations in particulate As concentrations (B), distribution coefficients (C), and percentage of dissolved As (D) from the later monitoring survey (light blue line illustrate the tidal cycle; the solid green/red line and lighter zone represent the DGT results and their standard deviations).

The monitoring surveys revealed patterns in temporal variability of As fractions during the tidal cycle. In both observed periods, the As-dis concentration was the lowest during high tide and increased 4 to 5-fold during low tide. In comparison, the As-dis concentration in the Dijle River, collected approximately 200 m after the confluence with the Zenne River (D1), the measured values varied between 1.2 $\mu\text{g L}^{-1}$ at high tide to 2.3 $\mu\text{g L}^{-1}$ at low tide (data not shown). The concentrations of particulate As measured in 2021 range between 61.4–

158.9 $\mu\text{g g}^{-1}$ (**Fig. 6B**). Although the concentrations of both, particulate and dissolved As, increase during the low tide, the distribution coefficient is lower at low tide ($K_D = 18,500$) and increases at high tide ($K_D = 70,500$) (**Fig. 6C**). A significantly higher portion of As is thus represented by the dissolved fraction during low tide (64–72%) compared to only 29–37% during high tide in 2021 (**Fig. 6D**).

A general good agreement is observed between the TWA concentrations calculated from the grab samplings and the DGT-determined concentrations measured by all resins. The TWA value from 2021 seems to be underestimated by 25.8% in comparison to the result of Lewatit FO 36 and ZrO_2 DGTs. Nevertheless, it is possible that the chosen sampling frequency was not sufficient to record dynamic changes in As concentrations, thereby resulting in an underestimation of the calculated TWA. This is further supported by the very good agreement between the DGT-determined concentrations measured by both resins that were deployed simultaneously.

The results of this study demonstrate the benefits of the DGT application in a dynamic environment such as tidal rivers when large temporal variations in the concentrations are found, where grab sampling may provide highly variable results (**Fig. 2**). The DGT-determined concentrations better reflect the actual load of As in the water without the need for frequent water sampling as well as providing information on the lability of the As species. Comparable to what we observed in the other sampling sites of the Zenne River (**Fig. 5**), the DGT results are equal to the TWA concentrations which indicates that the labile fraction of As predominates in the water column of the Zenne river. Therefore, it can be assumed that all of the As measured as a dissolved fraction may be potentially available to biota. This is comparable to what has been observed in other studies. Gontijo et al. [30] compared DGT with ultrafiltration (UF) (1kDa) and dissolved concentrations and found that at most sampling sites, the dissolved As was predominantly present as labile As (42–98%, with a good agreement between DGT-As and

UF-As), despite Fe and Al being predominantly present in the colloidal form. At four sites, the colloidal fraction of As accounted for 29–57% of the dissolved As. Likewise, Panther et al. [31] demonstrated the complexation of As in the presence of fulvic acids (FA), typical Fe concentrations found in surface waters ($\mu\text{g/L}$ levels) and the presence of FeO(OH) colloids. Increasing the concentration of Fe (III), thus also the concentration of FeO(OH) colloids, increased the colloidal As fraction. However, the presence of FA in the same system increased the labile form of As because it may limit the adsorption of As on FeO(OH) colloids, or may even displace As adsorbed to FeO(OH) due to their competition [32].

The overall findings confirm that there is an important point source of As between Z9 and Z11 resulting in large temporal variability in As concentrations in the water column at the downstream part of the river. The variability is driven by the tidal cycle due to dilution with the water of the Dijle River during rising tide at the mouth of the Zenne. This explains the large variability in As-dis and As-SPM measured in the different surveys in this study (**Fig. 2**) as well as the observations reported by other researchers in historical studies. For instance, in the study of Baeyens et al. from 2003 [14], approximately 2–3 times higher concentrations of dissolved and particulate As were found in the downstream part of the Zenne. Moreover, a single As-dis concentration of $17 \mu\text{g L}^{-1}$ was reported in the same study. Similarly, a single concentration peak of $27.8 \mu\text{g L}^{-1}$ was found by Andreae and Andreae in 1989 [15] in Hombeek that corresponds to our station Z12.

3.3 Source of As elevated concentrations in the downstream part of the Zenne River

Since an important increase of both dissolved and particulate As was observed for all sampling campaigns between Z9 (34 km) and Z11 (41 km) all possible contributors of As input in this area were identified: two river tributaries (the Woluwe and the Tangebeek rivers), an overflow structure from the Canal Brussels-Rupel, a combined sewer overflow (CSO), and

several (15) industrial effluents. In addition, the Tangebeek also receives a CSO, industrial effluents, and the effluents of WWTP Grimbergen close to its confluence with the Zenne. Data on the concentrations of As in the different sources (Woluwe River, Canal, CSO) were obtained by the authors in the OSIRIS and SUBLIMUS projects and combined with data from the Flemish Environmental Monitoring Agency (Vlaamse Milieu Maatschappij, VMM, www.geoloket.vmm.be/Geoviews/) for the Zenne River, its tributaries and the Dijle River (**Table 1** and **Fig. S3**).

In order to quantify the importance of each of these contributors as a source for As, a mass balance was calculated for dissolved arsenic between Z9 and Z11. Note that there were not enough data to do the same evaluation for particulate As. Average daily fluxes of dissolved As were computed in Z9 and Z11, at the outlet of Woluwe and Tangebeek rivers, Canal overflow and CSO from yearly waterflow measurements and average As concentration data. Data used are averages for the period 2010–2016; values and data sources are summarized in **Table 1**. Daily fluxes of arsenic are then computed and put together to establish a mass balance (**Fig. 7**).

Table 1 Average daily waterflow and dissolved arsenic concentrations (As-dis) used in the mass balance.

Station	Waterflow (m ³ d ⁻¹)	Provider	As-dis (μg L ⁻¹)	Provider
Zenne:				
Zenne-Z9	754,872	Flowbru 2010-2016 (1)	1.29 (0.26)	this study + additional measurements (5)
Zenne-Z11	855,207	Waterinfo 2010-2016 (2)	9.5 (5.1)	this study + additional measurements (5)
To Zenne:				
Woluwe outlet	40,515	OSIRIS water mass balance (3)	1.45 (0.59)	additional measurements (5)
Tangebeek outlet	27,993	OSIRIS water mass balance (3)	176 (58)	VMM (4)
Canal overflow	21,105	OSIRIS water mass balance (3)	2.06 (0.38)	additional measurements (5)
CSO	3,858	VMM (4)	1.29 (0.29)	additional measurements (6)
To Tangebeek:				
CSO	34	VMM (4)	1.29 (0.29)	additional measurements (6)

(1) www.flowbru.be; (2) www.waterinfo.be; (3) Carbonnel et al. 2016 [33]; (4) Vlaamse Milieu Maatschappij, www.geoloket.vmm.be/Geoviews/; (5) performed by the authors between 2010 and 2016; (6) performed by the authors between 2010 and 2016 in untreated sewage from Brussels. The As-dis values are averages for the period 2010–2016 with standard deviations in brackets. CSO – combined sewer overflow.

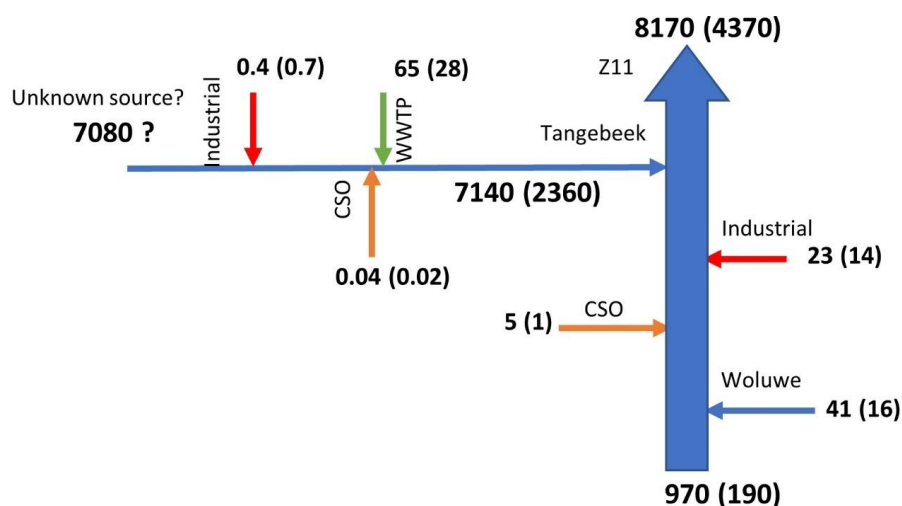


Fig. 7 Average daily fluxes of dissolved arsenic (in g day^{-1}) in the Zenne between stations Z9 and Z11 (values are averages for the period 2010–2016 with standard deviations in brackets; CSO – combined sewer overflow; WWTP – wastewater treatment plant).

First, we can verify that the mass balance for the Zenne is closed with sources of As corresponding to the concentration difference observed between Z11 and Z9. Results show that the daily As fluxes between Z9 and Z11 are multiplied by a factor of 8 (from 970 to 8170 g day^{-1}). Regarding sources, surprisingly, the small Tangebeek, only contributing 5% to the Zenne water discharge (**Table 1**), contributes by 87% to the As load carried by the Zenne, which is much more than any other source, including CSO and industries. This extremely high load of As in the Tangebeek cannot be explained by presently reported sources of contamination such as CSO and industries (both negligible) and WWTP effluents (1% of the Tangebeek load). According to VMM data, the median values of As concentrations from the station located in Tangebeek right before its confluence with the Zenne (VMM station no. 357800) are in the range 110.0–225.5 $\mu\text{g L}^{-1}$ (**Fig. 8**) and thus by two orders of magnitude higher than the concentrations found in the Zenne (Z9), Woluwe River, Canal and CSOs (1–2 $\mu\text{g L}^{-1}$; **Table 1**).

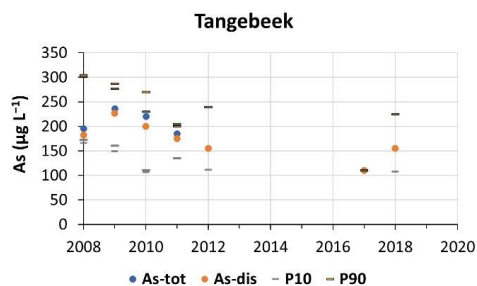


Fig. 8 Evolution of dissolved and total As concentrations (As-dis, As-tot) during 2008–2020 at station no. 357800 on the Tangebeek based on the data from VMM online database (data expressed as median values with 10th (P10) and 90th (P90) percentiles for n = 6–12).

To identify the origin of elevated As concentrations found in Tangebeek, the data from five monitoring stations along this river from the period 2009–2020 were further evaluated (**Fig. 9A**). The results revealed alarming concentrations of As found at station no. 35800 on the Tangebeek with an average value reaching up to 2561 $\mu\text{g L}^{-1}$ of As-dis (**Fig. 9B**). These high concentrations have been observed since the onset of the VMM monitoring in the early 2000s! Given the location of this monitoring station, it is assumed that the source of As is located within a dense industrial zone located 3.5 km upstream from the confluence with the Zenne and before the confluence of the Tangebeek with the Maalbeek (red area in **Fig. 9A**). This is further supported by average values of As concentrations at stations no. 358100 located upstream of this industrial area (2.4 $\mu\text{g L}^{-1}$ of As-dis) and no. 35700 located on Maalbeek (2.2 $\mu\text{g L}^{-1}$ of As-dis) reported during the same period. After the confluence of both streams at station no. 357900, the high concentration of As is diluted and decreases to 465.2 $\mu\text{g L}^{-1}$ of As-tot (only data from 2002 available). Further dilution occurs by another tributary and the outlet of the WWTP Grimbergen. Before the confluence of Tangebeek and Zenne, the concentration of As-dis drops to the average value of 176 $\mu\text{g L}^{-1}$.

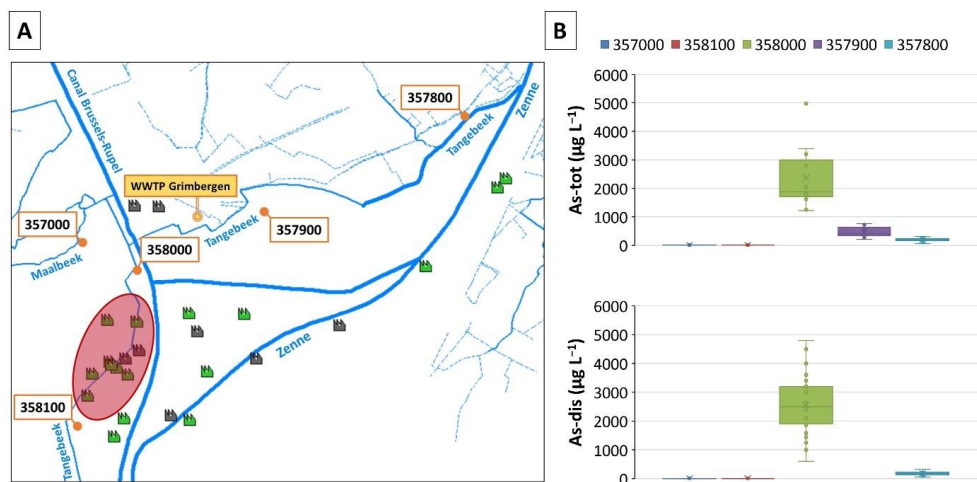


Fig. 9 (A) Monitoring stations along Tangebeek with industrial area where As source is located (highlighted in red). (B) Box plots of total and dissolved As concentrations (As-dis, As-tot) reported at these stations based on data from VMM online database (box includes values between 25th and 75th percentiles with the line inside indicating median value and the cross indicating mean value; the whiskers indicate minimum and maximum values; circles represent inner data points).

As none of the present industries reports significant releases of As, inputs from this site could come from a historical industrial activity that probably contaminated the groundwater sources in this zone. A possible historical source may be a former sulphuric acid factory extracting pyrite minerals. However, this requires further investigation.

3.4 Geochemistry of As in sediments of the Zenne River

3.4.1 Total As content in the sediments along the Zenne River

An overview of the compiled data of results collected between 2012 and 2021 on total As concentrations in sediments along the Zenne River is shown in **Fig. 10**. The total As concentrations in the section upstream of the confluence with the Tangebeek range from 1.4 to 8.8 $\mu\text{g g}^{-1}$ (average 4.3 $\mu\text{g g}^{-1}$) and are comparable to background values found in small, relatively unimpacted streams in Flanders (VMM, www.geoloket.vmm.be/Geoviews/). According to data from Foregs Geochemical Atlas of Europe [27], the geochemical background concentration of As in stream sediments in Belgium is around 9.4 $\mu\text{g g}^{-1}$. After the confluence

with the Tangebeek (Z11–Z14, which coincides with the tidal section of the river), the concentrations of As range from 3.8 to 27.5 $\mu\text{g g}^{-1}$ (average 11.7 $\mu\text{g g}^{-1}$). Before the confluence with the Tangebeek, the concentrations of particulate As in SPM are around 10–20 $\mu\text{g g}^{-1}$ and increase sharply at Z11 up to over 200 $\mu\text{g g}^{-1}$ (**Fig. 2B**), whereas in the tidal section, As-SPM varies from 61 to 159 $\mu\text{g g}^{-1}$ during a tidal cycle (**Fig. 6B**). The increase in As concentrations in the sediments due to the settling of the contaminated particles shows that the downstream section also serves as a trap, partially removing the As transported downstream.

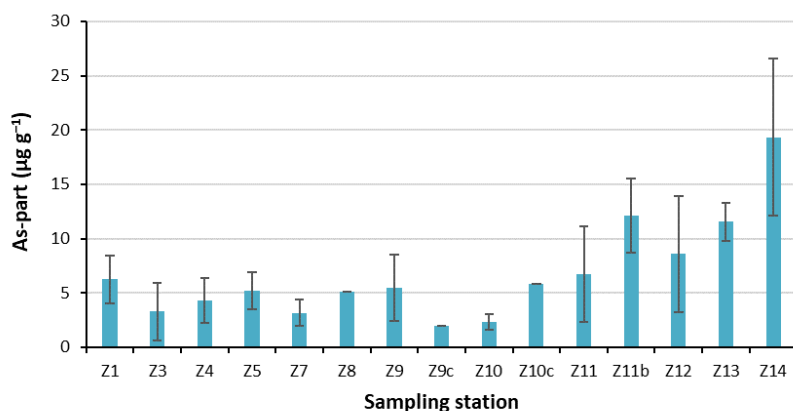


Fig. 10 Total As concentrations in the sediment samples along the Zenne River, compiled data of 2012–2021, fraction < 1mm.

3.4.2 Sequential extractions of sediments along the Zenne River

To evaluate the mobility of sediment-bound arsenic, the BCR sequential extraction procedure was performed on the sediments from the Brussels region as well as from the tidal Zenne in 2013 (stations Z5–Z14, 20–58 km). The sediment samples in the Brussels area were collected by BIM (Brussels Instituut Milieubeheer) and thus the sampling stations were slightly different from those used in this study (the approximate position corresponding to the stations of this study is expressed by the symbol ~). The distribution of Fe, Mn, and As in the four fractions (F1–4) that were separated within the successive extraction steps is shown in **Fig. 11**.

In the upper section of the river, Fe is predominantly (around 70%) bound to the residual fraction and will be present as the natural minerals. In the tidal section, the reducible fraction becomes more important accounting for 20–70% of the Fe present. The redox cycling of Fe in these sediments results in the formation of authigenic iron (oxyhydr)oxide mineral phases. The exchangeable fraction is relatively more important in the upstream area (10–20%) than in the tidal section (0–20%). The oxidizable fraction also increases in the tidal area due to the formation of sulphide phases. For Mn, the exchangeable and carbonate fraction predominates in all sediments but especially in the upstream area. Comparable to Fe, the reducible fraction increases from < 10% upstream to > 30% in the tidal section. The redox cycling of Mn leads to the formation of manganese (oxyhydr)oxides. The residual fraction accounts for 10–20% upstream and decreases to < 5% in the tidal zone. The oxidizable fraction was generally only a few percent, except for Z9 and Z10b.

Arsenic is essentially bound in the reducible fraction (F2) and represents predominating fraction at stations Z8, Z11, Z11b, Z12, and Z13 (34–58%). Arsenic found in this fraction is bound to the Fe and Mn (oxyhydr)oxides which are considered key factors controlling As mobility in sediments. The exchangeable and carbonate fraction (F1) is also very important and represents the most significant fraction at stations ~Z7, Z9–9c, Z9, and Z14 where it accounts for 34–41% of the total As content. This fraction generally consists of metals in porewater, weakly sorbed metals, and carbonates which can be liberated from the solid phase by the reduction of the pH in the environment. Therefore, it can be assumed that a significant fraction of As is easily available in the sediments of the Zenne river. The oxidisable fraction (F3) of As is, in general, the least representative one in the tidal zone (7–14% at stations ~Z5, Z11b, Z12, Z13, and Z14). This fraction is represented by elements bound to organic fraction and oxidisable sulphides. The residual fraction (F4) of As (generally consisting of refractory material, non-oxidisable sulphides, and refractory minerals) is then the least representative (6–13%) at

upstream stations (~Z7 to Z11). One exception is found at station ~Z5 in the Brussels area where the residual fraction predominates (46%). The importance of the residual fraction increases in the tidal section, probably due to the incorporation of As on non-oxidizable sulphides.

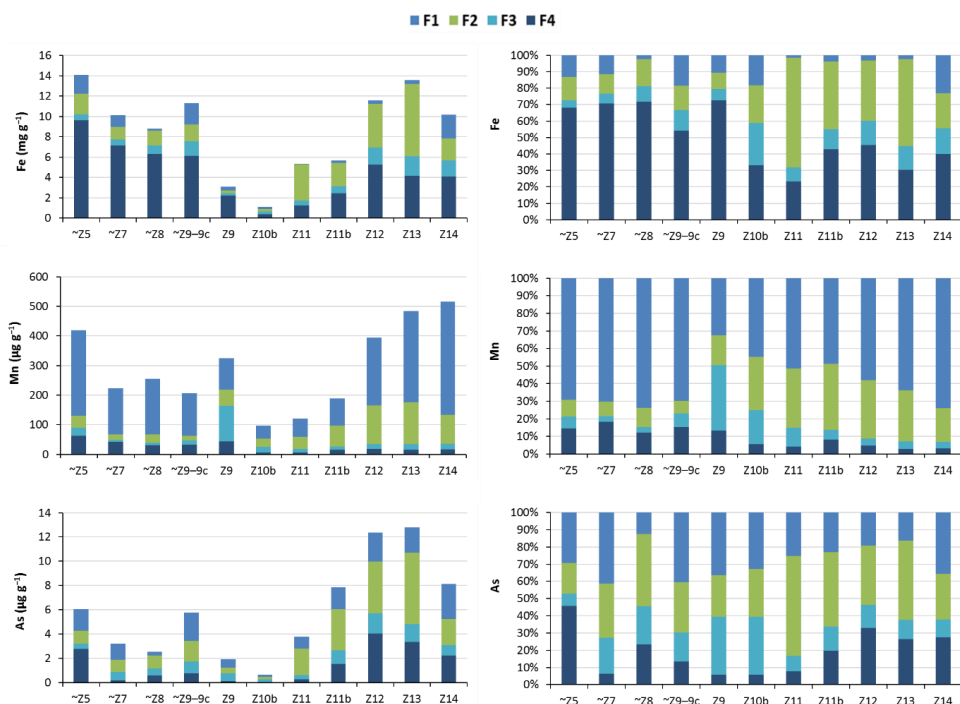


Fig. 11 Iron, manganese, and arsenic sequential extractions of sediments in the Brussels region and the tidal Zenne, 2013 (F1 – exchangeable and carbonate fraction; F2 – reducible fraction; F3 – oxidisable fraction; F4 – residual fraction).

3.4.3 The dissolved and labile As, Fe, and Mn concentrations in porewater

Concentrations of As, Fe, and Mn in sediments porewater (PW-As/Fe/Mn) and the DGT-labile concentrations (DGT-As/Fe/Mn) were determined at the upstream station Z5 (20 km) and at the tidal station Z14 (58 km) in June 2020 and are shown in **Fig. 12**. The DGTs utilizing Lewatit FO 36 resin and ZrO_2 were used for the determination of total labile As while 3-MFS was used for the specific measurement of labile As(III). Labile fractions of Fe and Mn were

determined by Chelex-100 DGTs. The depth profiles of redox potential and pH at both stations are shown in **Fig. S4**.

At station Z5, substantial remobilization of As appears below the water-sediment interface with the maximum concentration of dissolved As in porewater of $12.2 \mu\text{g L}^{-1}$ at -1 cm , and another peak observed at -9 cm . The same trends can be seen for the porewater profiles of Mn and Fe indicating that As distribution in sediments is governed by the reductive mobilisation from Mn and Fe (oxyhydr)oxides. The total labile DGT-As (Lewatit FO 36) shows a maximum at -1.5 cm and accounts for 9–21% of the PW-As. The same trends are found for DGT-Fe and DGT-Mn. In the first 3–4 cm depth, porewater concentrations are comparable to the DGT concentrations of Fe and Mn, but in the deeper layers, the increase in porewater concentrations is not observed in the DGT profiles indicating that the species formed are not DGT labile (possibly in the form of organic colloids) and/or that the remobilisation rates from the sediment phase are lower in the deeper layers. The DGT-As(III) (3-MFS) is very low in the overlying water but shows a maximum at -1.5 cm depth, accounting for 117 and 140% in relation to total DGT-As determined by ZrO_2 and Lewatit FO 36, respectively. The As(III) concentrations further follow the profile of total DGT-As until the bottom.

In the muddy sediments of the intertidal flat at station Z14, the maximum dissolved concentration of As found in porewater is achieved at -7 cm depth with $335.7 \mu\text{g L}^{-1}$ As and is thus 28 times higher than in Z5. The labile fraction of total DGT-As (Lewatit FO 36) increases below the water-sediment interface, peaks at -2 cm , and then remains fairly stable till the bottom with $20.6 \pm 3.6 \mu\text{g L}^{-1}$ accounting for 7–34% of PW-As. Regarding the speciation of labile arsenic at station Z14, reduction of As(V) already occurs in the overlying water, where As(III) accounts for 100% of the total labile As. The profile of As(III) further copies the profile of total DGT-As (Lewatit FO 36 and ZrO_2), accounting for 100% or more (up to 206%) of total labile DGT-As until 6 cm depth and around 75% at 10–13 cm depth. The overestimation of

DGT-As(III) in relation to total DGT-As observed at Z14 between -2 and -6 cm depth can be attributed to spatial heterogeneity of sediments since Lewatit FO 36 and ZrO_2 were always deployed back-to-back, while 3-MFS DGT probe was deployed next to them. However, the DGT-labile concentrations of As measured by all three binding phases were overall in very good agreement indicating that the reducing conditions found in both sediments enhance the reduction of As, which is thus predominantly present as As(III) [14, 34]. The dissolved Fe and Mn concentrations at station Z14 reached their maximum at -7 cm depth and thus coincide with that of As. The labile fraction of both metals sharply increases within the first centimetres below the water-sediment interface and remains fairly stable from about -3 cm till the bottom with concentrations of $19.1 \pm 1.8 \text{ mg L}^{-1}$ of Fe and $1839 \pm 413 \text{ } \mu\text{g L}^{-1}$ of Mn.

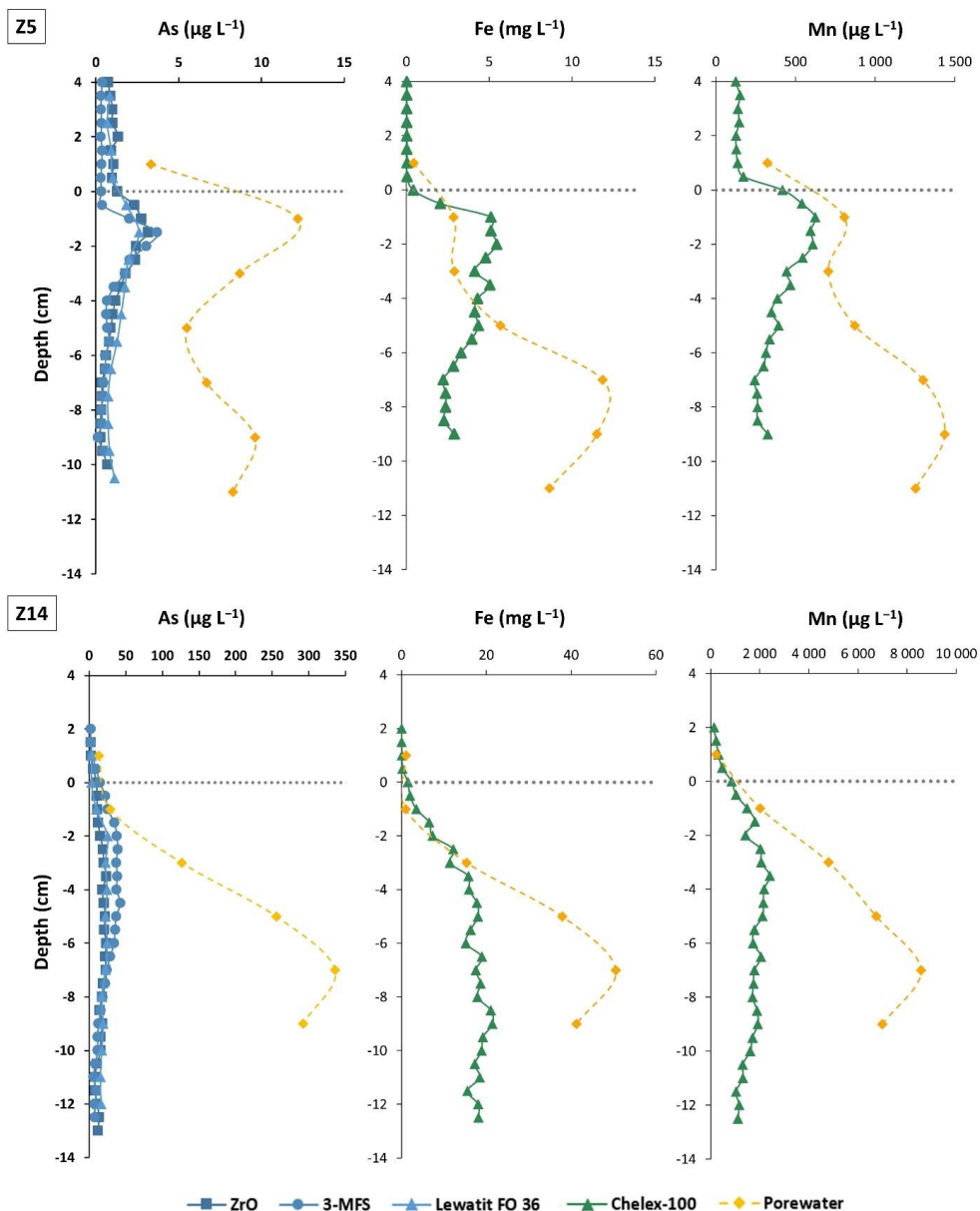


Fig. 12 The depth profiles of dissolved and DGT-determined concentrations of As, Fe, and Mn in sediment porewater at stations Z5 and Z14, June 2020 (grey dotted line represents water-sediment interface).

The low fraction of DGT labile As species at depths below 2 cm probably indicate the presence of mixed colloids of As, Fe, and Mn with organic matter (OM). As binding to OM may occur via ternary complexes through the formation of a metal-cation bridge [35] or thiol-

bonding to sulfhydryl groups of OM [36]. In addition, OM plays an important role in stabilizing redox-sensitive authigenic minerals and associated As [37] explaining the presence of As(V) in the deeper layers.

The simultaneous concentration peaks of As as well as Fe and Mn observed below the water-sediment interface correspond to the reductive mobilisation of As from the Mn and Fe (oxyhydr)oxides and subsequent release of all three elements to porewater. A strong positive correlation between As and Mn labile concentrations across the whole vertical profile was observed at stations Z5 and Z14 ($r = 0.91$ and 0.82 , respectively) while a medium positive correlation was observed between As and Fe labile concentrations at these stations ($r = 0.65$ and 0.73 , respectively). The reason for the lower correlation level between As and Fe is a slight delay of the Fe peaks which suggests that As is primarily released from the Fe (oxyhydr)oxides by reductive desorption and the dissolution of the Fe mineral itself occurs later. The reducing conditions found in both sediments also enhance the reduction of As, which is thus predominantly present as As(III) [14, 34].

3.4.4 Diffusive benthic fluxes of As

Diffusive transport at the water-sediment interface was calculated for stations Z5 and Z14 based on the observed porewater profiles. Data used for the flux calculations as well as the fluxes calculated for the zones Z1 to Z10 (based on the Z5 profile) and Z11 to Z14 (based on the Z14 profile) are shown in **Table 2**.

Table 2 Data used for calculations of benthic fluxes of arsenic with resulting fluxes calculated for zones Z1–Z10 and Z11–Z14.

	Porosity	D_{sed}	dC / dx	F_D	Zone	Area	Flux
		($cm^2 s^{-1}$)		($\mu g m^{-2} d^{-1}$)		(km^2)	($g d^{-1}$)
Z5	0.6	4.55×10^{-6}	6	14.2	Z1–Z10	0.35	5
Z14	0.85	6.94×10^{-6}	45	229	Z11–Z14	0.23	53

The diffusive benthic fluxes of As account for 5 g d^{-1} in the Brussels region and 53 g d^{-1} in the tidal section. The fluxes in the downstream part of the river can however be significantly higher due to bioturbation and resuspension of bottom sediments caused by tidal currents. Compared to the important point source from the Tangebeek the benthic flux account for less than 1% of the input to the river.

4 Conclusions

Downstream transport of As in the Zenne River is completely dominated by the presence of an important point source located on the tributary Tangebeek. Dissolved As concentrations in the Zenne River increase from 1.6 to $9.6\text{ }\mu\text{g L}^{-1}$ and particulate As from 15.5 to $120.4\text{ }\mu\text{g g}^{-1}$ after the confluence with the Tangebeek. Current industrial activities cannot explain the observed concentrations. Historical sources as well as distribution and speciation of As in surface water, groundwater, sediments, and soils in the Tangebeek and its surroundings need to be performed to evaluate the potential impact on human health.

The point source results in large temporal variability in the downstream tidal section of the Zenne River, where the water is diluted with Dijle water during rising tide. The DGT technique was used to assess time-weighted average concentrations of labile As species. The results showed that the DGT-determined As concentrations were equal to the average concentrations calculated from the grab samplings in all sections of the river, indicating a potential bioavailability of the As species and the benefits of DGT to measure average concentrations in dynamic environments.

Arsenic concentrations in the sediment also show an increasing trend downstream. The reducible fraction is the main binding fraction for As and porewater geochemistry is dominated by the reductive dissolution of Mn and Fe oxyhydroxides. As(III) dominates the speciation of labile As species in porewater. The DGT-labile fraction of As accounts for 7–34% of the total

dissolved As concentrations in porewater, indicating the presence of colloidal As species, which are not DGT-labile. Although As porewater concentrations are significantly higher than the concentrations in the surface water, the calculated benthic fluxes only account for 1% of the downstream transport, highlighting the importance of the point source on the behaviour of As.

References

- [1] Smedley, P.L. & Kinniburgh, D. A review of the source, behaviour and distribution of arsenic in natural waters. *Applied Geochemistry*. 2002, (17), 517-568. DOI:10.1016/S0883-2927(02)00018-5.
- [2] Irving, E.C., Lowell, R.B., Culp, J.M., Liber, K., Xie, Q. & Kerrich, R. Effects of arsenic speciation and low dissolved oxygen condition on the toxicity of arsenic to a lotic mayfly. *Environmental Toxicology and Chemistry: An International Journal*. 2008, (27), 583-590.
- [3] Basta, N.T., Rodriguez, R.R. & Casteel, S.W. Bioavailability and Risk of Arsenic Exposure by the Soil Ingestion Pathway. In: Environmental Chemistry of Arsenic, Frankenberger Jr, W.T. Ed., *CRC Press*, 2001.
- [4] Mason, R.P. Trace metals in freshwaters. In: Trace metals in aquatic systems, *Wiley Online Library*, 2013.
- [5] Akter, K.F., Owens, G., Davey, D.E. & Naidu, R. Arsenic speciation and toxicity in biological systems. In: Reviews of environmental contamination and toxicology, *Springer*, 2005, pp. 97-149.
- [6] Guéguen, C. & Dominik, J. Partitioning of trace metals between particulate, colloidal and truly dissolved fractions in a polluted river: the Upper Vistula River (Poland). *Applied Geochemistry*. 2003, (18), 457-470. DOI:10.1016/S0883-2927(02)00090-2.
- [7] Hargreaves, A.J., Vale, P., Whelan, J., Constantino, C., Dotro, G., Campo, P. & Cartmell, E. Distribution of trace metals (Cu, Pb, Ni, Zn) between particulate, colloidal and truly dissolved fractions in wastewater treatment. *Chemosphere*. 2017, (175), 239-246. DOI:10.1016/j.chemosphere.2017.02.034.
- [8] Choe, K.-Y., Gill, G.A. & Lehman, R. Distribution of particulate, colloidal, and dissolved mercury in San Francisco Bay estuary. 1. Total mercury. *Limnology and Oceanography*. 2003, (48), 1535-1546. DOI:10.4319/lo.2003.48.4.1547.
- [9] Kumar, R., Rani, M., Gupta, H. & Gupta, B. Trace metal fractionation in water and sediments of an urban river stretch. *Chemical Speciation & Bioavailability*. 2014, (26), 200-209. DOI:10.3184/095422914X14142369069568.
- [10] Gailardet, J., Viers, J. & Durpé, B. Trace Elements in River Waters. In: Treatise on Geochemistry: Surface and Ground Water, Weathering, and Soils, Drever, J.I. Ed., *Elsevier*, 2005, Vol. 5.
- [11] Zhang, F., Lin, B. & Sun, J. Current reversals in a large tidal river. *Estuarine, Coastal and Shelf Science*. 2019, (223), 74-84. DOI:10.1016/j.ecss.2019.04.017.
- [12] MacCready, P. Estuarine adjustment to changes in river flow and tidal mixing. *Journal of Physical Oceanography*. 1999, (29), 708-726. DOI:10.1175/1520-0485(1999)029<0708:EATCIR>2.0.CO;2.
- [13] Wang, X., Kong, F., Li, Y., Li, Q., Wang, C., Zhang, J. & Xi, M. Effect of simulated tidal cycle on DOM, nitrogen and phosphorus release from sediment in Dagu River-Jiaozhou Bay

estuary. *Science of the Total Environment*. 2021, (783), 147158. DOI:10.1016/j.scitotenv.2021.1471.

[14] Baeyens, W., de Brauwere, A., Brion, N., De Gieter, M. & Leermakers, M. Arsenic speciation in the river Zenne, Belgium. *Science of the Total Environment*. 2007, (384), 409-419. DOI:10.1016/j.scitotenv.2007.05.044.

[15] Andreae, M. & Andreae, T. Dissolved arsenic species in the Schelde estuary and watershed, Belgium. *Estuarine, Coastal and Shelf Science*. 1989, (29), 421-433. DOI:10.1016/0272-7714(89)90077-2.

[16] Brion, N., Verbanck, M.A., Bauwens, W., Elskens, M., Chen, M. & Servais, P. Assessing the impacts of wastewater treatment implementation on the water quality of a small urban river over the past 40 years. *Environmental Science and Pollution Research*. 2015, (22), 12720-12736. DOI:10.1007/s11356-015-4493-8.

[17] Garnier, J., Brion, N., Callens, J., Passy, P., Deligne, C., Billen, G., Servais, P. & Billen, C. Modeling historical changes in nutrient delivery and water quality of the Zenne River (1790s–2010): The role of land use, waterscape and urban wastewater management. *Journal of Marine Systems*. 2013, (128), 62-76. DOI:10.1016/j.jmarsys.2012.04.001.

[18] Bi, Q. & Toorman, E.A. Mixed-sediment transport modelling in Scheldt estuary with a physics-based bottom friction law. *Ocean Dynamics*. 2015, (65), 555-587. DOI:10.1007/s10236-015-0816-z.

[19] UWW Directive 91/271/ECC. Directive on urban waste water treatment. *Official Journal of the European Community Council*, 135/40-135/52, 1991.

[20] Ouattara, N.K., Garcia-Armisen, T., Anzil, A., Brion, N. & Servais, P. Impact of wastewater release on the faecal contamination of a small urban river: The Zenne River in Brussels (Belgium). *Water, Air, & Soil Pollution*. 2014, (225), 1-12. DOI:10.1007/s11270-014-2043-5.

[21] Rauret, G., López-Sánchez, J., Sahuquillo, A., Rubio, R., Davidson, C., Ure, A. & Quevauviller, P. Improvement of the BCR three step sequential extraction procedure prior to the certification of new sediment and soil reference materials. *Journal of Environmental Monitoring*. 1999, (1), 57-61. doi:10.1039/a807854h

[22] Larios, R., Fernández-Martínez, R. & Rucandio, I. Comparison of three sequential extraction procedures for fractionation of arsenic from highly polluted mining sediments. *Analytical and Bioanalytical Chemistry*. 2012, (402), 2909-2921. DOI:10.1007/s00216-012-5730-3.

[23] Leermakers, M., Mbachou, B.E., Husson, A., Lagneau, V. & Descostes, M. An alternative sequential extraction scheme for the determination of trace elements in ferrihydrite rich sediments. *Talanta*. 2019, (199), 80-88. DOI:10.1016/j.talanta.2019.02.053.

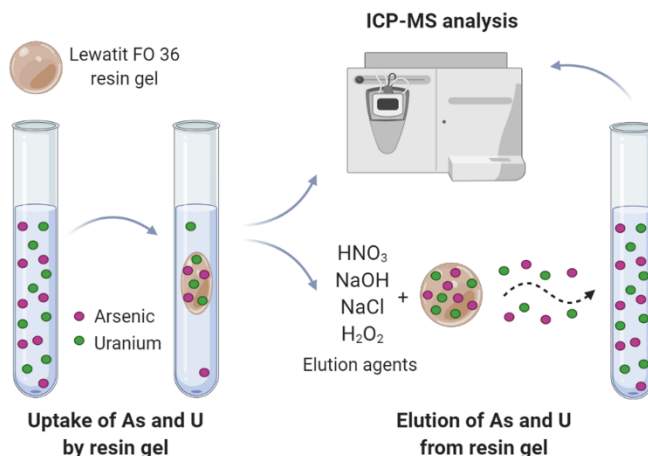
[24] Li, Y. S. Gregory (1974) Diffusion of ions in seawater and in deep-sea sediments. *Geochimica et Cosmochimica Acta*. 1974, (38), 703-714. DOI:10.1016/0016-7037(74)90145-8.

- [25] Homoky, W.B., Weber, T., Berelson, W.M., Conway, T.M., Henderson, G.M., Van Hulten, M., Jeandel, C., Severmann, S. & Tagliabue, A. Quantifying trace element and isotope fluxes at the ocean–sediment boundary: a review. *Philosophical Transactions of the Royal Society A: Mathematical, Physical and Engineering Sciences*. 2016, (374), 20160246. DOI:10.1098/rsta.2016.0246.
- [26] Boudreau, B.P. Diagenetic models and their implementation: Modelling Transport and Reactions in Aquatic Sediments, *Springer*, 1997.
- [27] Salminen, R., Batista, M.J., Bidovec, M., Demetriades, A., De Vivo, B., De Vos, W., Duris, M., Gilucis, A., Gregorauskiene, V., Halamic, J., Heitzmann, P., Lima, A., Jordan, G., Klaver, G., Klein, P., Lis, J., Locutura, J., Marsina, K., Mazreku, A., O'Connor, P.J., Olsson, S.Å., Ottesen, R.-T., Petersell, V., Plant, J.A., Reeder, S., Salpeteur, I., Sandström, H., Siewers, U., Steenfelt, A. & Tarvainen, T. FOREGS - Geochemical Atlas of Europe, Association of the Geological Surveys of The European Union (EuroGeoSurveys), *Geological Survey of Finland, Espoo*, 2005.
- [28] VLAREM II. Decision of the Flemish Government of 24/06/2021 concerning general and sectoral regulations with regard to environmental issues. Appendix 2.3.1 Basic Environmental Quality Standards for Surface Water from 01/10/2019. *Belgian Official Gazette*.
- [29] Smolíková, V., Pelcová, P., Ridošková, A., Hedbávný, J. & Grmela, J. Development and evaluation of the iron oxide-hydroxide based resin gel for the diffusive gradient in thin films technique. *Analytica Chimica Acta*. 2020, (1102), 36-45. DOI:10.1016/j.aca.2019.12.042.
- [30] Gontijo, E.S., Watanabe, C.H., Monteiro, A.S., Tonello, P.S., da Silva, G.A., Friese, K., Roeser, H.M. & Rosa, A.H. Distribution and bioavailability of arsenic in natural waters of a mining area studied by ultrafiltration and diffusive gradients in thin films. *Chemosphere*. 2016, (164), 290-298. DOI:10.1016/j.chemosphere.2016.08.107.
- [31] Panther, J.G., Stillwell, K.P., Powell, K.J. & Downard, A.J. Development and application of the diffusive gradients in thin films technique for the measurement of total dissolved inorganic arsenic in waters. *Analytica Chimica Acta*. 2008, (622), 133-142. DOI:10.1016/j.aca.2008.06.004.
- [32] Simeoni, M.A., Batts, B.D. & McRae, C. Effect of groundwater fulvic acid on the adsorption of arsenate by ferrihydrite and gibbsite. *Applied Geochemistry*. 2003, (18), 1507-1515. DOI:10.1016/S0883-2927(03)00074-X.
- [33] Carbonnel, V., Brion, N., Elskens, M., Claeys, P. & Verbanck, M. Building water and chemicals budgets over a complex hydrographic network. In: European Congress of the International Association for Hydro-environment engineering and Research: Sustainable hydraulics in the era of global change, Erpicum, S., Dewals, B., Archambeau, P., Piroton, M. Eds., *CRC Press*, Liege Belgium, 2016, pp. 77-77.
- [34] Aftabtalab, A., Rinklebe, J., Shaheen, S.M., Niazi, N.K., Moreno-Jiménez, E., Schaller, J. & Knorr, K.-H. Review on the interactions of arsenic, iron (oxy)(hydr) oxides, and dissolved organic matter in soils, sediments, and groundwater in a ternary system. *Chemosphere*. 2022, (286), 131790. DOI:10.1016/j.chemosphere.2021.131790.

- [35] Hoffmann, M., Mikutta, C. & Kretzschmar, R. Arsenite binding to natural organic matter: spectroscopic evidence for ligand exchange and ternary complex formation. *Environmental Science & Technology*. 2013, (47), 12165-12173. DOI:10.1021/es4023317.
- [36] Wang, Y., Le Pape, P., Morin, G., Asta, M.P., King, G., Bártová, B., Suvorova, E., Fruttschi, M., Ikogou, M. & Pham, V.H.C. Arsenic speciation in Mekong Delta sediments depends on their depositional environment. *Environmental Science & Technology*. 2018, (52), 3431-3439. DOI:10.1021/acs.est.7b05177.
- [37] Miller, C.B., Parsons, M.B., Jamieson, H.E., Ardakani, O.H., Patterson, R.T. & Galloway, J.M. Mediation of arsenic mobility by organic matter in mining-impacted sediment from sub-Arctic lakes: implications for environmental monitoring in a warming climate. *Environmental Earth Sciences*. 2022, (81), 1-20. DOI:10.1007/s12665-022-10213-2.

5.4 Optimization of elution protocol for simultaneous determination of arsenic and uranium by Lewatit FO 36-DGT

Smolíková, V., Pelcová, P., Ridošková, A., Leermakers, M. Simultaneous determination of arsenic and uranium by the Diffusive Gradients in Thin Films technique using Lewatit FO 36: Optimization of elution protocol. *Talanta*, 2021, 228 (122234), IF 5.386.



The novel DGT technique for the determination of arsenic presented in this work (**Chapter 5.1**) utilizes commercially available resin Lewatit FO 36. Besides the high selectivity of its functional groups of iron oxide-hydroxide for oxyanions, the resin also acts as a weakly basic ion exchanger thanks to tertiary amine functional groups ($-\text{CH}_2-\text{N}(\text{CH}_3)_2$). Therefore, among others, it can also bind negatively charged uranium complexes [280]. Arsenic and uranium are the two main targeted analytes of this work and it was therefore intended to evaluate whether this resin gel could act as a suitable DGT binding phase for uranium determination as well. Since arsenic and uranium often occur simultaneously in mining environments [28-30], it would be beneficial to have a DGT design that can quantitatively determine both analytes at the same time.

Even though the test of uptake efficiency showed very good sorption abilities of Lewatit FO 36 DGTs towards both elements, the current elution protocol was incompatible with the ICP-MS analyses. As mentioned previously (**Chapter 4.4.1**),

a highly concentrated mixture of NaOH and NaCl (0.25 M and 0.17 M, respectively) used for arsenic elution from Lewatit FO 36 resin gels causes polyatomic ion interferences and thus make it impossible to determine arsenic content in the eluates. A new and simple elution protocol was therefore proposed and optimized allowing the simultaneous determination of arsenic and uranium by Lewatit FO 36-DGTs. The best elution efficiency ($90.3 \pm 3.9\%$ for As and $85.2 \pm 3.1\%$ for U) was obtained when 5 mL of 1 M NaOH at 70 °C was used. This elution protocol is simple, allows the processing of a large number of samples in one batch thanks to the elimination of the use of microwave extraction, and enables the analysis of eluates by ICP-MS.

The combination of NaCl and NaOH was initially used because of the recommendation by the manufacturer of the resin and since it has been widely used by other researchers for the regeneration of iron oxide-based sorbents. However, the presence of chlorides has been proven to not have a significant role in the elution of As from the functional groups. In fact, based on information obtained from the manufacturer, the use of NaCl in the recommended elution protocol was related to the original purpose of application – as a sorbent of As from potable water supplies. The NaOH increases pH which leads to deprotonation of the FeO(OH) functional groups which causes electrostatic repulsion of As species that have a negative charge at $\text{pH} > 10$. Nevertheless, the sorbent in this form could not be used for the treatment of drinking water due to the resulting high pH which would result in the release of OH^- from the regenerated resin during subsequent use. The addition of NaCl thus causes an exchange of OH^- groups for Cl^- , and the resin can be re-used for treatment of drinking water. For Supplementary Information see **Chapter 12.2**.



Short communication

Simultaneous determination of arsenic and uranium by the diffusive gradients in thin films technique using Lewatit FO 36: Optimization of elution protocol

Vendula Smolíková^{a,b}, Pavlína Pelcová^b, Andrea Ridošková^{b,c}, Martine Leermakers^{a,*}

^a Analytical, Environmental and Geochemistry, Vrije Universiteit Brussel, Pleinlaan 2, 1050, Brussels, Belgium

^b Department of Chemistry and Biochemistry, Mendel University in Brno, Zemědělská 1, CZ-613 00, Brno, Czech Republic

^c CEITEC – Central European Institute of Technology, Mendel University in Brno, Zemědělská 1, CZ-613 00, Brno, Czech Republic



ARTICLE INFO

Keywords:

Diffusive gradients in thin films technique

Arsenic

Uranium

Elution procedure

ABSTRACT

The sorption ability of Lewatit FO 36-DGT resin gel, which has been developed for arsenic determination, towards uranium was tested by batch experiments within this study for the first time. Since the uptake efficiency of uranium was $99.0 \pm 0.4\%$ and the maximum uptake capacity was not achieved even at the U spike of $1250 \mu\text{g}$ in the solution, the Lewatit FO 36 resin seems to be a suitable binding phase for DGT resin gels for the determination of uranium. The resin gel also does not display any significant sorption selectivity in favour of one element over another. A novel protocol for simultaneous elution of arsenic and uranium from Lewatit FO 36 resin gel was therefore proposed in this study. The elution efficiencies of $90.3 \pm 3.9\%$ and $85.2 \pm 3.1\%$ for As and U, respectively, were obtained using 5 mL of 1 M NaOH at 70°C for 24 h. The comparison with the original elution protocol using microwave-assisted elution by 0.25 M NaOH and 0.17 M NaCl at 130°C for 16 min indicates, that the novel elution protocol provides good results in the performance of arsenic elution and, in addition, allows simultaneous elution of uranium. Moreover, the elimination of NaCl from the elution process allows a fast and simple analysis of both elements using ICP-MS, and therefore, the Lewatit FO 36-DGT technique can become more commonplace among laboratories without the need to modify the analytical method as proposed in the original study.

1. Introduction

The diffusive gradient in thin films (DGT) technique is considered to be an effective tool for *in-situ* determination of labile species of various contaminants in the environment. Although it has been successfully used for the determination of nutrients (ammonium, nitrate, phosphorus) or various organic compounds (antibiotics, bisphenols, pesticides, endocrine disruptors, pharmaceuticals, etc.) it is nowadays mostly used for its original purpose – determining the concentration of the labile species of trace metals [1,2]. In our previously published work [3], a new resin gel utilizing Lewatit FO 36 was developed and evaluated for the determination of four bioavailable arsenic species (As(III), As(V), monomethylarsonic acid, dimethylarsinic acid) in the aquatic environment. But besides the high selectivity of iron oxide-hydroxide functional

groups of Lewatit FO 36 for oxyanions, the resin also acts as a weakly basic ion exchanger thanks to tertiary amine functional groups ($-\text{CH}_2-\text{N}(\text{CH}_3)_2$). Therefore it can also bind natural organic matter such as tannins, lignins, negatively charged uranium complexes, chromate, and others [4]. Arsenic and uranium often occur simultaneously in mining environments [5–7]. Their simultaneous measurement by the DGT technique may be thus beneficial for environmental studies as it may improve understanding of geochemical cycling of these co-occurring contaminants and may contribute to the assessment of their potential bioavailability to biota.

When using the DGT technique, the elution of analytes accumulated on the binding phase requires special attention as it may significantly contribute to the uncertainties of the DGT measurement [8]. Therefore, each novel binding phase undergoes thorough testing of elution

Abbreviations: DGT, diffusive gradient in thin films technique; ET-AAS, electrothermal atomic absorption spectrometry; ICP-MS, inductively coupled plasma mass spectrometry; MDL, method detection limit.

* Corresponding author.

E-mail address: mleermak@vub.be (M. Leermakers).

<https://doi.org/10.1016/j.talanta.2021.122234>

Received 6 November 2020; Received in revised form 13 February 2021; Accepted 16 February 2021

Available online 19 February 2021

0039-9140/© 2021 Elsevier B.V. All rights reserved.

procedures (with key variables of the used elution agent, its concentration, and volume together with the elution time and temperature) in order to achieve the highest elution yield with high reproducibility. The elution protocol of Lewatit FO 36 resin gel proposed in the original study [3] utilizes the mixture of 0.17 M sodium chloride and 0.25 M sodium hydroxide as an elution agent (according to the recommendation of the resin manufacturer [4]) in combination with microwave-assisted extraction at 130 °C for 16 min. Although the obtained quantitative elution yield of arsenic content was $98.4 \pm 2.0\%$, the measurement of arsenic concentration in high chlorides matrix may be challenging due to the interference effect of chlorides during analysis. The proposed elution protocol is therefore not suitable for analysis by inductively coupled plasma mass spectrometry (ICP-MS), which is currently one of the most common analytical techniques for elemental analysis in laboratories.

Given that the Lewatit FO 36 resin has a great potential to be a suitable DGT binding phase for uranium, the uptake efficiency and uptake capacity of Lewatit FO 36 resin gel towards uranium were evaluated in this study. The selectivity of this DGT binding phase for a range of As and U concentrations in different ratios was evaluated as well to assess its suitability for application in a real environment. Due to the need for practical sample analysis by conventional ICP-MS, a new elution protocol for simultaneous measurement of both elements, As and U, was proposed and evaluated within this study.

2. Materials and methods

2.1. Reagents and chemicals

All chemicals were of analytical reagent or higher grade. Chemicals used for DGT gels production and the preparation protocol are described in a previous study [3]. Arsenic standard solution 1000 mg L^{-1} in 2% HNO_3 (Merck, Germany) and uranium standard solution 1000 mg L^{-1} in 2% HNO_3 (SPEX CertiPrep, UK) were used for the preparation of experimental solutions and for calibration of ICP-MS together with the internal standard of indium (Alfa Aesar, addition to a final concentration of $1 \text{ } \mu\text{g L}^{-1}$). The HNO_3 was used for material cleaning (HNO_3 produced by distillation apparatus), gels extraction, and sample acidification (Optima Grade, Fisher Scientific, USA). The NaCl, NaOH, NaNO_3 (all Merck, Germany), and H_2O_2 (suprapure, Fisher Scientific, USA) were used for gel extraction. The pH was measured by multi-meter WTW 3430 and adjusted to a desired value by diluted HNO_3 or NaOH if necessary.

2.2. Uptake efficiency

Experimental solutions (0.01 M NaNO_3 ; pH = 5; spiked with $20 \text{ } \mu\text{g L}^{-1}$ of As and U) were prepared 24 h before the start of the experiment so that the carbon content in the solution equilibrate with atmospheric CO_2 . To evaluate the uptake efficiency of Lewatit FO 36 resin gel, a single resin gel disc (5 replicates) was immersed into 10 mL of experimental solution and shaken for 24 h. The concentration of both elements in the experimental solution was determined at the beginning and end of the experiment by ICP-MS. The difference between the initial mass (M_i) and the remaining mass (M_r) of analytes in the solution indicated the total analyte mass accumulated on the resin gel disc (M_a). The efficiency of As and U uptake was expressed as the uptake factor (f_u), using Eq. (1). A control experiment for evaluation of As and U sorption on the walls of tubes was performed as well.

$$f_u = (M_i - M_r) / M_i * 100\% \quad (1)$$

2.3. Elution efficiency

The gel discs removed from the experimental solution were rinsed with Milli-Q water and the accumulated As and U were eluted using various elution agents (HNO_3 , NaOH, NaCl, H_2O_2) or their mixtures. The

mixture of NaOH and H_2O_2 has already been successfully used as an elution agent for elution of As [9,10] or U [11,12] from other DGT resin gels. The molarity and volume of elution agents in combination with extraction temperature varied within 7 variants (Table 1) in order to achieve the highest possible efficiency of elution of both analytes. The tested molarity of elution agents and extraction conditions were selected with respect to the previous studies dealing with the elution of As and U from DGT resin gels [10,11]. The extraction in the conventional drying oven at the temperature of 70 °C allows to increase the elution efficiency and at the same time does not disturb the material of the polypropylene extraction tubes [13]. Resin gel blanks (gel discs that were not deployed into the experimental solution) were eluted as well. After 24 h of elution, the samples were centrifuged if necessary and diluted ten times by 2% (v/v) HNO_3 prior to analysis. The eluted mass of As and U (M_e) was used for the calculation of the elution factor (f_e) using Eq. (2).

$$f_e = (M_e / M_a) * 100\% \quad (2)$$

2.4. Diffusion coefficient of U towards Lewatit FO 36

Since resin gels utilizing Lewatit FO 36 resin were originally developed for the determination of arsenic, its diffusion coefficient was determined in the previous study [3]. But diffusion coefficient of U towards this resin gel was determined within this study by the time-dependence experiment. The DGTs were deployed in 2 L of well-stirred 0.01 M NaNO_3 spiked with $20 \text{ } \mu\text{g L}^{-1}$ of U (with the addition of $0.983 \text{ mM L}^{-1} \text{ NaHCO}_3$ to buffer the solution to pH 7.56 [14]) and a duplicates of DGT units were retrieved from the solution after 2, 4, 8, 24, 48 h. The diffusion coefficient (D , $\text{cm}^2 \text{ s}^{-1}$) was calculated from the slope of a linear regression of the U mass accumulated on a resin gel and normalized for the solution concentration (M/c) as a function of time using Eq. (3), where Δg is the thickness of diffusive layer consisting of diffusive gel and membrane filter ($0.080 + 0.0125 \text{ cm}$), and A is the exposed area (3.14 cm^2). The diffusion coefficient was corrected to the temperature using the Stokes-Einstein relation [15].

$$D = \text{slope} * \Delta g / A \quad (3)$$

2.5. Uptake capacity of the Lewatit FO 36 resin gel

The uptake capacity is commonly determined by exposing a resin gel to a high concentration of analyte until equilibrium is reached. A single Lewatit FO 36 resin gel disc (3 replicates) was immersed into 5 mL of 0.01 M NaNO_3 solution (pH 5.0) with U concentration range of $0.1\text{--}250 \text{ mg L}^{-1}$ and let shaken for 24 h. The gels were subsequently eluted using the new elution protocol proposed in this study. The U mass eluted from the gel disc (M_e) was compared to the mass that was expected to be accumulated on the gel disc (M_a) based on the difference between the initial and remaining U mass in the solution. This enabled us to validate the results and evaluate whether the elution efficiency is independent of the amount of metal bound on the gel disc. Since the new elution protocol was also tested for As, the same experiment was performed with both elements in parallel.

Table 1
Variants of the tested elution protocols.

Variant	Elution agent	Elution volume	Elution temperature
A	Concentrated HNO_3	1 mL	70 °C
B	$0.25 \text{ M NaOH} + 0.17 \text{ M NaCl}$	1 mL	70 °C
C	$1 \text{ M NaOH} + 1 \text{ M H}_2\text{O}_2$	1 mL	18 °C ^a
D	$1 \text{ M NaOH} + 1 \text{ M H}_2\text{O}_2$	5 mL	70 °C
E	$2 \text{ M NaOH} + 1 \text{ M H}_2\text{O}_2$	2.5 mL	70 °C
F	1 M NaOH	1 mL	18 °C ^a
G	1 M NaOH	5 mL	70 °C

^a Laboratory temperature.

2.6. Selectivity of the Lewatit FO 36 resin gel for arsenic and uranium

To evaluate whether the Lewatit FO 36 resin gel favour one of the tested elements over the other, the series of solutions with As + U spike of various concentrations and ratios were prepared (Table 2). The concentration ranges were chosen concerning the average concentrations of As and U in the natural environment that are generally quite low ($<10 \mu\text{g L}^{-1}$ in freshwater and $1.5 \mu\text{g L}^{-1}$ in seawater for As [16], and $0.3 \mu\text{g L}^{-1}$ in freshwater and $3.3 \mu\text{g L}^{-1}$ in seawater for U [17,18]). The variant j (10 mg L^{-1} of each element) then represented extreme conditions. A single Lewatit FO 36 resin gel disc (3 replicates) was immersed into 10 mL of each solution prepared in 0.01 M NaNO_3 (pH 5.0) and the tubes were shaken for 24 h. The uptake efficiency of both elements was calculated by the difference between the initial and remaining masses in the solution as described in Section 2.2. The elution of the gels using the new elution protocol proposed in this study was performed as well.

2.7. Analytical methods and data analysis

Arsenic and uranium concentration in all samples was determined by the sector field inductively coupled plasma mass spectrometry (SF-ICP-MS, Element II, Thermo Fisher Scientific Bremen GmbH, Germany), for instrumental parameters see Supplementary Information. The accuracy of sample analysis was verified by the analysis of reference samples (river water SLRS6, National Research Council Canada). Arsenic and uranium concentration in the certified reference material (SLRS-6) was $108 \pm 4\%$ and $103 \pm 5\%$ of certified values, respectively. Analysis of blank resin gels (5 replicates) was performed for the determination of the method detection limit (MDL). Analytical software STATISTICA13 (StatSoft, Czech Republic) was used for data analysis. One-way analysis of variance (ANOVA test) was used to determine the statistically significant differences between DGT performances. A statistically significant difference of the results was declared when p-value was below the level of significance $\alpha = 0.05$. The Tukey's Honest Significant Difference post-hoc test was performed to identify statistically different results.

3. Results and discussion

3.1. Uptake and elution efficiency

The average uptake efficiency of arsenic and uranium towards Lewatit FO 36 resin gel ($n = 15$) was $98.7 \pm 0.6\%$ and $99.0 \pm 0.4\%$, respectively. No sorption of As and U onto the tube walls was observed within the control experiment. The previous study showed excellent sorption ability of Lewatit FO 36 resin gel towards arsenic whose As(III) and As(V) compounds are predominantly neutral or anionic in the pH range > 4 [3]. In terms of uranium, it is mostly present in the natural surface water under oxic conditions in the hexavalent oxidation state U(VI), while under anoxic conditions in groundwater (e.g. in confined aquifers) it is present in tetravalent oxidation state U(IV). Other oxidation states (trivalent and pentavalent) of uranium are generally not relevant for ecotoxicological studies because they are considered unstable in the natural environment [17]. Hexavalent compounds are also highly soluble and mobile and are present either as free uranyl ion (UO_2^{2+}) or complexed with ligands such as OH^- , Cl^- , CO_3^{2-} , PO_4^{3-} , F^- , SO_4^{2-} [19]. However, both free uranyl ion and the most common carbonate complexes are predominantly neutral or anionic in the same pH range as arsenic and are therefore bound by functional groups of Lewatit FO 36 resin.

Table 2

Arsenic and uranium concentration ratios for evaluation of Lewatit FO 36 selectivity.

Variant	a	b	c	d	e	f	g	h	i	j
As ($\mu\text{g L}^{-1}$)	1	1	1	10	10	10	100	100	100	10,000
U ($\mu\text{g L}^{-1}$)	1	10	100	1	10	100	1	10	100	10,000

Comparison of elution efficiencies of all tested elution agents is given in Fig. 1. Concentrated HNO_3 (A) was an effective elution agent for uranium (although with a large standard deviation of 8.3%) but as already demonstrated in the original study by Smolíková et al. [3], it is not a suitable eluent for arsenic elution from Lewatit FO 36 resin gel. The elution mixture of 0.25 M NaOH and 0.17 M NaCl, originally proposed in the mentioned study, provided unsatisfactory recoveries of both elements (B), but the results pointed out the strong effect of the temperature on the elution efficiency. In the original protocol using this elution agent in combination with microwave-assisted extraction (130°C for 16 min), the elution efficiency of arsenic was 34.8% higher compared to the result in this study, where only the temperature of 70°C was used. The resulting elution efficiency was therefore insufficient for DGT calculations since the minimum generally accepted value of f_e should be at least 80% as it is a typical value for metals [2]. Even though the higher temperature of microwave-assisted extraction allows achieving higher elution efficiency, its practical use may be restrictive due to the low number of samples processed in one batch and generally higher demands on laboratory equipment. Therefore, the extraction of DGT resin gels in a conventional drying oven at 70°C is generally preferred and was used in this study as well. To avoid the use of chloride-containing eluents which cause interferences during analyses, the mixture of NaOH and H_2O_2 (C, D, E) was used. There is a statistically significant difference ($p < 0.05$) of elution efficiency between variant C and variants D, E for both elements. But whereas the use of a higher temperature and elution agent volume reduced the elution efficiency of uranium, the elution efficiency of arsenic was conversely increased. Therefore, the higher temperature and volume of the elution agent seems to be crucial for the elution of arsenic. On the other hand, a statistically significant improvement in the elution efficiency of uranium between variants D and E ($p < 0.05$) suggests that a higher ratio of elution agents in favour of NaOH to H_2O_2 (from 1:1 to 2:1) can increase the uranium elution despite the negative effect of higher temperature. The presence of H_2O_2 at the higher temperature, therefore, seems to have a negative effect on the elution of uranium from Lewatit FO 36 resin gel. For this reason, a simple 1M NaOH was used as the other variant of the elution agent. As evident from the obtained results, laboratory temperature and eluent volume of 1 mL were insufficient for elution of both elements (F). The elevated extraction temperature (70°C) and a higher volume of eluent (5 mL) (G) nevertheless provided excellent elution efficiency of As ($90.3 \pm 3.9\%$) and U ($85.2 \pm 3.1\%$). Since there was no statistical difference ($p > 0.05$) in the elution efficiencies of As in variants D, E, and G, it is

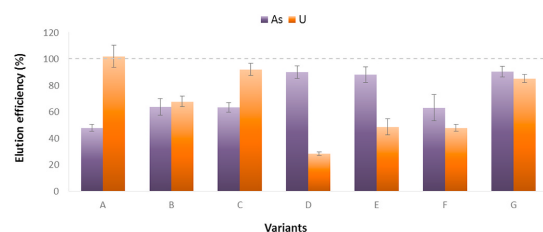


Fig. 1. Comparison of elution efficiency of each elution agent variant: A – concentrated $\text{HNO}_3/70^\circ\text{C}$; B – 0.25 M NaOH + 0.17 M NaCl/ 70°C ; C – 1 M NaOH + 1 M $\text{H}_2\text{O}_2/18^\circ\text{C}$; D – 1 M NaOH + 1 M $\text{H}_2\text{O}_2/70^\circ\text{C}/5 \text{ mL}$; E – 2 M NaOH + 1 M $\text{H}_2\text{O}_2/70^\circ\text{C}/2.5 \text{ mL}$; F – 1 M NaOH/ 18°C ; G – 1 M NaOH/ $70^\circ\text{C}/5 \text{ mL}$ (error bars for $n = 5$).

obvious that H_2O_2 has no role in the elution process of arsenic from Lewatit FO 36 resin gel. Even though the elution efficiency of arsenic is 8.0% lower compared to the one of the original study [3], the advantages of simultaneous elution of both elements and the possibility of analysing the samples by ICP-MS are undoubtedly more beneficial. Moreover, the elution factors of both elements are higher than the minimum generally accepted value of 80% and, in addition, with excellent repeatability with deviations below 5%. For the results of statistical analysis see Supplementary Information.

3.2. Diffusion coefficient of U towards Lewatit FO 36

The diffusion coefficient of U calculated within this study from the time-dependence experiment (Fig. 2) was $4.38 \pm 0.06 \times 10^{-6} \text{ cm}^2 \text{ s}^{-1}$ (0.01 M NaNO_3 solution, pH 7.56, at 25°C), which is in good agreement with the average value of $D = 4.44 \pm 0.22 \times 10^{-6} \text{ cm}^2 \text{ s}^{-1}$ obtained by Drozdak et al. [12] for Chelex, Metsorb, and Diphonix resin gels. Drozdak et al. [12] also demonstrated in their study that the diffusion coefficients of U may vary in the literature, with differences being given by the used DGT binding phase in combination with the experimental conditions (solution composition and pH). This causes the changes in uranium speciation in solution (such as the formation of anionic uranyl carbonates species), resulting in a lower affinity towards the resin or lower uptake kinetics.

3.3. Uptake capacity of the Lewatit FO 36 resin gel

Generally, a high uptake capacity of the DGT binding phase towards the studied analyte is required to avoid its saturation during *in-situ* deployment. Very high uptake capacity of the Lewatit FO 36 resin gel towards As was demonstrated in the original study [3], and therefore, the uptake capacity towards U was investigated as well.

The expected U mass accumulated per gel disc (based on the difference between the initial and remaining mass in the solution) plotted versus the U concentration in the original solution is shown in Fig. 3A. The Lewatit FO 36 resin gel effectively accumulated uranium even though the U mass in the initial solution was 1250 μg which proves its very high uptake capacity. Given that the saturation of resin gel was not achieved, the total uptake capacity of Lewatit FO 36 towards uranium has not been established. In comparison with other binding phases used for the determination of U, the uptake capacity of Lewatit FO 36 is comparable or much higher than the capacities reported by Drozdak et al. [12,20]. In these studies, the maximum uptake capacities of PIWBA, Chelex-100, and Metsorb resins were determined as 99.9–249.9 μg of U per gel disc. The best results were so far achieved with Diphonix resin, the capacity of which was not fulfilled even when the U spike was up to 2500 μg .

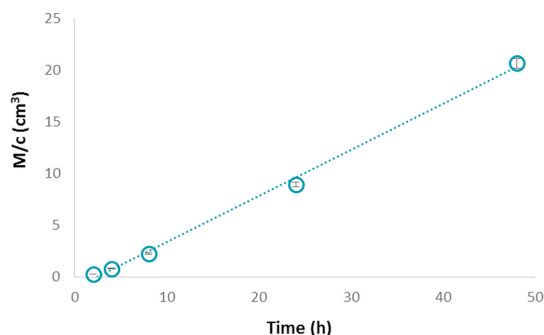


Fig. 2. Time-dependence experiment of U uptake by Lewatit FO 36 resin gel (deployment solution of 0.01 M NaNO_3 ; U 20 $\mu\text{g L}^{-1}$; pH 7.56; $n = 3$).

However, even though the uptake capacity of the Lewatit FO 36 resin gel was demonstrated to be very high, important information regarding the efficiency of the elution protocol proposed in this study was revealed. The results of U mass eluted from the gels showed that the elution efficiency is dependent on the amount of U accumulated on the resin gel disc and is actually able to release only up to $112.2 \pm 8.7 \mu\text{g}$ of accumulated U (Fig. 3A). To verify the data for As, the uptake capacity test and subsequent elution of the gels were performed in the same way (Fig. 3B). The results showed that only $122.3 \pm 8.4 \mu\text{g}$ of accumulated As was released from the gel during elution even though the accumulated mass was much higher. Since the total masses of both analytes eluted from gels are very similar, it seems that the elution agent (1 M NaOH at 70°C) reached its maximum elution capacity. Based on the results of different volumes of eluent and especially elution temperature, the authors believe, that increasing the eluent volume or extraction temperature may increase the elution efficiency. Nevertheless, with respect to the practical use of DGTs and also the average concentrations of arsenic ($<10 \mu\text{g L}^{-1}$ in freshwater and $1.5 \mu\text{g L}^{-1}$ in seawater [16]) and uranium ($0.3 \mu\text{g L}^{-1}$ in freshwater and $3.3 \mu\text{g L}^{-1}$ in seawater [17,18]), the obtained results still suggest the possible deployment over long time periods in natural waters. Regarding the most common deployment period (24 h), the Lewatit FO 36-DGTs can be applied in natural waters with concentrations up to 6.51 mg L^{-1} of As or 8.73 mg L^{-1} of U.¹ Therefore, the potential distortion of the results can occur only in the case of application in an environment where the concentrations of both elements would be extremely high.

3.4. Selectivity of the Lewatit FO 36 resin gel for arsenic and uranium

Although the uptake capacity of both studied elements was determined to be very high, a series of experiments evaluating the influence of the simultaneous presence of As and U on the course of their sorption was performed at different concentration ratios (Fig. 4). The results showed that even at the highest concentration ratio of As and U (variant j with $10:10 \text{ mg L}^{-1}$), the uptake efficiency of both elements was $97.9 \pm 0.7\%$ and $95.9 \pm 1.4\%$, respectively. With respect to the results obtained in Section 3.3, the elution of the gels was performed as well in order to validate the elution efficiency when both analytes are accumulated at the same time. The resulting eluted masses of variants a–i corresponded overall to 94.6–105.5% of the masses accumulated on the gels. However, this result was expected given the fact that the As and U spike in the most concentrated variant i was only 1 μg of each element. On the contrary in the variant j, where the As and U spike corresponded to 100 μg of each element, the total accumulated mass (200 μg) on the gel disc exceeded the maximum mass that can be released from the gel using the proposed elution protocol as stated in Section 3.3. Thus, the elution efficiencies obtained for variant j were $50.3 \pm 5.5\%$ for As and $67.7 \pm 9.1\%$ for U. When expressing these results as total masses, this corresponds to $48.9 \pm 5.4 \mu\text{g}$ of As and $63.9 \pm 8.6 \mu\text{g}$ of U and therefore $\sim 113 \mu\text{g}$ as a sum of eluted analytes. This result thus confirms the observations from the previous experiment and indicates the insufficient strength of the eluent when the total mass of the accumulated analytes exceeds $\sim 110 \mu\text{g}$.

3.5. Method detection limit

The blank values of Lewatit FO 36 resin gel eluted by 5 mL of 1 M NaOH, was calculated as $0.21 \pm 0.04 \text{ ng}$ for As, and $0.16 \pm 0.02 \text{ ng}$ for U. The MDL was calculated for 24 h deployment using the thickness of the diffusion layer (0.0925 cm), exposed area (3.14 cm^2) and the diffusion coefficient of As and U towards Lewatit FO 36 ($6.41 \times 10^{-6} \text{ cm}^2 \text{ s}^{-1}$ [3]

¹ The maximum As/U concentration in natural waters for DGT application calculated for $M_{\text{As}} = 122.3 \mu\text{g As}$; $M_{\text{U}} = 112.2 \mu\text{g}$; $\Delta g = 0.0925 \text{ cm}$; $A = 3.14 \text{ cm}^2$; $t = 24 \text{ h}$; $D_{\text{As}} = 6.41 \times 10^{-6} \text{ cm}^2 \text{ s}^{-1}$; $D_{\text{U}} = 4.38 \times 10^{-6} \text{ cm}^2 \text{ s}^{-1}$.

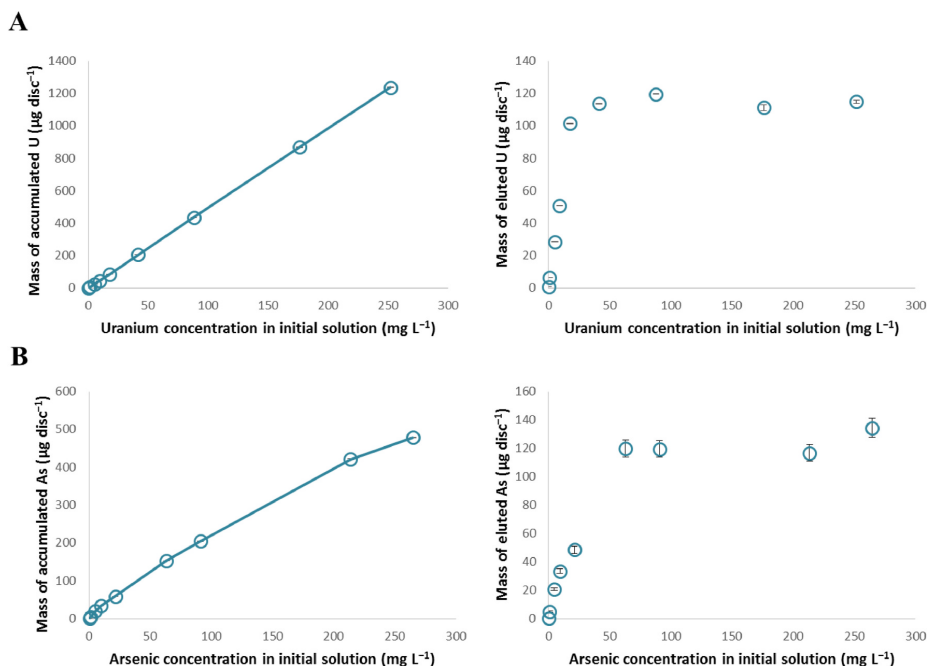


Fig. 3. Uptake capacity and elution efficiency of new elution protocol over the high concentration range of uranium (A) and arsenic (B) (error bars for $n = 3$).

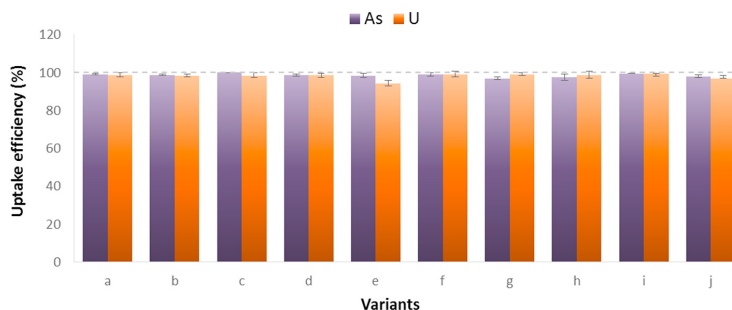


Fig. 4. Evaluation of the Lewatit FO 36 resin gel selectivity for As and U at different concentration ratios: a – 1:1; b – 1:10; c – 1:100; d – 10:1; e – 10:10; f – 10:100; g – 100:1; h – 100:10; i – 100:100; j – 10,000:10,000 (concentrations in $\mu\text{g L}^{-1}$; error bars for $n = 3$).

and $4.38 \times 10^{-6} \text{ cm}^2 \text{ s}^{-1}$, respectively). The calculation was made from three times the standard deviations of resin gel blank values. The resulting MDLs were $0.04 \mu\text{g L}^{-1}$ for As and $0.02 \mu\text{g L}^{-1}$ for U.

4. Conclusions

The excellent sorption abilities of Lewatit FO 36-DGT resin gel towards uranium and arsenic were demonstrated within this study by quantitative uptake efficiency of $98.7 \pm 0.6\%$ for As and $99.0 \pm 0.4\%$ for U. Moreover, the resin gel has extremely high uptake capacity for U that was not saturated even at a U spike of $1250 \mu\text{g}$ in the solution. It has also been shown that the resin gel does not show signs of selectivity in favour of one element over another. These results suggest that this novel resin gel can be used for the simultaneous determination of both elements in the real aquatic environment. An optimized elution procedure for the simultaneous elution of As and U from Lewatit FO 36 resin gel using 5

mL of 1 M NaOH at 70°C resulted in an elution efficiency of $90.3 \pm 3.9\%$ for As and $85.2 \pm 3.1\%$ for U. The elimination of NaCl from the original elution protocol allows simple analysis of samples by ICP-MS and therefore enables the widespread use of the new Lewatit FO 36 resin gel in many laboratories. Although the results revealed that the proposed elution protocol may be insufficient for elution of accumulated masses over $\sim 110 \mu\text{g}$ per gel disc or higher, with respect to common concentrations of both studied elements in the natural environments, this would be a problem only under extreme conditions. However, our results pointed to the need for thorough testing in the introduction of new elution procedures, which should always be verified in terms of both uptake and elution efficiency over concentration ranges.

Declaration of competing interest

The authors declare that they have no known competing financial

interests or personal relationships that could have appeared to influence the work reported in this paper.

Acknowledgements

This work was supported by the CEITEC 2020 (LQ1601) and by the project PROFISH CZ.02.1.01/0.0/0.0/16_019/0000869, which is financed by the European Regional Development Fund in the Operational Programme Research, Development and Education and The Czech Ministry of Education, Youth and Sports. Graphical abstract was created with BioRender.com.

Appendix A. Supplementary data

Supplementary data to this article can be found online at <https://doi.org/10.1016/j.talanta.2021.122234>.

Author contribution

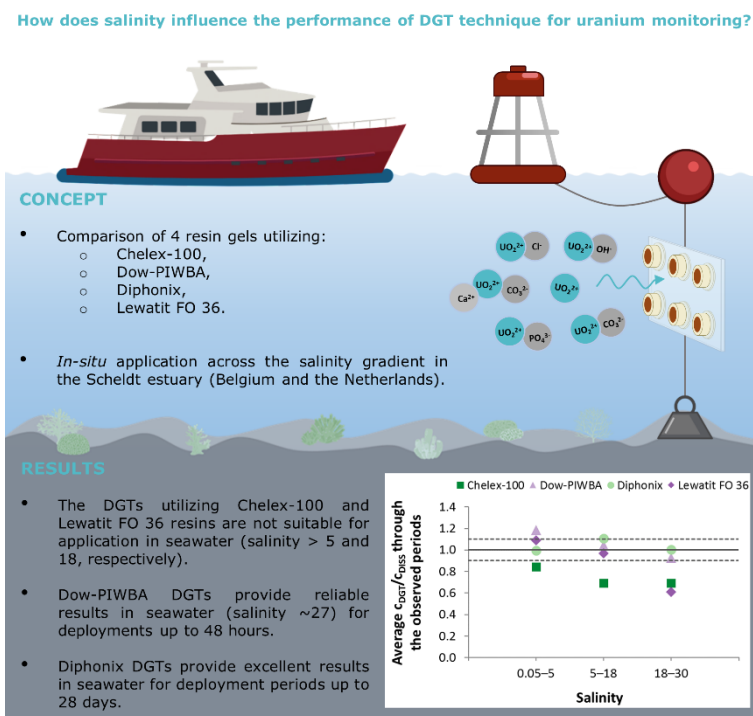
Vendula Smolřková; Investigation, Methodology, Formal analysis, Writing – original draft, Pavřlna Pelcová; Writing – review & editing, Andrea Ridořková; : Writing – review & editing, Martine Leermakers: Conceptualization, Supervision, Methodology, Writing – review & editing.

References

- [1] C. Li, S. Ding, L. Yang, Y. Wang, M. Ren, M. Chen, X. Fan, E. Lichtfouse, Diffusive gradients in thin films: devices, materials and applications, *Environ. Chem. Lett.* (2018) 1–31.
- [2] W. Davison, *Diffusive Gradients in Thin-Films for Environmental Measurements*, Cambridge University Press, 2016.
- [3] V. Smolřková, P. Pelcová, A. Ridořková, J. Hedbávný, J. Grmela, Development and evaluation of the iron oxide-hydroxide based resin gel for the diffusive gradient in thin films technique, *Anal. Chim. Acta* 1102 (2020) 36–45.
- [4] Lanxess, Product Information – Lewatit® FO 36, 2011. <https://www.lenntech.com/Data-sheets/Lewatit-FO-36-L.pdf>.
- [5] A. Abdelouas, Uranium mill tailings: geochemistry, mineralogy, and environmental impact, *Elements* 2 (6) (2006) 335–341.
- [6] J.M. Blake, S. Avasarala, K. Artyushkova, A.-M.S. Ali, A.J. Brearley, C. Shuey, W. P. Robinson, C. Nez, S. Bill, J. Lewis, Elevated concentrations of U and co-occurring metals in abandoned mine wastes in a northeastern Arizona Native American community, *Environ. Sci. Technol.* 49 (14) (2015) 8506–8514.
- [7] R. Donahue, M. Hendry, Geochemistry of arsenic in uranium mine mill tailings, Saskatchewan, Canada, *Appl. Geochem.* 18 (11) (2003) 1733–1750.
- [8] A. Kreuzeder, J. Santner, H. Zhang, T. Prohaska, W.W. Wenzel, Uncertainty evaluation of the diffusive gradients in thin films technique, *Environ. Sci. Technol.* 49 (3) (2015) 1594–1602.
- [9] F. Tan, X. Jiang, X. Qiao, D. Sun, J. Gao, X. Quan, J. Chen, S. Ren, Y. Wang, Development of cerium oxide-based diffusive gradients in thin films technique for in-situ measurement of dissolved inorganic arsenic in waters, *Anal. Chim. Acta* 1052 (2019) 65–72.
- [10] Q. Sun, J. Chen, H. Zhang, S. Ding, Z. Li, P.N. Williams, H. Cheng, C. Han, L. Wu, C. Zhang, Improved diffusive gradients in thin films (DGT) measurement of total dissolved inorganic arsenic in waters and soils using a hydrous zirconium oxide binding layer, *Anal. Chem.* 86 (6) (2014) 3060–3067.
- [11] C.M. Hutchins, J.G. Panther, P.R. Teasdale, F. Wang, R.R. Stewart, W.W. Bennett, H. Zhao, Evaluation of a titanium dioxide-based DGT technique for measuring inorganic uranium species in fresh and marine waters, *Talanta* 97 (2012) 550–556.
- [12] J. Drozdak, M. Leermakers, Y. Gao, V. Phrommavanh, M. Descostes, Evaluation and application of Diffusive Gradients in Thin Films (DGT) technique using Chelex®-100, Metsorb™ and Diphonix® binding phases in uranium mining environments, *Anal. Chim. Acta* 889 (2015) 71–81.
- [13] M. Leermakers, V. Phrommavanh, J. Drozdak, Y. Gao, J. Nos, M.J.C. Descostes, DGT as a useful monitoring tool for radionuclides and trace metals in environments impacted by uranium mining, case study of the Sagnes wetland in France 155 (2016) 142–151.
- [14] G.S. Turner, G.A. Mills, J.L. Burnett, S. Amos, G.R. Fones, Evaluation of diffusive gradients in thin-films using a Diphonix® resin for monitoring dissolved uranium in natural waters, *Anal. Chim. Acta* 854 (2015) 78–85.
- [15] H. Zhang, W. Davison, Diffusional characteristics of hydrogels used in DGT and DET techniques, *Anal. Chim. Acta* 398 (2–3) (1999) 329–340.
- [16] W. Goessler, D. Kuehnelt, Analytical methods for the determination of arsenic and arsenic compounds in the environment, in: W.T. Frankenberger Jr. (Ed.), *Environmental Chemistry of Arsenic*, CRC Press, 2001.
- [17] Z. Karpas, Determination of Uranium in Environmental Samples, *Analytical Chemistry of Uranium: Environmental, Forensic, Nuclear, and Toxicological Applications*, CRC Press, 2014.
- [18] S.J. Markich, Uranium speciation and bioavailability in aquatic systems: an overview, *Sci. World J.* 2 (2002).
- [19] R.B.M. Sparovek, J. Fleckenstein, E.J.L.V. Schnug, Issues of uranium and radioactivity in natural mineral waters 51 (4) (2001) 149–158.
- [20] J. Drozdak, M. Leermakers, Y. Gao, V. Phrommavanh, M. Descostes, Novel speciation method based on Diffusive Gradients in Thin Films for in situ measurement of uranium in the vicinity of the former uranium mining sites, *Environ. Pollut.* 214 (2016) 114–123.

5.5 Comparative study evaluating the salinity influence on the performance of different DGT binding phases for uranium determination – the Scheldt Estuary (Belgium)

Smolíková, V., Pelcová, P., Ridošková, A., Leermakers, M. Diffusive Gradients in Thin-Films technique for uranium monitoring along a salinity gradient: A comparative study on the performance of Chelex-100, Dow-PIWBA, Diphonix, and Lewatit FO 36 resin gels in the Scheldt Estuary. *Talanta*, 2021, 240 (123168). IF 5.386.



The Diffusive Gradients in Thin films is a broadly used and beneficial passive sampling technique for the determination of trace elements in the environment. Therefore, many studies are dealing with the development and evaluation of new DGT binding gels containing various sorbents in order to obtain a robust technique providing accurate and reliable results of the DGT measurement. Similarly, number of studies focuses on the development and evaluation of the DGT designs for U determination using sorbents such

as Chelex-100 [240, 241], Diphonix [180, 238], Dowex 2×8-400 [239], Dow-PIWBA [242], MnO₂ [240], Metsorb [241], Lewatit FO 36 [274], Spheron-Oxin [243], or Whatman DE 81 [236]. Nevertheless, the data about their practical application in the real environment are lacking in the literature as they are mostly limited to a few *in-situ* trials. When developing a novel DGT design, the sorption ability of the binding phase towards the targeted analyte is usually studied in the presence of interfering ions. But these tests performed under laboratory conditions are generally limited to a few major analytes that may be potentially co-adsorbed with the desired analyte or that can interact with the analyte in the solution. However, the simulated conditions can never fully reflect the complexity of the real aquatic environment. Therefore, a thorough evaluation of the DGT performance in the real environment of various conditions is a crucial step to validate the capability of the binding phase to provide robust and reliable results.

For this reason, a comparative study of the performance of four selected DGT designs utilizing Chelex-100, Diphonix, Dow-PIWBA, and Lewatit FO 36 resins for the determination of uranium in the real environment is presented in this chapter. In order to evaluate their efficiency under various conditions, the DGTs were tested across the salinity gradient in the Scheldt estuary (Belgium) during four campaigns over the period 2014–2021. The results revealed that Chelex-100 and Lewatit FO 36 are not suitable DGT binding phases for U determination in seawater. Although Dow-PIWBA DGTs provided excellent performance along the whole salinity gradient, the long-term deployment trial in seawater revealed that the resin gel accumulates U only for up to 2 days. The best performance was achieved by Diphonix DGTs that provided results with a very good agreement between DGT-determined and dissolved U concentrations across the whole salinity gradient. Moreover, the long-term deployment trial revealed that Diphonix resin is the only binding phase providing exceptional results even after 28 days of deployment in seawater (~28 PSU). The results of this study undoubtedly demonstrated that thorough testing of the DGT technique in a natural environment is a crucial prerequisite for obtaining reliable data and a better understanding of the biogeochemical behaviour of trace elements in the environment. For Supplementary Information see **Chapter 12.3**.



Diffusive Gradients in Thin-films technique for uranium monitoring along a salinity gradient: A comparative study on the performance of Chelex-100, Dow-PIWBA, Diphonix, and Lewatit FO 36 resin gels in the Scheldt estuary

Vendula Smolíková^{a,b}, Pavlína Pelcová^b, Andrea Ridošková^b, Martine Leermakers^{a,*}

^a Analytical, Environmental and Geochemistry, Vrije Universiteit Brussel, Pleinlaan 2, Brussels, Belgium

^b Department of Chemistry and Biochemistry, Mendel University in Brno, Zemědělská 1, CZ-613 00, Brno, Czech Republic

ARTICLE INFO

Keywords:

Diffusive gradients in thin-films
Passive sampling
Uranium monitoring
Uranium speciation
Salinity gradient
Scheldt estuary

ABSTRACT

Monitoring of uranium in the environment using the Diffusive Gradients in Thin-films (DGT) technique gains importance as it can provide unique information about the bioavailability of the element and allows its long-term *in-situ* measurement. Hence, in this study, four DGT binding phases (Chelex-100, Dow-PIWBA, Diphonix, and Lewatit FO 36 resins) were evaluated for uranium monitoring to assess the robustness of their performance in estuarine and marine environments. These DGTs were deployed along the Scheldt estuary (Belgium and the Netherlands) over four campaigns between 2014 and 2021. The DGT performance (ratio of the DGT-determined vs. dissolved U concentration in grab water sample) varied with the water salinity. The Chelex-100 DGTs generally provided good performance in freshwater (median ratios close to 1.0), but an inverse correlation with the increasing salinity was observed (median ratios 0.7 at the stations with salinity >5). The Lewatit FO 36 DGTs provided good performance in the salinity range 0–18 (median ratios 1.0). However, a strong negative influence was observed at stations with high salinity levels (>18, ratio 0.6) and during the long-term deployment in seawater (ratios <0.5 over deployment periods ≥2 days). The Dow-PIWBA and Diphonix DGTs provided overall similar results with excellent performances along the whole salinity gradient (median ratios 1.1 and 1.0, respectively). Nevertheless, the long-term deployment trial in seawater (salinity ~27) revealed the robustness of Diphonix DGTs that provided outstanding results even after 28 days of deployment (ratio 1.0). The differences in the performance of tested DGT resins were mostly given by the changes of U speciation along the salinity gradient. The speciation modelling of U showed that calcium uranyl carbonate complexes dominate along the Scheldt estuary (from 97 to 86% seawards) with increasing fraction of $\text{UO}_2(\text{CO}_3)_3^{4-}$ (from 2 to 14%) towards the mouth.

1. Introduction

Environmental pollution monitoring programs are nowadays gaining in importance around the world, partially due to the increasing acceptance of social responsibility for the impact of human activities on the environment [1,2]. Alongside other significantly targeted analytes, there is an increasing need for the monitoring of uranium. The concentration of uranium in the terrestrial and aquatic environment is not only given by its natural abundance and release from the geological background but can be influenced by anthropogenic activities such as uranium mining and milling or its processing in the nuclear industry [3]. Monitoring of uranium in the environment represents a challenge for

ecotoxicological studies as the total concentration and isotopic composition of uranium provides information about radiological toxicity but not necessarily about the chemical toxicity which is related to uranium speciation [4]. While there are different approaches for water quality monitoring, including continual *in-situ* measurement (e.g., electrodes for dissolved oxygen or pH), the monitoring of trace metals is generally performed by discrete sampling in time series. However, this approach may provide variable and misleading results, especially in dynamic environments with fluctuating analyte concentrations. A continual *in-situ* sampling approach using the Diffusive Gradients in Thin-films (DGT) technique stands out for its ability to determine mobile and labile forms of the monitored analyte (“free ions” and their labile

Abbreviations: DGT, diffusive gradient in thin-films technique; ICP-MS, inductively coupled plasma mass spectrometry.

* Corresponding author. Vrije Universiteit Brussel - AMGC, Pleinlaan 2, 1050, Brussels, Belgium.

E-mail address: mleermak@vub.be (M. Leermakers).

<https://doi.org/10.1016/j.talanta.2021.123168>

Received 20 September 2021; Received in revised form 10 December 2021; Accepted 21 December 2021

Available online 22 December 2021

0039-9140/© 2021 Elsevier B.V. All rights reserved.

complexes) over a certain time period, thus providing the time-weighted average concentrations. As a result, it is possible to obtain crucial information about uranium bioavailability which better reflects the ecotoxicological status of the environment [5–8].

The principle of the DGT technique is based on the diffusion of analytes through a diffusive gel and its subsequent accumulation on a binding gel (resin embedded in hydrogel). The analyte mass accumulated on the binding gel is then eluted and analysed by instrumental technique [9,10]. In addition to the original purpose of the DGT technique as a tool for measuring trace metals in the aquatic environment [6, 10–12], it is also used for the determination of nutrients [13–16], radioactive elements [17–22], platinum group elements [23–25], rare-earth elements [26,27], and various organic compounds (such as phenolic compounds [28], antibiotics [29], or pesticides [30] as summarized in work of Guibal et al. [31] and references cited therein) in water, sediment or soil, as well as other matrices such as food [32,33]. The advantages of using the DGT technique are: the pre-concentration of analytes that allows for measurements at low environmental concentrations, the ability to obtain time-integrated concentrations of analytes, and the possibility of simultaneous deployments of DGTs in the water and sediment in the studied area, thus obtaining more complex information about the geochemistry of the investigated analyte [34]. Therefore, there are many studies dealing with the development and evaluation of new binding gels containing different resins in order to obtain a robust technique that can be applied in various environmental conditions without affecting the accuracy and reliability of DGT measurement.

From its first use in 1994 [10], Chelex-100 has become the most commonly used resin for DGT measurements. Chelex-100 is a chelating resin with iminodiacetate acid as functional groups, and as such, it has a high affinity for cationic species (mainly transition metals). It is also often used for uranium measurements in freshwater environments [35–39]. However, its performance for uranium determination in the natural environment can be unsatisfactory since it is not exclusively selective for U and its binding sites may become saturated by competing ions. Moreover, the uranium species formed in solution (often anionic or neutral) may show a low affinity for Chelex-100 and slow dissociation kinetics within the diffusive layer, resulting in non-perfect sink conditions [37,40]. This is especially apparent when DGTs are deployed in complex matrices such as seawater or when deployed for longer periods [41,42]. Therefore, Chelex-100 has been replaced by other binding phases (*i.e.*, Diphonix [17,43], Dowex 2 × 8–400 [44], MnO₂ [41], Metsorb [42], Dow-PIWBA [45], Spheron-Oxin [46], or Lewatit FO 36 [47]) more suitable for the selective determination of uranium. Their binding mechanisms are either based on chelation (Diphonix and Spheron-Oxin), sorption (Metsorb and MnO₂), anion exchange (Dowex 2 × 8–400), or both sorption and anion exchange (Dow-PIWBA and Lewatit FO 36). Nevertheless, while the sorption ability of DGT binding phases in the presence of interfering ions is usually investigated during their development, the tests are limited to a few major potential co-adsorbing analytes. These simulated conditions can never fully reflect the complexity of the aquatic environment. Moreover, the data about the practical application of the DGT technique for uranium measurements (U-DGT) in the real environment are generally lacking in the literature as they are mostly limited to a few *in-situ* trials. A thorough evaluation of the DGT performance in the real environment of various conditions is therefore necessary, as it is a crucial step to validate the capability of the binding phase to provide robust and reliable results.

For this reason, four resins (Chelex-100, Dow-PIWBA, Diphonix, and Lewatit FO 36) for uranium determination were selected and their abilities evaluated along the salinity gradient to investigate the influence of the changing U speciation on the DGT performance. The study area of the Scheldt estuary (Belgium and the Netherlands) is characterized by salinity ranging from freshwater (<0.05), oligohaline (0.05–5), mesohaline (5–18) to polyhaline (18–30) waters [48]. Moreover, the river passes through the industrial area of Antwerp (Belgium)

and its pollution status is thus considerably influenced by anthropogenic activities [12,49–52]. This industrial area also coincides with the turbidity maximum of the estuary and can thus complicate processes related to the early stages of estuarine mixing. All of the tested resins had been thoroughly evaluated under laboratory conditions in the earlier studies and have been shown to have sufficient sorption abilities towards U regarding their sorption capacity (200 µg disc⁻¹, 2500 µg disc⁻¹, 99 µg disc⁻¹, and 1250 µg disc⁻¹ for Chelex-100, Dow-PIWBA, Diphonix, and Lewatit FO 36, respectively) or their performance across the pH range typical for natural waters (pH = 4–8) [17,45,47,53]. In the present study, the DGTs utilizing these tested resins were deployed along the Scheldt estuary within four campaigns over the period 2014–2021 in order to find the most reliable DGT binding phase for uranium monitoring in the freshwater and marine environment.

2. Materials and methods

2.1. Reagents and chemicals

All chemicals were of analytical reagent grade or higher. Milli-Q water (Millipore, USA) was used for the preparation of gels and solutions, as well as for cleaning DGT devices. Acrylamide 40% (w/v) (Merck, Germany), agarose-derived DGT cross-linker (2%) (DGT Research Ltd., UK), ammonium persulfate (APS) (Merck, Germany), N, N,N',N'-tetramethylethylenediamine (TEMED) (Merck, Germany) and resins Chelex®-100 (Bio-Rad, USA), Diphonix® (Eichrom Technologies, USA), Dow-PIWBA (The Dow Chemical Company, USA) and Lewatit® FO 36 (Lanxess, Germany) were used for gel preparation. The nitric acid was used for material cleaning (HNO₃ produced by distillation apparatus Berghof, Germany), samples acidification, and gels extraction (Optima Grade, Fisher Scientific, USA). The 1-hydroxyethane-1,1-diphosphonic acid (HEDPA) 60% (w/v) in H₂O (Sigma-Aldrich, Germany) and sodium hydroxide (Merck, Germany) were used for gel extraction. The stock solution of uranium of 1000 mg L⁻¹ in 2% HNO₃ (SPEX CertiPrep, UK) was used for calibration of the ICP-MS. Indium (Alfa Aesar, USA) was used as the internal standard for U analysis (addition to a final concentration of 1 µg L⁻¹).

2.2. Study site and sampling

The studied area is located on the border of northern Belgium and southwestern Netherlands and is a dynamic ecosystem of the Scheldt estuary (Fig. 1). Uranium monitoring in water was performed at 8 stations on the Scheldt River (HEM, S22, S15, S12, S09, S07, S04, S01) during the campaigns on R.V. Belgica in March 2014, 2019, 2020, and 2021. Moreover, a long-term deployment was performed at 2 stations in the Zeebrugge harbour (HZ1 and HZ2) during the campaigns in 2020 and 2021. For geographical coordinates of all sampling stations and an overview of used resin gels during all campaigns see Table S1 in the Supplementary Information (SI).

Water samples were taken directly from the rigid hull inflatable boat (RHIB) at the sampling stations using 2 L polypropylene (PP) bottles at the start and end of the DGT deployment. The sampling bottles for U and major cations were pre-cleaned by 1% HNO₃ for at least 24 h and thoroughly rinsed with Milli-Q water and seawater prior to use on-site. A separate sampling bottle was used for nutrients, anions, alkalinity, and dissolved organic carbon (DOC) (pre-cleaned by 1% HCl to avoid contamination for NO₃⁻ analysis). Representative water samples were filtered through 0.45 µm membrane syringe filters and acidified to 1% HNO₃ for trace metals and major cation analysis. Samples for DOC analysis were stored in pre-combusted (550 °C for 3 h) glass bottles and samples for nutrients, anions, and alkalinity analysis were stored in polyethylene (PE) bottles. Water physico-chemical parameters (pH, temperature, salinity, dissolved oxygen) were measured at each sampling station by multi-parameter instruments VWR MU 6100H and WTW 3430.

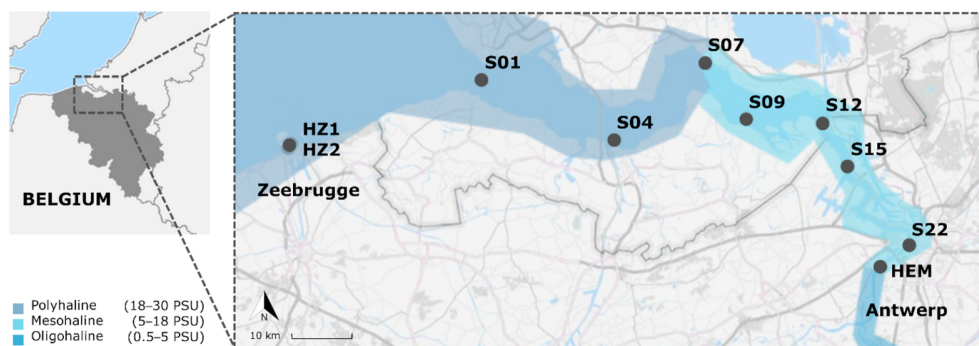


Fig. 1. Studied area with sampling stations along the Scheldt estuary and in the Zeebrugge harbour with a visualization of salinity areas (data of salinity areas adapted from Vlaams Instituut voor de Zee [54]).

2.3. Preparation, assembly, and deployment of DGTs

The DGT pistons, glass, and plastic equipment used for gels handling were cleaned in 5% (v/v) HNO_3 for at least 24 h and thoroughly rinsed with Milli-Q water prior to use. The gel stock solution was prepared using 15% (v/v) acrylamide and 0.3% (v/v) DGT cross-linker. The polymerization reaction of the gel solution was initiated by freshly prepared 10% (w/v) APS and catalysed by TEMED. The polyacrylamide (PAM) diffusive gels were prepared according to the protocol described in the literature [6] with a resulting thickness of 0.08 cm. The same protocol was slightly modified for the preparation of each type of PAM resin gel with a thickness of 0.04 cm (see detailed information in Table 1). The Diphonix, Dow-PIWBA, and Lewatit FO 36 resins were ground (Pulverisette Type 02.102, Fritsch, Germany) and sieved on a PE sieve (50 μm) prior to use. Thoroughly mixed gel solution with a resin was cast between two glass plates and allowed to polymerize at 45 °C for 1 h. After 24 h hydration in Milli-Q water, gel sheets were cut using a plastic circle cutter (diameter 2.5 cm) and stored in 0.01 M NaNO_3 at 4 °C prior to use.

DGT pistons (DGT Research Ltd., UK) with an exposure window of 3.14 cm^2 were used for water deployment. Polyvinyl fluoride (PVDF) Durapore® membrane filters of 0.45 μm pore size (Merck, Germany) were pre-cleaned in 5% (v/v) HNO_3 for 24 h and thoroughly rinsed with Milli-Q water prior to use. The DGT plastic housings were loaded with resin gel, covered by PAM diffusive gel and membrane filter, and enclosed by a cap with an exposure window. Assembled DGT units were stored at 4 °C in zip-lock bags and kept moisturized with 0.01 M NaNO_3 prior to deployment.

The DGTs were deployed while navigating upstream from the mouth to Antwerp and retrieved the next day while navigating downstream. The method of DGT deployment in water varied over the years as shown in Fig. 2. During campaigns in 2014 and 2019, the DGTs were loaded in Perspex open plates that were directly attached by nylon rope to the buoy on top and to anchor on the bottom (A). In 2019, one series of Chelex-100 DGTs was tied back to back by a fishing line and placed in filter tubes (filter element for Pluviofilter, pore size 90 μm , BWT, Austria), which were then deployed in the same way as the open plates

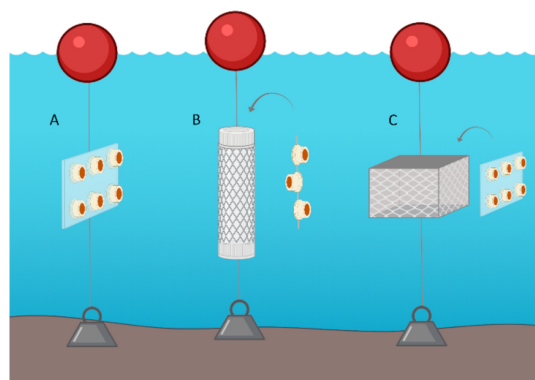


Fig. 2. The method of DGT deployment in water column using an open plate (A), filter tube (pore size 90 μm) (B), or open plate enclosed in a polypropylene cage (perforation size 2 cm) (C). Each construction is attached by nylon rope to the buoy on top and to anchor on the bottom.

(B). During the 2020 and 2021 campaigns, DGT pistons were loaded in Perspex plates and enclosed in a polypropylene cage (perforation size 2 cm) before attachment (C). Each type of resin gel was deployed in 4–6 replicates per station. In the estuary, the DGT deployment ranged from 12 to 24 h. For the long-term deployment trial, the DGTs were deployed for 2 and 28 days (station HZ1) or 6 and 21 days (station HZ2).

2.4. Evaluation of the DGT performance

2.4.1. Elution efficiency

For accurate determination of uranium mass accumulated on DGT resin gel, it is necessary to use a suitable elution agent and the appropriate elution factor for calculations. The elution factor indicates the elution efficiency of the used eluent in relation to the total amount of analyte accumulated on the gel. As the Chelex-100 [38,44], Diphonix [17,43], and Dow-PIWBA [45,55] resin gels are widely used for uranium determination, the validated elution protocols have been followed in this study. The U mass accumulated on Chelex-100 was eluted by 1 ml of 1 M HNO_3 at laboratory temperature. The 1 ml of 1 M HEDPA at laboratory temperature and 1 ml of concentrated HNO_3 at 70 °C were used for elution of Diphonix and Dow-PIWBA resin gels, respectively, as recommended by Drozdak et al. [17,45]. The 5 ml of 1 M NaOH at 70 °C was used for elution of Lewatit FO 36 resin gels according to Smolková

Table 1

Preparation protocol of PAM resin gels (reagents used per 10 ml of gel solution).

	Chelex-100 [6]	Diphonix [17]	Dow-PIWBA [45]	Lewatit FO 36 [53]
Resin (g)	4	2	2	1.25
10% APS (μl)	50	360	300	240
TEMED (μl)	15	90	120	120

et al. [47]. The elution factors (f_e) of 0.83 ± 0.02 , 0.79 ± 0.04 , 0.88 ± 0.01 , and 0.85 ± 0.03 were used for calculation of the uranium mass accumulated on Chelex-100, Diphonix, Dow-PIWBA, and Lewatit FO 36 resin gels, respectively [17,45,47].

2.4.2. DGT calculations

Uranium mass (M , ng) accumulated on the resin gel disc is calculated from the concentration of U measured by analytical technique in the eluent (c_e) using Eq. (1), where V is the total volume of gel and elution agent and f_e is the elution factor as described in 2.4.1.

$$M = c_e \cdot V / f_e \quad (1)$$

Uranium concentration determined by DGT (c_{DGT} , $\mu\text{g L}^{-1}$) is then calculated from the uranium mass using Eq. (2), where Δg is the thickness of diffusive layer consisting of diffusive gel and membrane filter (0.0925 cm), D is the diffusion coefficient of U ($4.40 \times 10^{-6}\text{ cm}^2\text{ s}^{-1}$ at 25°C [17]), A is the exposed area (3.14 cm^2), and t is the deployment time (s).

$$c_{DGT} = M \cdot \Delta g / (D \cdot A \cdot t) \quad (2)$$

2.5. Analytical methods and statistical analysis of results

Uranium concentration in all samples was determined by sector field inductively coupled plasma mass spectrometry (SF-ICP-MS, Element II, Thermo Fisher Scientific Bremen GmbH, Germany). Water samples were diluted ten times before analysis. Method accuracy was verified by the analysis of blank samples and adequate reference materials. For water analysis, the standard reference material SLRS-6 (river water, National Research Council Canada) and SPS-SW2 (surface water level 2, Spectrapure Standards AS, Norway) were used. Uranium concentration in both reference materials ranged between 97 and 108% of certified values. Major cations (Ca^{2+} , K^+ , Mg^{2+} , Na^+) were also measured by SF-ICP-MS. NO_3^- , PO_4^{3-} , NH_4^+ , and Si were measured by segmented flow analysis (QuAAtro Nutrient Analyser); Cl^- and SO_4^{2-} were measured by Ion chromatography (Metrohm IC Professional). Alkalinity was measured by automatic titration (Mettler Toledo). Dissolved organic carbon (DOC) was measured by mass spectrometry (HiPerTOC, Thermo).

The geochemical speciation software Visual MINTEQ 3.1 and the Stockholm Humic Model (SHM) was used to assess uranium speciation in the Scheldt estuary. Analytical software STATISTICA13 (StatSoft) was used for data analysis. The Pearson's correlation coefficient (r) was used to describe the relationship between parameters and a one-way analysis of variance (ANOVA test) was used to determine the statistically significant differences between DGT performances and dissolved U concentrations analysed in water samples. A statistically significant difference in the results was declared when the p -value was below the level of significance $\alpha = 0.05$.

3. Results and discussion

3.1. Estuarine geochemistry of uranium

Physico-chemical parameters measured during the campaigns are shown in the Supplementary Information (Table S2). For 2014, the data of major cations and anions as well as DOC are also presented as they are used for the speciation calculations (Table S3). Since all campaigns during 2014–2021 were performed in the same season (usually the first week of March), the temperature, pH, salinity, and oxygen concentrations in the water were overall very similar. The water temperature varied between 5.9 and 8.9°C and pH generally shows a slight increase from 7.73 to 8.40 towards the mouth (the exact temperature of each sampling station was nevertheless used for DGT calculations to achieve the most accurate results). Similarly, the oxygen concentrations increased seawards from 7.2 to 12.3 mg L^{-1} . The salinity varied from 0.2

to 1.0 at station HEM, located upstream of Antwerp to 24.9 – 25.7 at station S01.

Increasing trends along the estuary were found in 2014 for the concentrations of Ca^{2+} (93 – 290 mg L^{-1}), K^+ (18 – 249 mg L^{-1}), Mg^{2+} (34 – 815 mg L^{-1}), Na^+ (241 – 6536 mg L^{-1}), Cl^- (510 – $16,536\text{ mg L}^{-1}$), and SO_4^{2-} (119 – 2160 mg L^{-1}). On the contrary, decreasing trends seawards were found for the concentration of the DOC (6.926 – 1.135 mg L^{-1}), PO_4^{3-} (0.24 – 0.15 mg L^{-1}), NH_4^+ (0.32 – 0.06 mg L^{-1}), Si (3.78 – 1.07 mg L^{-1}) and NO_3^- (16.20 – 5.75 mg L^{-1}).

The concentrations of dissolved uranium increased seawards from $0.96 \pm 0.16\text{ }\mu\text{g L}^{-1}$ at station HEM to $3.17 \pm 0.67\text{ }\mu\text{g L}^{-1}$ at station S01 during observed periods. A strong positive correlation between salinity and dissolved uranium concentration was observed (Fig. 3, for Pearson's coefficients, see Table S4 in the SI). This indicates a conservative behaviour of U during estuarine mixing which is in an agreement with what has been observed in many other estuaries [56,57]. The dissolved uranium concentration of $2.86\text{ }\mu\text{g L}^{-1}$ at the salinity level of 30 reported in those studies also corresponds with the observations of this study.

3.2. The method of DGT deployment

The effect of the deployment method on the DGT performance was evaluated for Chelex-100 as this resin gel was the only one deployed in all three ways shown in Fig. 2. Deploying DGTs in unprotected open plates (Fig. 2A) may either result in damage of the filter membrane (either by floating material or by fish) or high tidal currents and high turbidity may allow particles to be pushed in the filter sealings and is therefore not recommended in such dynamic environments. For U, there was no statistically significant difference between the uranium results of DGTs deployed in open plates and enclosed in filter tubes during the 2019 campaign except for station S01 ($p < 0.05$). Nevertheless, the authors believe that the best option is the use of open plates enclosed in a plastic cage (Fig. 2C). This deployment method ensures a natural water flow that is not affected by a fine filter (pore size of only $90\text{ }\mu\text{m}$) of the filter as it may be in the case of the filter tubes (Fig. 2B), there is no direct contact of DGT units with the walls of the protective cage and at the same time, the DGT units are protected from the damage by larger objects and high tidal currents.

3.3. Influence of salinity on the U-DGT performance in water

The evaluation of salinity influence on the U-DGT performance was based on the results of campaigns in 2014, 2019, 2020, and 2021 (Fig. 4). Due to extreme weather conditions in 2020, it was impossible to retrieve DGTs from all sampling stations, and therefore some data are not available. To evaluate the DGT performance, the uranium concentrations determined by DGTs (c_{DGT}) were compared with the dissolved uranium concentrations analysed in water samples (c_{DISS}) and c_{DGT}/c_{DISS} ratio was evaluated. If all dissolved U species are labile, the c_{DGT}/c_{DISS} ratio approaches 1. However, it must be taken into account, that the DGT results are influenced by the variability of the U concentration at a given location over time as the technique provides a time-weighted average concentration. Since the total dissolved concentrations could only be measured at the start and end of the deployment time, they do not reflect the true changes in concentrations during deployment. Therefore, in dynamic environments such as river estuaries, the grab sampling may provide misleading results in contrary to the DGT-determined time-integrated concentrations [58].

Chelex-100 resin gels provided results coinciding with the dissolved uranium concentration by the c_{DGT}/c_{DISS} ratio of 1.11 , 1.16 , and 0.99 at the station HEM over 2014, 2019, and 2021 campaigns, respectively. But with increasing salinity towards the sea, the agreement with the dissolved uranium fraction gradually declines to 0.69 , 0.68 , and 0.73 (measured at the station S01 during the same sampling periods). In 2020, the overall c_{DGT}/c_{DISS} ratios were very low (0.32 – 0.56) at all stations. Nevertheless, a strong negative correlation between salinity

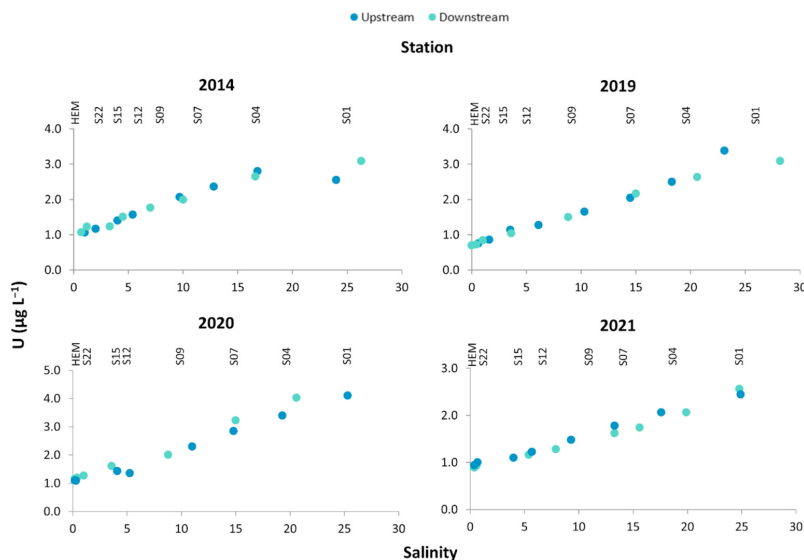


Fig. 3. The concentration of dissolved uranium ($0.45 \mu\text{m}$) in the function of salinity along the Scheldt estuary during field campaigns in 2014–2021. A transect from S01 to HEM was performed on the first day (upstream) and from HEM to S01 on the following day (downstream).

and Chelex-100 performance was observed within all campaigns of 2014–2021 with Pearson's correlation coefficients $r = -0.81$, -0.64 (or -0.97 for DGTs deployed in filter tubes), -0.92 , and -0.46 , respectively.

The Dow-PIWBA DGTs generally provided very good agreement with the dissolved uranium concentrations. In 2014, the DGT results were predominantly not statistically different ($p > 0.05$) from the dissolved uranium concentration with the $c_{\text{DGT}}/c_{\text{DISS}}$ ratios varying between 0.96 and 1.16. In 2019, the $c_{\text{DGT}}/c_{\text{DISS}}$ ratio varied between 1.34 and 1.01 from station HEM to S01, respectively. But these results were also skewed by the lack of samples ($n = 3$) due to the loss of DGTs. Nevertheless, the results of the 2020 campaign show excellent agreement between DGT and dissolved uranium concentrations with $c_{\text{DGT}}/c_{\text{DISS}}$ ratios varying between 0.90 and 1.07. Since the results of this campaign are the average of 6 replicates of DGT units per station, they are more reliable than the results of the previous year. In 2021 the overall $c_{\text{DGT}}/c_{\text{DISS}}$ ratio varied in the range of 1.01–1.49 between stations HEM and S07. Nevertheless, it is obvious that there might be some influence of the salinity at the station S01, where the samplers were deployed for the longest period and the resulting $c_{\text{DGT}}/c_{\text{DISS}}$ ratio was only 0.66. The statistical analysis revealed a medium to strong negative correlation between the Dow-PIWBA DGT performance and increasing salinity throughout the observed years ($r = -0.38$, -0.91 , -0.53 , -0.93) but it must be taken into account that the results were mostly statistically non-significantly different from dissolved uranium concentration.

Diphonix resin gels provided overall comparable results with Dow-PIWBA resin gels, with very good agreement between the DGT-determined and dissolved uranium concentration at all stations. In 2019 the $c_{\text{DGT}}/c_{\text{DISS}}$ ratios varied between 0.95 and 1.25, in 2020, the ratios varied between 0.83 and 1.21, and in 2021 the ratios varied between 0.92 and 1.05. Diphonix also determined higher uranium concentrations at stations HEM and S09 in 2019 just like Dow-PIWBA indicating a possible increase of uranium concentration between grab sampling. Nevertheless, this was not the case in 2021. No significant correlation between Diphonix-DGT performance and salinity gradient was observed in 2019 ($r = -0.27$) and a medium positive correlation was observed in 2020 and 2021 ($r = 0.53$ and 0.60).

Lewatit FO 36 resin gel was tested for uranium determination under field conditions for the first time in the 2020 campaign. The results of this study show a strong negative correlation between this DGT type performance and salinity gradient ($r = -0.75$) and gradually decreasing $c_{\text{DGT}}/c_{\text{DISS}}$ ratio from 1.09 to 0.87 between S22 and S07 stations, respectively. In 2021 similarly to Dow-PIWBA resin, the $c_{\text{DGT}}/c_{\text{DISS}}$ ratio varied in the range of 1.32–0.89 between the HEM and S07 stations with a significant decrease at station S01 ($c_{\text{DGT}}/c_{\text{DISS}} = 0.66$) resulting in a strong negative correlation between the salinity and Lewatit FO 36 performance ($r = -0.79$).

3.4. Long-term uranium monitoring

The Chelex-100, Diphonix, Dow-PIWBA, and Lewatit FO 36 DGTs were evaluated for the long-term monitoring trials (with deployment times of 2, 6, 21, or 28 days) (Fig. 5). The water salinity at the station HZ1, where the long-term deployment was performed in 2020, was ~ 28 , with $\text{pH} = 7.92 \pm 0.04$, and a temperature of 8.05 ± 1.75 °C. The parameters at the station HZ2 from 2021 were similar – with the salinity of ~ 26 , $\text{pH} = 8.0 \pm 0.03$, and temperature of 6.67 ± 1.16 °C. The results of the DGT-determined U concentrations indicate that at the end of the deployment period, only Diphonix DGTs accumulated uranium which resulted in excellent agreement with the dissolved uranium concentrations ($c_{\text{DGT}}/c_{\text{DISS}} = 0.93, 0.94, 0.81$, and 0.96 after 2, 6, 21, or 28 days, respectively). This can also be observed from the U mass accumulation per gel disc over the deployment time which was compared to theoretical U mass that would be accumulated under the perfect sink conditions. The Dow-PIWBA and Lewatit FO 36 DGTs provided underestimated U concentrations which agreed with the dissolved U concentration by only 9.6–14.0% and 2.9–4.6%, respectively, at the end of the trials. A significant decrease in the U uptake on the Lewatit FO 36 resin was observed already after 2 days of deployment. The Chelex-100 DGTs were deployed only for 28 days (in 2020) and provided strongly underestimated results which agreed with the dissolved U concentration by less than 1%.

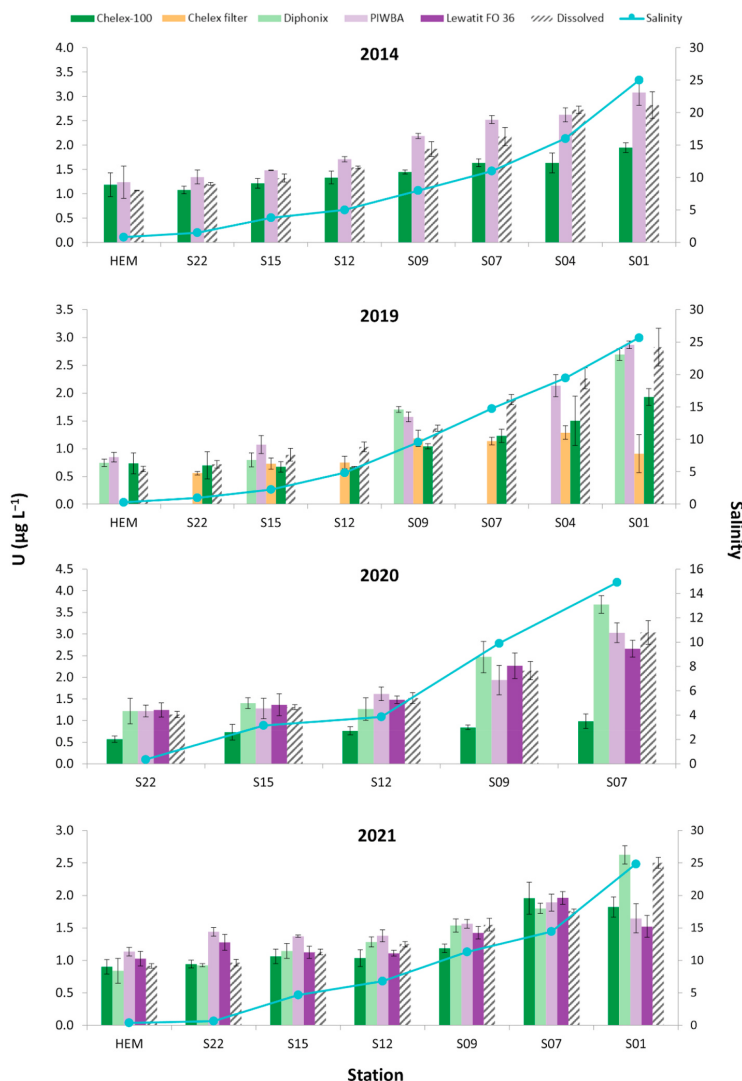


Fig. 4. A comparison of the DGT technique performance (utilizing Chelex-100, Diphonix, Dow-PIWBA, and Lewatit FO 36 resins) with the dissolved U concentrations in the function of the increasing salinity (grey line) along the Scheldt estuary during campaigns in 2014–2021 ($n = 4-6$, mean \pm standard deviation). Chelex filter corresponds to Chelex-100 units deployed in a filter tube.

3.5. Discussion

3.5.1. Uranium speciation in the Scheldt estuary

In the natural surface water under oxic conditions, uranium is present mostly in the hexavalent oxidation state U(VI) i.e., in the form of the uranyl ion (UO_2^{2+}). Under these conditions, uranium is generally complexed with ligands such as OH^- , Cl^- , CO_3^{2-} , PO_4^{3-} , F^- , SO_4^{2-} [59]. One of the most important uranium complexes found in the natural aquatic environment is represented by uranyl carbonates with the neutral or anionic $\text{UO}_2(\text{CO}_3)_x$ species dominating between pH 4–12. In solutions containing Ca at neutral and alkaline pH the very stable ternary $\text{Ca}_2\text{UO}_2(\text{CO}_3)_3(\text{aq})$ and $\text{CaUO}_2(\text{CO}_3)_3^{2-}$ complexes are formed. In addition, speciation of uranyl in freshwater may be affected by the

concentration of organic ligands – especially humic substances that form stable uranyl complexes and contribute to the element's migration in aquatic systems [60]. In rivers, more than 90% of uranium may be associated with colloidal fraction, either in relation to iron colloids or through interactions with humic or humin acids. The colloidal fraction governs transport mechanisms of uranium in aquatic systems, but its representation tends to diminish linearly as salinity increases. In estuarine environments, less than 5% of uranium is associated with this fraction at the salinity of 3 [61,62]. It is likely that during initial estuarine mixing, the riverine uranium associated with Fe-organic rich colloids, is removed. This removal is due to colloidal aggregation into larger particles that can sink on a short time-scale.

Calculating U speciation with geochemical modelling is strongly

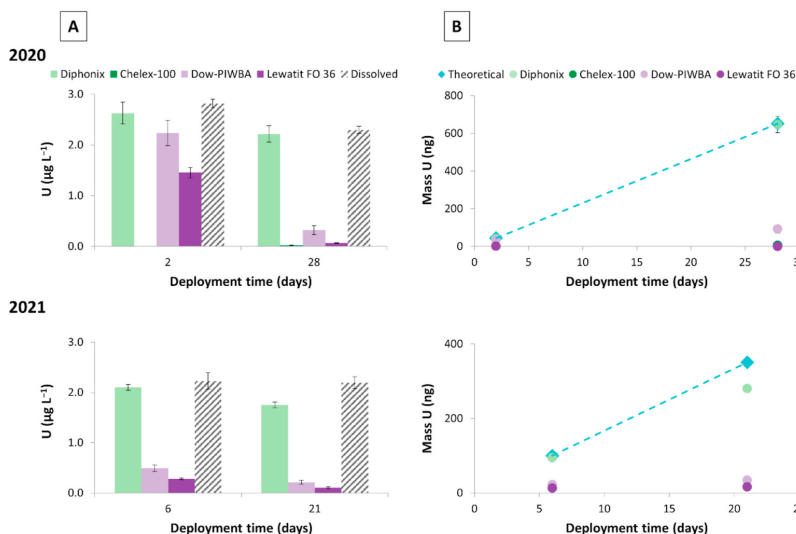


Fig. 5. Long-term deployment of DGTs (utilizing Chelex-100, Diphonix, Dow-PIWBA, and Lewatit FO 36 resins) in seawater at the station HZ1 (2020, salinity ~ 28 , pH = 7.92 ± 0.04) and HZ2 (2021, salinity ~ 26 , pH = 8.0 ± 0.03) with a comparison of the DGT-determined vs. dissolved U concentrations (A) and U masses accumulated per gel disc vs. theoretical values assuming the perfect sink conditions (obtained with Eq. (2) using the concentration of dissolved U during the deployment; $D = 4.40 \times 10^{-6} \text{ cm}^2 \text{ s}^{-1}$ at 25°C ; $\Delta g = 0.0925 \text{ cm}$; and $A = 3.14 \text{ cm}^2$) (B).

dependant on the completeness of the thermodynamic databases used, affecting especially stable ternary earth alkaline uranyl carbonate complexes [63–66]. In addition, the composition of organic matter is not well known. In the present study, we calculated the U speciation in the Scheldt estuary using Visual MINTEQ 3.1. For the complexation of U with DOC, the Stockholm Humic Matter model was selected [40] and the composition of DOC was estimated as 80% fulvic acids and 20% humic acids [67,68]. The results of the calculations are shown in Fig. 6. Calcium uranyl carbonate complexes dominate throughout the whole estuary accounting for 97% of the species in the riverine end member (HEM) and 86% at the mouth (S01). The $\text{UO}_2(\text{CO}_3)_2^{2-}$ fraction, humic and fulvic acid complexes account for less than 1% of the dissolved U species. An important increase in the $\text{UO}_2(\text{CO}_3)_3^{4-}$ fraction from 2 to 14% is observed seawards.

3.5.2. Influence of uranium speciation on the binding properties of different resin gels

The DGT-determined concentration is dependent on both the mobility (diffusion) and the lability of the metal species [69] and is also operationally defined by the selection of experimental parameters (pore size of the diffusive layer, diffusive layer thickness, the affinity of binding phase, etc.). The differences in the performance of DGT resins tested in this study are influenced by the properties of their functional groups which show different affinities towards uranium species. Chelex-100 is a chelating ion-exchange resin with iminodiacetate (IDA)

functional groups. The structure of the IDA groups changes with pH and so the performance of DGTs utilizing Chelex-100 resin is pH-dependent as well. At neutral and alkaline pH the IDA groups have a negative charge and thus pose a high affinity towards divalent metals such as Ca, Cd, Co, Cr, Cu, Fe, Mg, Mn, Ni, Pd, or Zn [70,71]. However, the negative charge of the functional groups is also the cause of electrostatic repulsion of uranyl anionic species ($\text{CaUO}_2(\text{CO}_3)_3^{2-}$, $\text{UO}_2(\text{CO}_3)_2^{2-}$, $\text{UO}_2(\text{CO}_3)_3^{4-}$) that predominate in seawater at pH ~ 8 [42]. However, Zhao et al. [40] showed that $\text{UO}_2(\text{CO}_3)_2^{2-}$ has a high uptake rate on Chelex-100 DGTs in comparison to $\text{UO}_2(\text{CO}_3)_3^{4-}$ which has the lowest uptake rate. This can explain the systematic decrease in $c_{\text{DGT}}/c_{\text{DISS}}$ with increasing salinity as the $\text{UO}_2(\text{CO}_3)_3^{4-}$ increases from 2 to 14% and the contribution of $\text{UO}_2(\text{CO}_3)_2^{2-}$ is negligible in the Scheldt estuary according to the speciation calculations. Another factor that plays a role is the accumulation rate of calcium uranyl carbonate species on the resin gel. Laboratory experiments performed in our lab (unpublished data) have shown that deploying Chelex-100 DGTs in solutions rich in calcium and carbonate for a 14-day period while using double resin gels, result in a non-linear accumulation of U on the resin gels over time. Moreover, U starts to accumulate on the second resin gel after 2 days (by 6%) and this fraction increases to 40% after 14 days. In such cases, the non-perfect sink conditions prevail and the simple DGT formula cannot be used. This explains the low accumulation of U on Chelex-100 DGTs during the long deployment (28 days).

Dow-PIWBA resin is a polyphenol impregnated weak base anion exchanger. In general, polyphenols bind uranium through chelation and ion exchange with their functional groups (i.e., hydroxyl, carbonyl, carboxyl) [72,73]. Unlike Chelex-100, this resin is able to operate across a wide range of pH (3–9) and its performance is independent of the ionic strength in the range from 0.1 mM to 0.7 M NaNO_3 , but the U adsorption starts to decrease at Ca concentrations above 200 mg/L and concentrations $> 500 \text{ mg/L}$ [45]. In the Scheldt estuary, for a 24 h deployment, a good agreement is observed between c_{DGT} and c_{DISS} . However, the resin is not suitable for long-term monitoring in seawater as its binding sites started to show signs of saturation after 6 days of deployment in the station with a salinity of 26–28. Likewise, our laboratory experiments with double resin layers, deploying Dow-PIWBA DGTs in calcium carbonate-rich waters for 14 days (unpublished data) show that accumulation on the second resin starts to occur after 7 days.

Diphonix is a strong cation-chelating resin with diphosphonic acid

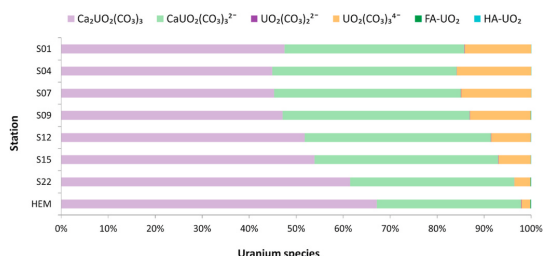


Fig. 6. Speciation of U in the Scheldt estuary calculated with Visual MINTEQ (input data from 2014 in Supplementary information).

and sulphonic acid functional groups. Therefore, it acts as a dual mechanism polymer, with a sulfonic acid cation exchange group allowing rapid access (mostly non-specific) of ions into the polymeric network, and the diphosphonic acid group being responsible for selective binding a number of metal cations. The Diphonix resin exhibits an extraordinarily strong affinity for actinides, especially in the tetra- and hexavalent oxidation states. Its main advantage is the extremely high binding capacity as Diphonix resin gel disc does not show signs of saturation even after loading 2500 µg of U per gel disc [17] and thus has a significantly higher capacity compared to Dow-PIWBA resin with the capacity of only 100 µg of U per gel disc [45]. Another advantage is its resilience towards the influence of external factors such as interfering ions (Ca^{2+} , PO_4^{3-} , SO_4^{2-} and HCO_3^-) or extreme pH conditions on its performance [17]. Diphonix was the only resin able to quantitatively accumulate U over long deployment periods indicating its performance is affected neither by saturation of the binding sites by competing ions nor by U speciation in the solution. Diphonix resin was originally used for DGT measurement by Drozdak et al. [17] and Turner et al. [43]. In the latter study, the field deployments revealed linear accumulation of U by DGTs in freshwater for the duration of 7 days while in seawater, the results matched the course of U uptake predicted by simple DGT formula (Eq. (2)) for 3 days only. However, this is not the case of this study, where Diphonix provided excellent agreement with dissolved U concentration in seawater (salinity ~27) even after 28 days of deployment. This can be attributed to slight differences in the preparation of Diphonix resin gels. In this work, the protocol by Drozdak et al. [17] was followed but in contrast to previously mentioned studies, the resin was ground and sieved to a resulting particle size <50 µm before the gel production. This not only improved the homogeneity of the resulting gels but could also increase the already high binding capacity. As a result, the interference effects of any co-adsorbed analytes could be better suppressed. Comparable results were also found in our laboratory experiments in calcium carbonate rich waters using double resin gel layers. Linear accumulation was observed for up to 30 days with no accumulation on the second resin layer (unpublished data).

Lewatit FO 36 is a weakly basic ion-exchange resin that is doped with a nano-scaled film of iron oxide-hydroxide with a high affinity for oxyanions such as As, P, Si, V, or Sb [74]. Even though the efficiency of this resin should not be influenced by the presence of chlorides (as stated by the manufacturer and as demonstrated in the original study developing the Lewatit FO 36-DGT technique [53]), this fact is declared for the determination of arsenic. But the sorption mechanism of arsenic and uranium by this resin differs. While arsenic is bound by a specific, reversible reaction involving hydroxy-groups on the iron oxide-hydroxide surface, uranium predominantly reacts with the weakly basic anion exchange group ($-\text{CH}_2-\text{N}(\text{CH}_3)_2$). And these groups may become easily saturated by chlorides or other competing anions in seawater. The mechanism of U uptake by ferrihydrite is also known. Nevertheless, the uranyl carbonate complexes present in seawater have a lower affinity towards $\text{FeO}(\text{OH})$ functional groups at intermediate pH and therefore, the uptake by tertiary amine group likely prevails [75, 76]. Thus, the results indicate the possible use of this resin for the U determination in freshwater environments, but its performance may be hampered in seawater or when deployed over a longer period in seawater.

The performance of the DGT technique during long-term deployments may be generally hampered by the formation of biofilm on the surface of the samplers as it acts as an additional diffusion layer [77]. However, no biofilm formation on the samplers has been observed on the surface of DGT samplers during the long-term deployment trials in this study. Moreover, biofouling would affect the performance of all DGT devices despite the utilized resin.

4. Conclusions

The salinity influence on the performance of the DGT technique for

uranium monitoring was investigated in this extensive comparative study for the first time. Results of four field expeditions performed over the period 2014–2021 were compared in order to subject the selected U binding phases to thorough testing in estuarine and marine environmental conditions. The U concentrations along the Scheldt estuary ranged from $0.96 \pm 0.16 \mu\text{g L}^{-1}$ at station HEM located in Antwerp (salinity 0.2–1.0) to $3.17 \pm 0.67 \mu\text{g L}^{-1}$ at station S01 located in the mouth of the Scheldt estuary (salinity 23.1–26.3). In this study, the differences in the performance of tested DGT resins were related to the changes of U speciation along the salinity gradient for the 24 h deployments. The speciation modelling of U showed that calcium uranyl carbonate complexes dominate along the Scheldt estuary (from 97 to 86% seawards) and that the fraction of $\text{UO}_2(\text{CO}_3)_3^{4-}$ showed an increasing trend seaward (from 2 to 14%). This change in U speciation may explain the systematic decrease of U accumulated on the Chelex-100 DGT with increasing salinity. Chelex-100 cannot be used for long-term measurement of U due to competition and saturation effects. The Lewatit FO 36 DGT provided overall reliable results and the DGT-determined concentrations agreed with the dissolved U concentrations up to salinity 18, but the performance decreased at higher salinity levels (>18) and especially during the long-term deployment in seawater (deployment period >24 h). The Dow-PIWBA DGT could be used throughout the whole salinity gradient for 24 h deployments, but in seawater performance dropped after 48 h. The most robust performance along the salinity gradient was achieved by Diphonix DGTs. The U-DGT fraction determined by this resin was in very good agreement with the dissolved uranium concentrations across the whole salinity gradient. Moreover, the long-term deployment trial revealed that Diphonix resin is the only binding phase providing comparable results even after 28 days of deployment in seawater (salinity ~27). The results of this study thus demonstrated that thorough testing of the DGT technique in a natural environment is a crucial prerequisite for obtaining reliable data and application of the DGT as a speciation tool.

Author statement

Vendula Smolíková: Investigation, Methodology, Validation, Formal analysis, Writing – Original Draft, **Pavína Pelcová:** Writing – Review & Editing, **Andrea Ridošková:** Writing – Review & Editing, **Martine Leermakers:** Conceptualization, Supervision, Methodology, Resources, Writing – Review & Editing.

Declaration of competing interest

The authors declare that they have no known competing financial interests or personal relationships that could have appeared to influence the work reported in this paper.

Acknowledgements

Ship time on the R.V. Belgica was provided by BELSPO and RBINS–OD Nature. Authors would like to thank the crew members of the research vessel Belgica. This work was also supported by the project PROFISH CZ.02.1.01/0.0/0.0/16.019/0000869, which is financed by the European Regional Development Fund in the Operational Programme Research, Development and Education and The Czech Ministry of Education, Youth and Sports. Graphical abstract and illustrations in this work were created with BioRender.com.

Appendix A. Supplementary data

Supplementary data to this article can be found online at <https://doi.org/10.1016/j.talanta.2021.123168>.

References

- [1] D.-P. Häder, A.T. Banaszak, V.E. Villafañe, M.A. Narvarte, R.A. González, E. W. Helbling, Anthropogenic pollution of aquatic ecosystems: emerging problems with global implications, *Sci. Total Environ.* 713 (2020) 136586.
- [2] V. Kumar, R.D. Parihar, A. Sharma, P. Bakshi, G.P.S. Sidhu, A.S. Bali, I. Karouzias, R. Bhardwaj, A.K. Thukral, Y. Gyasi-Agyei, Global evaluation of heavy metal content in surface water bodies: a meta-analysis using heavy metal pollution indices and multivariate statistical analyses, *Chemosphere* 236 (2019) 124364.
- [3] D.K. Gupta, C. Walther, Uranium in Plants and the Environment, Springer, 2020.
- [4] T. Mathews, K. Beaugelin-Seiller, J. Garnier-Laplace, R. Gilbin, C. Adam, C. Della-Vedova, A probabilistic assessment of the chemical and radiological risks of chronic exposure to uranium in freshwater ecosystems, *Environ. Sci. Technol.* 43 (17) (2009) 6684–6690.
- [5] R. Dunn, P. Teasdale, J. Warnken, M. Jordan, J. Arthur, Evaluation of the in situ, time-integrated DGT technique by monitoring changes in heavy metal concentrations in estuarine waters, *Environ. Pollut.* 148 (1) (2007) 213–220.
- [6] H. Zhang, W. Davison, Performance characteristics of diffusion gradients in thin films for the in situ measurement of trace metals in aqueous solution, *Anal. Chem.* 67 (19) (1995) 3391–3400.
- [7] W. Davison, Diffusive Gradients in Thin-Films for Environmental Measurements, Cambridge University Press, 2016.
- [8] A. Kot-Wasik, B. Zabiegała, M. Urbanowicz, E. Dominiak, A. Wasik, J. Namieśnik, Advances in passive sampling in environmental studies, *Anal. Chim. Acta* 602 (2) (2007) 141–163.
- [9] C. Li, S. Ding, L. Yang, Y. Wang, M. Ren, M. Chen, X. Fan, E. Lichtfouse, Diffusive gradients in thin films: devices, materials and applications, *Environ. Chem. Lett.* (2018) 1–31.
- [10] W. Davison, H. Zhang, In situ speciation measurements of trace components in natural waters using thin-film gels, *Nature* 367 (6463) (1994) 546–548.
- [11] F. Degryse, E. Smolders, DGT and bioavailability, in: W. Davison (Ed.), Diffusive Gradients in Thin-Films for Environmental Measurements, Cambridge University Press, 2016.
- [12] C. Gaulier, C. Zhou, W. Guo, A. Bratic, P.-J. Superville, G. Billon, W. Baeyens, Y. Gao, Trace metal speciation in North Sea coastal waters, *Sci. Total Environ.* 692 (2019) 701–712.
- [13] M. Ren, S. Ding, D. Shi, Z. Zhong, J. Cao, L. Yang, D.C. Tsang, D. Wang, D. Zhao, Y. Wang, A new DGT technique comprised in a hybrid sensor for the simultaneous measurement of ammonium, nitrate, phosphorus and dissolved oxygen, *Sci. Total Environ.* (2020) 138447.
- [14] J. Huang, W.W. Bennett, P.R. Teasdale, N.R. Kankanamge, D.T. Welsh, A modified DGT technique for the simultaneous measurement of dissolved inorganic nitrogen and phosphorus in freshwaters, *Anal. Chim. Acta* 988 (2017) 17–26.
- [15] Z. Feng, N. Wang, M. He, L. Yang, Y. Wang, T. Sun, Simultaneous sampling of dissolved orthophosphate and ammonium in freshwaters using diffusive gradients in thin films with a mixed binding phase, *Talanta* 186 (2018) 176–182.
- [16] H. Yao, N. You, H.-G. Cao, L.-X. Kang, J.-B. Wu, Y.-J. Zhao, H.-T. Fan, Y.-L. Yi, In-situ sampling of available calcium using diffusive gradients in thin-films technique based on benzo-crown ether-functionalised silica as the binding agent, *Environ. Chem.* 15 (4) (2018) 205–214.
- [17] J. Drozdak, M. Leermakers, Y. Gao, V. Phrommavanh, M. Descostes, Evaluation and application of Diffusive Gradients in Thin Films (DGT) technique using Chelex®-100, Metsorb™ and Diphonix® binding phases in uranium mining environments, *Anal. Chim. Acta* 889 (2015) 71–81.
- [18] M. Leermakers, Y. Gao, J. Navez, A. Poffijn, K. Croes, W. Baeyens, Radium analysis by sector field ICP-MS in combination with the Diffusive Gradients in Thin Films (DGT) technique, *J. Anal. At. Spectrom.* 24 (8) (2009) 1115–1117.
- [19] C. Murdock, M. Kelly, L.-Y. Chang, W. Davison, H. Zhang, DGT as an in situ tool for measuring radocesium in natural waters, *Environ. Sci. Technol.* 35 (22) (2001) 4530–4535.
- [20] R. Cusnir, P. Steinmann, F.o. Bochud, P. Froidevaux, A DGT technique for plutonium bioavailability measurements, *Environ. Sci. Technol.* 48 (18) (2014) 10829–10834.
- [21] M.A. French, H. Zhang, J.M. Pates, S.E. Bryan, R.C. Wilson, Development and performance of the diffusive gradients in thin-films technique for the measurement of technetium-99 in seawater, *Anal. Chem.* 77 (1) (2005) 135–139.
- [22] L.-Y. Chang, W. Davison, H. Zhang, M. Kelly, Performance characteristics for the measurement of Cs and Sr by diffusive gradients in thin films (DGT), *Anal. Chim. Acta* 368 (3) (1998) 243–253.
- [23] E. Abdulbur-Alfakhoury, S. Van Zutphen, M. Leermakers, Development of the diffusive gradients in thin films technique (DGT) for platinum (Pt), palladium (Pd), and rhodium (Rh) in natural waters, *Talanta* 203 (2019) 34–48.
- [24] E. Abdulbur-Alfakhoury, G. Trommter, N. Brion, D. Dumoulin, M. Reichstädter, G. Billon, M. Leermakers, W. Baeyens, Distribution of platinum (Pt), palladium (Pd), and rhodium (Rh) in urban tributaries of the Scheldt River assessed by diffusive gradients in thin films technique (DGT), *Sci. Total Environ.* 784 (2021) 147075.
- [25] G. Trommter, D. Dumoulin, G. Billon, Development and validation of DGT passive samplers for the quantification of Ir, Pd, Pt, Rh and Ru: a challenging application in waters impacted by urban activities, *Talanta* 223 (2021) 121707.
- [26] Y. Yuan, S. Ding, Y. Wang, L. Zhang, M. Ren, C. Zhang, Simultaneous measurement of fifteen rare earth elements using diffusive gradients in thin films, *Anal. Chim. Acta* 1031 (2018) 98–107.
- [27] L.J. Alakangas, F.A. Mathurin, M. Åström, Diverse fractionation patterns of rare earth elements in deep fracture groundwater in the Baltic Shield-progress from utilisation of diffusive gradients in thin-films (DGT) at the Äspö hard rock laboratory, *Geochim. Cosmochim. Acta* 269 (2020) 15–38.
- [28] N. You, Y. Chen, Q.-X. Zhang, Y. Zhang, Z. Meng, H.-T. Fan, In-situ monitoring of phenol in surface waters by diffusive gradients in thin films technique based on the nanocomposites of zero-valent iron@ biochar, *Sci. Total Environ.* 735 (2020) 139553.
- [29] N. You, S. Chen, Y. Wang, H.-T. Fan, L.-N. Sun, T. Sun, In situ sampling of tetracycline antibiotics in culture wastewater using diffusive gradients in thin films equipped with graphene nanoplatelets, *Environ. Res.* 191 (2020) 110089.
- [30] R. Guibal, R. Buzier, A. Charriau, S. Lissalde, G. Guibaud, Passive sampling of anionic pesticides using the Diffusive Gradients in Thin Films technique (DGT), *Anal. Chim. Acta* 966 (2017) 1–10.
- [31] R. Guibal, R. Buzier, S. Lissalde, G. Guibaud, Adaptation of diffusive gradients in thin films technique to sample organic pollutants in the environment: an overview of o-DGT passive samplers, *Sci. Total Environ.* 693 (2019) 133537.
- [32] H. Chen, L. Guo, M. Zhang, J. Gu, K. Zhong, L. Bo, J. Li, Determination of lead in soybean sauces by the diffusive gradients in thin films technique, *Food Chem.* 165 (2014) 9–13.
- [33] M. Reichstädter, P. Divis, E.A. Alfakhoury, Y. Gao, Simultaneous Determination of Mercury, Cadmium and Lead in Fish Sauce Using Diffusive Gradients in Thin-Films Technique, *Talanta*, 2020, p. 121059.
- [34] G.S. Turner, G.A. Mills, M.J. Bowes, J.L. Burnett, S. Amos, G.R. Fones, Evaluation of DGT as a long-term water quality monitoring tool in natural waters; uranium as a case study, *Environ. Sci.: Proc. Impacts* 16 (3) (2014) 393–403.
- [35] J. Drozdak, M. Leermakers, Y. Gao, M. Elskens, V. Phrommavanh, M. Descostes, Uranium aqueous speciation in the vicinity of the former uranium mining sites using the diffusive gradients in thin films and ultrafiltration techniques, *Anal. Chim. Acta* 913 (2016) 94–103.
- [36] M. Leermakers, V. Phrommavanh, J. Drozdak, Y. Gao, J. Nos, M. Descostes, DGT as a useful monitoring tool for radionuclides and trace metals in environments impacted by uranium mining: case study of the Sagnes wetland in France, *Chemosphere* 155 (2016) 142–151.
- [37] W. Li, J. Zhao, C. Li, S. Kiser, R.J. Cornett, Speciation measurements of uranium in alkaline waters using diffusive gradients in thin films technique, *Anal. Chim. Acta* 575 (2) (2006) 274–280.
- [38] J.H. Pedrobom, C.E. Eismann, A.A. Menegário, J.A. Galhardi, K.S. Luko, T. de Araujo Dourado, C.H. Kiang, In situ speciation of uranium in treated acid mine drainage using the diffusion gradients in thin films technique (DGT), *Chemosphere* 169 (2017) 249–256.
- [39] A. Martin, C. Landesman, A. Lépinay, C. Roux, J. Champion, P. Chardon, G. Montavon, Flow rock influence on uranium and trace elements release in water from the waste rock pile of the former La Commanderie uranium mine (France), *J. Environ. Radioact.* 208 (2019) 106010.
- [40] J. Zhao, R. Cornett, C. Chakrabarti, Assessing the uranium DGT-available fraction in model solutions, *J. Hazard Mater.* 384 (2020) 121134.
- [41] G.S. Turner, G.A. Mills, P.R. Teasdale, J.L. Burnett, S. Amos, G.R. Fones, Evaluation of DGT techniques for measuring inorganic uranium species in natural waters: interferences, deployment time and speciation, *Anal. Chim. Acta* 739 (2012) 37–46.
- [42] C.M. Hutchins, J.G. Panther, P.R. Teasdale, F. Wang, R.R. Stewart, W.W. Bennett, H. Zhao, Evaluation of a titanium dioxide-based DGT technique for measuring inorganic uranium species in fresh and marine waters, *Talanta* 97 (2012) 550–556.
- [43] G.S. Turner, G.A. Mills, J.L. Burnett, S. Amos, G.R. Fones, Evaluation of diffusive gradients in thin-films using a Diphonix® resin for monitoring dissolved uranium in natural waters, *Anal. Chim. Acta* 854 (2015) 78–85.
- [44] W. Li, C. Li, J. Zhao, R.J. Cornett, Diffusive gradients in thin films technique for uranium measurements in river water, *Anal. Chim. Acta* 592 (1) (2007) 106–113.
- [45] J. Drozdak, M. Leermakers, Y. Gao, V. Phrommavanh, M. Descostes, Novel speciation method based on Diffusive Gradients in Thin Films for in situ measurement of uranium in the vicinity of the former uranium mining sites, *Environ. Pollut.* 214 (2016) 114–123.
- [46] M. Gregusova, B. Docekál, New resin gel for uranium determination by diffusive gradient in thin films technique, *Anal. Chim. Acta* 684 (1–2) (2011) 142–146.
- [47] V. Smolíková, P. Pelcová, A. Ridošková, M. Leermakers, Simultaneous determination of arsenic and uranium by the diffusive gradients in thin films technique using Lewatit FO 36: optimization of elution protocol, *Talanta* 228 (2021) 122234.
- [48] F.D. Por, Hydrobiological notes on the high-salinity waters of the Sinai Peninsula, *Mar. Biol.* 14 (2) (1972) 111–119.
- [49] W. Baeyens, B. Van Eck, C. Lambert, R. Wollast, L. Goeyens, General Description of the Scheldt Estuary, Trace Metals in the Westerschelde Estuary: A Case-Study of a Polluted, Partially Anoxic Estuary, Springer, 1998, pp. 1–14.
- [50] P. Meire, T. Ysebaert, S. Van Damme, E. Van den Bergh, T. Maris, E. Struyf, The Scheldt estuary: a description of a changing ecosystem, *Hydrobiologia* 540 (1–3) (2005) 1–11.
- [51] M. Leermakers, S. Galletti, S. De Galan, N. Brion, W. Baeyens, Mercury in the southern North sea and Scheldt estuary, *Mar. Chem.* 75 (3) (2001) 229–248.
- [52] W. Guo, K. Van Langenhove, T. Vandermarken, M.S. Denison, M. Elskens, W. Baeyens, Y. Gao, In situ measurement of estrogenic activity in various aquatic systems using organic diffusive gradients in thin-film coupled with ERE-CALUX bioassay, *Environ. Int.* 127 (2019) 13–20.
- [53] V. Smolíková, P. Pelcová, A. Ridošková, J. Hedbávný, J. Grmela, Development and evaluation of the iron oxide-hydroxide based resin gel for the diffusive gradient in thin films technique, *Anal. Chim. Acta* 1102 (2020) 36–45.
- [54] VlaamsInstituutvoordeZee, ScheldeMonitor Geoviewer, 2020. Oostende, Belgium.

- [55] A. Husson, M. Leermakers, M. Descostes, V. Lagneau, Environmental geochemistry and bioaccumulation/bioavailability of uranium in a post-mining context—The Bois-Noirs Limouzat mine (France), *Chemosphere* 236 (2019) 124341.
- [56] H. Windom, R. Smith, F. Niencheski, C. Alexander, Uranium in rivers and estuaries of globally diverse, smaller watersheds, *Mar. Chem.* 68 (4) (2000) 307–321.
- [57] E. Strady, G. Blanc, J. Schäfer, A. Coyne, A. Dabrin, Dissolved uranium, vanadium and molybdenum behaviours during contrasting freshwater discharges in the Gironde Estuary (SW France), *Estuar. Coast Shelf Sci.* 83 (4) (2009) 550–560.
- [58] J.G. Rodríguez, I. Amouroux, M.J. Belzunce-Segarra, P. Bersuder, T. Bolam, M. Caetano, I. Carvalho, M.M.C. Dos Santos, G.R. Fones, J.-L. Gonzalez, Assessing variability in the ratio of metal concentrations measured by DGT-type passive samplers and spot sampling in European seawaters, *Sci. Total Environ.* 783 (2021) 147001.
- [59] R.B.M. Sparovek, J. Fleckenstein, E. Schnug, Issues of uranium and radioactivity in natural mineral waters, *Landbauforschung Volkenrode* 51 (4) (2001) 149–158.
- [60] A.C. Hogan, R.A. van Dam, S.J. Markich, C. Camilleri, Chronic toxicity of uranium to a tropical green alga (*Chlorella* sp.) in natural waters and the influence of dissolved organic carbon, *Aquat. Toxicol.* 75 (4) (2005) 343–353.
- [61] P. Andersson, D. Porcelli, G. Wasserburg, J. Ingri, Particle transport of 234U–238U in the Kalix river and in the Baltic sea, *Geochem. Cosmochim. Acta* 62 (3) (1998) 385–392.
- [62] D. Porcelli, P. Andersson, G. Wasserburg, J. Ingri, M. Baskaran, The importance of colloids and mires for the transport of uranium isotopes through the Kalix River watershed and Baltic Sea, *Geochem. Cosmochim. Acta* 61 (19) (1997) 4095–4113.
- [63] W. Dong, S.C. Brooks, Determination of the formation constants of ternary complexes of uranyl and carbonate with alkaline earth metals (Mg²⁺, Ca²⁺, Sr²⁺, and Ba²⁺) using anion exchange method, *Environ. Sci. Technol.* 40 (15) (2006) 4689–4695.
- [64] E.L. Mühr-Ebert, F. Wagner, C. Walther, Speciation of uranium: compilation of a thermodynamic database and its experimental evaluation using different analytical techniques, *Appl. Geochem.* 100 (2019) 213–222.
- [65] P.E. Reiller, M. Descostes, Development and application of the thermodynamic database PRODATA dedicated to the monitoring of mining activities from exploration to remediation, *Chemosphere* (2020) 126301.
- [66] J. Lartigue, B. Charrasse, B. Reile, M. Descostes, Aqueous inorganic uranium speciation in European stream waters from the FOREGS dataset using geochemical modelling and determination of a U bioavailability baseline, *Chemosphere* 251 (2020) 126302.
- [67] S. Meylan, N. Odzak, R. Behra, L. Sigg, Speciation of copper and zinc in natural freshwater: comparison of voltammetric measurements, diffusive gradients in thin films (DGT) and chemical equilibrium models, *Anal. Chim. Acta* 510 (1) (2004) 91–100.
- [68] A. Charriau, L. Lesven, Y. Gao, M. Leermakers, W. Baeyens, B. Ouddane, G. Billon, Trace metal behaviour in riverine sediments: role of organic matter and sulfides, *Appl. Geochem.* 26 (1) (2011) 80–90.
- [69] J. Galceran, J. Puy, Interpretation of diffusion gradients in thin films (DGT) measurements: a systematic approach, *Environ. Chem.* 12 (2) (2015) 112–122.
- [70] Ø.A. Garmo, O. Royset, E. Steinnes, T.P. Flaten, Performance study of diffusive gradients in thin films for 55 elements, *Anal. Chem.* 75 (14) (2003) 3573–3580.
- [71] Bio-Rad Laboratories, **Chelex® 100 and Chelex 20 Chelating Ion Exchange Resin - Instruction Manual**, 2000. <https://www.bio-rad.com/webroot/web/pdf/lsr/literature/LIT200.pdf>.
- [72] J. Liu, J. Li, X. Yang, Q. Song, C. Bai, Y. Shi, L. Zhang, C. Liu, S. Li, L. Ma, Facile preparation of polyphenolic hydroxyl functionalized uranium-selective chelating sorbent: simple oxidation of styrene-divinylbenzene copolymer microparticles by Hummers method, *Mater. Lett.* 97 (2013) 177–180.
- [73] M.A. Mahmoud, Separation of U (VI) ions from the aqueous phase onto polyphenol silica nanocomposite in the batch adsorption system, *Alex. Eng. J.* 60 (4) (2021) 3819–3827.
- [74] Lanxess, **Product Information – Lewatit® FO 36**, 2011. <https://www.lanxess.com/Data-sheets/Lewatit-FO-36-L.pdf>.
- [75] M. Wazne, G.P. Korfiatis, X. Meng, Carbonate effects on hexavalent uranium adsorption by iron oxyhydroxide, *Environ. Sci. Technol.* 37 (16) (2003) 3619–3624.
- [76] S.D. Yusan, S.A. Erenturk, Sorption behaviors of uranium (VI) ions on α -FeOOH, *Desalination* 269 (1–3) (2011) 58–66.
- [77] E. Uher, H. Zhang, S. Santos, M.-H.L.n. Tusseau-Vuillemin, C. Gourlay-Francé, Impact of biofouling on diffusive gradient in thin film measurements in water, *Anal. Chem.* 84 (7) (2012) 3111–3118.

6 CONCLUSIONS

The aim of this work was the development and evaluation of Diffusive Gradients in Thin films technique for environmental application. A particular interest of this study lied in the investigation of arsenic and uranium in the aquatic environment. To be able to study their speciation and biogeochemistry, a novel DGT technique utilizing commercially available resin Lewatit FO 36 was successfully developed, characterized, and validated by *in-situ* applications in natural aquatic environments.

The novel DGT resin gel utilizing Lewatit FO 36 is easy to produce and provides accurate and reproducible results. The Lewatit FO 36 resin gel has a high sorption capacity (~535 μg per gel disc) towards all four tested arsenic species (As^{III} , As^{V} , monomethylarsonic acid (MMA), and dimethylarsinic acid (DMA)) and its sorption ability is not influenced in the pH range 4–8 or in the presence of interfering analytes such as chlorides and humic acid. Only a very high concentration of phosphates (10 mg L^{-1}) caused a slight decrease (around 10%) in the diffusion coefficients of MMA and As^{V} species which can be explained by the chemical analogy of PO_4^{3-} and AsO_4^{3-} . The phosphates may therefore compete for the binding sites on the resin and thus decrease the efficiency of arsenates uptake. Similarly, the presence of iron (1 mg L^{-1}) caused a decrease in the uptake of all tested As species, due to the formation of As-Fe complexes which are not labile and thus do not contribute to the DGT-determined fraction. Nevertheless, regarding the common concentrations of phosphates (0.05 mg L^{-1}) and iron (less than 0.3 mg L^{-1}), these negative effects may be considered negligible for applications in most natural waters. However, it is always important to consider the influence of iron on arsenic speciation particularly in areas, where higher concentrations of iron may occur, and take this into account for data interpretation.

The performance of the DGT technique utilizing Lewatit FO 36 resin gels was validated by several applications in natural waters. Very good results were obtained during deployment in the water reservoir Zászkalská (Neřežín, Czech Republic) in the vicinity of the former cinnabar mine, where the DGTs linearly accumulated As for up to 49 days. Although the DGT performance at the end of this experiment was influenced

by the formation of biofilm, the agreement between DGT-determined and dissolved As concentration in the water was 91–93%. The following application of the Lewatit FO 36 DGTs focused on the investigation of As bioavailability in arsenic and iron-rich water from natural mineral springs Hronovka and Regnerka (Hronov, Czech Republic). Although it was expected that the bioavailability of As in mineral water will be reduced by the high Fe content (as it was observed during the development of Lewatit FO 36 DGTs), the obtained DGT-determined concentrations fully corresponded to the dissolved As concentrations analysed directly in grab water samples. For this reason, it is assumed that the composition of the mineral water (especially high concentrations of sulphates, sulphides, or phosphates) prevents the complexation of arsenic and iron, and arsenic is thus completely available to DGT and potentially to the biota.

Arsenic distribution and geochemistry in water and sediments of the Zenne River were investigated based on the research findings from the years 2010–2021. The combination of passive and sampling techniques and analysis of historical data revealed that the downstream transport of As in the Zenne River is completely dominated by the presence of an important point source located on the tributary Tangebeek. After the confluence of Zenne with this tributary, the concentrations of As in water sediments sharply increase and affects the downstream part of the river. Since this part is influenced by the tide, large temporal variability in As concentrations can be observed in this area as due to the dilution with the Dijle water during rising tide. The study has demonstrated the benefits of DGT application in this dynamic environment, where the technique provides time-weighted average concentrations of labile As species. The investigation of geochemical behaviour of As in sediments showed that the reducible fraction is the main binding fraction for As and porewater geochemistry is dominated by the reductive dissolution of Mn and Fe oxyhydroxides. In sediment porewaters As is predominantly present as non-DGT labile species (66–93%) and the DGT labile As fraction is dominated by As(III). Flux calculations evaluating the relative importance of different As sources to the Zenne River revealed that the point source on Tangebeek contributes for 87% of the As load carried by the Zenne River.

The results pointed out the presence of As source located in the industrial area downstream of Brussels where a sharp increase of As concentrations is observed in water and sediments. Large temporal variability in As concentrations in the tidal zone is found with the dissolved and particulate As concentrations generally being 4–5 times higher during low tide. Comparison with the historical data (2003) demonstrated changes in the partitioning of As between the dissolved and particulate phases. Currently, lower concentrations of dissolved As are generally found along the Zenne River as a result of oxygen restoration due to the operation of the wastewater treatment plants in the Brussels area. The study also highlighted the benefits of the DGT application in a dynamic environment such as tidal rivers where water grab sampling may provide variable and misleading results. On the contrary, the time-integrated As concentrations provided by the DGT technique are more informative. The investigation of As geochemistry in sediments then showed that As mobility in this area is predominantly driven by reductive desorption or dissolution from the iron/manganese (oxyhydr)oxides.

The initial development process of the Lewatit FO 36 DGT binding phase also resulted in the optimization of a novel ET-AAS method. Since the highly concentrated mixture of NaOH and NaCl (both 10 g L^{-1}) was originally used for the elution of arsenic from Lewatit FO 36 resin gels, the determination of As content in eluates was complicated by the loss of arsenic content during the pyrolysis step and interferences caused by the matrix of elution agent. To avoid these complications, the proposed method combines a unique graphite furnace temperature program with the cool-down pre-atomization step and modification of the graphite furnace surface by tungsten carbides. The method enables the analysis of As in solution samples without any samples pre-treatment and is characterized by high accuracy and precision. Although the method was initially proposed for the analysis of As in the eluents of the Lewatit FO 36 resin gels, it can find broader application. Since the method utilizes standard addition calibration, it can be applied on high salinity samples without the knowledge of the exact concentration of chlorides. This enables its application for the analysis of seawater or mineral water samples.

Further laboratory testing of the Lewatit FO 36 resin gel revealed its ability to simultaneously determine arsenic and uranium. The resin gel has a high sorption capacity (~1250 µg per gel disc) towards uranium and does not display any significant sorption selectivity in favour of one element over another. A novel protocol for simultaneous elution of arsenic and uranium from Lewatit FO 36 resin gel was also proposed in this study. It utilizes 1 M NaOH in combination with a higher temperature (70 °C). In comparison with the original elution protocol, the novel method provides good results in As elution and, in addition, allows simultaneous elution of U. Moreover, the elimination of NaCl from the elution process allows a fast and simple analysis of both elements using ICP-MS, and therefore, the Lewatit FO 36-DGT technique can become more commonplace among laboratories without the need to modify the analytical method as proposed in the original study.

The final chapter focused on the evaluation of the salinity influence on the DGT performance for uranium monitoring in the estuarine and marine environment. Four selected DGT binding phases (Chelex-100, Diphonix, Dow-PIWBA, and Lewatit FO 36 resins) were tested by *in-situ* deployment along the Scheldt estuary (Belgium) within four campaigns between 2014–2021. The concentrations of dissolved uranium in this area exhibit typical conservative behaviour along the salinity gradient. The speciation modelling of U showed that calcium uranyl carbonate complexes dominate along the Scheldt estuary (from 97 to 86% seawards) and that the fraction of $\text{UO}_2(\text{CO}_3)_3^{4-}$ showed an increasing trend seaward (from 2 to 14%). This change in U speciation may explain the systematic decrease of U accumulated on the Chelex-100 DGT with increasing salinity. Chelex-100 cannot be used for long-term measurement of U due to competition and saturation effects. The Lewatit FO 36 DGT provided overall reliable results and the DGT-determined concentrations agreed with the dissolved U concentrations up to salinity 18, but the performance decreased at higher salinity levels (> 18) and especially during the long-term deployment in seawater (deployment period > 24 h). This suggests that the resin could be valuable for simultaneous monitoring of As and U in a freshwater environment (such as mining-impacted areas) but further research investigating the influence of other competing ions is necessary. The Dow-PIWBA DGT could be used

throughout the whole salinity gradient for 24h deployments, but its performance drop after 48 h in seawater. The most robust performance along the salinity gradient was achieved only by Diphonix DGTs as this resin provided good results even after 28 days of deployment in seawater (~27 PSU). Therefore, the results of this study demonstrated that thorough testing of the DGT technique in a natural environment is a crucial prerequisite for obtaining reliable data and application of the DGT as a speciation tool.

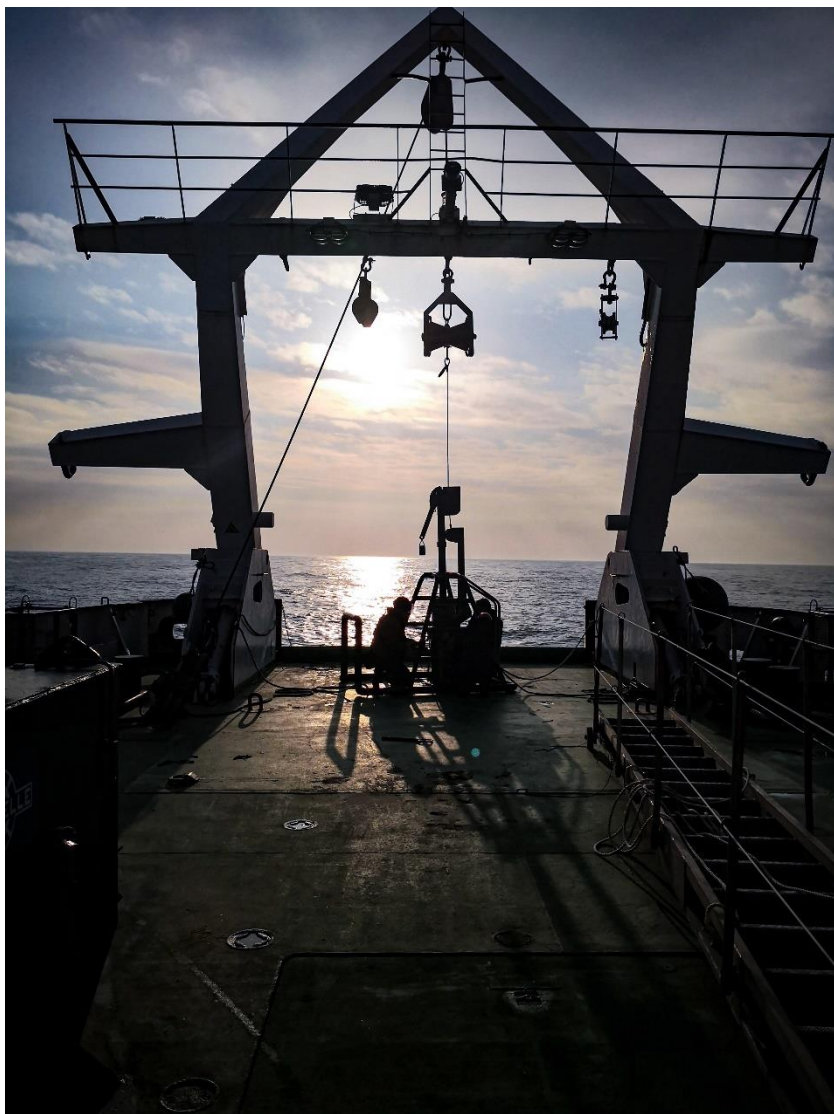
7 FUTURE PERSPECTIVES

Within this work, the Lewatit FO 36 resin was proved to be a reliable DGT binding phase with a great potential for As and/or U monitoring in natural environments. However, regarding the nature of the functional groups of this resin (and technical information provided by the manufacturer), it is also capable of selective adsorption of other species of oxyanions such as HPO_4^{2-} , HSiO_3^- , HSbO_4^{2-} , HVO_4^{2-} , MoO_4^{2-} , SeO_4^{2-} , *etc.* Therefore, the evaluation of the sorption abilities of Lewatit FO 36 towards other oxyanions belongs among our future interests. Field expeditions on the RV Belgica using the Lewatit FO 36 resin are planned.

Knowledge of the speciation of As is essential for the understanding of its environmental fate and toxicity. The Lewatit FO 36 resin effectively binds As(III), As(V), MMAs and DMAs and up to now only total As measurements were made. Future perspectives involve the selective elution of the different species or simultaneous elution followed by chromatographic separation. The aim is to apply these developments in uranium mining sites in Canada where high arsenic concentrations are observed.

Other perspectives also include the completion of studies which are currently ongoing and are therefore not included in this thesis. These studies were performed in cooperation with Orano Mining and focused on the application of the DGT technique as a monitoring tool for uranium and other trace elements. One such study evaluates whether the DGT technique can be used as a long-term monitoring tool for uranium in surface water and groundwater at an active nuclear site (Tricastin, France). To find the design of the DGT technique for uranium monitoring over longer time periods, extensive laboratory testing with various binding phases (Chelex-100, Iontosorb Oxin, Diphonix, and Dow-PIWBA resins, or their mixtures) was performed and followed by *in-situ* application on the site. Another field expedition is currently planned. Another study focuses on the mapping of the speciation and bioavailability of U in mining sites in France. The monitoring was already performed in the Pays de Loire region and Burgundy in France. The outcomes of these studies will be potentially used for the implementation of the future water quality standards (Water Framework Directive) in

which the U concentrations and toxicity in the function of the composition of the surface water are the subjects of discussions with the safety authorities.



(Collection of sediment core during sampling cruise in the Belgian coastal zone in 2021).

8 REFERENCES

- [1] Journal Citation Reports. Journal Categories ranked by Number of Journals. *Clarivate Analytics*. URL: <https://jcr.clarivate.com/jcr/browse-category-list>. [cited 11/10/2021].
- [2] Czernuszenko, W. & Rowinski, P. Water quality hazards and dispersion of pollutants, *Springer Science & Business Media*, 2005.
- [3] World Health Organization. Arsenic in Drinking-water: Background Document for Development of WHO Guidelines for Drinking-water Quality. 2011.
- [4] World Health Organization. Uranium in Drinking-water: Background Document for Development of WHO Guidelines for Drinking-water Quality. 2012.
- [5] Davison, W. & Zhang, H. In situ speciation measurements of trace components in natural waters using thin-film gels. *Nature*. 1994, (367), 546-548. DOI:10.1038/367546a0.
- [6] Menegário, A.A., Yabuki, L.N.M., Luko, K.S., Williams, P.N. & Blackburn, D.M. Use of diffusive gradient in thin films for in situ measurements: a review on the progress in chemical fractionation, speciation and bioavailability of metals in waters. *Analytica Chimica Acta*. 2017, (983), 54-66. DOI:10.1016/j.aca.2017.06.041.
- [7] Davison, W. Diffusive gradients in thin-films for environmental measurements, *Cambridge University Press* 2016.
- [8] Gaulier, C., Zhou, C., Gao, Y., Guo, W., Reichstädter, M., Ma, T., Baeyens, W. & Billon, G. Investigation on trace metal speciation and distribution in the Scheldt estuary. *Science of the Total Environment*. 2021, (757), 143827. DOI:10.1016/j.scitotenv.2020.143827.
- [9] Rodríguez, J.G., Amouroux, I., Belzunce-Segarra, M.J., Bersuder, P., Bolam, T., Caetano, M., Carvalho, I., Dos Santos, M.M.C., Fones, G.R. & Gonzalez, J.-L. Assessing variability in the ratio of metal concentrations measured by DGT-type passive samplers and spot sampling in European seawaters. *Science of the Total Environment*. 2021, (783), 147001. DOI:10.1016/j.scitotenv.2021.147001.
- [10] Elias, L.P., Menegário, A.A., Hernández, A.H., Eismann, C.E., Viana, J.L.M., Pedrobom, J.H., de Oliveira Junior, E.G., Barbiero, L. & Fostier, A.H. In situ fractionation and redox speciation of arsenic in soda lakes of Nhecolândia (Pantanal, Brazil) using the diffusive gradients in thin films (DGT) technique. *Chemosphere*. 2021, 132592. DOI:10.1016/j.chemosphere.2021.132592.

- [11] Zhao, J., Cornett, R. & Chakrabarti, C. Assessing the uranium DGT-available fraction in model solutions. *Journal of Hazardous Materials*. 2020, (384), 121134. DOI:10.1016/j.jhazmat.2019.121134.
- [12] Søndergaard, J., Bach, L. & Gustavson, K. Measuring bioavailable metals using diffusive gradients in thin films (DGT) and transplanted seaweed (*Fucus vesiculosus*), blue mussels (*Mytilus edulis*) and sea snails (*Littorina saxatilis*) suspended from monitoring buoys near a former lead–zinc mine in West Greenland. *Marine Pollution Bulletin*. 2014, (78), 102-109. DOI:10.1016/j.marpolbul.2013.10.054.
- [13] Pelcová, P., Vičarová, P., Ridošková, A., Dočekalová, H., Kopp, R., Mareš, J. & Poštulková, E. Prediction of mercury bioavailability to common carp (*Cyprinus carpio* L.) using the diffusive gradient in thin film technique. *Chemosphere*. 2017, (187), 181-187. DOI:10.1016/j.chemosphere.2017.08.097.
- [14] Zhang, S., Wang, Y., Pervaiz, A., Kong, L. & He, M. Comparison of diffusive gradients in thin-films (DGT) and chemical extraction methods for predicting bioavailability of antimony and arsenic to maize. *Geoderma*. 2018, (332), 1-9. DOI:10.1016/j.geoderma.2018.06.023.
- [15] Wen, Y., Li, W., Yang, Z., Zhuo, X., Guan, D.-X., Song, Y., Guo, C. & Ji, J. Evaluation of various approaches to predict cadmium bioavailability to rice grown in soils with high geochemical background in the karst region, Southwestern China. *Environmental Pollution*. 2020, (258), 113645. DOI:10.1016/j.envpol.2019.113645.
- [16] Town, R.M., Chakraborty, P. & van Leeuwen, H. Dynamic DGT speciation analysis and applicability to natural heterogeneous complexes. *Environmental Chemistry*. 2009, (6), 170. DOI:10.1071/EN08091.
- [17] Dunn, R., Teasdale, P., Warnken, J., Jordan, M. & Arthur, J. Evaluation of the in situ, time-integrated DGT technique by monitoring changes in heavy metal concentrations in estuarine waters. *Environmental Pollution*. 2007, (148), 213-220. DOI:10.1016/j.envpol.2006.10.027.
- [18] Montero, N., Belzunce-Segarra, M., Gonzalez, J.-L., Larreta, J. & Franco, J. Evaluation of diffusive gradients in thin-films (DGTs) as a monitoring tool for the assessment of the chemical status of transitional waters within the Water Framework Directive. *Marine Pollution Bulletin*. 2012, (64), 31-39. DOI:10.1016/j.marpolbul.2011.10.028.
- [19] Turner, G.S., Mills, G.A., Bowes, M.J., Burnett, J.L., Amos, S. & Fones, G.R. Evaluation of DGT as a long-term water quality monitoring tool in natural waters; uranium as a case study. *Environmental Science: Processes & Impacts*. 2014, (16), 393-403. DOI:10.1039/C3EM00574G.

- [20] Zhou, C., Gaulier, C., Luo, M., Guo, W., Baeyens, W. & Gao, Y. Fine scale measurements in Belgian coastal sediments reveal different mobilization mechanisms for cationic trace metals and oxyanions. *Environment International*. 2020, (145), 106140. DOI:10.1016/j.envint.2020.106140.
- [21] Viana, J.L.M., de Souza, A.F., Hernández, A.H., Elias, L.P., Eismann, C.E., Rezende-Filho, A.T., Barbiero, L., Menegario, A.A. & Fostier, A.H. In situ arsenic speciation at the soil/water interface of saline-alkaline lakes of the Pantanal, Brazil: A DGT-based approach. *Science of the Total Environment*. 2022, (804), 150113. DOI:10.1016/j.scitotenv.2021.150113.
- [22] Husson, A., Leermakers, M., Descostes, M. & Lagneau, V. Environmental geochemistry and bioaccumulation/bioavailability of uranium in a post-mining context—The Bois-Noirs Limouzat mine (France). *Chemosphere*. 2019, (236), 124341. DOI:10.1016/j.chemosphere.2019.124341.
- [23] Martin, A., Montavon, G. & Landesman, C. A combined DGT-DET approach for an in situ investigation of uranium resupply from large soil profiles in a wetland impacted by former mining activities. *Chemosphere*. 2021, (279), 130526. DOI:10.1016/j.chemosphere.2021.130526.
- [24] Cesbron, F., Metzger, E., Launeau, P., Deflandre, B., Delgard, M.-L., Thibault de Chanvalon, A., Geslin, E., Anschutz, P. & Jézéquel, D. Simultaneous 2D imaging of dissolved iron and reactive phosphorus in sediment porewaters by thin-film and hyperspectral methods. *Environmental Science & Technology*. 2014, (48), 2816-2826. DOI:10.1021/es404724r.
- [25] Stockdale, A., Davison, W. & Zhang, H. 2D simultaneous measurement of the oxyanions of P, V, As, Mo, Sb, W and U. *Journal of Environmental Monitoring*. 2010, (12), 981-984. DOI:10.1039/B925627J.
- [26] Zhou, Y., Wang, H., Zhang, Y., Cai, Y., Yin, H., Yang, Z., Li, Q. & Yuan, H. Availability and diffusion kinetic process of phosphorus in the water–sediment interface assessed by the high-resolution DGT technique. *Journal of Soils and Sediments*. 2021, (21), 3274-3288. DOI:10.1007/s11368-021-02954-7.
- [27] Zhou, C., Gao, Y., Gaulier, C., Luo, M., Zhang, X., Bratkic, A., Davison, W. & Baeyens, W. Advances in understanding mobilization processes of trace metals in marine sediments. *Environmental Science & Technology*. 2020, (54), 15151-15161. DOI:10.1021/acs.est.0c05954.
- [28] Abdelouas, A. Uranium mill tailings: geochemistry, mineralogy, and environmental impact. *Elements*. 2006, (2), 335-341. DOI:10.2113/gselements.2.6.335.

- [29] Blake, J.M., Avasarala, S., Artyushkova, K., Ali, A.-M.S., Brearley, A.J., Shuey, C., Robinson, W.P., Nez, C., Bill, S. & Lewis, J. Elevated concentrations of U and co-occurring metals in abandoned mine wastes in a northeastern Arizona Native American community. *Environmental Science and Technology*. 2015, (49), 8506-8514. DOI:10.1021/acs.est.5b01408.
- [30] Donahue, R. & Hendry, M. Geochemistry of arsenic in uranium mine mill tailings, Saskatchewan, Canada. *Applied Geochemistry*. 2003, (18), 1733-1750. DOI:10.1016/S0883-2927(03)00106-9.
- [31] IUPAC. Compendium of Chemical Terminology (the "Gold Book"). 2nd ed. Compiled by A. D. McNaught and A. Wilkinson, *Blackwell Science Oxford*, 1997.
- [32] Morel, F., Milligan, A. & Saito, M. Marine Bioinorganic Chemistry: The Role of Trace Metals in the Oceanic Cycles of Major Nutrients. In: *Treatise on Geochemistry: The Oceans and Marine Geochemistry*, Elderfield, H. Ed., *Elsevier*, 2006, Vol. 6, pp. 113-140.
- [33] Lindh, U. Biological functions of the elements. In: *Essentials of medical geology: Impacts of the natural environment on public health*, Selinus, O. Ed., *Springer*, 2005.
- [34] World Health Organization. Trace elements in human nutrition and health. 1996.
- [35] Pérez-Granados, A.M. & Vaquero, M.P. Silicon, aluminium, arsenic and lithium: essentiality and human health implications. *Journal of Nutrition Health and Aging*. 2002, (6), 154-162.
- [36] Uthus, E.O. c. *The Journal of Trace Elements in Experimental Medicine*. 2003, (16), 345-355. DOI:10.1002/jtra.10044.
- [37] Živkov Baloš, M., Jakšić, S. & Ljubojević Pelić, D. The role, importance and toxicity of arsenic in poultry nutrition. *World's Poultry Science Journal*. 2019, (75), 375-386. DOI:10.1017/S0043933919000394.
- [38] Duker, A.A., Carranza, E.J.M. & Hale, M. Arsenic geochemistry and health. *Environment International*. 2005, (31), 631-641. DOI:10.1016/j.envint.2004.10.020.
- [39] Goessler, W. & Kuehnelt, D. Analytical Methods for the Determination of Arsenic and Arsenic Compounds in the Environment. In: *Environmental Chemistry of Arsenic*, Frankenberger Jr, W.T. Ed., *CRC Press*, 2001.
- [40] Agency for Toxic Substances and Disease Registry (ATSDR). Toxicological profile for arsenic, *Atlanta, GA: U.S. Department of Health and Human Services, Public Health Service*, 2007.

- [41] Toujaguez, R., Ono, F., Martins, V., Cabrera, P., Blanco, A., Bundschuh, J. & Guilherme, L. Arsenic bioaccessibility in gold mine tailings of Delita, Cuba. *Journal of Hazardous Materials*. 2013, (262), 1004-1013. DOI:10.1016/j.jhazmat.2013.01.045.
- [42] Kabata-Pendias, A. Trace elements in soils and plants, *CRC press*, 2010.
- [43] Smedley, P., Edmunds, W. & Pelig-Ba, K. Mobility of arsenic in groundwater in the Obuasi gold-mining area of Ghana: some implications for human health. *Geological Society, London, Special Publications*. 1996, (113), 163-181. DOI:10.1144/GSL.SP.1996.113.01.13.
- [44] Smedley, P.L. & Kinniburgh, D. A review of the source, behaviour and distribution of arsenic in natural waters. *Applied Geochemistry*. 2002, (17), 517-568. DOI:10.1016/S0883-2927(02)00018-5.
- [45] Basta, N.T., Rodriguez, R.R. & Casteel, S.W. Bioavailability and Risk of Arsenic Exposure by the Soil Ingestion Pathway. In: *Environmental Chemistry of Arsenic*, Frankenberger Jr, W.T. Ed., *CRC Press*, 2001.
- [46] Herath, I., Vithanage, M., Bundschuh, J., Maity, J.P. & Bhattacharya, P. Natural arsenic in global groundwaters: distribution and geochemical triggers for mobilization. *Current Pollution Reports*. 2016, (2), 68-89. DOI:10.1007/s40726-016-0028-2.
- [47] Hering, J.G. & Kneebone, P.E. Biogeochemical Controls on Arsenic Occurrence and Mobility in Water Supplies. In: *Environmental Chemistry of Arsenic*, Frankenberger Jr, W.T. Ed., *CRC Press*, 2001.
- [48] Mason, R.P. Trace metals in freshwaters. In: *Trace metals in aquatic systems*, *Wiley Online Library*, 2013.
- [49] O'Day, P.A., Vlassopoulos, D., Root, R. & Rivera, N. The influence of sulfur and iron on dissolved arsenic concentrations in the shallow subsurface under changing redox conditions. *Proceedings of the National Academy of Sciences*. 2004, (101), 13703-13708. DOI:10.1073/pnas.0402775101.
- [50] Szramek, K., Walter, L.M. & McCall, P. Arsenic mobility in groundwater/surface water systems in carbonate-rich Pleistocene glacial drift aquifers (Michigan). *Applied Geochemistry*. 2004, (19), 1137-1155. DOI:10.1016/j.apgeochem.2004.01.012.
- [51] Bauer, M. & Blodau, C. Mobilization of arsenic by dissolved organic matter from iron oxides, soils and sediments. *Science of the Total Environment*. 2006, (354), 179-190. DOI:10.1016/j.scitotenv.2005.01.027.

- [52] Wu, Z., Ren, H., McGrath, S.P., Wu, P. & Zhao, F.-J. Investigating the contribution of the phosphate transport pathway to arsenic accumulation in rice. *Plant Physiology*. 2011, (157), 498-508. DOI:10.1104/pp.111.178921.
- [53] Pothier, M.P., Lenoble, V., Garnier, C., Misson, B., Rentmeister, C. & Poulain, A.J. Dissolved organic matter controls of arsenic bioavailability to bacteria. *Science of the Total Environment*. 2020, (716), 137118. DOI:10.1016/j.scitotenv.2020.137118.
- [54] Karpas, Z. Fundamental properties of uranium and its compounds, the nuclear fuel cycle, and analytical methods used for characterizing uranium. In: Analytical chemistry of uranium: environmental, forensic, nuclear, and toxicological applications, *CRC press* 2014.
- [55] Grenthe, I., Drozdynski, J., Fujino, T., Buck, E.C., Albrecht-Schmitt, T.E. & Wolf, S.F. Uranium. In: The chemistry of the actinide and transactinide elements, Morss, L.R., Edelstein, N.M., Fuger, J. Eds., *Springer*, 2010.
- [56] Karpas, Z. Determination of Uranium in Environmental Samples. In: Analytical chemistry of uranium: environmental, forensic, nuclear, and toxicological applications, *CRC press* 2014.
- [57] Markich, S.J. Uranium speciation and bioavailability in aquatic systems: an overview. *The Scientific World Journal*. 2002, (2). DOI:10.1100/tsw.2002.130.
- [58] Srivastava, R.R., Pathak, P. & Perween, M. Environmental and Health Impact due to Uranium Mining. In: Uranium in Plants and the Environment, Gupta, D.K., Walther, C. Eds., *Springer* 2020.
- [59] Sparovek, R.B.M., Fleckenstein, J. & Schnug, E. Issues of uranium and radioactivity in natural mineral waters. *Landbauforschung Volkenrode*. 2001, (51), 149-158.
- [60] Stewart, B.D., Mayes, M.A. & Fendorf, S. Impact of uranyl– calcium– carbonate complexes on uranium (VI) adsorption to synthetic and natural sediments. *Environmental Science & Technology*. 2010, (44), 928-934. DOI:10.1021/es902194x.
- [61] Dong, W. & Brooks, S.C. Determination of the formation constants of ternary complexes of uranyl and carbonate with alkaline earth metals (Mg^{2+} , Ca^{2+} , Sr^{2+} , and Ba^{2+}) using anion exchange method. *Environmental Science & Technology*. 2006, (40), 4689-4695. DOI:10.1021/es0606327.
- [62] Endrizzi, F. & Rao, L. Chemical speciation of uranium (VI) in marine environments: complexation of calcium and magnesium Ions with $[(UO_2)(CO_3)_3]^{4-}$ and the effect on the extraction of uranium from seawater. *Chemistry–A European Journal*. 2014, (20), 14499-14506. DOI:10.1002/chem.201403262.

- [63] Cumberland, S.A., Douglas, G., Grice, K. & Moreau, J.W. Uranium mobility in organic matter-rich sediments: A review of geological and geochemical processes. *Earth-Science Reviews*. 2016, (159), 160-185. DOI:10.1016/j.earscirev.2016.05.010.
- [64] Novotnik, B., Chen, W. & Evans, R.D. Uranium bearing dissolved organic matter in the porewaters of uranium contaminated lake sediments. *Applied Geochemistry*. 2018, (91), 36-44. DOI:10.1016/j.chemosphere.2007.06.032.
- [65] Adriano, D.C. Bioavailability of trace metals. In: Trace Elements in Terrestrial Environments: Biogeochemistry, Bioavailability and Risks of metals, *Springer*, 2001.
- [66] Michalke, B. & Caroli, S. Speciation of trace elements. In: Essentials of medical geology: Impacts of the natural environment on public health, Selinus, O. Ed., *Springer*, 2005.
- [67] Drexler, J., Fisher, N., Henningsen, G., Lanno, R., McGeer, J., Sappington, K. & Beringer, M. Issue paper on the bioavailability and bioaccumulation of metals. In: US Environmental Protection Agency, Risk Assessment Forum, 2003.
- [68] Nikinmaa, M. Factors Affecting the Bioavailability of Chemicals. In: An introduction to aquatic toxicology, *Elsevier*, 2014.
- [69] de Paiva Magalhães, D., da Costa Marques, M.R., Baptista, D.F. & Buss, D.F. Metal bioavailability and toxicity in freshwaters. *Environmental Chemistry Letters*. 2015, (13), 69-87. DOI:10.1007/s10311-015-0491-9.
- [70] Wallace, J.B., Hutchens, J.J. & Grubaugh, J.W. Transport and storage of FPOM. In: Methods in stream ecology, Hauer, F.R., Lamberti, G. Eds., *Academic Press*, 2011.
- [71] de Souza Machado, A.A., Spencer, K., Kloas, W., Toffolon, M. & Zarfl, C. Metal fate and effects in estuaries: A review and conceptual model for better understanding of toxicity. *Science of the Total Environment*. 2016, (541), 268-281. DOI:10.1016/j.scitotenv.2015.09.045.
- [72] Lead, J.R. & Wilkinson, K.J. Environmental colloids and particles: current knowledge and future developments. In: Environmental colloids and particles: behaviour, separation and characterisation, Wilkinson, K.J., Lead, J.R. Eds., *John Wiley & Sons*, 2007, Vol. 10.
- [73] Hargreaves, A.J., Vale, P., Whelan, J., Constantino, C., Dotro, G., Campo, P. & Cartmell, E. Distribution of trace metals (Cu, Pb, Ni, Zn) between particulate, colloidal and truly dissolved fractions in wastewater treatment. *Chemosphere*. 2017, (175), 239-246. DOI:10.1016/j.chemosphere.2017.02.034.

- [74] Choe, K.-Y., Gill, G.A. & Lehman, R. Distribution of particulate, colloidal, and dissolved mercury in San Francisco Bay estuary. 1. Total mercury. *Limnology and Oceanography*. 2003, (48), 1535-1546. DOI:10.4319/lo.2003.48.4.1547.
- [75] Kumar, R., Rani, M., Gupta, H. & Gupta, B. Trace metal fractionation in water and sediments of an urban river stretch. *Chemical Speciation & Bioavailability*. 2014, (26), 200-209. DOI:10.3184/095422914X14142369069568.
- [76] Gailardet, J., Viers, J. & Durpé, B. Trace Elements in River Waters. In: *Treatise on Geochemistry: Surface and Ground Water, Weathering, and Soils*, Drever, J.I. Ed., *Elsevier*, 2005, Vol. 5.
- [77] Lindh, U. Uptake of elements from a biological point of view. In: *Essentials of medical geology: Impacts of the natural environment on public health*, Selinus, O. Ed., *Springer*, 2005.
- [78] Brown, P.L. & Markich, S. Evaluation of the free ion activity model of metal-organism interaction: extension of the conceptual model. *Aquatic Toxicology*. 2000, (51), 177-194. DOI:10.1016/S0166-445X(00)00115-6.
- [79] Worms, I., Simon, D.F., Hassler, C. & Wilkinson, K. Bioavailability of trace metals to aquatic microorganisms: importance of chemical, biological and physical processes on biouptake. *Biochimie*. 2006, (88), 1721-1731. DOI:10.1016/j.biochi.2006.09.008.
- [80] Javanbakht, V., Alavi, S.A. & Zilouei, H. Mechanisms of heavy metal removal using microorganisms as biosorbent. *Water Science and Technology*. 2014, (69), 1775-1787. DOI:10.2166/wst.2013.718.
- [81] Moiseenko, T. Bioavailability and Ecotoxicity of Metals in Aquatic Systems: Critical Contamination Levels. *Geochemistry International*. 2019, (57), 737-750. DOI:10.31857/S0016-7525647675-688.
- [82] Luoma, S.N. Bioavailability of trace metals to aquatic organisms—a review. *Science of the Total Environment*. 1983, (28), 1-22. DOI:10.1016/s0048-9697(83)80004-7.
- [83] Batley, G.E., Apte, S.C. & Stauber, J.L. Speciation and bioavailability of trace metals in water: progress since 1982. *Australian Journal of Chemistry*. 2004, (57), 903-919. DOI:10.1071/CH04095.
- [84] Kumaresan, M. & Riyazuddin, P. Overview of speciation chemistry of arsenic. *Current Science*. 2001, 837-846.

- [85] Akter, K.F., Owens, G., Davey, D.E. & Naidu, R. Arsenic speciation and toxicity in biological systems. In: Reviews of environmental contamination and toxicology, *Springer*, 2005, pp. 97-149.
- [86] Donat, J. & Dryden, C. Transition metals and heavy metal speciation. In: Marine chemistry and geochemistry, Turekian, K.K., Steele, J., Thorpe, S. Eds., *Elsevier*, 2010.
- [87] Cutter, G.A. Metalloids and oxyanions. In: Marine chemistry and geochemistry, Turekian, K.K., Steele, J., Thorpe, S. Eds., *Elsevier*, 2010.
- [88] Jan, A.T., Azam, M., Siddiqui, K., Ali, A., Choi, I. & Haq, Q.M. Heavy metals and human health: mechanistic insight into toxicity and counter defense system of antioxidants. *International Journal of Molecular Sciences*. 2015, (16), 29592-29630. DOI:10.3390/ijms161226183.
- [89] Chakraborti, D. Arsenic: Occurance in Groundwater. In: Encyclopedia of environmental health, Nriagu, J.O. Ed., *Elsevier*, 2019.
- [90] Wu, X., Cobbina, S.J., Mao, G., Xu, H., Zhang, Z. & Yang, L. A review of toxicity and mechanisms of individual and mixtures of heavy metals in the environment. *Environmental Science and Pollution Research*. 2016, (23), 8244-8259. DOI:10.1007/s11356-016-6333-x.
- [91] Keith, L.S., Faroon, O.M. & Fowler, B.A. Uranium. In: Handbook on the Toxicology of Metals, Nordberg, G.F., Fowler, B.A., Nordberg, M. Eds., *Academic press*, 2014.
- [92] Paunesku, T. & Woloschak, G.E. Genome effects and mutational risk of radiation. In: Encyclopedia of environmental health, Nriagu, J.O. Ed., *Elsevier*, 2019.
- [93] Goulet, R.R., Fortin, C. & Spry, D.J. Uranium. In: Homeostasis and Toxicology of Non-Essential Metals, Wood, C.M., Farrell, A.P., Brauner, C.J. Eds., 2012.
- [94] Galhardi, J.A., Bonotto, D.M., Erismann, C.E. & da Silva, Y.J.A.B. Biogeochemistry of Uranium in Tropical Environment. In: Uranium in Plants and the Environment, Gupta, D.K., Walther, C. Eds., *Springer* 2020.
- [95] Karpas, Z. Exposure, Toxicity and Biomonitoring of Uranium Exposure. In: Analytical chemistry of uranium: environmental, forensic, nuclear, and toxicological applications, *CRC press* 2014.
- [96] Agency for Toxic Substances and Disease Registry (ATSDR). Toxicological profile for uranium, *Atlanta, GA: U.S. Department of Health and Human Services, Public Health Service*, 2013.

- [97] Miller, A.C., Stewart, M., Brooks, K., Shi, L. & Page, N. Depleted uranium-catalyzed oxidative DNA damage: absence of significant alpha particle decay. *Journal of Inorganic Biochemistry*. 2002, (91), 246-252. DOI:10.1016/s0162-0134(02)00391-4.
- [98] Rump, A., Eder, S., Lamkowski, A., Hermann, C., Abend, M. & Port, M. A quantitative comparison of the chemo-and radiotoxicity of uranium at different enrichment grades. *Toxicology Letters*. 2019, (313), 159-168. DOI:10.1016/j.toxlet.2019.07.004.
- [99] Singhal, R., Preetha, J., Karpe, R., Tirumalesh, K., Kumar, S. & Hegde, A. The use of ultra filtration in trace metal speciation studies in sea water. *Environment International*. 2006, (32), 224-228. DOI:10.1016/j.envint.2005.08.015.
- [100] Monteiro, A.S.C., Parat, C., Rosa, A.H. & Pinheiro, J.P. Towards field trace metal speciation using electroanalytical techniques and tangential ultrafiltration. *Talanta*. 2016, (152), 112-118. DOI:10.1016/j.talanta.2016.01.053.
- [101] John, D.A. & Leventhal, J.S. Bioavailability of metals. In: Preliminary compilation of descriptive geoenvironmental mineral deposit models, Du Bray, E.A. Ed., *US Geological Survey Denver, CO*, 1995.
- [102] Filgueiras, A., Lavilla, I. & Bendicho, C. Chemical sequential extraction for metal partitioning in environmental solid samples. *Journal of Environmental Monitoring*. 2002, (4), 823-857. DOI:10.1039/B207574C.
- [103] Gleyzes, C., Tellier, S. & Astruc, M. Fractionation studies of trace elements in contaminated soils and sediments: a review of sequential extraction procedures. *Trends in Analytical Chemistry*. 2002, (21), 451-467. DOI:10.1016/S0165-9936(02)00603-9.
- [104] Tessier, A., Campbell, P.G. & Bisson, M. Sequential extraction procedure for the speciation of particulate trace metals. *Analytical Chemistry*. 1979, (51), 844-851. DOI:10.1021/ac50043a017.
- [105] Ure, A., Quevauviller, P., Muntau, H. & Griepink, B. Speciation of heavy metals in soils and sediments. An account of the improvement and harmonization of extraction techniques undertaken under the auspices of the BCR of the Commission of the European Communities. *International Journal of Environmental Analytical Chemistry*. 1993, (51), 135-151. DOI:10.1080/03067319308027619.
- [106] Vutchev, M. & Lalor, G. Inorganic and organic geochemistry techniques. In: Essentials of medical geology: Impacts of the natural environment on public health, Selinus, O. Ed., *Springer*, 2005.

- [107] Companys, E., Galceran, J., Pinheiro, J., Puy, J. & Salaün, P. A review on electrochemical methods for trace metal speciation in environmental media. *Current Opinion in Electrochemistry*. 2017, (3), 144-162. DOI:10.1016/j.coelec.2017.09.007.
- [108] Mota, A., Pinheiro, J. & Simões Gonçalves, M. Electrochemical methods for speciation of trace elements in marine waters. Dynamic aspects. *The Journal of Physical Chemistry A*. 2012, (116), 6433-6442. DOI:10.1021/jp2124636.
- [109] Cindrić, A.-M., Marcinek, S., Garnier, C., Salaün, P., Cukrov, N., Oursel, B., Lenoble, V. & Omanović, D. Evaluation of diffusive gradients in thin films (DGT) technique for speciation of trace metals in estuarine waters-A multimethodological approach. *Science of the Total Environment*. 2020, (721), 137784. DOI:10.1016/j.scitotenv.2020.137784.
- [110] Degryse, F. & Smolders, E. DGT and Bioavailability. In: Diffusive gradients in thin-films for environmental measurements, Davison, W. Ed., *Cambridge University Press* 2016.
- [111] Sans-Duñó, J., Cecilia, J., Galceran, J. & Puy, J. Availability of metals to DGT devices with different configurations. The case of sequential Ni complexation. *Science of the Total Environment*. 2021, (779), 146277. DOI:10.1016/j.scitotenv.2021.146277.
- [112] Van Leeuwen, H.P., Town, R.M., Buffle, J., Cleven, R.F., Davison, W., Puy, J., van Riemsdijk, W.H. & Sigg, L. Dynamic speciation analysis and bioavailability of metals in aquatic systems. *Environmental Science & Technology*. 2005, (39), 8545-8556. DOI:10.1021/es050404x.
- [113] Morabito, R. Extraction techniques in speciation analysis of environmental samples. *Fresenius' Journal of Analytical Chemistry*. 1995, (351), 378-385. DOI:10.1007/BF00322906.
- [114] Cornelis, R. & Nordberg, M. General Chemistry, Sampling, Analytical Methods and Speciation. In: Handbook on the Toxicology of Metals, Nordberg, G.F., Fowler, B.A., Nordberg, M. Eds., *Academic press*, 2014.
- [115] Krasnodębska-Ostręga, B., Sadowska, M. & Biaduń, E. Sample Pretreatment for Trace Speciation Analysis. *Physical Sciences Reviews*. 2017, (2). DOI:10.1515/psr-2017-8005.
- [116] Grotti, M., Terol, A. & Todoli, J. Speciation analysis by small-bore HPLC coupled to ICP-MS. *Trends in Analytical Chemistry*. 2014, (61), 92-106. DOI:10.1016/j.trac.2014.06.009.
- [117] Liu, Y.M. & Cheng, J.K. Elemental speciation analysis in capillary electrophoresis. *Electrophoresis*. 2003, (24), 1993-2012. DOI:10.1002/elps.200305409.

- [118] Terlecka, E. Arsenic speciation analysis in water samples: A review of the hyphenated techniques. *Environmental Monitoring and Assessment*. 2005, (107), 259-284. DOI:10.1007/s10661-005-3109-z.
- [119] Shraim, A., Chiswell, B. & Olszowy, H. Speciation of arsenic by hydride generation–atomic absorption spectrometry (HG–AAS) in hydrochloric acid reaction medium. *Talanta*. 1999, (50), 1109-1127. DOI:10.1016/s0039-9140(99)00221-0.
- [120] Houserová, P., Matějček, D., Kubáň, V., Pavlíčková, J. & Komárek, J. Liquid chromatographic–cold vapour atomic fluorescence spectrometric determination of mercury species. *Journal of Separation Science*. 2006, (29), 248-255. DOI:10.1002/jssc.200500300.
- [121] Cerveira, C., Pozebon, D., de Moraes, D.P. & de Fraga, J.C.S. Speciation of inorganic arsenic in rice using hydride generation atomic absorption spectrometry (HG–AAS). *Analytical Methods*. 2015, (7), 4528-4534. DOI:10.1039/C5AY00563A.
- [122] Harrington, C.F. The speciation of mercury and organomercury compounds by using high-performance liquid chromatography. *Trends in Analytical Chemistry*. 2000, (19), 167-179. DOI:10.1016/S0165-9936(99)00190-9.
- [123] Feldmann, J., Salaün, P. & Lombi, E. Critical review perspective: elemental speciation analysis methods in environmental chemistry–moving towards methodological integration. *Environmental Chemistry*. 2009, (6), 275-289. DOI:10.1071/EN09018.
- [124] Santos, J.S., Teixeira, L.S., Dos Santos, W.N., Lemos, V.A., Godoy, J.M. & Ferreira, S.L. Uranium determination using atomic spectrometric techniques: an overview. *Analytica Chimica Acta*. 2010, (674), 143-156. DOI:10.1016/j.aca.2010.06.010.
- [125] Perkin Elmer. Atomic Spectroscopy: A guide to selecting the appropriate technique and system. https://www.perkinelmer.com/lab-solutions/resources/docs/BRO_WorldLeaderAAICPMSICPMS.pdf. [cited 14/11/2020].
- [126] Thermo Elemental. AAS, GFAAS, ICP or ICP-MS? Which technique should I use?: An elementary overview of element analysis. <https://oliver.chemistry.ucsc.edu/122/Lab5%20Handout.pdf>. [cited 14/11/2020].
- [127] Westall, J., Zachary, J. & Morel, F. MINEQL: A computer program for the calculation of chemical equilibrium composition of aqueous systems. Technical note. MIT: Cambridge, MA, 1976.
- [128] Allison, J.D., Brown, D.S. & Novo-Gradac, K.J. MINTEQA2/PRODEFA2: A geochemical assessment model for environmental systems: version 3.0 user's manual,

Environmental Research Laboratory, Office of Research and Development, US Environmental Protection Agency, 1991.

[129] Parkhurst, D.L. & Appelo, C. User's guide to PHREEQC (Version 2): A computer program for speciation, batch-reaction, one-dimensional transport, and inverse geochemical calculations. *Water-Resources Investigations Report*. 1999, (99), 312. DOI:10.3133/wri994259.

[130] Van der Lee, J. Thermodynamic and mathematical concepts of CHESS. MINES ParisTech, 1998.

[131] Bethke, C. Geochemical reaction modeling: Concepts and applications, *Oxford University Press*, 1996.

[132] Puigdomènech, I. MEDUSA and HYDRA: Software for Chemical Equilibrium Calculations. Royal Institute of Technology, Stockholm, Sweden, 2004.

[133] Tipping, E. WHAMC-A chemical equilibrium model and computer code for waters, sediments, and soils incorporating a discrete site/electrostatic model of ion-binding by humic substances. *Computers & Geosciences*. 1994, (20), 973-1024. DOI:10.1016/0098-3004(94)90038-8.

[134] Zhu, C. & Anderson, G. Computer Programs for Geochemical Modeling. In: Environmental applications of geochemical modeling, *Cambridge University Press*, 2002.

[135] Wanner, H. The NEA Thermochemical Data Base Project. *Radiochimica Acta*. 1988, (44), 325-330. DOI:10.1524/ract.1988.4445.2.325.

[136] Delany, J. & Lundeen, S. The LLNL thermodynamic database. *Lawrence Livermore National Laboratory Report UCRL-21658*. Lawrence Livermore National Laboratory, Livermore, California, USA. 1990.

[137] Giffaut, E., Grivé, M., Blanc, P., Vieillard, P., Colàs, E., Gailhanou, H., Gaboreau, S., Marty, N., Made, B. & Duro, L. Andra thermodynamic database for performance assessment: ThermoChimie. *Applied Geochemistry*. 2014, (49), 225-236. DOI:10.1016/j.apgeochem.2014.05.007.

[138] Reiller, P.E. & Descostes, M. Development and application of the thermodynamic database PRODATA dedicated to the monitoring of mining activities from exploration to remediation. *Chemosphere*. 2020, 126301. DOI:10.1016/j.chemosphere.2020.126301.

[139] Morel, F. Principles of aquatic chemistry, *Wiley New York*, 1983.

- [140] Smith, K.S., Balistrieri, L.S. & Todd, A.S. Using biotic ligand models to predict metal toxicity in mineralized systems. *Applied Geochemistry*. 2015, (57), 55-72. DOI:10.1016/j.apgeochem.2014.07.005.
- [141] Pagenkopf, G.K. Gill surface interaction model for trace-metal toxicity to fishes: role of complexation, pH, and water hardness. *Environmental Science & Technology*. 1983, (17), 342-347. DOI:10.1021/es00112a007.
- [142] Hassler, C.S., Slaveykova, V.I. & Wilkinson, K. Some fundamental (and often overlooked) considerations underlying the free ion activity and biotic ligand models. *Environmental Toxicology and Chemistry*. 2004, (23), 283-291. DOI:10.1897/03-149.
- [143] Campbell, P.G., Errécalde, O., Fortin, C., Hiriart-Baer, V.P. & Vigneault, B. Metal bioavailability to phytoplankton—applicability of the biotic ligand model. *Comparative Biochemistry and Physiology Part C: Toxicology & Pharmacology*. 2002, (133), 189-206. DOI:10.1016/S1532-0456(02)00104-7.
- [144] Hesslein, R.H. An in situ sampler for close interval pore water studies. *Limnology and Oceanography*. 1976, (21), 912-914. DOI:10.4319/lo.1976.21.6.0912.
- [145] Bailon, M.X., Park, M.-o. & Hong, Y. Passive sampling methods for assessing the bioaccumulation of heavy metals in sediments. *Current Pollution Reports*. 2019, (5), 129-143. DOI:10.1007/s40726-019-00111-w.
- [146] Teasdale, P.R., Batley, G.E., Apte, S.C. & Webster, I.T. Pore water sampling with sediment peepers. *Trends in Analytical Chemistry*. 1995, (14), 250-256. DOI:10.1016/0165-9936(95)91617-2.
- [147] Davison, W. & Zhang, H. Introduction to DGT. In: Diffusive gradients in thin-films for environmental measurements, Davison, W. Ed., *Cambridge University Press* 2016.
- [148] Peijnenburg, W.J., Teasdale, P.R., Reible, D., Mondon, J., Bennett, W.W. & Campbell, P.G. Passive sampling methods for contaminated sediments: State of the science for metals. *Integrated Environmental Assessment and Management*. 2014, (10), 179-196. DOI:10.1002/ieam.1502.
- [149] Davison, W., Grime, G., Morgan, J. & Clarke, K. Distribution of dissolved iron in sediment pore waters at submillimetre resolution. *Nature*. 1991, (352), 323-325. DOI:10.1038/352323a0.
- [150] Gao, Y., Leermakers, M., Elskens, M., Billon, G., Ouddane, B., Fischer, J.-C. & Baeyens, W. High resolution profiles of thallium, manganese and iron assessed by DET and DGT techniques in riverine sediment pore waters. *Science of the Total Environment*. 2007, (373), 526-533. DOI:10.1016/j.scitotenv.2006.11.047.

- [151] Dočekalová, H., Clarisse, O., Salomon, S. & Wartel, M. Use of constrained DET probe for a high-resolution determination of metals and anions distribution in the sediment pore water. *Talanta*. 2002, (57), 145-155. DOI:10.1016/S0039-9140(01)00679-8.
- [152] Temminghoff, E.J., Plette, A.C., Van Eck, R. & Van Riemsdijk, W.H. Determination of the chemical speciation of trace metals in aqueous systems by the Wageningen Donnan Membrane Technique. *Analytica Chimica Acta*. 2000, (417), 149-157. DOI:10.1016/S0003-2670(00)00935-1.
- [153] Donnan, F.G. cc. *Chemical Reviews*. 1924, (1), 73-90. DOI:10.1021/cr60001a003.
- [154] Cox, J.A., Slonawska, K., Gatchell, D.K. & Hiebert, A.G. Metal speciation by Donnan dialysis. *Analytical Chemistry*. 1984, (56), 650-653. DOI:10.1021/ac00268a014.
- [155] Vega, F.A., Weng, L., Temminghoff, E.J. & van Riemsdijk, W.H. Donnan Membrane Technique (DMT) for Anion Measurement. *Analytical Chemistry*. 2010, (82), 2932–2939. DOI:10.1021/ac9029339.
- [156] Fitch, A. & Helmke, P.A. Donnan equilibrium/graphite furnace atomic absorption estimates of soil extract complexation capacities. *Analytical Chemistry*. 1989, (61), 1295-1298. DOI:10.1021/AC00186A023.
- [157] Weng, L., Vega, F.A. & Van Riemsdijk, W.H. Strategies in the application of the Donnan membrane technique. *Environmental Chemistry*. 2011, (8), 466-474. DOI:10.1071/EN11021.
- [158] Pan, Y., Koopmans, G.F., Bonten, L.T., Song, J., Luo, Y., Temminghoff, E.J. & Comans, R.N. In-situ measurement of free trace metal concentrations in a flooded paddy soil using the Donnan Membrane Technique. *Geoderma*. 2015, (241), 59-67. DOI:10.1016/j.geoderma.2014.11.003.
- [159] Kalis, E.J., Weng, L., Dousma, F., Temminghoff, E.J. & Van Riemsdijk, W.H. Measuring free metal ion concentrations in situ in natural waters using the Donnan membrane technique. *Environmental Science & Technology*. 2006, (40), 955-961. DOI:10.1021/es051435v.
- [160] Parat, C. & Pinheiro, J. ISIDORE, a probe for in situ trace metal speciation based on Donnan membrane technique with related electrochemical detection part 1: Equilibrium measurements. *Analytica Chimica Acta*. 2015, (896), 1-10. DOI:10.1016/j.aca.2015.07.016.

- [161] Senn, D.B., Griscom, S.B., Lewis, C.G., Galvin, J.P., Chang, M.W. & Shine, J.P. Equilibrium-based sampler for determining Cu²⁺ concentrations in aquatic ecosystems. *Environmental Science & Technology*. 2004, (38), 3381-3386. DOI:10.1021/es0353614.
- [162] Dong, Z., Lewis, C.G., Burgess, R.M. & Shine, J.P. The Gellyfish: An in situ equilibrium-based sampler for determining multiple free metal ion concentrations in marine ecosystems. *Environmental Toxicology and Chemistry*. 2015, (34), 983-992. DOI:10.1002/etc.2893.
- [163] Pesavento, M., Alberti, G. & Biesuz, R. Analytical methods for determination of free metal ion concentration, labile species fraction and metal complexation capacity of environmental waters: a review. *Analytica Chimica Acta*. 2009, (631), 129-141. DOI:10.1016/j.aca.2008.10.046.
- [164] Parthasarathy, N. & Buffle, J. Capabilities of supported liquid membranes for metal speciation in natural waters: application to copper speciation. *Analytica Chimica Acta*. 1994, (284), 649-659. DOI:10.1016/0003-2670(94)85069-0.
- [165] Bayen, S., Wilkinson, K.J. & Buffle, J. The permeation liquid membrane as a sensor for free nickel in aqueous samples. *Analyst*. 2007, (132), 262-267. DOI:10.1039/b615298h.
- [166] Unsworth, E.R., Warnken, K.W., Zhang, H., Davison, W., Black, F., Buffle, J., Cao, J., Cleven, R., Galceran, J. & Gunkel, P. Model predictions of metal speciation in freshwaters compared to measurements by in situ techniques. *Environmental Science & Technology*. 2006, (40), 1942-1949. DOI:10.1021/es051246c.
- [167] Gramlich, A., Tandy, S., Slaveykova, V.I., Duffner, A. & Schulin, R. The use of permeation liquid membranes for free zinc measurements in aqueous solution. *Environmental Chemistry*. 2012, (9), 429-437. DOI:10.1071/EN12103.
- [168] Parthasarathy, N., Pelletier, M. & Buffle, J. Permeation liquid membrane for trace metal speciation in natural waters: Transport of liposoluble Cu (II) complexes. *Journal of Chromatography A*. 2004, (1025), 33-40. DOI:10.1016/j.chroma.2003.10.083.
- [169] Kingston, J.K., Greenwood, R., Mills, G.A., Morrison, G.M. & Persson, L.B. Development of a novel passive sampling system for the time-averaged measurement of a range of organic pollutants in aquatic environments. *Journal of Environmental Monitoring*. 2000, (2), 487-495. DOI:10.1039/b003532g.
- [170] Allan, I.J., Knutsson, J., Guigues, N., Mills, G.A., Fouillac, A.-M. & Greenwood, R. Chemcatcher® and DGT passive sampling devices for regulatory monitoring of trace metals in surface water. *Journal of Environmental Monitoring*. 2008, (10), 821-829. DOI:10.1039/b802581a.

- [171] Allan, I.J., Knutsson, J., Guigues, N., Mills, G.A., Fouillac, A.-M. & Greenwood, R. Evaluation of the Chemcatcher and DGT passive samplers for monitoring metals with highly fluctuating water concentrations. *Journal of Environmental Monitoring*. 2007, (9), 672-681. DOI:10.1039/b701616f.
- [172] Aguilar-Martínez, R., Gómez-Gómez, M.M. & Palacios-Corvillo, M.A. Mercury and organotin compounds monitoring in fresh and marine waters across Europe by Chemcatcher passive sampler. *International Journal of Environmental Analytical Chemistry*. 2011, (91), 1100-1116. DOI:10.1080/03067310903199534.
- [173] Vrana, B., Allan, I.J., Greenwood, R., Mills, G.A., Dominiak, E., Svensson, K., Knutsson, J. & Morrison, G. Passive sampling techniques for monitoring pollutants in water. *Trends in Analytical Chemistry*. 2005, (24), 845-868. DOI:10.1016/j.trac.2005.06.006.
- [174] Gaulier, C., Zhou, C., Guo, W., Bratkic, A., Superville, P.-J., Billon, G., Baeyens, W. & Gao, Y. Trace metal speciation in North Sea coastal waters. *Science of the Total Environment*. 2019, (692), 701-712. DOI:10.1016/j.scitotenv.2019.07.314.
- [175] Ren, M., Ding, S., Shi, D., Zhong, Z., Cao, J., Yang, L., Tsang, D.C., Wang, D., Zhao, D. & Wang, Y. A new DGT technique comprised in a hybrid sensor for the simultaneous measurement of ammonium, nitrate, phosphorus and dissolved oxygen. *Science of the Total Environment*. 2020, 138447. DOI:10.1016/j.scitotenv.2020.138447.
- [176] Panther, J.G., Stewart, R.R., Teasdale, P.R., Bennett, W.W., Welsh, D.T. & Zhao, H. Titanium dioxide-based DGT for measuring dissolved As (V), V (V), Sb (V), Mo (VI) and W (VI) in water. *Talanta*. 2013, (105), 80-86. DOI:10.1016/j.talanta.2012.11.070.
- [177] Huang, J., Bennett, W.W., Teasdale, P.R., Kankanamge, N.R. & Welsh, D.T. A modified DGT technique for the simultaneous measurement of dissolved inorganic nitrogen and phosphorus in freshwaters. *Analytica Chimica Acta*. 2017, (988), 17-26. DOI:10.1016/j.aca.2017.08.024.
- [178] Feng, Z., Wang, N., He, M., Yang, L., Wang, Y. & Sun, T. Simultaneous sampling of dissolved orthophosphate and ammonium in freshwaters using diffusive gradients in thin films with a mixed binding phase. *Talanta*. 2018, (186), 176-182. DOI:10.1016/j.talanta.2018.04.045.
- [179] Chang, L.-Y., Davison, W., Zhang, H. & Kelly, M. Performance characteristics for the measurement of Cs and Sr by diffusive gradients in thin films (DGT). *Analytica Chimica Acta*. 1998, (368), 243-253. DOI:10.1016/S0003-2670(98)00215-3.
- [180] Drozdak, J., Leermakers, M., Gao, Y., Phrommavanh, V. & Descostes, M. Evaluation and application of Diffusive Gradients in Thin Films (DGT) technique using

Chelex®-100, Metsorb™ and Diphonix® binding phases in uranium mining environments. *Analytica Chimica Acta*. 2015, (889), 71-81. DOI:10.1016/j.aca.2015.07.057.

[181] Leermakers, M., Gao, Y., Navez, J., Poffijn, A., Croes, K. & Baeyens, W. Radium analysis by sector field ICP-MS in combination with the Diffusive Gradients in Thin Films (DGT) technique. *Journal of Analytical Atomic Spectrometry*. 2009, (24), 1115-1117. DOI:10.1039/B821472G.

[182] Murdock, C., Kelly, M., Chang, L.-Y., Davison, W. & Zhang, H. DGT as an in situ tool for measuring radiocesium in natural waters. *Environmental Science & Technology*. 2001, (35), 4530-4535. DOI:10.1021/es0100874.

[183] Cusnir, R., Steinmann, P., Bochud, F.o. & Froidevaux, P. A DGT technique for plutonium bioavailability measurements. *Environmental Science & Technology*. 2014, (48), 10829-10834. DOI:10.1021/es501149v.

[184] French, M.A., Zhang, H., Pates, J.M., Bryan, S.E. & Wilson, R.C. Development and performance of the diffusive gradients in thin-films technique for the measurement of technetium-99 in seawater. *Analytical Chemistry*. 2005, (77), 135-139. DOI:10.1021/ac048774b.

[185] Abdulbur-Alfakhoury, E., Van Zutphen, S. & Leermakers, M. Development of the diffusive gradients in thin films technique (DGT) for platinum (Pt), palladium (Pd), and rhodium (Rh) in natural waters. *Talanta*. 2019, (203), 34-48. DOI:10.1016/j.talanta.2019.05.038.

[186] Abdulbur-Alfakhoury, E., Trommetter, G., Brion, N., Dumoulin, D., Reichstädter, M., Billon, G., Leermakers, M. & Baeyens, W. Distribution of platinum (Pt), palladium (Pd), and rhodium (Rh) in urban tributaries of the Scheldt River assessed by diffusive gradients in thin films technique (DGT). *Science of the Total Environment*. 2021, (784), 147075. DOI:10.1016/j.scitotenv.2021.147075.

[187] Trommetter, G., Dumoulin, D. & Billon, G. Development and validation of DGT passive samplers for the quantification of Ir, Pd, Pt, Rh and Ru: A challenging application in waters impacted by urban activities. *Talanta*. 2021, (223), 121707. DOI:10.1016/j.talanta.2020.121707.

[188] Ding, S., Xu, D., Wang, Y., Wang, Y., Li, Y., Gong, M. & Zhang, C. Simultaneous measurements of eight oxyanions using high-capacity diffusive gradients in thin films (Zr-oxide DGT) with a high-efficiency elution procedure. *Environmental Science & Technology*. 2016, (50), 7572-7580. DOI:10.1021/acs.est.6b00206.

[189] Price, H.L., Teasdale, P.R. & Jolley, D.F. An evaluation of ferrihydrite-and Metsorb™-DGT techniques for measuring oxyanion species (As, Se, V, P): Effective

capacity, competition and diffusion coefficients. *Analytica Chimica Acta*. 2013, (803), 56-65. DOI:10.1016/j.aca.2013.07.001.

[190] Österlund, H., Chlot, S., Faarinen, M., Widerlund, A., Rodushkin, I., Ingri, J. & Baxter, D.C. Simultaneous measurements of As, Mo, Sb, V and W using a ferrihydrite diffusive gradients in thin films (DGT) device. *Analytica Chimica Acta*. 2010, (682), 59-65. DOI:10.1016/j.aca.2010.09.049.

[191] Li, K., Liu, Z., Shi, X., Wei, T.-j., Ma, L.Q. & Luo, J. Novel in situ method based on diffusive gradients in thin-films with lanthanum oxide nanoparticles for measuring As, Sb, and V and in waters. *Journal of Hazardous Materials*. 2020, (383), 121196. DOI:10.1016/j.jhazmat.2019.121196.

[192] Yuan, Y., Ding, S., Wang, Y., Zhang, L., Ren, M. & Zhang, C. Simultaneous measurement of fifteen rare earth elements using diffusive gradients in thin films. *Analytica Chimica Acta*. 2018, (1031), 98-107. DOI:10.1016/j.aca.2018.05.067.

[193] Alakangas, L.J., Mathurin, F.A. & Åström, M. Diverse fractionation patterns of Rare Earth Elements in deep fracture groundwater in the Baltic Shield–Progress from utilisation of Diffusive Gradients in Thin-films (DGT) at the Äspö Hard Rock Laboratory. *Geochimica et Cosmochimica Acta*. 2020, (269), 15-38. DOI:10.1016/j.gca.2019.10.026.

[194] Li, C., Ding, S., Yang, L., Wang, Y., Ren, M., Chen, M., Fan, X. & Lichtfouse, E. Diffusive gradients in thin films: devices, materials and applications. *Environmental Chemistry Letters*. 2018, 1-31. DOI:10.1007/s10311-018-00839-9.

[195] Reichstädter, M., Divis, P., Alfakhoury, E.A. & Gao, Y. Simultaneous determination of mercury, cadmium and lead in fish sauce using Diffusive Gradients in Thin-films technique. *Talanta*. 2020, 121059. DOI:10.1016/j.talanta.2020.121059.

[196] Chen, H., Guo, L., Zhang, M., Gu, J., Zhong, K., Bo, L. & Li, J. Determination of lead in soybean sauces by the diffusive gradients in thin films technique. *Food Chemistry*. 2014, (165), 9-13. DOI:10.1016/j.foodchem.2014.05.105.

[197] Scally, S., Davison, W. & Zhang, H. In situ measurements of dissociation kinetics and labilities of metal complexes in solution using DGT. *Environmental Science & Technology*. 2003, (37), 1379-1384. DOI:10.1021/es0202006.

[198] Davison, W. & Zhang, H. Principles of measurements in simple solutions. In: Diffusive gradients in thin-films for environmental measurements, Davison, W. Ed., *Cambridge University Press* 2016.

[199] Baeyens, W., Gao, Y., Davison, W., Galceran, J., Leermakers, M., Puy, J., Superville, P.-J. & Beguery, L. In situ measurements of micronutrient dynamics in open

seawater show that complex dissociation rates may limit diatom growth. *Scientific Reports*. 2018, (8), 1-11. DOI:10.1038/s41598-018-34465-w.

[200] Davison, W. & Zhang, H. Progress in understanding the use of diffusive gradients in thin films (DGT)–back to basics. *Environmental Chemistry*. 2012, (9), 1-13. DOI:10.1071/EN11084.

[201] Davison, W. & Zhang, H. Diffusion layer properties. In: Diffusive gradients in thin-films for environmental measurements, Davison, W. Ed., *Cambridge University Press* 2016.

[202] Pichette, C., Zhang, H., Davison, W. & Sauvé, S. Preventing biofilm development on DGT devices using metals and antibiotics. *Talanta*. 2007, (72), 716-722. DOI:10.1016/j.talanta.2006.12.014.

[203] Uher, E., Zhang, H., Santos, S., Tusseau-Vuillemin, M.-H.I.n. & Gourlay-Francé, C. Impact of biofouling on diffusive gradient in thin film measurements in water. *Analytical Chemistry*. 2012, (84), 3111-3118. DOI:10.1021/ac2028535.

[204] Pelcová, P., Dočekalová, H. & Kleckerová, A. Determination of mercury species by the diffusive gradient in thin film technique and liquid chromatography–atomic fluorescence spectrometry after microwave extraction. *Analytica Chimica Acta*. 2015, (866), 21-26. DOI:10.1016/j.aca.2015.01.043.

[205] Dočekalová, H. & Diviš, P. Application of diffusive gradient in thin films technique (DGT) to measurement of mercury in aquatic systems. *Talanta*. 2005, (65), 1174-1178. DOI:10.1016/j.talanta.2004.08.054.

[206] Diviš, P., Leermakers, M., Dočekalová, H. & Gao, Y. Mercury depth profiles in river and marine sediments measured by the diffusive gradients in thin films technique with two different specific resins. *Analytical and Bioanalytical Chemistry*. 2005, (382), 1715-1719. DOI:10.1007/s00216-005-3360-8.

[207] Reichstädter, M., Gao, Y., Diviš, P., Ma, T., Gaulier, C. & Leermakers, M. Cysteine-modified silica resin in DGT samplers for mercury and trace metals assessment. *Chemosphere*. 2021, (263), 128320. DOI:10.1016/j.chemosphere.2020.128320.

[208] Shiva, A.H., Teasdale, P.R., Bennett, W.W. & Welsh, D.T. A systematic determination of diffusion coefficients of trace elements in open and restricted diffusive layers used by the diffusive gradients in a thin film technique. *Analytica Chimica Acta*. 2015, (888), 146-154. DOI:10.1016/j.aca.2015.07.027.

[209] Li, W., Teasdale, P.R., Zhang, S., John, R. & Zhao, H. Application of a poly (4-styrenesulfonate) liquid binding layer for measurement of Cu²⁺ and Cd²⁺ with the

diffusive gradients in thin-films technique. *Analytical Chemistry*. 2003, (75), 2578-2583. DOI:10.1021/ac020658q.

[210] Blom, L.B., Morrison, G.M., Roux, M.S., Mills, G. & Greenwood, R. Metal diffusion properties of a Nafion-coated porous membrane in an aquatic passive sampler system. *Journal of Environmental Monitoring*. 2003, (5), 404-409. DOI:10.1039/B107959J.

[211] Persson, L.B., Morrison, G.M., Friemann, J.-U., Kingston, J., Mills, G. & Greenwood, R. Diffusional behaviour of metals in a passive sampling system for monitoring aquatic pollution. *Journal of Environmental Monitoring*. 2001, (3), 639-645. DOI:10.1039/B107959J.

[212] Panther, J.G., Stillwell, K.P., Powell, K.J. & Downard, A.J. Perfluorosulfonated ionomer-modified diffusive gradients in thin films: tool for inorganic arsenic speciation analysis. *Analytical Chemistry*. 2008, (80), 9806-9811. DOI:10.1021/ac801678u.

[213] Larner, B.L. & Seen, A.J. Evaluation of paper-based diffusive gradients in thin film samplers for trace metal sampling. *Analytica Chimica Acta*. 2005, (539), 349-355. DOI:10.1016/j.aca.2005.03.007.

[214] de Almeida, E., do Nascimento Filho, V.F. & Menegário, A.A. Paper-based diffusive gradients in thin films technique coupled to energy dispersive X-ray fluorescence spectrometry for the determination of labile Mn, Co, Ni, Cu, Zn and Pb in river water. *Spectrochimica Acta Part B: Atomic Spectroscopy*. 2012, (71), 70-74. DOI:10.1016/j.sab.2012.05.006.

[215] de Oliveira, W., de Carvalho, M.d.F.B., de Almeida, E., Menegário, A.A., Domingos, R.N., Brossi-Garcia, A.L., do Nascimento Filho, V.F. & Santelli, R.E. Determination of labile barium in petroleum-produced formation water using paper-based DGT samplers. *Talanta*. 2012, (100), 425-431. DOI:10.1016/j.talanta.2012.08.013.

[216] Liu, S., Qin, N., Song, J., Zhang, Y., Cai, W., Zhang, H., Wang, G. & Zhao, H. A nanoparticulate liquid binding phase based DGT device for aquatic arsenic measurement. *Talanta*. 2016, (160), 225-232. DOI:10.1016/j.talanta.2016.06.064.

[217] Fan, H.-T., Liu, J.-X., Sui, D.-P., Yao, H., Yan, F. & Sun, T. Use of polymer-bound Schiff base as a new liquid binding agent of diffusive gradients in thin-films for the measurement of labile Cu²⁺, Cd²⁺ and Pb²⁺. *Journal of Hazardous Materials*. 2013, (260), 762-769. DOI:10.1016/j.jhazmat.2013.05.049.

[218] Fan, H.-T., Sun, T., Li, W., Sui, D., Jin, S. & Lian, X. Sodium polyacrylate as a binding agent in diffusive gradients in thin-films technique for the measurement of Cu²⁺

and Cd²⁺ in waters. *Talanta*. 2009, (79), 1228-1232. DOI:10.1016/j.talanta.2009.04.049.

[219] Li, W., Zhao, H., Teasdale, P.R. & Wang, F. Trace metal speciation measurements in waters by the liquid binding phase DGT device. *Talanta*. 2005, (67), 571-578. DOI:10.1016/j.talanta.2005.03.018.

[220] Sui, D.-P., Fan, H.-T., Li, J., Li, Y., Li, Q. & Sun, T. Application of poly (ethyleneimine) solution as a binding agent in DGT technique for measurement of heavy metals in water. *Talanta*. 2013, (114), 276-282. DOI:10.1016/j.talanta.2013.05.027.

[221] Bennett, W.W., Arsic, M., Panther, J.G., Welsh, D.T. & Teasdale, P.R. Binding layer properties. In: Diffusive gradients in thin-films for environmental measurements, Davison, W. Ed., *Cambridge University Press* 2016.

[222] Garmo, Ø.A., Røyset, O., Steinnes, E. & Flaten, T.P. Performance study of diffusive gradients in thin films for 55 elements. *Analytical Chemistry*. 2003, (75), 3573-3580. DOI:10.1021/ac026374n.

[223] Lucas, A.R., Reid, N., Salmon, S.U. & Rate, A.W. Quantitative assessment of the distribution of dissolved Au, As and Sb in groundwater using the diffusive gradients in thin films technique. *Environmental Science & Technology*. 2014, (48), 12141-12149. DOI:10.1021/es502468d.

[224] Rolisola, A.M., Suárez, C.A., Menegário, A.A., Gastmans, D., Kiang, C.H., Colaço, C.D., Garcez, D.L. & Santelli, R.E. Speciation analysis of inorganic arsenic in river water by Amberlite IRA 910 resin immobilized in a polyacrylamide gel as a selective binding agent for As (v) in diffusive gradient thin film technique. *Analyst*. 2014, (139), 4373-4380. DOI:10.1039/c4an00555d.

[225] Tan, F., Jiang, X., Qiao, X., Sun, D., Gao, J., Quan, X., Chen, J., Ren, S. & Wang, Y. Development of cerium oxide-based diffusive gradients in thin films technique for in-situ measurement of dissolved inorganic arsenic in waters. *Analytica Chimica Acta*. 2019, (1052), 65-72. DOI:10.1016/j.aca.2018.11.023.

[226] Luo, J., Zhang, H., Santner, J. & Davison, W. Performance characteristics of diffusive gradients in thin films equipped with a binding gel layer containing precipitated ferrihydrite for measuring arsenic (V), selenium (VI), vanadium (V), and antimony (V). *CA analytical chemistry*. 2010, (82), 8903-8909. DOI:10.1021/ac101676w.

[227] Moreno-Jimenez, E., Six, L., Williams, P.N. & Smolders, E. Inorganic species of arsenic in soil solution determined by microcartridges and ferrihydrite-based diffusive gradient in thin films (DGT). *Talanta*. 2013, (104), 83-89. DOI:10.1016/j.talanta.2012.11.007.

- [228] Panther, J.G., Stillwell, K.P., Powell, K.J. & Downard, A.J. Development and application of the diffusive gradients in thin films technique for the measurement of total dissolved inorganic arsenic in waters. *Analytica Chimica Acta*. 2008, (622), 133-142. DOI:10.1016/j.aca.2008.06.004.
- [229] Bennett, W.W., Teasdale, P.R., Panther, J.G., Welsh, D.T. & Jolley, D.F. New diffusive gradients in a thin film technique for measuring inorganic arsenic and selenium (IV) using a titanium dioxide based adsorbent. *Analytical Chemistry*. 2010, (82), 7401-7407. DOI:10.1021/ac101543p.
- [230] Sebutsoe, X., Chimuka, L., Tutu, H. & Cukrowska, E. Development and evaluation of a DGT sampler using functionalised cross-linked polyethyleimine for the monitoring of arsenic and selenium in mine impacted wetlands. *Chemosphere*. 2020, (In Press). DOI:10.1016/j.chemosphere.2020.128975.
- [231] Garnier, J.-M., Garnier, J., Jézéquel, D. & Angeletti, B. Using DET and DGT probes (ferrihydrite and titanium dioxide) to investigate arsenic concentrations in soil porewater of an arsenic-contaminated paddy field in Bangladesh. *Science of the Total Environment*. 2015, (536), 306-315. DOI:10.1016/j.scitotenv.2015.07.065.
- [232] Gorny, J., Lesven, L., Billon, G., Dumoulin, D., Noiriél, C., Pirovano, C. & Made, B. Determination of total arsenic using a novel Zn-ferrite binding gel for DGT techniques: Application to the redox speciation of arsenic in river sediments. *Talanta*. 2015, (144), 890-898. DOI:10.1016/j.talanta.2015.07.016.
- [233] Sun, Q., Chen, J., Zhang, H., Ding, S., Li, Z., Williams, P.N., Cheng, H., Han, C., Wu, L. & Zhang, C. Improved diffusive gradients in thin films (DGT) measurement of total dissolved inorganic arsenic in waters and soils using a hydrous zirconium oxide binding layer. *Analytical Chemistry*. 2014, (86), 3060-3067. DOI:10.1021/ac404025e.
- [234] Guan, D.-X., Williams, P.N., Luo, J., Zheng, J.-L., Xu, H.-C., Cai, C. & Ma, L.Q. Novel precipitated zirconia-based DGT technique for high-resolution imaging of oxyanions in waters and sediments. *Environmental Science & Technology*. 2015, (49), 3653-3661. DOI: 10.1021/es505424m.
- [235] Bennett, W.W., Teasdale, P.R., Panther, J.G., Welsh, D.T. & Jolley, D.F. Speciation of dissolved inorganic arsenic by diffusive gradients in thin films: selective binding of As(III) by 3-mercaptopropyl-functionalized silica gel. *Analytical Chemistry*. 2011, (83), 8293-8299. DOI:10.1021/ac202119t.
- [236] Li, W., Zhao, J., Li, C., Kiser, S. & Cornett, R.J. Speciation measurements of uranium in alkaline waters using diffusive gradients in thin films technique. *Analytica Chimica Acta*. 2006, (575), 274-280. DOI:10.1016/j.aca.2006.05.092.

- [237] Vandenhove, H., Antunes, K., Wannijn, J., Duquene, L. & Van Hees, M. Method of diffusive gradients in thin films (DGT) compared with other soil testing methods to predict uranium phytoavailability. *Science of the Total Environment*. 2007, (373), 542-555. DOI:10.1016/j.scitotenv.2006.12.023.
- [238] Turner, G.S., Mills, G.A., Burnett, J.L., Amos, S. & Fones, G.R. Evaluation of diffusive gradients in thin-films using a Diphonix® resin for monitoring dissolved uranium in natural waters. *Analytica Chimica Acta*. 2015, (854), 78-85. DOI:10.1016/j.aca.2014.11.023.
- [239] Li, W., Li, C., Zhao, J. & Cornett, R.J. Diffusive gradients in thin films technique for uranium measurements in river water. *Analytica Chimica Acta*. 2007, (592), 106-113. DOI:10.1016/j.aca.2007.04.012.
- [240] Turner, G.S., Mills, G.A., Teasdale, P.R., Burnett, J.L., Amos, S. & Fones, G.R. Evaluation of DGT techniques for measuring inorganic uranium species in natural waters: interferences, deployment time and speciation. *Analytica Chimica Acta*. 2012, (739), 37-46. DOI:10.1016/j.aca.2012.06.011.
- [241] Hutchins, C.M., Panther, J.G., Teasdale, P.R., Wang, F., Stewart, R.R., Bennett, W.W. & Zhao, H. Evaluation of a titanium dioxide-based DGT technique for measuring inorganic uranium species in fresh and marine waters. *Talanta*. 2012, (97), 550-556. DOI:10.1016/j.talanta.2012.05.012.
- [242] Drozdak, J., Leermakers, M., Gao, Y., Phommavanh, V. & Descostes, M. Novel speciation method based on Diffusive Gradients in Thin Films for in situ measurement of uranium in the vicinity of the former uranium mining sites. *Environmental Pollution*. 2016, (214), 114-123. DOI:10.1016/j.envpol.2016.04.004.
- [243] Gregusova, M. & Docekal, B. New resin gel for uranium determination by diffusive gradient in thin films technique. *Analytica Chimica Acta*. 2011, (684), 142-146. DOI:10.1016/j.aca.2010.11.002.
- [244] Gorny, J., Dumoulin, D., Alaimo, V., Lesven, L., Noiriél, C., Madé, B. & Billon, G. Passive sampler measurements of inorganic arsenic species in environmental waters: A comparison between 3-mercaptop-silica, ferrihydrite, Metsorb®, zinc ferrite, and zirconium dioxide binding gels. *Talanta*. 2019, (198), 518-526. DOI:10.1016/j.talanta.2019.01.127.
- [245] Huynh, T., Zhang, H. & Noller, B. Evaluation and application of the diffusive gradients in thin films technique using a mixed-binding gel layer for measuring inorganic arsenic and metals in mining impacted water and soil. *Analytical Chemistry*. 2012, (84), 9988-9995. DOI:10.1021/ac302430b.

- [246] Panther, J.G., Bennett, W.W., Welsh, D.T. & Teasdale, P.R. Simultaneous measurement of trace metal and oxyanion concentrations in water using diffusive gradients in thin films with a Chelex–Metsorb mixed binding layer. *Analytical Chemistry*. 2014, (86), 427-434. DOI:10.1021/ac402247j.
- [247] Wang, Y., Ding, S., Shi, L., Gong, M., Xu, S. & Zhang, C. Simultaneous measurements of cations and anions using diffusive gradients in thin films with a ZrO–Chelex mixed binding layer. *Analytica Chimica Acta*. 2017, (972), 1-11. DOI:10.1016/j.aca.2017.04.007.
- [248] Stockdale, A., Davison, W. & Zhang, H. High-resolution two-dimensional quantitative analysis of phosphorus, vanadium and arsenic, and qualitative analysis of sulfide, in a freshwater sediment. *Environmental Chemistry*. 2008, (5), 143-149. DOI:10.1071/EN07096.
- [249] Xu, L., Sun, Q., Ding, S., Gong, M. & Zhang, C. Simultaneous measurements of arsenic and sulfide using diffusive gradients in thin films technique (DGT). *Environmental Geochemistry Health*. 2018, (40), 1919-1929. DOI:10.1007/s10653-017-9968-8.
- [250] Kreuzeder, A., Santner, J., Prohaska, T. & Wenzel, W.W. Gel for simultaneous chemical imaging of anionic and cationic solutes using diffusive gradients in thin films. *Analytical Chemistry*. 2013, (85), 12028-12036. DOI:10.1021/ac403050f.
- [251] Pedrobom, J.H., Eismann, C.E., Menegário, A.A., Galhardi, J.A., Luko, K.S., de Araujo Dourado, T. & Kiang, C.H. In situ speciation of uranium in treated acid mine drainage using the diffusion gradients in thin films technique (DGT). *Chemosphere*. 2017, (169), 249-256. DOI:10.1016/j.chemosphere.2016.11.082.
- [252] Drozdak, J., Leermakers, M., Gao, Y., Elskens, M., Phommavanh, V. & Descostes, M. Uranium aqueous speciation in the vicinity of the former uranium mining sites using the diffusive gradients in thin films and ultrafiltration techniques. *Analytica Chimica Acta*. 2016, (913), 94-103. DOI:10.1016/j.aca.2016.01.052.
- [253] Altier, A., Jiménez-Piedrahita, M., Uribe, R., Rey-Castro, C., Galceran, J. & Puy, J. Time weighted average concentrations measured with Diffusive Gradients in Thin films (DGT). *Analytica Chimica Acta*. 2019, (1060), 114-124. DOI:10.1016/j.aca.2019.01.056.
- [254] Forsberg, J., Dahlqvist, R., Gelting-Nyström, J. & Ingri, J. Trace metal speciation in brackish water using diffusive gradients in thin films and ultrafiltration: comparison of techniques. *Environmental Science & Technology*. 2006, (40), 3901-3905. DOI:10.1021/es0600781.

- [255] Öhlander, B., Forsberg, J., Österlund, H., Ingri, J., Ecke, F. & Alakangas, L. Fractionation of trace metals in a contaminated freshwater stream using membrane filtration, ultrafiltration, DGT and transplanted aquatic moss. *Geochemistry: Exploration, Environment, Analysis*. 2012, (12), 303-312. DOI:10.1144/geochem2012-125.
- [256] Leermakers, M., Phommavanh, V., Drozdak, J., Gao, Y., Nos, J. & Descostes, M. DGT as a useful monitoring tool for radionuclides and trace metals in environments impacted by uranium mining: case study of the Sagnes wetland in France. *Chemosphere*. 2016, (155), 142-151. DOI:10.1016/j.chemosphere.2016.03.138.
- [257] Gontijo, E.S., Watanabe, C.H., Monteiro, A.S., Tonello, P.S., da Silva, G.A., Friese, K., Roeser, H.M. & Rosa, A.H. Distribution and bioavailability of arsenic in natural waters of a mining area studied by ultrafiltration and diffusive gradients in thin films. *Chemosphere*. 2016, (164), 290-298. DOI:10.1016/j.chemosphere.2016.08.107.
- [258] Ridošková, A., Pelfrêne, A., Douay, F., Pelcová, P., Smolíková, V. & Adam, V. Bioavailability of mercury in contaminated soils assessed by the diffusive gradient in thin film technique in relation to uptake by *Miscanthus*× *giganteus*. *Environmental Toxicology and Chemistry*. 2019, (38), 321-328. DOI:10.1002/etc.4318.
- [259] Pelcová, P., Zouharová, I., Ridošková, A. & Smolíková, V. Evaluation of mercury availability to pea parts (*Pisum sativum* L.) in urban soils: Comparison between diffusive gradients in thin films technique and plant model. *Chemosphere*. 2019, (234), 373-378. DOI:10.1016/j.chemosphere.2019.06.076.
- [260] Bade, R., Oh, S. & Shin, W.S. Diffusive gradients in thin films (DGT) for the prediction of bioavailability of heavy metals in contaminated soils to earthworm (*Eisenia foetida*) and oral bioavailable concentrations. *Science of the Total Environment*. 2012, (416), 127-136. DOI:10.1016/j.scitotenv.2011.11.007.
- [261] Amirbahman, A., Massey, D.I., Lotufo, G., Steenhaut, N., Brown, L.E., Biedenbach, J.M. & Magar, V.S. Assessment of mercury bioavailability to benthic macroinvertebrates using diffusive gradients in thin films (DGT). *Environmental Science: Processes & Impacts*. 2013, (15), 2104-2114. DOI:10.1039/c3em00355h.
- [262] Pelcová, P., Vičarová, P., Dočekalová, H., Poštulková, E., Kopp, R., Mareš, J. & Smolíková, V. The prediction of mercury bioavailability for common carp (*Cyprinus carpio* L.) using the DGT technique in the presence of chloride ions and humic acid. *Chemosphere*. 2018, (211), 1109-1112. DOI:10.1016/j.chemosphere.2018.07.202.
- [263] Luider, C.D., Crusius, J., Playle, R.C. & Curtis, P.J. Influence of natural organic matter source on copper speciation as demonstrated by Cu binding to fish gills, by ion selective electrode, and by DGT gel sampler. *Environmental Science & Technology*. 2004, (38), 2865-2872. DOI:10.1021/es030566y.

- [264] Clarisse, O., Lotufo, G., Hintelmann, H. & Best, E. Biomonitoring and assessment of monomethylmercury exposure in aqueous systems using the DGT technique. *Science of the Total Environment*. 2012, (416), 449-454. DOI:10.1016/j.scitotenv.2011.11.077.
- [265] Yin, H., Cai, Y., Duan, H., Gao, J. & Fan, C. Use of DGT and conventional methods to predict sediment metal bioavailability to a field inhabitant freshwater snail (*Bellamya aeruginosa*) from Chinese eutrophic lakes. *Journal of Hazardous Materials*. 2014, (264), 184-194. DOI:10.1016/j.jhazmat.2013.11.030.
- [266] Røyset, O., Rosseland, B.O., Kristensen, T., Kroglund, F., Garmo, Ø.A. & Steinnes, E. Diffusive gradients in thin films sampler predicts stress in brown trout (*Salmo trutta* L.) exposed to aluminum in acid fresh waters. *Environmental Science & Technology*. 2005, (39), 1167-1174. DOI:10.1021/es049538l.
- [267] Pelfrêne, A., Waterlot, C. & Douay, F. Investigation of DGT as a metal speciation tool in artificial human gastrointestinal fluids. *Analytica Chimica Acta*. 2011, (699), 177-186. DOI:10.1016/j.aca.2011.05.024.
- [268] Pelfrêne, A., Waterlot, C. & Douay, F. In vitro digestion and DGT techniques for estimating cadmium and lead bioavailability in contaminated soils: Influence of gastric juice pH. *Science of the Total Environment*. 2011, (409), 5076-5085. DOI:10.1016/j.scitotenv.2011.08.032.
- [269] Liu, Z.-D., Li, H.-B., Fang, X., Zhang, H., Ma, L.Q. & Luo, J. Investigating lead species and bioavailability in contaminated soils: coupling DGT technique with artificial gastrointestinal extraction and in vivo bioassay. *Environmental Science & Technology*. 2019, (53), 5717-5724. DOI:10.1021/acs.est.8b06918.
- [270] Zhang, H. & Davison, W. Performance characteristics of diffusion gradients in thin films for the in situ measurement of trace metals in aqueous solution. *Analytical Chemistry*. 1995, (67), 3391-3400. DOI:10.1021/ac00115a005.
- [271] Pelcová, P., Dočekalová, H. & Kleckarová, A. Development of the diffusive gradient in thin films technique for the measurement of labile mercury species in waters. *Analytica Chimica Acta*. 2014, (819), 42-48. DOI:10.1016/j.chemosphere.2021.132545.
- [272] Pommier, A.-L., Simon, S., Buzier, R. & Guibaud, G. Evaluation of a mercapto-functionalized silica binding phase for the selective sampling of SeIV by Diffusive Gradients in Thin films. *Talanta*. 2019, (199), 590-595. DOI:10.1016/j.talanta.2019.02.086.
- [273] Smolíková, V., Pelcová, P., Ridošková, A., Hedbávný, J. & Grmela, J. Development and evaluation of the iron oxide-hydroxide based resin gel for the diffusive gradient in thin films technique. *Analytica Chimica Acta*. 2020, (1102), 36-45. DOI:10.1016/j.aca.2019.12.042.

- [274] Smolíková, V., Pelcová, P., Ridošková, A. & Leermakers, M. Simultaneous determination of arsenic and uranium by the diffusive gradients in thin films technique using Lewatit FO 36: Optimization of elution protocol. *Talanta*. 2021, (228), 122234. DOI:10.1016/j.talanta.2021.122234.
- [275] Zhang, H. & Davison, W. Diffusional characteristics of hydrogels used in DGT and DET techniques. *Analytica Chimica Acta*. 1999, (398), 329-340. DOI:10.1016/S0003-2670(99)00458-4.
- [276] Branch, S., Ebdon, L., Ford, M., Foulkes, M. & O'Neill, P. Determination of arsenic in samples with high chloride content by inductively coupled plasma mass spectrometry. *Journal of Analytical Atomic Spectrometry*. 1991, (6), 151-154. DOI:10.1039/JA9910600151.
- [277] Chen, Z., Khan, N.I., Owens, G. & Naidu, R. Elimination of chloride interference on arsenic speciation in ion chromatography inductively coupled mass spectrometry using an octopole collision/reaction system. *Microchemical Journal*. 2007, (87), 87-90. DOI:10.1016/j.microc.2007.05.011.
- [278] Slavin, W., Carnrick, G. & Manning, D. Chloride interferences in graphite furnace atomic absorption spectrometry. *Analytical Chemistry*. 1984, (56), 163-168. DOI:10.1021/ac00266a011.
- [279] Mester, Z. & Sturgeon, R.E. Detection of volatile arsenic chloride species during hydride generation: a new prospectus. *Journal of Analytical Atomic Spectrometry*. 2001, (16), 470-474. DOI:10.1039/B100750P.
- [280] Lanxess. Product information – Lewatit® FO 36. <https://www.lenntech.com/Data-sheets/Lewatit-FO-36-L.pdf>. [cited 23/10/2020].
- [281] European Environment Agency. Nutrients in freshwater in Europe. URL:<https://www.eea.europa.eu/data-and-maps/indicators/nutrients-in-freshwater/nutrients-in-freshwater-assessment-published-10>. [cited 20/10/2021].
- [282] SenGupta, A.K. Ion exchange in environmental processes: Fundamentals, applications and sustainable technology, *John Wiley & Sons*, 2017.
- [283] Zhang, H. & Davison, W. Use of diffusive gradients in thin-films for studies of chemical speciation and bioavailability. *Environmental Chemistry*. 2015, (12), 85-101. DOI:10.1071/EN14105.
- [284] Farrell, J. & Chaudhary, B.K. Understanding arsenate reaction kinetics with ferric hydroxides. *Environmental Science & Technology*. 2013, (47), 8342-8347. DOI:10.1021/es4013382.

- [285] Simeoni, M.A., Batts, B.D. & McRae, C. Effect of groundwater fulvic acid on the adsorption of arsenate by ferrihydrite and gibbsite. *Applied Geochemistry*. 2003, (18), 1507-1515. DOI:10.1016/S0883-2927(03)00074-X.
- [286] Xing, W. & Liu, G. Iron biogeochemistry and its environmental impacts in freshwater lakes. *Fresenius Environmental Bulletin*. 2011, (20), 1339-1345.
- [287] Kritzberg, E. & Ekström, S. Increasing iron concentrations in surface waters—a factor behind brownification? *Biogeosciences*. 2012, (9), 1465-1478. DOI:10.5194/bg-9-1465-2012.
- [288] Hendry, B., Bundschuh, J., Yoshizuka, K., Bryjak, M., Kabay, N., Bhattacharya, P. & Anaç, S. The Global Arsenic Problem: Challenges for Safe Water Production, Vol. 2. *CRC Press*, 2010.
- [289] Ouattara, N.K., Garcia-Armisen, T., Anzil, A., Brion, N. & Servais, P. Impact of wastewater release on the faecal contamination of a small urban river: The Zenne River in Brussels (Belgium). *Water, Air, & Soil Pollution*. 2014, (225), 1-12. DOI:10.1007/s11270-014-2043-5.
- [290] Baeyens, W., de Brauwere, A., Brion, N., De Gieter, M. & Leermakers, M. Arsenic speciation in the river Zenne, Belgium. *Science of the Total Environment*. 2007, (384), 409-419. DOI:10.1016/j.scitotenv.2007.05.044.
- [291] Andreae, M. & Andreae, T. Dissolved arsenic species in the Schelde estuary and watershed, Belgium. *Estuarine, Coastal and Shelf Science*. 1989, (29), 421-433. DOI:10.1016/0272-7714(89)90077-2.

9 ABBREVIATIONS

3-MFS	3-mercaptopropyl-functionalized silica
A	Exposure area of DGT sampler
AAS	Atomic adsorption spectrometry
AG	Agarose gel
ANOVA	Analysis of variance
APA	Agarose cross-linked polyacrylamide gel
APS	Ammonium persulphate
ASV	Anodic stripping voltammetry
BCR	Community Bureau of Reference
BLM	Biotic ligand model
c_{DGT}	Analyte concentration determined by DGT
CE	Capillary electrophoresis
CEC	Capillary electrochromatography
c_{SOL}	Analyte concentration in the bulk solution
CSV	Cathodic stripping voltammetry
CV-AFS	Cold vapour atomic fluorescence spectrometry
CZE	Capillary zone electrophoresis
D	Diffusion coefficient of the analyte
D_T	Diffusion coefficient of the analyte at the temperature T
D_{Ref}	Diffusion coefficient of the analyte at the temperature T_{Ref}
DBL	Diffusive boundary layer
DET	Diffusive equilibrium in thin films technique
Δg	Thickness of the diffusive layer
DGT	Diffusive gradients in thin films technique
DMA	Dimethylarsinic acid
DMT	Donnan membrane technique
DOM	Dissolved organic matter
ET-AAS	Electrothermal atomic absorption spectrometry

F-AAS	Flame atomic absorption spectrometry
FA	Fulvic acid
Fe ₃ O ₄ NPs	Nanoparticulate Fe ₃ O ₄
Fh	Ferrihydrite
FIAM	Free ion activity model
f _u	Uptake factor
f _e	Elution factor
GC	Gas chromatography
GE	Gel electrophoresis
GSH	Glutathione
HA	Humic acid
HFPLM	Hollow fibre permeable liquid membranes
HS	Humic substances
HEDPA	1- hydroxyethane-1,1-diphosphonic acid
HG-AAS	Hydride generation atomic absorption spectrometry
HPLC	High performance liquid chromatography
ICP -MS	Inductively coupled plasma mass spectrometry
ICP-OES	Inductively coupled plasma optical emission spectrometry
IDA	Iminodiacetic acid
IE	Ion-exchange
IEF	Isoelectric focusing
ISE	Ion-selective electrodes
J	Flux of analyte to a DGT sampler
LC	Liquid chromatography
LLE	Liquid-liquid extraction
LOD	Limit of detection
M	Mass of analyte accumulated in the DGT binding layer
M _a	Mass of analyte accumulated in the DGT binding layer
M _e	Mass of analyte eluted from the DGT binding layer
M _i	Initial mass of analyte in the solution

M_r	Remaining mass of analyte in the solution
MBL	Mixed binding layer
MDL	Material diffusive layer
MEKC	Micellar electrokinetic capillary electrochromatography
MMA	Monomethylarsonic acid
ML	Metal complex with ligand
M^{Z+}	Free metal ion
nano-La ₂ O ₃	Nanoparticulate lanthanum oxide
PES	Polyethersulphone
PLM	Permeation liquid membrane
PVDF	Polyvinyl fluoride
RG	Restricted gel
ROS	Reactive oxygen species
RP	Reversed phase
SAM	S-adenosylmethionine
SCPEI-PCPEI	Mixture of sulphonated and phosphonated cross-linked polyethylenimine
SE	Size-exclusion
SF-ICP-MS	Sector field inductively coupled plasma mass spectrometry
SPE	Solid-phase extraction
SPR-IDA	Suspended particulate reagent-iminodiacetate
SLM	Supported liquid membranes
δ^{MDL}	Thickness of the material diffusive layer
Δ^{DBL}	Thickness of the diffusive boundary layer
t	Time of DGT deployment
T	Temperature of the solution
T_{Ref}	Reference temperature of the solution (25 °C)
TEMED	N,N,N',N'-tetramethylenediamine
TMAO	Trimethylarsine oxide
TWA	Time-weighted average
WHAM	Windermere humic aqueous model

WHO

World health organization

Zn-ferrite

Zinc ferrite

10 LIST OF FIGURES

Fig. 3-1 Illustrative Pourbaix Eh-pH diagram of As-H-O system ($\text{As} = 10^{-5} \text{ M}$, $T = 25^\circ \text{C}$, created with Medusa Software (Royal Institute of Technology, Sweden)).	23
Fig. 3-2 Illustrative distribution diagram of arsenite (A) and arsenate (B) fractions in aqueous solution under different pH conditions ($\text{As} = 10^{-5} \text{ M}$, created with Medusa Software (Royal Institute of Technology, Sweden)).	23
Fig. 3-3 Illustrative Pourbaix Eh-pH diagram of U-H-O system ($\text{U} = 10^{-5} \text{ M}$, $T = 25^\circ \text{C}$, created with Medusa Software (Royal Institute of Technology, Sweden)).	25
Fig. 3-4 Illustrative distribution diagram of uranium fractions under different pH conditions in non-complexing environment (A) and in the presence of carbonates (B) ($\text{U} = 10^{-5} \text{ M}$, $\text{CO}_3^{2-} = 10^{-2} \text{ M}$ created with Medusa Software (Royal Institute of Technology, Sweden)).	25
Fig. 3-5 Illustrative scheme of trace elements pathways to aquatic ecosystems, their fractionation in water, and potential exposure pathways for living organisms.	28
Fig. 3-6 Trace element (metal(loid)) uptake by cell (M^{Z+} – free metal ion; ML – weak complex of metal and ligand; 1 – surface complexation; 2 – penetration of M or ML through the phospholipid layer; 3 – mediated transport; 4 – transport through ion pump/channel; 5 – endocytosis, A – mitochondria, B – nucleus, C – endoplasmic reticulum with ribosomes, D – Golgi apparatus, E - lysosome) (inspired by [56, 72, 74] and created with BioRender.com).	30
Fig. 3-7 Overview of selected analytical techniques used for elemental speciation analysis.	35
Fig. 3-8 Schematic comparison of detection limits/measurement range of selected analytical techniques used for elemental analysis (adapted from [112, 113]).	37
Fig. 3-9 Structure of the DGT piston and sediment probe with a resin gel, diffusive gel and membrane filter (A), and a schematic illustration of the steady-state concentration gradients generated during the uptake of free metal ions and fully labile/partially labile/inert metal complexes (B) (inspired by [186, 188], created with BioRender.com).	44
Fig. 4-1 Illustrative protocol for preparation of the DGT APA resin gel (created with BioRender.com).	55
Fig. 4-2 Schematic illustration of DGT deployment method when performing laboratory experiment (A) or when applied <i>in-situ</i> in streams (B) or deeper water of lake or sea (C) and deployment of DGT probes in sediments (D) (created with BioRender.com).	57
Fig. 4-3 Inner surface of the graphite tube before (A) and after (B) modification by tungsten carbides.	63

11 LIST OF TABLES

Table 3-1 Overview of binding phases used for analysis of arsenic or uranium by the DGT technique.	49
Table 4-1 Preparation protocol of resin gels (reagents used per 10 mL of gel solution).	54
Table 4-2 Elution protocols for resin gels used within this work.	58

12 LIST OF ANNEXES

12.1 Supplementary Information to Chapter 5.3

Ad Chapter 2 Materials and methods

Table S3 Location of sampling stations on the Zenne River.

Station	Location	Distance (km*)
Z1	Lembeek	0
Z1b	Lembeek	2
Z3	Beersel	13.2
Z4	Drogenbos	16.5
Z5	Anderlecht Industrie	19.9
Z5a	Anderlecht Veterinaire	22.5
Z7	Van Praet	29.7
Z8	Haren	33.0
Z9	Haren-Buda	33.8
Z9c	Vilvoorde Sluisstraat	35.9
Z10a	Vilvoorde Ziekenhuis	37.5
Z10b	Vilvoorde PB Gelatine	38.8
Z10c	Vilvoorde na kanaaldok	40.0
Z11	Eppegem	41.5
Z11b	Weerde Damstraat	43.3
Z11c	Weerde E19	45.0
Z11d	Zemst	46.2
Z12	Hombeek	51.5
Z13	Heffen	55.9
Z14	Zennegat	58.0

* The first station on the Zenne River is located at N 50° 42' 34.679", E 4° 13' 2.996".

Reagents and chemicals

All chemicals were of analytical reagent grade or higher. Milli-Q water (Millipore, USA) was used for the preparation of gels and solutions, as well as for cleaning DGT devices. The nitric acid was used for material cleaning (HNO_3 produced by distillation

apparatus Berghof, Germany), samples acidification, and gels extraction (Optima Grade, Fisher Scientific, USA). The DGT gels were prepared using acrylamide 40% (w/v) (Merck, Germany), agarose (Biorad, USA), agarose-derived DGT cross-linker (2%) (DGT Research Ltd., UK), ammonium persulfate (APS) (Merck, Germany), N,N,N',N'-tetramethylethylenediamine (TEMED) (Merck, Germany) and resins Chelex-100 (Bio-Rad, USA), Metsorb® (Graver Technologies Ltd., USA), Lewatit® FO 36 (Lanxess, Germany), and 3-mercaptopropyl-functionalized silica (3-MFS, 200–400 mesh; Sigma-Aldrich, Germany). The 3-MFS resin gels and diffusive gels were prepared with agarose (Bio-Rad, USA). The $\text{ZrOCl}_2 \times 8\text{H}_2\text{O}$ and MES (2-(N-morpholino)-ethanesulfonic acid) The sodium hydroxide (Merck, Germany) and potassium iodate (Sigma-Aldrich, Germany) were used for gel extraction. Hydrofluoric acid 40% (v/v), hydrochloric acid 37% (v/v) and boric acid 4% (w/v) (all Trace Metal Grade, Fisher Scientific, USA) were used for digestion. Acetic acid (Merck, Germany), hydroxylammonium chloride (Thermo Fisher, USA), hydrogen peroxide (Thermo Fisher, USA), and ammonium acetate (Merck, Germany) were used for sequential extractions. Zinc acetate, sodium sulphide, N,N-dimethyl-p-phenylenediamine sulphate, and ferric chloride (all Sigma-Aldrich, Germany) were used for preparation of solutions for the sulphide analysis. A multi-element standard solution (Merck XIII) was used for the preparation of the calibration standards for analysis of trace elements together with the internal standard of indium (Alfa Aesar, USA).

Ad Chapter 2.5 Protocol for manufacturing and handling the DGTs

The DGT pistons, glass, and plastic equipment used for gels handling were cleaned in 5% (v/v) HNO_3 for at least 24 h and thoroughly rinsed with Milli-Q water prior to use. The gel stock solution was prepared using 15% (v/v) acrylamide and 0.3% (v/v) DGT cross-linker. The polymerization reaction of the gel solution was initiated by freshly prepared 10% (w/v) ammonium persulfate (APS) and catalysed by N,N,N',N'-tetramethylethylenediamine (TEMED). For the preparation of the APA diffusive gels, 10 mL of gel solution was mixed with 70 μL of freshly prepared 10% (w/v) APS and 25 μL of TEMED according to the protocol described in the literature [1]. The agarose-

based diffusive gels were only used for DGTs utilizing 3-MFS resin gel and were prepared by dissolution of agarose (1.5% solution) in Milli-Q water at 80 °C. All of the diffusive gels were prepared with a resulting thickness of 0.08 cm.

The same protocol was slightly modified for the preparation of each type of resin gel with a resulting thickness of 0.04 cm (**Table S2**). The Lewatit FO 36 and Metsorb resins were ground (Pulverisette Type 02.102, Fritsch, Germany) and sieved on a Teflon sieve (50 µm) prior to use. Only the 3-MFS resin gels were prepared in AG according to protocol by Pommier et al. [2]. Thoroughly mixed gel solution with each resin was cast between two glass plates and let polymerized at 45 °C (APA gels) or room temperature (AG gels) for 1 h. The ZrO₂ resin gels were prepared by in-situ precipitation on the diffusive gel according to the protocol by Guan et al. [3]. After 24 h of hydration in Milli-Q water, the gel sheets were then cut using a plastic circle cutter (diameter 2.5 cm) or Teflon coated razor blade (2.5 × 32 cm for sediment probes) and stored in 0.01 M NaNO₃ at 4 °C prior to use.

Table S2 Preparation protocol of resin gels (reagents used per 10 ml of gel solution).

	Resin (g)	10% APS (µl)	TEMED (µl)
3-MFS* [4]	1	-	-
Chelex-100 [1]	4	50	15
Lewatit FO 36 [5]	1.25	240	120
Metsorb [6]	1	60	15
ZrO ₂ ** [3]	12.88 + 4.24	-	-

*The 3-MFS resin gel was prepared in agarose and thus no APS and TEMED were added.

** The masses correspond to ZrOCl₂ × 8H₂O and MES (2-(N-morpholino)-ethanesulfonic acid, respectively, used for *in-situ* precipitation of ZrO₂ on the diffusive gel prepared from 10 mL of gel solution. The amount of precipitated ZrO₂ in the resulting resin gel is however unknown.

The DGT pistons and probes (DGT Research Ltd., UK) (with an exposure window of 3.14 cm² and 27 cm², respectively) were used for water and sediment deployment. Polyvinyl fluoride (PVDF) Durapore® membrane filters of 0.45 µm pore size (Merck, Germany) were pre-cleaned in 10% (v/v) HNO₃ for 24 h and thoroughly rinsed with

Milli-Q water prior to use. The DGT plastic housings were loaded with resin gel, covered by diffusive gel and membrane filter, and capped by a tight-fitting outer sleeve with an exposure window. Assembled DGT units were stored at 4 °C in zip-lock bags and kept moisturized with 0.01 M NaNO₃ prior to deployment.

Elution protocol of resin gels

After disassembling the DGT piston-shaped units, the resin gel discs were rinsed with Milli-Q water and placed in the clean tube. The resin gels from sediment probes were sliced by Teflon coated razor blade at 0.5–1 cm interval and placed in the clean tube. The reagents used for the elution of each type of resin gel together with the elution procedures are shown in **Table S3**. Since the gel slices from sediment probes are smaller, half the volume of eluent was used in order to avoid unnecessary dilution of trace elements concentration. After elution, the samples were diluted ten times by Milli-Q water or 2% HNO₃ (in the cases where elution reagent was not an acid) and stored at 4 °C until analysis.

Table S3 Elution protocols for resin gels used within this work.

	Reagent	Volume*	Elution procedure	Elution factor
3-MFS [7]	1 M HNO ₃ + 0.01 M KIO ₃	1 mL	LT**, 24 h	0.8
Chelex-100 [1]	1 M HNO ₃	1 mL	LT, 24 h	0.8
Lewatit FO 36 [8]	1 M NaOH	5 mL	70 °C, 24 h	0.9
Metsorb [6]	1 M HNO ₃	1 mL	LT, 24 h	0.8
ZrO ₂ [3]	0.5 M NaOH	10 mL	LT, 24 h	0.9

* The eluent volume per gel disc. Half the volume of eluent was used for the extraction of gel slices from sediment probes.

** LT – Laboratory temperature (20 °C).

DGT calculations

Arsenic mass (M , ng) accumulated on the resin gel disc is calculated from the concentration of As measured by analytical technique in the eluent (c_e) using **Eq. 1**,

where V is the total volume of gel and elution agent and f_e is the elution factor as described in.

$$M = c_e \cdot V / f_e \quad (1)$$

Arsenic concentration determined by DGT (c_{DGT} , $\mu\text{g L}^{-1}$) is then calculated from the accumulated mass (M , ng), the thickness of diffusive layer consisting of diffusive gel and membrane filter (Δg , cm), the diffusion coefficient of As (D , $\text{cm}^2 \text{s}^{-1}$), the area of the exposure window (A , cm^2), and the deployment time (t , s) using **Eq. 2**.

$$c_{DGT} = M \cdot \Delta g / (D \cdot A \cdot t) \quad (2)$$

The diffusion coefficients of As at 25 °C used for calculations were as follows – $6.41 \times 10^{-6} \text{ cm}^2 \text{s}^{-1}$ for Lewatit FO 36 [5], $10.1 \times 10^{-6} \text{ cm}^2 \text{s}^{-1}$ for 3-MFS (As^{III}) [6], 6.78×10^{-6} for ZrO₂ [5], and $5.96 \times 10^{-6} \text{ cm}^2 \text{s}^{-1}$ for Metsorb (measured in the laboratory).

Ad Chapter 3 Results and discussion

Ad Chapter 3.1 Distribution of dissolved and particulate As in water along the Zenne River

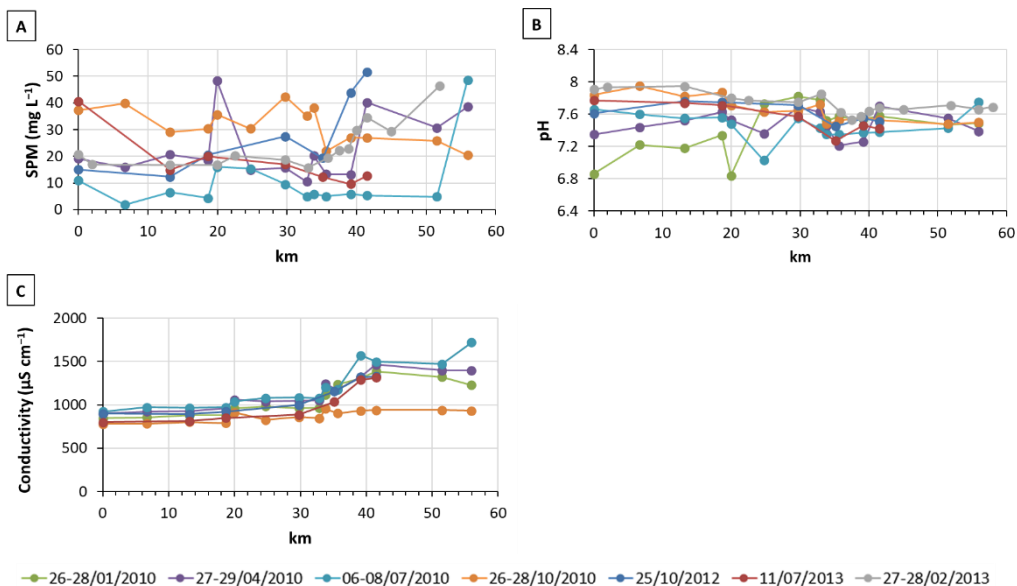


Fig. S1 Longitudinal profiles of the SPM (A), pH (B), and conductivity (C) along the Zenne River (0 km corresponds to station Z1 in Lembeek).

Ad Chapter 3.2 Temporal variability of As in the tidal zone and DGT time-integrated concentrations

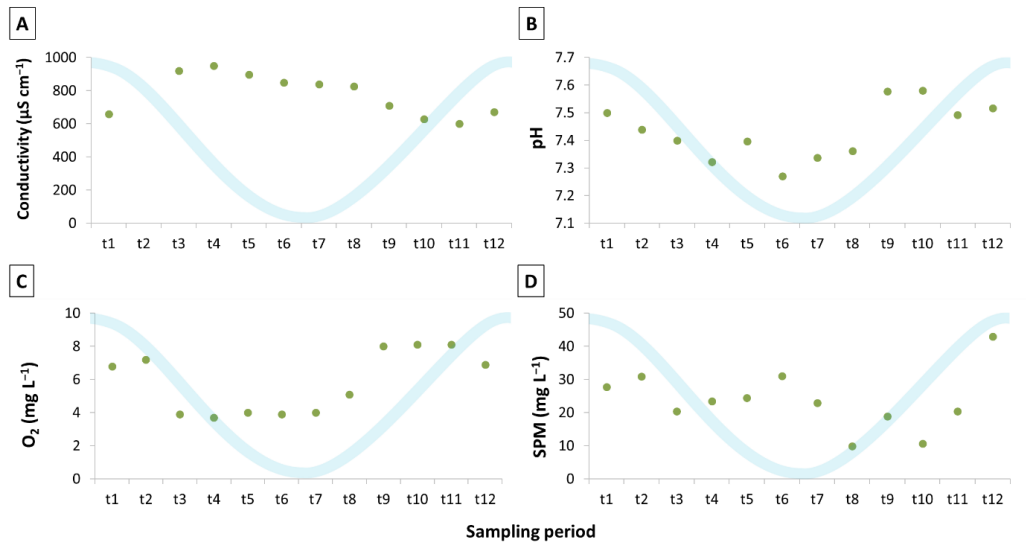


Fig. S2 Variation profiles of conductivity (A), pH (B), dissolved oxygen concentrations (C) and suspended particulate matter (D) at Z14 (Zennegat) during a tidal cycle, March 2021.

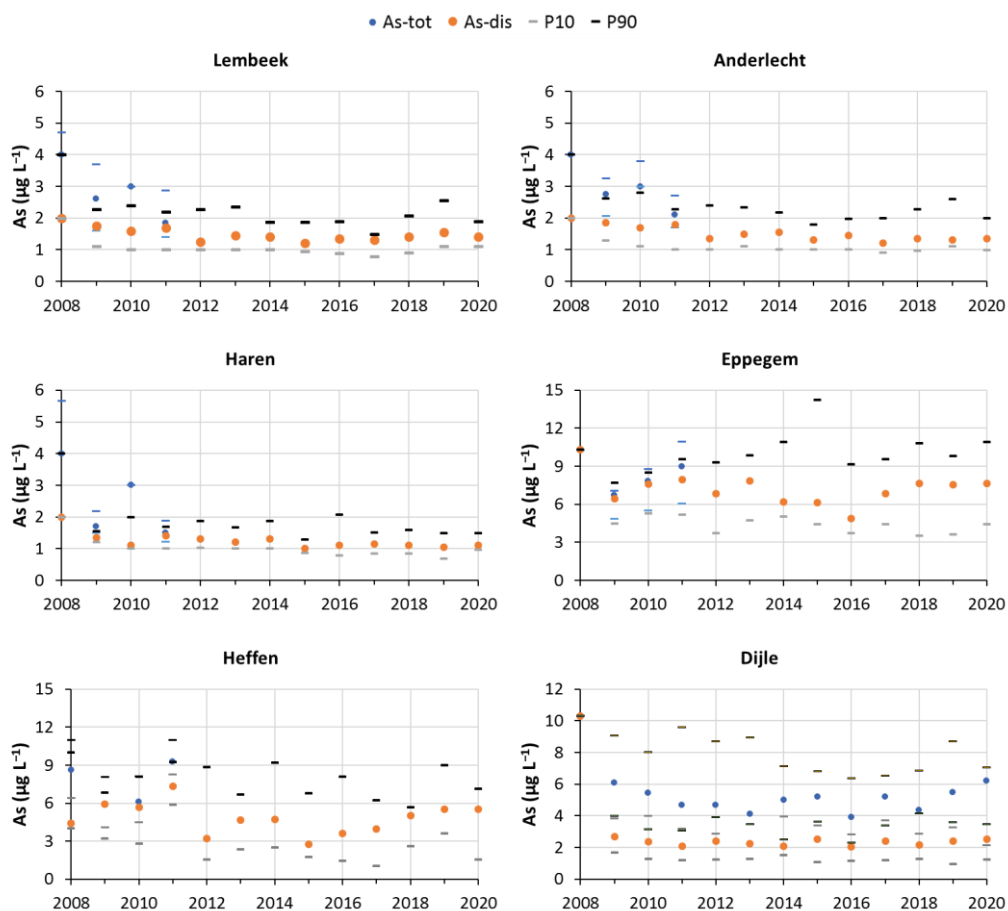


Fig. S3 Evolution of dissolved and total As concentrations (As-dis, As-tot) during 2008-2020 at stations Lembeek, Anderlecht, Haren, Eppegem, Heffen, and Dijle based on the data from VMM online database (data expressed as median values with 10th (P10) and 90th (P90) percentiles for n = 5–12).

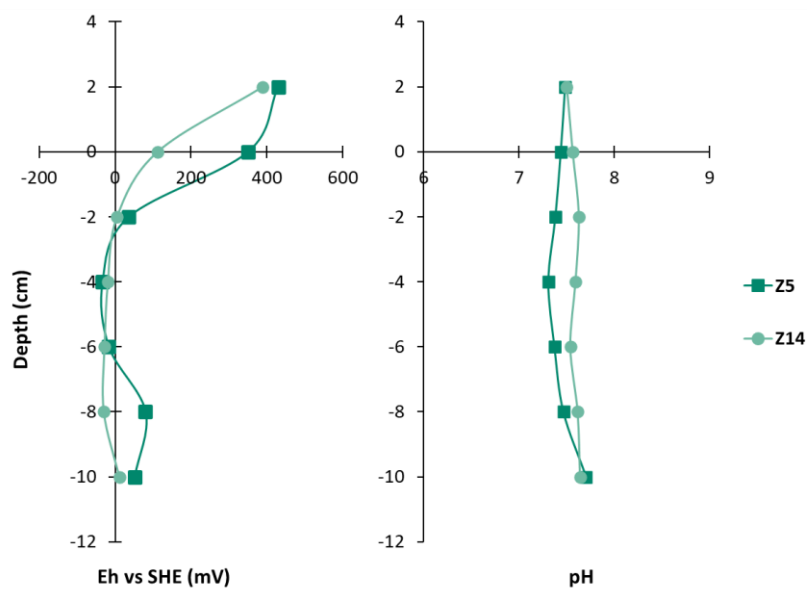


Fig. S4 The depth profiles of redox potential and pH in the sediments at stations Z5 and Z14 (June 2020).

- [1] Zhang, H. & Davison, W. Performance characteristics of diffusion gradients in thin films for the in situ measurement of trace metals in aqueous solution. *Analytical Chemistry*. 1995, (67), 3391-3400. DOI:10.1021/ac00115a005.
- [2] Pommier, A.-L., Simon, S., Buzier, R. & Guibaud, G. Evaluation of a mercapto-functionalized silica binding phase for the selective sampling of SeIV by Diffusive Gradients in Thin films. *Talanta*. 2019, (199), 590-595. DOI:10.1016/j.talanta.2019.02.086.
- [3] Guan, D.-X., Williams, P.N., Luo, J., Zheng, J.-L., Xu, H.-C., Cai, C. & Ma, L.Q. Novel precipitated zirconia-based DGT technique for high-resolution imaging of oxyanions in waters and sediments. *Environmental Science & Technology*. 2015, (49), 3653-3661. DOI: 10.1021/es505424m.
- [4] Reichstädter, M., Gao, Y., Diviš, P., Ma, T., Gaulier, C. & Leermakers, M. Cysteine-modified silica resin in DGT samplers for mercury and trace metals assessment. *Chemosphere*. 2021, (263), 128320. DOI:10.1016/j.chemosphere.2020.128320.
- [5] Smolíková, V., Pelcová, P., Ridošková, A., Hedbávný, J. & Grmela, J. Development and evaluation of the iron oxide-hydroxide based resin gel for the diffusive gradient in thin films technique. *Analytica Chimica Acta*. 2020, (1102), 36-45. DOI:10.1016/j.aca.2019.12.042.
- [6] Bennett, W.W., Teasdale, P.R., Panther, J.G., Welsh, D.T. & Jolley, D.F. New diffusive gradients in a thin film technique for measuring inorganic arsenic and selenium (IV) using a titanium dioxide based adsorbent. *Analytical Chemistry*. 2010, (82), 7401-7407. DOI:10.1021/ac101543p.
- [7] Bennett, W.W., Teasdale, P.R., Panther, J.G., Welsh, D.T. & Jolley, D.F. Speciation of dissolved inorganic arsenic by diffusive gradients in thin films: selective binding of AsIII by 3-mercaptopropyl-functionalized silica gel. *Analytical Chemistry*. 2011, (83), 8293-8299. DOI:10.1021/ac202119t.
- [8] Smolíková, V., Pelcová, P., Ridošková, A. & Leermakers, M. Simultaneous determination of arsenic and uranium by the diffusive gradients in thin films technique using Lewatit FO 36: Optimization of elution protocol. *Talanta*. 2021, (228), 122234. DOI:10.1016/j.talanta.2021.122234.

12.2 Supplementary Information to Chapter 5.4

Table S1 Instrumental parameters of the SF-ICP-MS used in this work.

Instrument	ELEMENT2 Thermo Finnigan
Forward power	1,350 W
Reflected power	< 2 W
Nebuliser	Concentric
Solution uptake rate	0.4 mL min ⁻¹ (pumped)
Spray chamber	Cyclonic
Sampling and skimmer cones	Ni (Thermo Finnigan)
Sample gas flow	1 to 1.5 L min ⁻¹
Cool argon flow rate	16 L min ⁻¹
Auxiliary argon flow rate	1.0 L min ⁻¹
Torch	Capacitive decoupling Pt shield torch
RF frequency	27.12 Mhz
Sensitivity	1 x 10 ⁶ cps per 1 ng mL ⁻¹ ¹¹⁵ In (in Low Resolution)
Autosampler	ESI SC 3 Fast
Take-up time	15 s
Wash time	10 s
Number of acquisition	6 (3 runs and 2 pass)
Mass window LR	150% for each isotope
Search window LR	150% for each isotope
Samples per peak LR	20
Integration window LR	80% for each isotope
Mass window HR	As75 65%, In115 125%
Search window HR	60%
Samples per peak HR	30
Integration window HR	60%
Scan type	E scan for each isotope
Integration type	Average for each isotope

Table S2 Tukey's post-hoc test matrices declaring the significant differences between variants of elution agents on the level of significance $\alpha=0.05$.

As							
Variant	A	B	C	D	E	F	G
A		0.00274	0.00343	0.00014	0.00014	0.00431	0.00014
B	0.00274		1.00000	0.00014	0.00014	0.99999	0.00014
C	0.00343	1.00000		0.00014	0.00014	1.00000	0.00014
D	0.00014	0.00014	0.00014		0.99879	0.00014	1.00000
E	0.00014	0.00014	0.00014	0.99879		0.00014	0.99563
F	0.00431	0.99999	1.00000	0.00014	0.00014		0.00014
G	0.00014	0.00014	0.00014	1.00000	0.99563	0.00014	

U							
Variant	A	B	C	D	E	F	G
A		0.00000	0.12929	0.00000	0.00000	0.00000	0.00118
B	0.00000		0.00000	0.00000	0.00017	0.00009	0.00068
C	0.12929	0.00000		0.00000	0.00000	0.00000	0.56143
D	0.00000	0.00000	0.00000		0.00006	0.00011	0.00000
E	0.00000	0.00017	0.00000	0.00006		0.99999	0.00000
F	0.00000	0.00009	0.00000	0.00011	0.99999		0.00000
G	0.00118	0.00068	0.56143	0.00000	0.00000	0.00000	

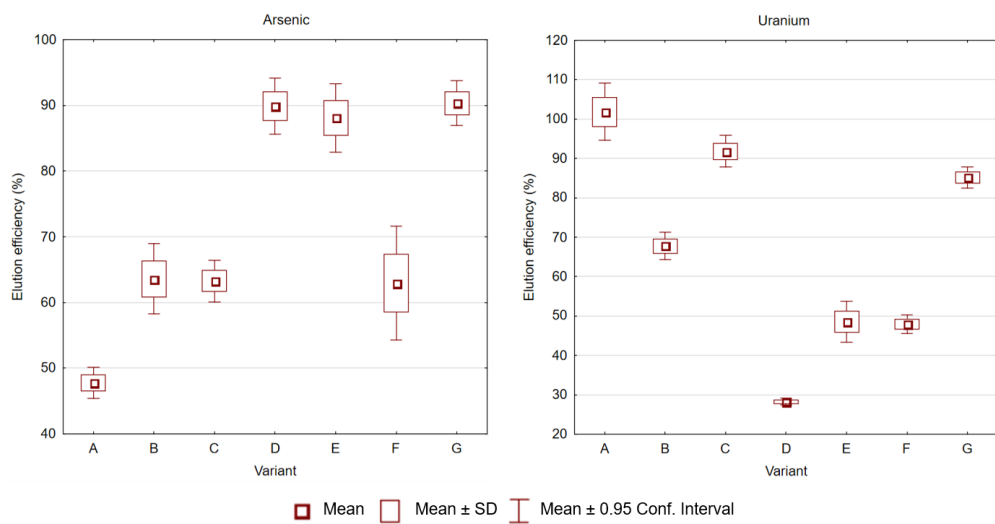


Fig. S1 Box plots showing significant differences between elution variants expressed as mean, standard deviation, and mean $\pm 1.96 \times$ SD.

12.3 Supplementary Information to Chapter 5.5

Table S1 Sampling stations on the Scheldt estuary and Belgian coast.

Location	Sampling station	Geographical coordinates		Results available for each campaign ^a			
		Latitude	Longitude	2014	2019	2020	2021
Scheldt estuary	HEM	51°11.57'N	04°20.15'E	CH, P	CH, P, D	*	CH, P, D, L
	S22	51°14.20'N	04°23.70'E	CH, P	CH	CH, P, D, L	CH, P, D, L
	S15	51°18.80'N	04°16.40'E	CH, P	CH, P, D	CH, P, D, L	CH, P, D, L
	S12	51°21.90'N	04°13.50'E	CH, P	CH	CH, P, D, L	CH, P, D, L
	S09	51°22.20'N	04°04.20'E	CH, P	CH, P, D	CH, P, D, L	CH, P, D, L
	S07	51°26.10'N	03°59.30'E	CH, P	CH	CH, P, D, L	CH, P, D, L
	S04	51°20.50 'N	03°50.50'E	CH, P	CH, P	*	*
	S01	51°24.80'N	03°34.40'E	CH, P	CH, P, D	*	CH, P, D, L
Zeebrugge harbour	HZ1	51°20.41'N	03°12.20'E			CH, P, D, L (l-t)	
	HZ2	51°19.87'N	03°11.97'E				P, D, L (l-t)

^a CH – Chelex-100; P – Dow-PIWBA; D – Diphonix; L – Lewatit FO 36; l-t – long term deployment.

* Missing data due to unfavorable weather conditions for DGT retrieval or loss of DGTs.

Table S2 Physico-chemical parameters of water from stations HEM–S01 during campaigns 2014–2021 (average values of n=2 obtained from upstream and downstream sampling).

Parameter	Year	Station							
		HEM	S22	S15	S12	S09	S07	S04	S01
Temperature (°C)	2014	7.40	7.40	7.40	7.00	6.40	6.10	6.00	6.00
	2019	8.90	8.75	8.90	8.90	8.25	8.10	8.05	7.95
	2020	8.80	8.25	8.30	8.25	7.80	8.05	8.05	7.61
	2021	8.30	8.40	8.00	8.10	7.10	6.50	5.90	6.30
pH	2014	7.80	7.90	7.90	8.00	8.00	8.09	8.10	8.05
	2019	7.81	7.88	7.90	8.00	8.04	8.01	8.04	8.01
	2020	8.38	8.16	8.09	7.97	8.04	8.06	8.05	8.04
	2021	7.73	7.78	7.94	7.96	7.90	7.95	7.98	7.96
Salinity	2014	0.9	1.6	3.7	5	8.4	11.4	16.7	25.2
	2019	0.3	1	2.3	4.9	9.6	14.8	19.5	25.7
	2020	0.2	0.4	3.1	3.9	9.9	14.9	20	25.3
	2021	0.4	0.7	4.7	6.8	11.3	14.5	18.8	24.9
Oxygen (mg L ⁻¹)	2014	8.8	8.0	8.0	8.0	7.7	10.7	11.6	12.3
	2019	9.5	9.6	9.8	11.5	11.1	11.7	12.2	11.5
	2020	8.7	9.3	10.8	11.0	11.2	11.5	11.4	11.8
	2021	7.2	7.6	9.8	10.5	11.1	11.6	11.9	12.3

Table S3 Physico-chemical parameters and concentrations of major cations, anions, and DOC analysed in the Scheldt Estuary (upstream sampling, 2014) and used as input data for the geochemical speciation of uranium.

Parameter	Station							
	HEM	S22	S15	S12	S09	S07	S04	S01
Salinity	1.0	2.0	4.0	5.4	9.7	12.8	16.8	24.0
Temperature (°C)	6.7	7.0	7.2	7.0	6.4	6.2	6.1	6.2
pH	7.8	7.9	7.9	8.0	8.0	8.1	8.1	8.1
Alkalinity (meq L ⁻¹)	3.9	3.9	3.8	3.7	3.6	3.5	3.3	2.9
O ₂ (mg L ⁻¹)	8.8	8.0	8.0	8.0	7.7	10.7	11.6	12.3
DOC (mg L ⁻¹)	6.925	6.923	4.712	7.988	5.244	1.851	1.683	1.135
Ca ²⁺ (mg L ⁻¹)	93	101	118	129	170	193	231	290
K ⁺ (mg L ⁻¹)	18	27	47	58	105	132	175	249
Mg ²⁺ (mg L ⁻¹)	34	65	131	178	332	427	573	815
Na ⁺ (mg L ⁻¹)	241	511	1,069	1,425	2,664	3,436	4,606	6,536
Cl ⁻ (mg L ⁻¹)	510	1,075	2,414	2,979	5,847	7,563	10,621	16,536
SO ₄ ²⁻ (mg L ⁻¹)	119	189	333	414	762	1,208	1,874	2,261
PO ₄ ³⁻ (mg L ⁻¹)	0.24	0.24	0.26	0.23	0.25	0.23	0.20	0.15
NH ₄ ⁺ (mg L ⁻¹)	0.32	0.23	0.11	0.04	0.05	0.04	0.04	0.06
Si (mg L ⁻¹)	3.78	3.24	3.05	2.75	2.56	2.03	1.85	1.07
NO ₃ ⁻ (mg L ⁻¹)	16.20	16.04	15.04	14.24	12.36	11.23	9.24	5.75
U (µg L ⁻¹)	1.07	1.2	1.32	1.54	1.92	2.18	2.73	2.82

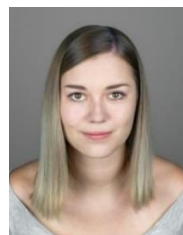
Table S4 Matrix of Pearson-type correlation between salinity and dissolved uranium concentration at stations HEM–S01.

		Dissolved U concentration			
		2014	2019	2020	2021
Salinity	2014	0.957099			
	2019		0.985534		
	2020			0.987798	
	2021				0.982811

12.4 Curriculum Vitae

Personal information

Name: Smolíková Vendula
Date of birth: 17/02/1993
E-mail: vendula.smolikova.vs@gmail.com
Researcher ID: H-8903-2018
ORCID: 0000-0001-5404-9553



Education

2020–present Joint PhD between Mendel University in Brno & Vrije Universiteit Brussel

- Faculty of AgriSciences, Mendel University in Brno, Czech Republic Science & Faculty of Sciences and Bio-Engineering Sciences, Vrije Universiteit Brussel, Belgium
- Topic: Determination of Trace Elements in the Aquatic Environment Using Diffusive Gradients in Thin Films Technique

2017–present PhD, Agricultural Chemistry

- Faculty of AgriSciences, Mendel University in Brno, Czech Republic
- Topic: Determination of Trace Elements in the Aquatic Environment Using Diffusive Gradients in Thin Films Technique

2015–2017 Master's degree, Food Quality and Safety

- Faculty of AgriSciences, Mendel University in Brno, Czech Republic
- Topic: Selected heavy metals in marine fish products

2012–2015 Bachelor's degree, Food Chemistry and Technology

- Faculty of AgriSciences, Mendel University in Brno, Czech Republic
- Topic: Determination of mercury in *Pangasius hypophthalmus* and evaluation of the potential risks of its consumption

Work experience

03/2021–02/2022 Researcher

Analytical, Environmental & Geo- Chemistry department, VUB, Belgium

02/2019–12/2019 Researcher

- Department of Chemistry and Biochemistry, MENDELU, Czech Republic

02/2017–12/2019 Research assistant

- CEITEC Brno University of Technology, Czech Republic
-

Internships

03–05/2019 PhD Traineeship, Vrije Universiteit Brussel, AMGC

- Development of DGT passive sampling techniques for uranium in mining environments and evaluation of its applicability as monitoring tool

07/2019 Master Traineeship, State Veterinary Institute Jihlava

- Processing of food samples and their analysis in the laboratory of gas chromatography.
-

Publications

- **Smolikova, V.**, Pelcova, P., Ridoskova, A., Leermakers, M. (2022). Diffusive gradients in thin-films technique for uranium monitoring along a salinity gradient: a comparative study on the performance of Chelex-100, Dow-PIWBA, Diphonix, and Lewatit FO 36 resin gels in the Scheldt estuary. *Talanta*, 240, 123168.
- Stepankova, H., Swiatkowski, M., Kruszynski, R., Svec, P., Michalkova, H., **Smolikova, V.**, Ridoskova, A., Splichal, Z., Michalek, P., Richtera, L., Kopel, P., Adam, V., Heger, Z., Rex, S. (2021). The Anti-Proliferative Activity of Coordination Compound-Based ZnO Nanoparticles as a Promising Agent Against Triple Negative Breast Cancer Cells. *International Journal of Nanomedicine*, 16, 4431.
- **Smolikova, V.**, Pelcova, P., Ridoskova, A., & Leermakers, M. (2021). Simultaneous determination of arsenic and uranium by the diffusive gradients in thin films technique using Lewatit FO 36: Optimization of elution protocol. *Talanta*, 228, 122234.
- **Smolikova, V.**, Pelcova, P., Ridoskova, A., Hedbavny, J., Grmela, J. (2020). Development and evaluation of the iron oxide-hydroxide based resin gel for the diffusive gradient in thin films technique. *Analytica Chimica Acta*, 1102, 36-45.
- Pelcova, P., Zouharova, I., Ridoskova, A., **Smolikova, V.** (2019). Evaluation of mercury availability to pea parts (*Pisum sativum* L.) in urban soils: comparison between diffusive gradients in thin films technique and plant model. *Chemosphere*, 234, 373-378.
- Ridoskova, A., Pelfrene, A., Douay, F., Pelcova, P., **Smolikova, V.**, Adam, V. (2019). Bioavailability of mercury in contaminated soils assessed by the

diffusive gradient in thin film technique in relation to uptake by *Miscanthus x giganteus*. *Environmental Toxicology And Chemistry*, 32 (2), 321-328.

- Brtnicky, M., Pecina, V., Hladky, J., Radziemska, M., Koudelkova, Z., Klimanek, M., Richtera, L., Adamcova, D., Elbl, J., Galiova, M.V., Balakova, L., Kynicky, J., **Smolikova, V.**, Houska, J., Vaverkova, M.D. (2019). Assessment of phytotoxicity, environmental and health risks of historical urban park soils. *Chemosphere*, 220, 678-686.
- Horky, P., Skalickova, S., Urbankova, L., Baholet, D., Kociova, S., Bytesnikova, Z., Kabourkova, E., Lackova, Z., Cernei, N., Gagić, M., Milosavljević, V., **Smolikova, V.**, Vaclavkova, E., Nevrkla, P., Knot, P., Krystofova, O., Hynek, D., Kopel, P., Skladanka, J., Adam, V., Smerkova, K. (2019). Zinc phosphate-based nanoparticles as a novel antibacterial agent: in vivo study on rats after dietary exposure. *Journal of Animal Science and Biotechnology*, 10(17).
- Pelcova, P., Vicarova, P., Docekalova, H., Postulkova, E., Kopp, R., Mares, J., **Smolikova, V.** (2018). The prediction of mercury bioavailability for common carp (*Cyprinus carpio* L.) using the DGT technique in the presence of chloride ions and humic acid. *Chemosphere*, 211, 1109-1112.
- Urbankova, L., Horky, P., Skladanka, J., Pribilova, M., **Smolikova, V.**, Nevrkla, P., Cernei, N., Lackova, Z., Hedbavny, J., Ridoskova, A., Adam, V., Kopel, P. (2018). Antioxidant status of rats' blood and liver affected by sodium selenite and selenium nanoparticles. *PeerJ*, (5) e4862.

Conferences

2020 VLIZ 2021, Conference Marine Science Day held by Vlaams Instituut voor de Zee

- The potential of diffusive gradients in thin films (DGT) technique as a monitoring tool for uranium in the aquatic environment (poster)

2020 MVBM 2020, Conference Mladá voda břehy mele 2020 held by Young Water Professionals Czech Republic

- The diffusive gradients in thin films for arsenic evaluation in the aquatic ecosystems (presentation)

2019 MendelNet 2019, The International Scientific PhD Students Conference

- Determination of arsenic bioavailability in mineral springs in the Czech Republic (presentation)

2019 DGT 2019, The 6th conference on Diffusive Gradients in Thin Films

- Evaluation and development of DGT as a monitoring tool at an uranium industrial site (presentation)
- 2019 ICCE-2019**, 17th International Conference on Chemistry and the Environment
- Direct determination of arsenic in high salinity samples by graphite furnace atomic absorption (poster)
- 2018 MendelNet 2018**, The International Scientific PhD Students Conference
- Modification of electrothermal atomic absorption spectrometry for determination of arsenic in high salinity samples (presentation)
- 2018 ISEAC-40**, International Conference on Environmental & Food Monitoring
- Development and evaluation of the diffusive gradient in thin film technique for determination of arsenic in aquatic environment (presentation)
- 2016 MendelNet 2016**, The International Scientific PhD Students Conference
- Determination of heavy metals in fish products (presentation)

Research expeditions

- North Sea and Scheldt estuary campaign on board of the RV Belgica (2019–2021)
- Burgundy, France (07/2021)
- Pays de la Loire region, France (10/2020)
- Tricastin, France (05/2019)

Projects

- 2019 Principal investigator of IGA MENDELU**
- Development and evaluation of the diffusive gradient in thin film technique for determination of arsenic bioavailability in the aquatic environment
- 2019 Co-investigator of IGA MENDELU**
- Development of Electrochemical DNA Biosensor for the Detection of DNA Methylation Associated with Cancer

Awards

- 2019**
- 1st place, MendelNet conference 2019. Section: Applied Chemistry and Biochemistry

2018

- 1st place, MendelNet conference 2018. Section: Applied Chemistry and Biochemistry

2017

- Rector award for outstanding study results, MENDELU, Czech Republic
- Dean award for outstanding master thesis, MENDELU, Czech Republic

2015

- Rector award for outstanding study results, MENDELU, Czech Republic